Interactions of the pentameric acetylcholine receptor subunits of nematodes

Jennifer Darcie Noonan
Institute of Parasitology
McGill University
Montreal – Canada

A thesis submitted to McGill University in partial fulfillment of the requirements of the degree of Doctor of Philosophy.

Abstract

Pentameric ligand-gated ion channels (pLGICs) represent an ancient signaling receptor family. Through a series of subunit gene duplication events followed by functional divergence, animals have expanded their receptor gene family and by extension, their function. The precise function of a channel depends on its subunit composition and organization, therefore knowing the mechanisms determining this would provide valuable insight into receptor function and evolutionary change. Despite this, little is known about what determines which subunits come together to form a functional channel, in what arrangement, and how this relates to the underlying synthesis machinery. Nematodes have a relatively recent expansion of their pLGIC gene family that allows us to study specific examples of how functional fine-tuning occurs. This thesis set out to use evolutionary examples of subunit compatibility, stoichiometry and interactions with synthesis machinery within the nematode channels. It was hypothesized that non-alpha subunits within a heteromeric receptor play an essential structural role and at least two must be present. Instances where a non-alpha subunit is no longer required, another non-alpha subunit will take its place. Loss of non-alpha subunit genes may lead to duplication and functional adaptation of an alpha subunit to become non-alpha. This regulation of receptor composition and arrangement will be influenced by the accessory protein network and these interactions may also change as a result. One of these receptors, the levamisole-sensitive acetylcholine receptor (L-AChR), fits the definition of a "perfect" heteromer because it requires five different subunits in a precise stoichiometry to be functional. By studying examples of L-AChR subunit gene duplications from related nematode species, I have identified specific sequences within non-alpha subunit types that mediate subunit organization and function. Attempts to reconstitute the homomeric ACR-16 from *Brugia malayi* in *Xenopus laevis* oocytes proved unsuccessful. To address this, I used a phylogenetic approach of characterizing ACR-16 from different related worm species to identify the cause. In doing so, I characterized a novel phylogenetic change in the ACR-16 requirement for new accessory proteins that occurs independent of pharmacology. An unexpected finding from this analysis was that one of these ACR-16 receptors no longer requires the RIC-3 accessory protein for heterologous expression; a highly uncharacteristic behaviour for this class of channel. Using a combination of chimeras and mutagenesis, I was then able to identify, down to a single amino acid residue, what region determines this observation. This work provides much needed insight into the mechanisms that determine subunit positioning and compatibility within heteromeric receptors. I also provide a novel method of using receptor phylogeny for investigating a change in accessory protein dependence. Finally, I show that accessory protein requirements can change rapidly and depend on a single amino acid. This work demonstrates how complex and dynamic subunits are in mediating compatibility and positioning within a receptor. It also highlights the importance of the underlying accessory protein network for functional expression in heterologous systems.

Résume

Les canaux ioniques pentamériques dépendant d'un ligand (pLGICs) représentent une ancienne famille de récepteurs de signalisation. Grâce à une série d'événements de duplication de gènes de sous-unités suivis d'une divergence fonctionnelle, les animaux ont étendu leur famille de gènes de récepteurs et, par extension, leur fonction. La fonction précise d'un canal dépend de la composition et de l'organisation de ses sous-unités. Par conséquent, la connaissance des mécanismes qui la déterminent permettrait de mieux comprendre la fonction des récepteurs et les changements évolutifs. Malgré cela, on connaît mal ce qui détermine les sous-unités qui se regroupent pour former un canal fonctionnel, la disposition de ces sous-unités, et comment cela est lié à la mécanique de synthèse sous-jacente. Les nématodes ont une expansion relativement récente de leur famille de gènes pLGIC, ce qui nous permet d'étudier des exemples spécifiques de la façon dont le peaufinage fonctionnel se produit. La présente thèse vise à utiliser des exemples évolutifs de la compatibilité des sous-unités, de la stœchiométrie et des interactions avec la mécanique de synthèse au sein des canaux des nématodes. On a émis l'hypothèse que les sous-unités non-alpha au sein d'un récepteur hétéromérique jouent un rôle structurel essentiel et qu'au moins deux doivent être présentes. Lorsqu'une sous-unité non-alpha n'est plus nécessaire, une autre sous-unité non-alpha prend sa place. La perte des gènes de la sous-unité non-alpha peut entraîner la duplication et l'adaptation fonctionnelle d'une sous-unité alpha pour devenir non-alpha. Cette régulation de la composition et de la disposition des récepteurs sera influencée par le réseau de protéines accessoires et ces interactions peuvent également changer en conséquence. L'un de ces récepteurs, le récepteur de l'acétylcholine sensible au lévamisole (L-AChR), correspond à la définition d'un hétéromère « parfait » car il nécessite cinq sous-unités différentes dans une stœchiométrie précise pour être fonctionnel. En étudiant des exemples de duplications de gènes de sous-unités L-AChR chez des nématodes apparentés, j'ai identifié des séquences spécifiques au sein de différents types de sous-unités alpha et non-alpha qui interviennent dans l'organisation et la fonction des sous-unités. Les tentatives de reconstitution de l'homomère ACR-16 de *Brugia malayi* dans des ovocytes se sont avérées infructueuses. Pour résoudre ce problème, j'ai utilisé une approche phylogénétique pour caractériser l'ACR-16 de différentes espèces de vers apparentés afin d'en identifier la cause. Ce faisant, j'ai caractérisé un nouveau changement phylogénétique dans la nécessité du ACR-16 pour de nouvelles protéines accessoires qui se produit indépendamment de la pharmacologie. Une découverte inattendue de cette analyse a été le fait que l'un de ces récepteurs ACR-16 ne nécessite plus la protéine accessoire RIC-3 pour une expression hétérologue, un comportement très peu caractéristique de cette classe de canaux. En utilisant une combinaison de chimères et de mutagénèse, j'ai pu identifier, jusqu'à un seul résidu d'acide aminé, la région qui détermine cette observation. Ce travail fournit des informations très utiles sur les mécanismes qui déterminent le positionnement et la compatibilité des sous-unités dans les récepteurs hétéromériques. Je fournis également une nouvelle méthode d'utilisation de la phylogénie des récepteurs pour étudier un changement dans la dépendance des protéines accessoires. Et enfin, je démontre que les besoins en protéines accessoires peuvent être extrêmes et dépendre d'un seul acide aminé. Ce travail démontre à quel point les sous-unités sont complexes et dynamiques, car différentes régions dans différents types de sous-unités interviennent dans la compatibilité et le positionnement au sein d'un récepteur. Il souligne également l'importance du réseau sous-jacent de protéines accessoires pour l'expression fonctionnelle dans des systèmes hétérologues et le fait qu'il devrait être examiné davantage.

Table of Contents

Acknowledgements

This thesis would never have been possible without the constant support that I have received from my parents Anne and Kevin. All of the opportunities that I have been given throughout my life are because of you, thank you, this thesis is for you. Thank you to my big brother Dr. Mike Noonan for providing me with an example of what a good scientist should be. I have looked up to you ever since we were kids, and still do. I also need to extend special thanks to my cousin Christie for scaring me in high school when I almost failed your science test. Your enthusiasm as my high school science teacher motivated me to study more which led to my scientific curiosity and passion for research.

Thank you to my supervisor Dr. Robin Beech for teaching me how to think like a scientist. Your methodological approach to asking and answering questions taught me how to critically analyze a situation and mature as a PhD student. Thank you for your constant patience when I came to you with my many questions, emails and negative PCRs, and thank you for seeing the potential in me when I started as a Masters intern.

Surviving grad school would not be possible without a supportive lab environment. Thank you to past and present lab members. In particular, Dr. Thomas Duguet for training me when I started and Dr. Mark Kaji for always helping me when something went wrong in the lab and listening to my rants (and for sharing the ultimate lab playlist!). Thank you to Dr. Georgia Limniatis for your many conversations and support, I admire you as a friend and a scientist. Thank you to all the of the students that I have trained in the lab, you have helped me grow as a leader and mentor.

To my PhD committee members, Dr. Jeff Xia and Dr. Reza Salavati, your support and feedback during committee meetings helped me stay on track with my projects. The years spent TAing for your courses allowed me to realize how much I enjoy teaching, thank you for providing me those opportunities.

Special thanks to Dr. Thavy Long, Dr. Tim Geary, Dr. Norma Bautista, Kathy Keller, and Mike Masse. Your conversations, assistance and moral support made every day at the Institute feel like home. Finally, thanks to anyone who even read this thesis from start to finish, I hope it’s not too painful.

Contribution of authors

In Chapter 2, the original *Xenopus laevis* oocyte expression plasmid containing the *Caenorhabditis elegans* levamisole-sensitive acetylcholine receptor (L-AChR) subunits cDNA sequences were a gift from Dr. Thomas Boulin (Thomas Boulin et al., 2008). The *Haemonchus contortus* L-AChR subunits and accessory proteins corresponding cDNAs in the *Xenopus laevis* oocyte expression plasmid were provided by Dr. C. Neveu and Dr. C. Charvet. The pTD2 *Xenopus laevis* oocyte expression plasmid was originally made by Dr. Thomas Duguet (T. Duguet, 2017). The dimers were originally cloned by Dr. Thomas Duguet (T. Duguet, 2017). The *unc-29.1* and *unc-29.1* chimeras (Chimera-1 & Chimera-2) were designed by Dr. Robin Beech. Marysa Antonakakis assisted with dimer and chimera electrophysiology and Gabby Lockwood assisted with chimera electrophysiology (not shown in this thesis).

In Chapter 3, the *unc-38* and *unc-63* coding sequences were manually annotated from the Wormbase Parasite genomes by Dr. Robin Beech (Bolt et al., 2018; Howe et al., 2016, 2017). The PAML analysis was performed by me. The *Brugia malayi* acetylcholine receptor subunit genes were cloned by Dr. Thomas Duguet, Sophia Bortulessi, and myself.

In Chapter 4, the coding sequences of *Ascaris suum*, *Dracunculus medinensis*, *Gonglyonema pulchrum* and *Thelazia callipaeda* were manually annotated from the Wormbase Parasite genomes by Dr. Robin Beech (Bolt et al., 2018; Howe et al., 2016, 2017). The *B. malayi* accessory proteins were cloned by me, and the *C. elegans* accessory proteins were synthesized using their genome-predicted coding sequences, obtained by Dr. Robin Beech. Rowena Groeneveld performed *C. elegans acr-16* knock-out (RB918) phenotype studies and worm microinjection (not included in this thesis).

In Chapters 5 and 6, the restriction enzyme modified sequences were engineered by Dr. Robin Beech and the resulting chimeras all cloned by me. The *A. suum* and *B. malayi* chimeras (Chimera-3 and Chimera-4) were designed by Dr. Robin Beech. The point mutations in Chapter 6 were designed and cloned by me. In Chapter 6 the homology models of *A. suum* and *D. medinensis* were made by me.

In Chapter 2 and 3, the idea of using dimers, chimeras and working on *B. malayi* AChRs came from Dr. Robin Beech. In Chapter 3 the idea of making *C. elegans:B. malayi* admixtures to test for individual *B. malayi* L-AChR subunit function came from me. In Chapter 4, the concept

of using ACR-16 Clade III as a model to track the inability to produce any functional *B. malayi* AChR in oocytes was my own. The stepwise process of testing for pharmacology changes and accessory protein effects was also my own. The extensive literature review search for accessory proteins to identify which ones to include was my idea and carried out by me. In Chapter 5, the pharmacological analysis of *B. malayi* acr-16 chimeras and identification of the regions that mediate the declining response was my own. In Chapter 6, the idea of using chimeras and point mutations to identify the regions in nematode AChRs that determines their requirement for RIC-3 was also mine. All of the ideas, methods, cloning and electrophysiology in Chapters 4-6 were carried out by me. This thesis was written by me and edited by Dr. Robin Beech and myself.

List of Abbreviations

ACh: Acetylcholine

AChR: Acetylcholine receptor

ACR: Acetylcholine receptor

AP: Accessory protein

Asu: *Ascaris suum*

AUP: Animal use protocol

BET: Betaine

BEPH: Bephenium

Bma: *Brugia malayi*

Bma-L-AChR: *B. malayi* levamisole sensitive acetylcholine receptor

Cel: *C. elegans*

Cel-acr-16: *C. elegans* acetylcholine receptor acr-16

Cel-L-AChR: *C. elegans* levamisole sensitive acetylcholine receptor

Cel-N-AChR: *C. elegans* nicotine sensitive acetylcholine receptor acr-16

cDNA: complimentary deoxyribonucleic acid

cRNA: complimentary ribonucleic acid

DA: Dopamine

Dme: *Dracunculus medinensis*

DMSO: Dimethyl suloxide

DNA: Deoxyribonucleic acid

dN/dS: Non-synonymous: synonymous substitution rate

ECD: Extracellular domain

EMC: ER membrane protein complex

EPI: epinephrine

ER: Endoplasmic reticulum

GABA: gamma-aminobutyricacid

Gpu: *Gonglyonema pulchrum*

Hco: *H. contortus*

Hco-L-AChR: *H. contortus* levamisole sensitive acetylcholine receptor

HGI: Helminth genome initiative

ICL: Intracellular loop

L-AChR: Levamisole sensitive acetylcholine receptor

N-AChR: Nicotine sensitive acetylcholine receptor

LEV: Levamisole

MOR: Morantel

MSA: Multiple sequence alignment

NIC: Nicotine

NOR: Norepinephrine

NMJ: Neuromuscular junction

NRA: Nicotine receptor associated protein

OXA: Oxantel

PCR: Polymerase chain reaction

pLGIC: pentameric ligand-gated ion channel

PYR: pyrantel

RIC: Resistance to inhibitors of cholinesterase

RNA: Ribonucleic acid

TEVC: Two-electrode voltage clamp electrophysiology

TM: Transmembrane domain

Tzc: *Thelazia callipaeda*

UNC: Uncoordinated

The ion channel gene names discussed in this thesis follow the nomenclature proposed by Beech et al., (2010). Italics represent gene names and capitals represent protein names.

List of Figures & Tables

Introduction

Musculature is a defining characteristic that separates animals from other organisms. At the center of this process are the pentameric ligand-gated ion channels (pLGICs). These membrane spanning receptors, composed of five structurally similar subunits, transmit specific extracellular cues into rapid changes in ion flux across cell membrane that eventually triggers muscle contraction (Corringer et al., 2000; Kandel et al., 2000). These receptors can be composed of five identical subunits (homomeric) or different subunits (heteromeric), and the precise function depends on subunit composition (Thompson et al., 2010; Wu et al., 2015). Subunit gene phylogeny confirms that this superfamily of ion channels predates multicellular life, with our single-celled ancestor inheriting a single subunit gene copy some 500 MYr ago (Tasneem et al., 2005). How did this single subunit give rise to the plethora of diverse animal receptors observed today? A series of gene duplications followed by sequence change led to the functional divergence of present day receptors.

Examples of these functional sequence changes that remain poorly understood include what sequence restricts subunits to specific, defined positions within heteromeric receptors, what sequence determines subunit subtypes and what sequences regulate requirements for the underlying assembly machinery? Answering these questions is difficult because the functional sequence changes have been masked by millions of years of time (Beech & Neveu, 2015; Tasneem et al., 2005). An ideal model to study receptor change must fulfill two criteria. First it must be a recent change in order to identify specific sequences. Second it must be generalizable to the entire pLGIC receptor family. The nematode pLGIC family fulfills these criteria. This receptor gene family has expanded within the nematodes, providing recent examples of functional change. As well, the high structure conservation between nematode and other animal receptors allows these changes and sequences to be applicable to all animal receptors.

Nematode acetylcholine (ACh) pLGIC subunits are classified into alpha or non-alpha types, depending on the presence or absence of a vicinal cysteine motif. The motif is central to ligand-gating as ligands bind at the interface of subunits. Alpha subunits that contain the motif provide the principal face of the binding pocket and non-alpha subunits that do not contain the motif provide the complementary face of the binding pocket. Therefore, subunit positioning is crucial to maintain this interface. The work in this thesis centers around three questions. What

sequences determine subunit positioning and compatibility? What sequences determine subunit subtype function? What sequences regulate requirements for accessory proteins?

The heteromeric levamisole-sensitive acetylcholine receptor (L-AChR) has been characterized from a number of worms. Due to gene duplication and loss events, each reconstituted receptor contains a different subunit composition and stoichiometry (Boulin et al., 2011; Boulin et al., 2008; Buxton et al., 2014; Williamson et al., 2009). For example, duplicated non-alpha UNC-29 subunits have differing abilities to produce functional receptors without the other non-alpha LEV-1 subunit (Duguet et al., 2016). As well, alpha subunit ACR-8 is also able to produce a receptor without LEV-1, whereas its paralog ACR-13 cannot (Blanchard et al., 2018). It is not currently known which subunit replaces LEV-1 in its absence, however subunit phylogeny suggests it is the other non-alpha subunit UNC-29, but this needs to be confirmed. These two duplication examples can be used to identify the sequence and regions restricting subunits in defined positions within the L-AChR. In Chapter 2, by using series of subunit dimers, I confirmed that the non-alpha UNC-29 indeed replaces LEV-1. Following this, by using a series of subunit chimeras, I identified the region in non-alpha subunits that mediate the ability to produce a receptor without LEV-1.

In some Clade III worms, duplicated L-AChR alpha subunits *unc-38* and *unc-63* have lost the vicinal cysteine motif which suggests an alpha to non-alpha subtype switch that may replace their previously lost non-alpha *lev-1* (Beech & Neveu, 2015). Identifying the sequences mediating this potential subunit subtype switch would provide insight into how subtypes evolved. In Chapter 3, I used a bioinformatic approach to predict functional change which can then be tested in oocytes. Selection pressure analysis predicted elevated substitution rates on the duplicate *unc-38* and *unc-63* copies with the intracellular loop and regions around the ligand-binding pocket containing these elevated rates. Unfortunately, despite many controls and conditions, no functional Clade III receptor was reconstituted in oocytes, including the nicotine sensitive acetylcholine receptor ACR-16 (N-AChR). This indicates that drastic changes occurred in the receptors from this group of worms, preventing their *ex vivo* reconstitution with traditional accessory proteins.

The inability to produce a homomeric N-AChR receptor from later Clade III worms also presents an interesting opportunity to explore what sequence changes regulate receptor requirements for accessory proteins. In Chapter 4, I used a novel approach of characterizing N-

AChR along its Clade III phylogeny using intermediate species, and found a slow, progressive change in the requirement for new accessory proteins. This change occurs independently of pharmacology and was partially reversed by including new accessory proteins (Chapter 4 & 5).

Finally, during the N-AChR characterization, one of the intermediate species no longer required any RIC-3 accessory protein to produce fully functional receptors in oocytes. This was unusual for an N-AChR and provided the perfect opportunity to identify the region mediating accessory protein requirement. Using a series of chimeras and single-residue mutagenesis, in Chapter 6, I narrowed down to a single amino acid residue that mediates RIC-3 requirement.

The work presented here answers some of the most basic mechanisms of receptor change. I confirmed that subunit positioning was likely determined early on in subunit evolution because only a non-alpha subunit can replace another non-alpha subunit. I have shown the inherent complexity in the regions that mediate subunit positioning and compatibility. As well, the signature of how evolutionary selection pressures act on duplicate subunits predicts that it is the intracellular loop and specific regions within the extracellular domain that functionally change subunit types. The inability to reconstitute any later Clade III receptor indicated severe changes to receptor synthesis. A phylogenetic characterization confirmed this is the case as Clade III N-AChR had a gradual decline in response which was partially reversed upon addition of new accessory proteins. This approach was novel and can explain why no functional acetylcholine receptor from other later Clade III receptors can be recorded in oocytes. Most strikingly, I have identified that RIC-3 accessory protein requirement can be extreme and depend on a single residue. In conclusion, the changes that determine subunit positioning, compatibility and subtypes are complex. As well, the work on accessory protein requirement highlights the importance of interpreting receptor change not only in the context of inter-subunit interactions, but in accessory protein interactions as well.

Chapter 1. Literature Review

1.1 Movement as a defining feature of animals

Movement is a defining feature of the animal kingdom that came with profound consequences. The evolution of a defined muscle system, estimated to have occurred prior to the Cambrian explosion (Holland, 2015; Smith & Harper, 2013), gave animals a competitive advantage over other organisms and each other. Not only movement within the environment became possible but traits such as the ability to chase prey, muscle-aided digestion, blood circulation and egg-laying become possible (Droser & Gehling, 2015). As a result, jaws, teeth and armoured bodies proliferated giving rise to the great diversity of modern-day animals (Droser & Gehling, 2015). The pentameric ligand-gated ion channels (pLGICs) are central to this because they transmit the nervous impulse that leads to muscle contraction. These receptors belong to a superfamily of protein receptors known as the ionotropic channels. These membrane-spanning channels respond to extracellular cues and induce rapid, specific responses allowing ion flux through them into cells. Neuromuscular contraction requires a fine-tuned, orchestrated sequence of events (Richmond & Jorgensen, 1999). The synaptic signal transfer from the nerve cell to the muscle cell must be both rapid and specific to ensure an appropriate timing, length, strength and location of muscle contraction (Kandel et al., 2000). Coordination of anionic and cationic channels is required since disrupting this inhibits the fine control of muscle contraction. As the gatekeepers central to this process, the pLGICs are targets of many chemicals, both natural toxins and synthetic drugs (Changeux et al., 1970; Holden dye & Walker 2007).

Present day pLGIC receptors, found in most animals, are either homomeric or heteromeric (Dent, 2006, 2010; Ortells, 2016; Ortells & Lunt, 1995; Tasneem et al., 2005). Understanding the mechanisms responsible for changes in ion-selectivity, ligand specificity, channel gating properties, receptor composition and subunit position is a problem of great importance in human medicine and the understanding of animal life. Despite the advances in understanding their structure and molecular details of their function, little is known about the factors that determine subunit composition, organization and assembly. Unfortunately, the long time, and therefore large number of sequence substitutions that have occurred since the Cambrian explosion obscure those responsible (Beech & Neveu, 2015; Dent, 2006). The

nematodes are a means to address these questions directly since expansion of their pLGIC family provides many examples of subunit duplication and functional divergence that are recent, with minimal sequence change. The focus of this thesis is the characterization of such events that can serve as models for this process.

1.2 Origin of pentameric ligand-gated ion channels and the importance of gene duplication & divergence

How did this diverse receptor family arise? The gene duplication hypothesis proposed by Ohno (1970) describes how gene duplication and functional divergence can explain the origin of biochemical complexity (Ohno, 1970). Genes cannot be created *de novo* so they must come from somewhere. A duplicated gene creates a redundancy where one copy can retain the original functionality while the other is released from the pressure to remain unchanged (Innan & Kondrashov, 2010). The majority of duplicated genes will be lost, but if not, selection pressure can now act on one or both genes in various ways to change them (Ohno, 1970). The consequences for duplicate genes may be altered quantity, timing or location of expression, a change, or the appearance of new functional capabilities and division of functions from a multifunctional ancestor to duplicates that specialize in a subset of these (Innan & Kondrashov, 2010). Gene duplication was, and continues to be, pivotal in driving pLGIC functional evolution (Beech & Neveu, 2015; Dent, 2010; Ortells, 2016). Examples of the different functional consequences that occur after gene duplication can be found in the pLGICs.

The primitive pLGIC was homopentameric (Beech & Neveu, 2015; Dent, 2006; Ortells, 2016; Ortells & Lunt, 1995; Tasneem et al., 2005) and functioned as a chemotactic receptor allowing unicellular organisms to sense their environment and control ion gradients (Ortells, 2016). The inheritance of a cationic pLGIC from the common ancestor with prokaryotes is monophyletic (Beech & Neveu, 2015; Dent, 2006; Ortells, 2016; Tasneem et al., 2005) followed by a rapid expansion in the number of pLGIC subunit genes approximately 500 MYr ago (Figure 1) (Dent, 2010; Ortells, 2016; Ortells & Lunt, 1995). Duplication and divergence produced a new class of channels that pass anions, instead of cations and these can inhibit membrane depolarization (Ortells, 2016; Ortells & Lunt, 1995; Tasneem et al., 2005). Further functional divergence gave rise to the main classes of pLGICs observed today that are defined by the neurotransmitter required for activation (Dent, 2006; Ortells, 2016; Tasneem et al., 2005). This

could be considered a first fine-tuning event refining control over the degree of activation. The animal pLGIC receptors also diversified to produce homomeric and heteromeric receptors where duplicate genes produce proteins that functionally diverge into distinct subunits and co-assemble into a single receptor. Of particular relevance for the pLGICs are changes in expression, changes in the ions conducted or the activating neurotransmitter and changes in subunit composition of the receptor. Examples of these can be found in the nematode pLGIC subunit expansion and can serve as models of how pLGIC change occurs in general. The following provides an overview of what might be expected given specific knowledge of the pLGIC gene family.

Binding of the activating neurotransmitter and gating of the conducted ion occurs at the interface between subunits (Corringer et al., 2000; Sine, 2002). Substitutions that alter binding or conductance would likely need to change multiple sites in a heteromeric receptor complex to be effective. A single substitution in the subunit of a homomeric receptor would alter all five sites simultaneously and so we might expect that changes in ligand specificity or conductance would be more effective in a homomeric receptor. In fact, a switch from conducting anions to cations occurred in the common ancestor of the gamma-aminobutyric acid (GABA)-gated cation channels EXP-1 (Beg & Jorgensen, 2003) and LGC-35 (Jobson et al., 2015), both of which are homomeric. The switch to binding glutamate as a neurotransmitter has occurred at least three times (Lynagh et al., 2015), a switch to binding biogenic amines happened twice (Beech et al., 2013), and a switch to binding acetylcholine occurred within the nematodes (Putrenko et al., 2005). In each case, this coincides with receptors that trace back to common ancestors that were likely homomeric.

The ligand-binding and gating mechanisms of pLGICs are highly conserved even though a large diversity of these receptors exists. A homopentamer is five-fold symmetrical, with five identical sites for neurotransmitter binding and yet simulations have shown that binding of two ligands molecules only is required to promote the asymmetry necessary for receptor opening (Mowrey et al., 2013). Cationic heteropentameric receptors have an arrangement of alpha and non-alpha subunits that optimizes this asymmetry (PDB 2BG9, 5KXI, etc) (Corringer et al., 2000). When a homomeric receptor subunit gene duplicates, two identical proteins are produced that could combine to form a single receptor if they are expressed in the same location. Since both copies are identical, they will compete for the same positions within the receptor. A competitive exclusion mechanism may result where the subunits accumulate substitutions that

functionally diverge them to the point of occupying different positions in the receptor. The consequence of this is a heteromeric receptor with defined subunit stoichiometry. Examples in nematodes where a heteromeric receptor has arisen from a homomeric ancestor include ACR-26/27 (Courtot et al., 2015) and ACR-21/LGC-4 (Handy-Hart, pers comm). In each case one of the two derived subunits has characteristics of the non-alpha type. One explanation would be to interpret this as selective adaptation for a fixed structural organization that optimizes the asymmetry required for channel opening (Mowrey et al., 2013). The sequence governing this change is not known and is a central theme of this thesis.

Further subunit specialization within heteropentamers can produce receptors where each subunit has a specific position within the final complex as shown by the many different solved 3D structures (eg PDB 2BG9; Unwin, 2005). The *Caenorhabditis elegans* levamisole-sensitive acetylcholine receptor (L-AChR) is an extreme example where five different genes encode the receptor. Removal of any one subunit leads to loss of the receptor (Figure 2B) (Boulin et al., 2008), which implies that no subunit can replace another and no subunit can occupy more than one location in the complex. By contrast, in the relatives of *C. elegans,* such as *Haemonchus contortus* and *Oesophagostomum dentatum*, subunits of the L-AChR both can produce functional receptors in different combinations (Boulin et al., 2011; Buxton et al., 2014; Duguet et al., 2016), suggesting the mechanisms determining position and composition are somewhat flexible and vary between species. This suggests that the L-AChR of nematodes may provide an experimentally accessible system to investigate these mechanisms.

Specific subunit duplications in L-AChR subunits directly relevant to this thesis are further discussed in Chapter 1.7, however spatial expression differences following duplication is also observed with L-AChR subunits. Duplications within the non-alpha group produced *acr-2, acr-3, lev-1* and *unc-29* and duplication within the alpha group produced *acr-13* and *acr-12* (Figure 2C) (Beech & Neveu, 2015; Dent, 2006; Mongan et al., 2002). Non-alpha LEV-1 and UNC-29 combine with the alpha subunits UNC-38, UNC-63 and ACR-13 to produce the body wall muscle L-AChR (Boulin et al., 2008). In contrast, the non-alpha ACR-2 and ACR-3 combine with UNC-38, UNC-63 and ACR-12 to produce a receptor with different pharmacology in neurons (Jospin et al., 2009). The ancestors of the duplicated subunits likely a formed a functional receptor with UNC-38 and UNC-63 and after duplication they were expressed in

different tissues and accumulated enough changes to be different subunits entirely to prevent competition of paralogous subunits for competing for the same receptor (Jospin et al., 2009).

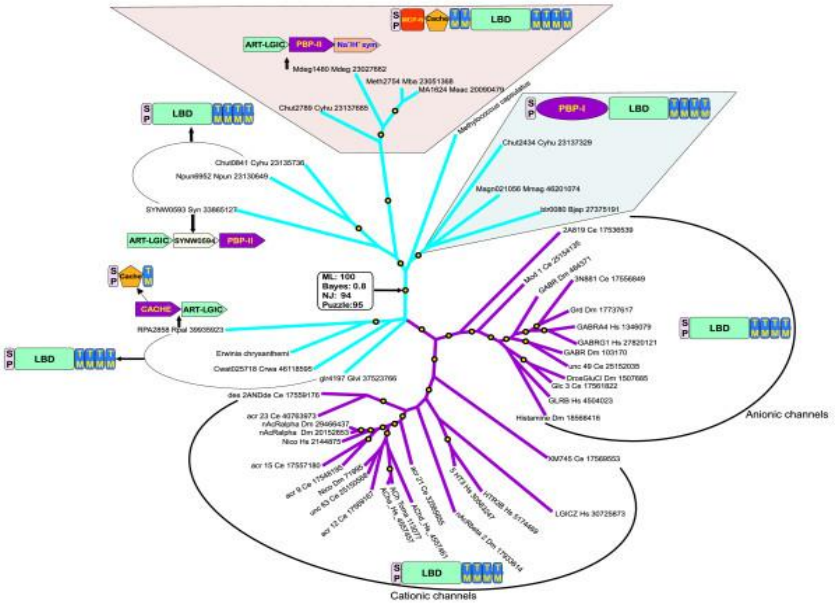

Figure 1. The origin of pLGICs.

The origin of present day pLGICs is believed to be monophyletic. Bacterial branches in blue and animal branches in purple. The ancestor of animals received one subunit gene copy (single purple branch) that duplicated and functionally diverged to produce the anionic and cationic channels. Within both families, more duplication and divergence events occurred which produced the classes of receptor families observed today. Used with permission from Tasneem et al., (2005)

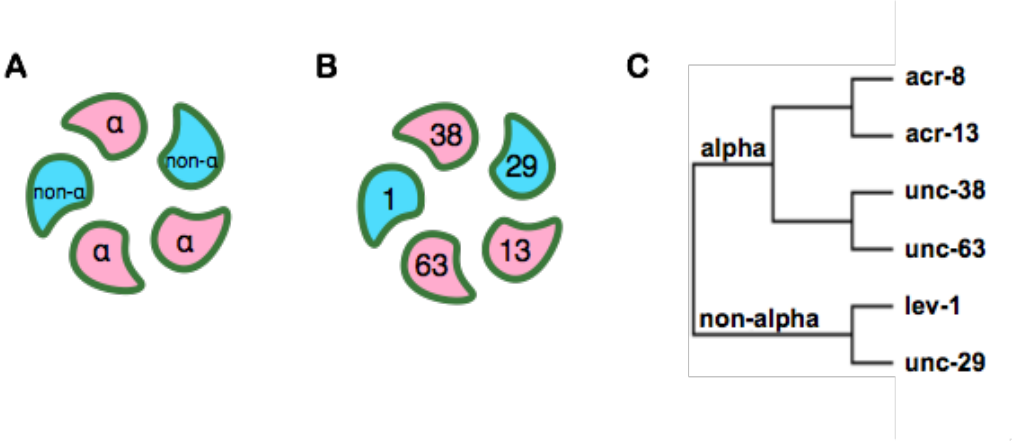

Figure 2. Nematode pLGIC subunit arrangement.

(A) The heteromeric L-AChR receptors have two non-alpha subunits (blue) separated by three alpha subunits (pink). (B) The proposed subunit positioning within the Cel-L-AChR model receptor. (C) Subunit phylogeny shows the alpha non-alpha split first, followed by further subtype divergence within each. Adapted from Duguet, (2017).

The vertebrate homologs of the nematode L-AChR subunits are also diverse. Vertebrates have alpha, beta, gamma, delta and epsilon subunits, with the alpha subunits being homologous to the nematode alpha subunits (Pedersen et al., 2019). Although the vertebrates have fewer subunit types compared to the nematodes, they can be combined in various ways producing receptors expressed in different locations with different pharmacology (Millar & Gotti, 2009). This is in contrast to the nematodes that have a larger diversity in subunits with more restricted subunit positioning. The duplication that produced the alpha and other subtypes occurred before the split that produced the invertebrates and the vertebrates, meaning that the nematodes serve as a model to understand the process that determines subunit function within a receptor.

The opposite of gene duplication is gene loss, when a subunit gene becomes lost in an ancestor and all its descendants as well. Loss balances gain and both processes together mean the gene landscape is constantly changing. Receptors that have been lost in insects, vertebrates and nematodes also means that compounds can selectively target one group and not the other (Dent, 2006). Many differences between *C. elegans* and parasite receptors are due to subunits being lost thus creating new receptor types (Boulin et al., 2011; Buxton et al., 2014). The dynamic nature of subunit gene loss and duplication suggests there is flexibility in the ability to produce a functional receptor. The nervous system is essential for survival, yet most pLGIC knock-outs have little to no noticeable phenotype (Lewis, et al., 1980a; Lewis et al., 1980b; Touroutine et al., 2004). This means that there is redundancy and adaptability within the receptor system. The balance between loss and duplication events poses questions about how they are related, if at all. Do duplications occur first, creating new functions, thus allowing previous functions to be unnecessary and lost? Or does the loss of a function create an environment promoting the retainment of a duplication? At least within the Clade III nematodes, loss of all non-alpha subunits except for *unc-29* predates the duplication of alpha subunits that seem to be becoming non-alpha (see Chapter 3) (Beech & Neveu, 2015; Coghlan et al., 2019; Williamson et al., 2007). However, receptor changes are not confined to just the channels themselves. How loss and duplication events extend to other cellular processes is not known. There exists a complex network of cellular machinery that regulates receptor expression (the details of which will be described in Chapter 1.6) (Green, 1999; Martin et al., 2012; Treinin & Jin, 2020). When a subunit duplicates and is undergoing functional change, the changes would likely affect how it interacts with its receptor synthesis machinery as well.

The examples presented here are nematode specific but are relevant to the receptor family as a whole. Nematodes represent an ideal model to study the process of receptor change in the family as whole because of the similarities between their origin and divergence. The gene expansion and subsequent functional divergence that occurred at the origin of the animals happened so long ago that the sequence changes mediating functional change have been masked by time (Beech & Neveu, 2015). In nematodes, a single subunit also inherited from an ancestor duplicated and diverged to produce the different nematode acetylcholine receptor (AChR) classes (Beech & Neveu, 2015; Dent, 2006, 2010; Jones et al., 2007). The duplications and divergence in the nematodes are relatively recent compared to those found at the origin in the animals and, thus, provide ideal models to study functional change. Furthermore, the conserved pLGIC structure allows for the findings in nematodes to be applicable to the receptor gene family as a whole. In fact, pLGICs are so conserved that chimeric receptors between eukaryotic and prokaryotic receptors are functional and a useful tool for studying receptor structure-function (Duret et al., 2011; Ghosh et al., 2017; Mnatsakanyan et al., 2015; Tillman et al., 2014). These receptors are separated by approximately 500 MY and in order to appreciate these phenomena, a detailed understanding of pLGIC structure is needed.

1.3 Structure of pentameric ligand-gated ion channels

In order to understand receptor change, a detailed understanding of receptor structure is necessary. Five subunits forming a radially symmetrical receptor complex is a defining feature of the pLGICs (Unwin, 1995, 2005). Each subunit is highly structurally similar; having a large extracellular domain (ECD), four transmembrane domains (TM1-4), and a large variable intracellular loop (ICL) (Figure 3 A, B) (Thompson et al., 2010). It is due to this high degree of structural conservation that the chimeric receptors between prokaryotes and eukaryotes are functional (Figure 4D) (Duret et al., 2011; Ghosh et al., 2017; Mnatsakanyan et al., 2015; Tillman et al., 2014). The ECD makes up the largest portion of the receptor and is where ligand binding occurs (Corringer et al., 2000; Smart & Paoletti, 2012; Thompson et al., 2010). The ECD of each subunit contains 10 β-strands that fold into a large β–sandwich, the ligand-binding pocket, and functional motifs including the Cys-loop, the C-loop, and the TM2-3 linker (Corringer et al., 2012; Dacosta & Baenziger, 2013; Thompson et al., 2010; Unwin, 2005). β–strands β1, β2, β3, β5, β6 and β8 form the inner β-sheet, and β–strands β4, β7, β9 and β10 form the outer β-sheet of the β–sandwich (Corringer et al., 2012; Dacosta & Baenziger, 2013; Smart &

Paoletti, 2012). Each of the five ECDs form a "donut" with a hole in the middle where extracellular ions flow down before reaching the channel pore (Corringer et al., 2000; Dacosta & Baenziger, 2013). The loop between β6 -β7 forms the Cys-loop, and the end of β10 continues to the beginning of TM1 (Corringer et al., 2012; Dacosta & Baenziger, 2013; Smart & Paoletti, 2012). The ECD along with the first transmembrane domain are the minimum structural regions required for synthesis and expression to the surface membrane and may participate in direct interactions with the synthesis machinery and other subunits regulating subunit compatibility (Neveu et al., 2010; Verrall & Hall, 1992). These regions therefore contain crucial regulatory and synthesis signal sequences, some of which are conserved from vertebrates to invertebrates (Eertmoed & Green, 1999; Sumikawa & Nishizaki, 1994; Wang et al., 2002). The ECD is where ligand binding occurs, but it is also the region where many positive and negative allosteric modulators bind (Changeux, 2018; Thompson et al., 2010). It is where the structural changes involved in gating begin and is therefore a critical region for receptor function.

The four transmembrane domains of each subunit traverse the plasma membrane as a bundle, anchoring the subunit in the membrane. The TM2 of each subunit lines the ion-permeable pore that allows the passage of ion across the membrane (Figure 4C) (Corringer et al., 1999; Keramidas et al., 2004; Unwin, 1995, 2005). This pore is lined with hydrophobic and charged residues that enable selectivity of ions that flow through (Corringer et al., 1999; Keramidas et al., 2004). Recently, a single substitution in this domain was found to completely determine if a subunit can be present twice in a heteromeric receptor (Emlaw et al., 2021), giving this region a previously unknown function in subunit compatibility and placement in the receptor. TM4 is the outermost domain from the central axis; and together with TM1 and TM3, interacts with membrane components (De Planque et al., 2004; Miyazawa et al., 2003). In unfavourable membrane conditions the TM4 undergoes a conformation change and hinges outwards, physically uncoupling the ECD from the TMs thereby stabilizing the receptor in an inactive state even in the presence of ligand (daCosta & Baenziger, 2009; Hénault et al., 2015). Due to its positioning as the outermost transmembrane domain, TM4 is in an ideal location to interact with membrane proteins involved in synthesis and modulation, however to our knowledge this idea has not been explored in detail. Immediately after TM4 is a short, variable length C-terminal tail that extends outwards from the membrane into the extracellular space. Apart from interacting with the cys-loop to influence channel gating (Alcaino et al., 2017) and a

binding site for some allosteric modulators (Jin & Steinbach, 2015; Paradiso et al., 2001), the tail is not known to have much function.

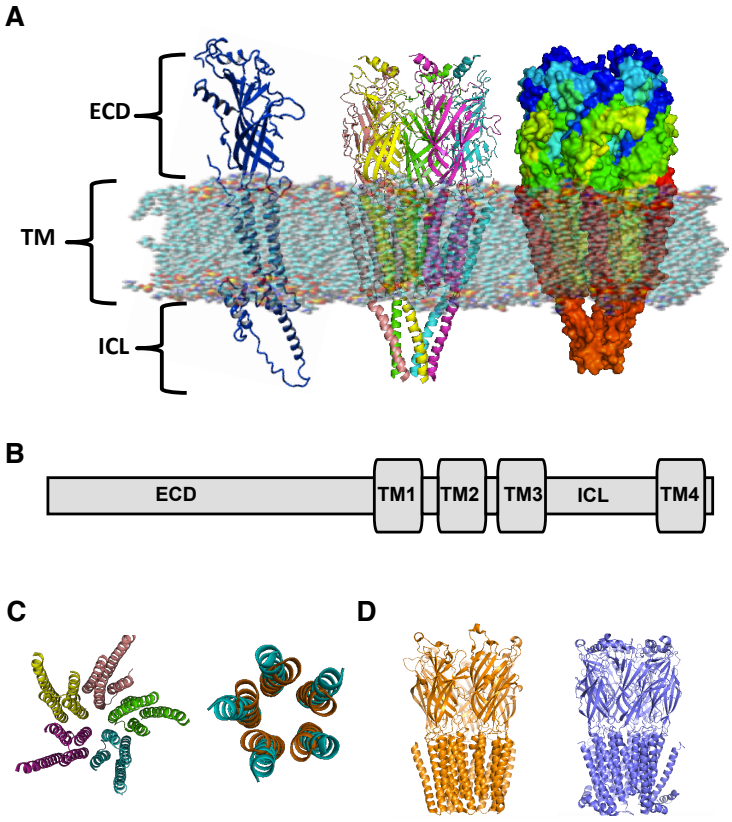

Figure 3. Structure of cys-loop pentameric ligand gated ion channels.
pLGICs are composed of five subunits and are embedded in cell surface membrane. They contain three main regions, a large extracellular domain (ECD) where ligand binding occurs, a series of transmembrane domains (TM) that anchor the receptor in the membrane, and a large intracellular loop (ICL). (A) Single subunit and pentamer structure embedded in the membrane (PDB: 3rqw). (B) Sequence-structure topology of cys-loop receptors. (C) Top-down view through the transmembrane domains and conformational changes in the TM2 during receptor gating (left, PDB:1oed; right, PDB: orange 4npq, cyan 3eam). (D) Conserved structure of receptors between bacterial GLIC receptor (orange, PDB 6F0I) and vertebrate nicotinic receptor (purple, PDB5KXI). Structures downloaded from the Protein Data Bank and manipulated in Pymol.

The intracellular loop, located between TM3 and TM4, is a highly variable region and little is known about its structure and function (Langlhofer & Villmann, 2016). It is believed that the loop interacts with intracellular cytoskeletal components involved in localization of the receptor to the membrane surface, clustering once at the surface, and endocytosis (Boulter et al., 1990; Kneussel & Betz, 2000). Post-translational modification of the ICL is also thought to play

a role in receptor pharmacology. Phosphorylation has been found to mediate receptor properties such as desensitization, ion permeability, and even stimulate expression (Huganir et al., 1986; O'Toole & Jenkins, 2011; Smart & Paoletti, 2012). The only known structures found in the loop are two alpha helices: MA and MX. The MA helix is a long and from each subunit forms a funnel, guiding ion flow out of the channel pore into the cell (Unwin, 2005). The shorter MX helix is nestled near the inner leaflet of the plasma membrane, and thought to be involved in receptor trafficking (Rudell et al., 2020). The details of the ICL structure and function remain a mystery. Bacterial receptors have a smaller ICL as compared to their eukaryotic counterparts (Tasneem et al., 2005). This suggests that primitive receptors had small ICLs and that the evolution of a large, variable ICL in eukaryotic receptors allowed for greater receptor diversity, regulation, and function (Goyal et al., 2011). The ICL is therefore an attractive candidate for regions determining subunit compatibility, positioning and function within a receptor. Using chimeric receptors, previous work has found that the minimum ICL length needed to ensure receptor function is approximately 70 amino acids (Baptista-Hon et al., 2013). Considering that eukaryotic ICLs are, on average, 150 amino acids, there remains much to be understood.

Motifs within pLGIC subunits have been well studied and characterized. Known functional AChR motifs include the Cys-loop, the C-loop, and the PAR/GEK motifs (Corringer et al., 2000; Keramidas et al., 2004). AChRs belong to a larger class of receptors known as the Cys-loop receptors. They are so aptly named because they contain a Cys-loop motif in the ECD. This motif contains two cysteine residues separated by 13 amino acids and is involved in receptor gating (Thompson et al., 2010). The Cys-loop is conserved in all eukaryotic pLGICs highlighting its functional importance (Thompson et al., 2010). Signal sequences in the ECD that ensure only properly folded subunits are expressed have also been described (Wang et al., 2002).

Ion selectivity is determined by specific residues within TM2. Cationic channels have a GEK or GER motif at the beginning of the TM2 sequence, whereas anionic channels have a PAR or AAR motif (Cymesa & Grosman, 2016; Jensen et al., 2005; Keramidas et al., 2004). Even though these motifs are at the beginning of the TM2 sequence, they are located at the bottom of the channel pore because TM2 crosses the membrane "bottom-up". The bottom region of the pore folds inwards, constricting the pore, thus creating a physical block preventing ion flow when the channel is inactive (Cymesa & Grosman, 2016; Sauguet et al., 2013). The GEK and PAR motifs, located in this region, therefore interact with the passing ions; the positive charges

in the PAR motif allow anions to pass, while the negative charges in the GEK motif allow cations to pass (Cymesa & Grosman, 2016; Jensen et al., 2005; Keramidas et al., 2004). Mutations in these motifs alter channel conductance and ion permeability (Wotring et al., 2003).

Most cationic alpha subunits contain a YXCC motif, the C-loop, in the ECD that is involved in ligand binding and the non-alpha subunits typically lack this motif (Corringer et al., 2000). Ligand binding occurs at the interface of two subunits where the subunit contributing the C-loop provides the principal face of the binding pocket, with the other subunit providing the complementary face of the binding pocket (Corringer et al., 2000; Dacosta & Baenziger, 2013; Smart & Paoletti, 2012; Taly et al., 2009; Thompson et al., 2010; Wu et al., 2015). For AChRs, the two adjacent subunits each contribute three loops from their respective β–sandwiches to form the ligand-binding pocket (Corringer et al., 2000; Dacosta & Baenziger, 2013; Thompson et al., 2010). The principal subunit contributes loops A (β2β3 loop), B (β4β5 loop), and C (β6β7 1oop) and the complementary subunit contributes loops D (β1β2 loop), E (β3β4 loop), and F (β5β6 loop) (Figure 4) (Taly et al., 2009; Thompson et al., 2010; Wu et al., 2015) . Conserved aromatic residues from these loops form the hydrophobic ligand-binding box (Figure 4) (Beech & Neveu, 2015; Corringer et al., 2000; Corringer et al., 2012; Dacosta & Baenziger, 2013; Taly et al., 2009; Thompson et al., 2010; Wu et al., 2015).

The structural changes involved in receptor opening have been described and are briefly overviewed (Figure 5) (Dacosta & Baenziger, 2013; Smart & Paoletti, 2012; Taly et al., 2009; Thompson et al., 2010). In the resting state, the principal face C-loop extends outwards from the central axis, exposing the binding pocket to solvent, when agonists bind, such as acetylcholine (ACh), it becomes oriented lengthwise into the pocket, with the positively charged nitrogen of ACh forming cation-π interactions with aromatic tryptophans and tyrosines. Upon ligand binding, the C-loop of the alpha subunit closes inwards and “hugs” the ligand in the pocket, this movement pulls the aromatic residues closer to the ligand thus strengthening their interaction. The structural changes in the residues of the loops causes the β–sandwich to hinge/rotate, which triggers the coupling cascade of ligand binding. The β1-β2, β6-β7 (cys-loop), and the β8-β9 loops of the ECD and the TM2-3 linker are involved in coupling the structural changes from the ECD to the rest of the protein. These three ECD loops rotate towards the TM2-TM3 linker, causing it to move radially outwards. This pulls TM2 leading to its straightening, allowing for ions to move down the pore into the cell. The pore is formed by rings with hydrophobic side

chains residues that strip the waters off the hydration shell that surrounds the ion, and by rings of charged residues that select for ion charge (Sauguet et al., 2013). The ions are then funneled through the MA helices of the ICL and into the cell. The TM2-TM3 linker is a well-studied linker involved in receptor gating (Campos-Caro et al., 1996; Grosman et al., 2000; Jha et al., 2007; Lee & Sine, 2005; Lynch et al., 1997). Mutations to this region, in particular a conserved proline, uncouple the ECD to the TMs, severely hindering receptor activity (Grosman et al., 2000). Receptor deactivation is quick and occurs when the structural changes cause the bottom of the pore to close in and constrict ion flux (Kinde et al., 2015).

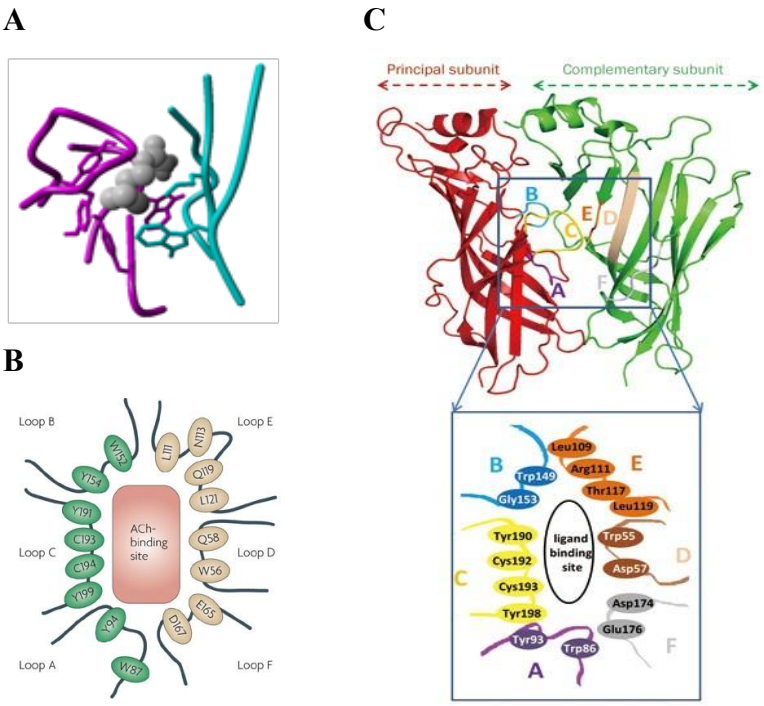

Figure 4. Cationic pLGIC acetylcholine ligand binding pocket. Ligand binding occurs at the interface between two subunits.

(A) The principal face (purple) and the complementary face (cyan) form a hydrophobic box for ligand binding. The shown ligand is a carbamylcholine. (B &C) Six loops, three from each subunit, form interactions with the ligand. (4A) used with permission from (Beech & Neveu, 2015); (4B) used with permission from Taly et al., (2009); (4C) used with permission from Wu et al., (2015)

The kinetics of pLGIC gating is an active field of study. The transition time from resting to open is very short and it quickly transitions to a desensitized state (Gielen & Corringer, 2018). Molecular dynamics suggests the desensitized state has a higher ligand affinity; favouring the desensitized state over open active state (Keramidas & Lynch, 2013). The desensitized state is

thought to act as a protective mechanism; if the receptor is open for the entire duration that the ligand is bound, the cell would be over-stimulated from an abundance of ion flux (Jones & Westbrook, 1996).

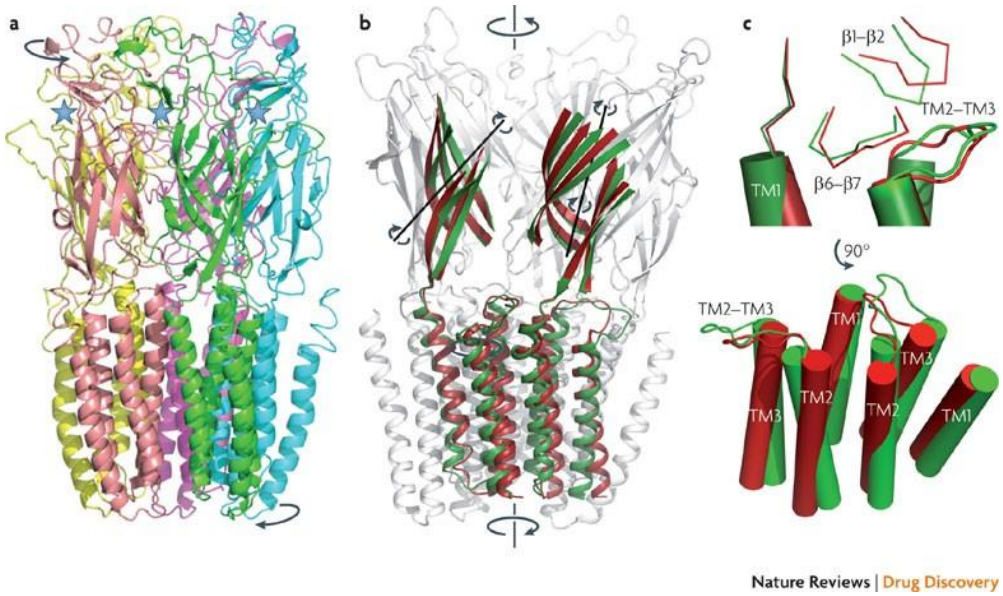

Figure 5. Structural changes during receptor gating.
Upon ligand binding, large conformational changes occur in the ECD (A, B) that propagate to the TMs (C) that allow the flux of ions through the pore created by the second transmembrane domain. Figure used with permission from Taly et al., (2009).

Although current understanding of the structural changes in pLGIC gating is extensive, there remains much to be understood. The majority of resolved pLGIC structures are prokaryotic (ex. PDB 6HZ3, 6I08, 5NJY, etc). These receptors are highly structurally homologous to eukaryotic receptors, however they lack the canonical cys-loop, which is critical in gating (Tasneem et al., 2005). As well, crystallization studies trap the protein complex at slightly different stages of a complex structural change, and putting the pieces together is not intuitive. Despite limitations in understanding the details of receptor gating, characteristics of receptor structure-function depend critically on the conserved binding pocket and by extension, maintaining subunit stoichiometry within the receptor.

As mentioned, ligand binding occurs at the interface between two subunits, therefore, each subunit contributes one ‘face’ of the pocket. The principle face contains the vicinal cysteine motif (C-loop) that is critical in receptor gating, whereas the complementary face does not

contain this motif (Corringer et al., 2000). In the nematodes, two subunit types exist, alpha subunits contain the vicinal cysteine motif whereas non-alpha subunits lack this motif. Because the cysteine motif is central to receptor gating, homomeric channels are composed of alpha subunits whereas heteromeric receptors are composed of a combination of alpha and non-alpha subunits. Thus, in a heteromeric receptor the alpha subunit provides the principle face of the binding pocket and the non-alpha subunit provides the complementary face (Corringer et al., 2000). The non-alpha subunits are not beside each other but are separated by alpha subunits (Figure 2) therefore two binding pockets are present. Even though any subunit interface can act as a ligand binding pocket, only two ligand molecules are needed to elicit full receptor activation (Mowrey et al., 2013). Since two ligand molecules bind in both homomeric and heteromeric receptors, receptor gating mechanisms were present early on in receptor evolution and have since been conserved. Subunits must also be confined to specific positions within a heteromeric receptor to maintain the alpha-non-alpha interface for ligand binding. Indeed, phylogeny of the L-AChR subunits shows that the split producing alpha and non-alpha subunits occurred first followed by further duplication and divergence within each subunit type (Figure 2C) (Beech & Neveu, 2015; Jones et al., 2007; Jones & Sattelle, 2008). Sequence changes that restrict the non-alpha/alpha subunits in a specific arrangement within the receptor therefore occurred early on in heteromeric receptor evolution and are necessary to maintain receptor function, yet they are not known. The sequences that restrict subunits to defined positions within a receptor are, by extension, also involved in subunit subtype change. Additionally, one must consider that these receptors do not act in isolation. How does subunit divergence and sequence change relate to the complex underlying synthesis machinery? These three themes are interlinked and form the focus of this thesis.

Addressing these questions is no simple feat. Functional fine-tuning that gave rise to the different classes of receptors and subunits occurred approximately 500 MYA (Tasneem et al., 2005). Therefore, the specific sequence and evolutionary signature that led to this divergence have been obscured with time. An ideal model to study receptor change must therefore fulfill two criteria. First, it must be a recent functional divergence with minimal sequence change in order to identify specific sequences, and second it must be generalizable to the entire pLGIC receptor family. The nematode pLGIC receptor family fulfills both these criteria.

1.4 Nematodes and the levamisole sensitive acetylcholine receptor

Nematodes are invertebrate roundworms that make up the second most abundant group of animals, behind insects, with reports estimating upwards of 10 million species (Blaxter & Koutsovoulos, 2015; Blaxter et al., 1998; Lee 2002). They are important for maintenance of both soil and marine ecosystems and can exist with both free-living or parasitic lifestyles (Lee 2002). Parasitic nematodes, helminths, are a significant social, economic and health burden to humans and animals (Abad et al., 2008; Lustigman et al., 2012; Roeber et al., 2013). Efforts to control helminth infections with the use of anthelmintics that target their nervous system pLGICs have proven very useful (Wolstenholme, 2011). However, the emergence of resistance threatens control schemes and so understanding the target receptors and how they may change from one species to another is an essential component of this endeavour.

Phylogenetic studies have classified the nematode Phylum into five distinct Clades encompassing both parasitic and free-living lifestyles: Clade I (Dorylaimia), Clade II (Enoplia), Clade III (Spirurina), Clade IV (Tylenchina), Clade V (Rhabditina) (Figure 6) (Blaxter & Koutsovoulos, 2015; Blaxter et al., 1998; Holterman et al., 2006; Mitreva et al., 2005; Parkinson et al., 2004). Despite their abundance and significance to ecosystems, less than a fraction of nematode species been described and even fewer have had their genomes sequenced (Blaxter & Koutsovoulos, 2015; Blaxter et al., 1998; Coghlan et al., 2019). The 50 Helminth Genome Initiative (HGI) was initiated to produce high quality draft genomes of 50 helminth species to improve both the understanding of their phylogeny and allow other researchers open source genome data for their work. To date over 150 helminth genomes have been released, which provide an excellent resource to identify recent examples of subunit gene duplication (Bolt et al., 2018; Coghlan et al., 2019; Howe et al., 2017).

The *C. elegans* nematode is a model organism and an ideal reference organism for comparison with others. The use of *C. elegans* as model organism has been widespread ever since the early genotype phenotype studies were made (Brenner 1974). These early studies noted that it is an easy organism to culture, its nervous system and anatomy is relatively simple and defined, with every cell division from zygote to adult mapped, allowing for the study of complex physiological functions in a "reduced" organism (Johnson et al., 2010; Markaki & Tavernarakis, 2010; Sulston et al., 1983). The first mutants screened for genes linked with the nervous system in *C. elegans* was for levamisole (LEV) resistance (Lewis et al., 1980a; Lewis et al., 1980b) that

led to reconstitution of the definitive L-AChR some 28 years later (Boulin et al., 2008). The reason for the delay in *ex vivo* receptor reconstitution was because of missing accessory proteins that needed to be included (Boulin et al., 2008; Fleming et al., 1997).

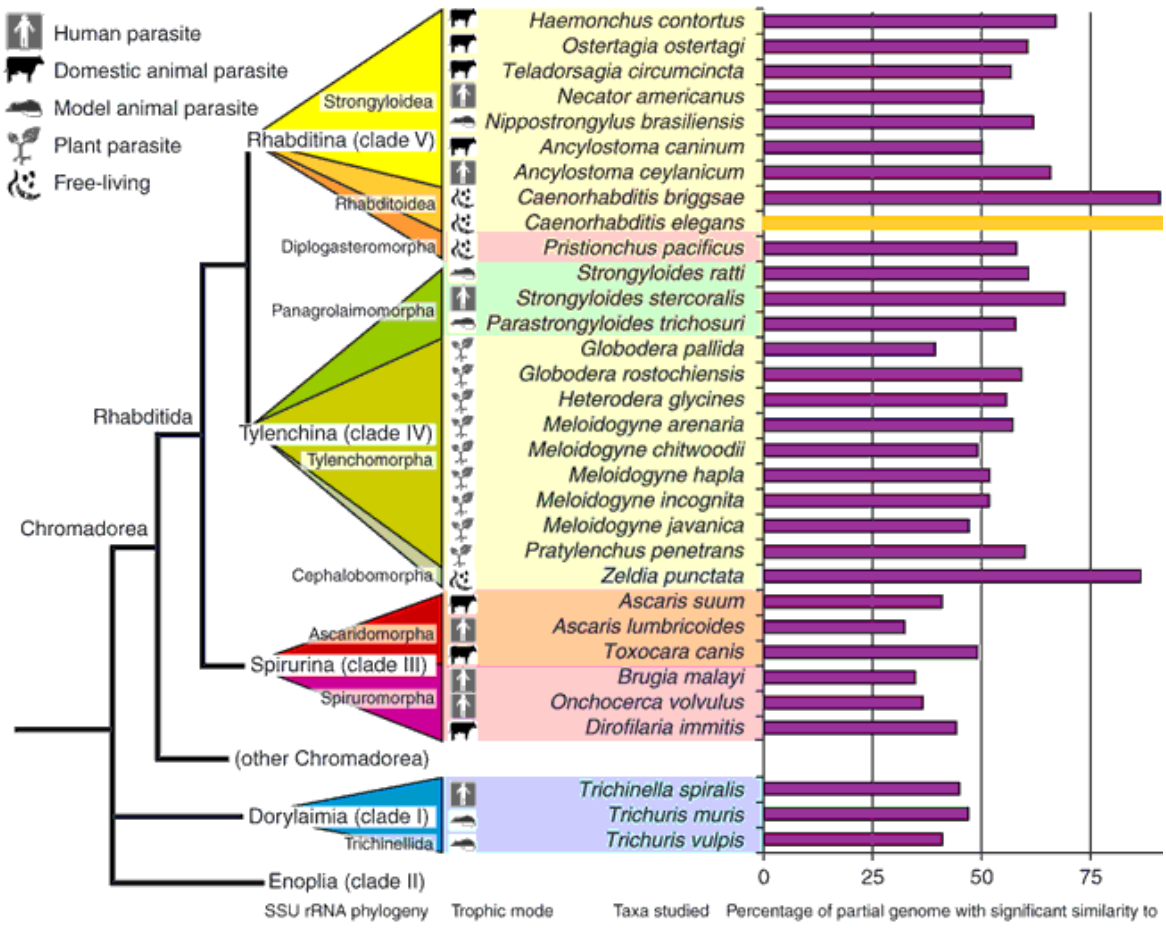

Figure 6. Nematode Clade classification

Nematodes are separated into Clades based on small subunit rRNA sequencing. The model nematode *C. elegans* groups within the Clade V worms. *H. contortus* also groups within the Clade V worms. *Brugia malayi* is a Clade III worm. Figure obtained with permission from Parkinson et al., (2004).

The sheer number and diversity of nematode subunits allows us to use recent examples of duplicate genes to examine how evolution changes these receptors (Beech & Neveu, 2015). The use of *C. elegans* as an experimental model for not only helminths but higher animals as well has led to the extensive characterization of a number of pLGICs. Of particular interest are two

cationic AChRs expressed in the same postsynaptic body wall muscle cells: the homomeric nicotine sensitive acetylcholine receptor (N-AChR) (ACR-16) and the heteromeric L-AChR respectively (Ben-Ami et al., 2009; Boulin et al., 2008; Martin et al., 2012; Touroutine et al., 2005; Williamson et al., 2009). There is also the anionic GABA receptor; UNC-49, in body wall muscle (Richmond & Jorgensen, 1999). The cationic receptors regulate muscle contraction while the anionic receptor regulates muscle relaxation, and all three receptors work in a coordinated effort to ensure appropriate contraction of the worm's body wall muscle (Richmond & Jorgensen, 1999). Interestingly, although the N-AChR and L-AChR both respond to ACh, one remains homomeric while the other is entirely heteromeric. The N-AChR contains the same ACR-16 subunit repeated five times whereas the L-AChR needs 5 different subunits (Ballivet et al., 1996; Boulin et al., 2008). It is not known what evolutionary pressures have kept the N-AChR homomeric and the L-AChR strictly heteromeric. The fact that both respond to the same ligand and are expressed in the same tissue limits the possible reasons why they would appear different (Ballivet et al., 1996; Boulin et al., 2008; Lewis et al., 1980a; Lewis et al., 1980b; Touroutine et al., 2005, 2004). Understanding how selective pressure can lead to different receptors expressed in the same synaptic junction would be a major step forward. These receptors, therefore, represent ideal models to understand basic evolutionary change.

As described above, early screens for genes that contribute to the nematode nervous system randomly inserted mutations into *C. elegans* and observed changes in worm phenotype. These screens identified 11 genes that either completely abolished the levamisole-sensitive phenotype or exhibited reduced sensitivity and uncoordinated body-wall muscle generated movements. Of these 11 genes, four were ion channel subunits (*lev-1, unc-29, unc-38*, and *unc-63*) and seven were accessory proteins. This work allowed for the initial identification of the genes involved in nematode cholinergic transmission.

Expression of three of the four subunits (*lev-1, unc-29,* and *unc-38*) in *X. laevis* oocytes, together but not individually, led to LEV induced currents that suggested these subunits produced an L-AChR. Although this was groundbreaking at the time, the measured currents were exceedingly small (maximal current of 10 nA), making it difficult to confirm its reliability (Fleming et al., 1997). It wasn't until years later when the correct subunits, in combination with accessory proteins, produced reliable responses in *Xenopus laevis* oocytes (Boulin et al., 2008). Using the initial *C. elegans* genetic screens along with newer work on the involvement of

specific pLGIC accessory proteins, Boulin and colleagues identified eight genes needed to produce a LEV-sensitive nematode channel (Boulin et al., 2008) . Of these eight genes, five were AChR subunits (*lev-1, unc-29, unc-38*, *unc-63* and *acr-13*) and three were ancillary proteins (*ric-3, unc-50,* and *unc-74*). The removal of any one of these either completely ablated the measured response or dramatically decreased it (Boulin et al., 2008).

This work not only identified the subunits required to produce the L-AChR, but it also highlighted the importance of co-injecting specific accessory proteins. Even though the *X. laevis* genome contains all three of the accessory proteins, they are either not expressed in high enough quantities in oocytes or are too divergent to be functional with the worm receptor (Bennett et al., 2012; Williams et al., 2005). Considering that it had taken over 20 years to reconstitute the L-AChR after its subunits were known, the significance of accessory proteins in receptor assembly and trafficking cannot be more stressed.

The Cel-L-AChR represents an ideal heteromeric receptor because all five subunits must be absolutely present to produce a functional channel. As mentioned, nematode cationic pLGICs fall into two classes of subunits; either alpha or non-alpha, and this distinction is critical in ligand binding (Corringer et al., 2000). The principal face of the ligand-binding subunit interface is defined by the C-loop that closes inwards and forms a shell around the bound ligand against the complementary face. Alpha subunits contain a YXCC motif in the C-loop that is required for ligand binding and can provide either the principal or complementary face of the pocket. Non-alpha subunits lack the motif and provide only the complementary face. In the nematode L-AChR subunits*, lev-1* and *unc-29* are non-alpha and *acr-13, unc-38,* and *unc-38* are alpha (Figure 2C). Heteropentameric receptors have an arrangement of alpha and non-alpha subunits that optimizes the asymmetry in ligand-binding; the non-alpha subunits do not sit directly beside each other in the channel and are thus separated by alpha subunits (Figure 2A) (Corringer et al., 2000; Mowrey et al., 2013).

Although the Cel-L-AChR is widely studied, its structural organization has yet to be resolved. Recent work has proposed a possible subunit arrangement by artificially fusing the C-terminal of one subunit to the N-terminal of another, forcing two subunits to be beside each other in the mature receptor. By adding the subunits in an incremental manner and testing functionality, subunit arrangement was proposed to be UNC-38:LEV-1:UNC-63:ACR-13:UNC-29 (Figure 2B) (Duguet, 2017). This proposed structure separates the two non-alpha subunits,

agreeing with previous work that the non-alpha subunits must not be positioned beside each other (Corringer et al., 2000; Mowrey et al., 2013). This work presents a major step forward into deciphering the subunit arrangement of this model receptor.

1.5 Details of the N-AChR in relation to the L-AChR and expression

In addition to the L-AChR, the homomeric ACR-16 N-AChR is also present in worm body wall muscle. The N-AChR is composed of five alpha type ACR-16 subunits (Ballivet et al., 1996). The early genetic screens that identified the L-ACh-R genes suggested that a second AChR was present in the same tissue because the uncoordinated phenotypes decreased as the worms aged and mapped to numerous other genes (Lewis et al., 1980a; Lewis et al., 1980b). The first evidence that the *acr-16* gene produces a homomeric receptor was not until 1996, when its pharmacological characterization in oocytes was compared to that of its vertebrate ortholog; the α7 AChR (Ballivet et al., 1996). ACR-16 knock-out *C. elegans* confirmed this receptor is present *in vivo* and forms a receptor independent to that of the L-AChR (Touroutine et al., 2005, 2004). The oocyte characterization of the Cel-L-AChR included the Cel-acr-16 and confirmed its requirement for RIC-3, but not UNC-50 nor UNC-74, suggesting the receptors, although expressed in the same tissue, are under somewhat different regulatory mechanisms (Boulin et al., 2008). More recently, other nematode ACR-16s have been characterized, including the Clade V *Ancylostoma caninum, Ancylostoma ceylanicum and Necator americanus,* the Clade III *Ascaris suum* and the Clade I *Trichuris suis* (Abongwa et al., 2016; Choudhary et al., 2019; Hansen et al., 2021; Kaji et al., 2020).

Acr-16 is widely conserved across animal species with a large diversity of genes found in the family (Coghlan et al., 2019). In nematodes, the *acr-16* clade of subunit genes has expanded, producing up to 9 subunit types, with many gene loss and duplication events (Coghlan et al., 2019). The diversity of *acr-16*, and its orthologs in other species, highlights its need to be conserved and expanded. Despite the large family of *acr-16* related genes, these receptors remain homomeric. Is it purely sequence change in the subunit that prevent their compatibility with subunits from other receptors? Or does it also involve the accessory proteins involved in assembly of the pentamer? Or is it a combination of both of these? Understanding to what extent receptors are similar and different, especially those expressed in the same synapse, is crucial in understanding the mechanisms involved that led to their divergence. In addition to sequence changes affecting the relationship between the subunits themselves, investigating how change

affects the accessory protein network must be considered as well since these receptors are subject to rigorous processing at every step of the expression pathway (Green, 1999; Treinin & Jin, 2020). The L-AChR and N-AChR are useful to understand to what extent different receptors share synthesis proteins.

1.6 Accessory protein network relevant to L- and N-AChR

The initial reconstitution of a robust L-AChR in *X. laevis* oocytes was difficult and produced little functional receptor. Success that was only achieved by including specific accessory proteins RIC-3, UNC-50 and UNC-74 shows that they are required for strong expression (Boulin et al., 2008; Lewis et al., 1980a; Lewis et al., 1980b). Other accessory proteins are known to be involved in *in vivo* L-AChR synthesis, yet their inclusion in oocytes is not required. The inability to express Bma-L-AChR nor Bma-N-AChR (see Chapter 3 on this) may be due to lack of required accessory proteins so it is important to understand their role in receptor assembly, stabilization, processing, and transport.

Expression of pLGIC receptors at the cell surface involves synthesis, stabilization and assembly in the ER, glycosylation in the golgi and trafficking to the cell surface (Green, 1999). Receptor-associated proteins (APs) play a crucial role in this (Treinin & Jin, 2020). Several are essential for cationic AChR expression and others continue to be identified in vertebrates and invertebrates alike (Choudhary et al., 2020; D'alessandro et al., 2018; S. Gu et al., 2016; Sharma et al., 2018). Subunits that make up the receptor are subject to many complex regulatory processes, with different chaperons involved at every step of the biosynthesis and expression pathway (Green, 1999; Green & Claudio, 1993; Millar & Harkness, 2008) (Figure 7). These include a number of proteins that are involved in subunit folding, assembly, transport and receptor placement within the neuromuscular junction (NMJ). Subunits are translated in the endoplasmic reticulum (ER) of post-synaptic cells before they are shuffled to the golgi apparatus before reaching the cell-surface membrane (Green, 1999). Nearly every region of the subunit has been implicated in subunit assembly and cell-surface expression, however many studies suggest the ECD and the TM1 as being the main regulators of receptor expression (Castillo et al., 2005; Eertmoed & Green, 1999; Sumikawa & Nishizaki, 1994; Verrall & Hall, 1992), however there is some evidence that suggests specific sequences within the ICL as well contribute to this intricate process (Rudell et al., 2020). Post-translational modification including glycosylation (at the ECD) and phosphorylation (at the ICL) occur in pLGICs and modulate functional properties of

the mature receptors and their surface expression (Huganir et al., 1986; Rudell et al., 2020). Given the complex nature and lack of a detailed understanding of pLGIC folding, assembly and transport, it is highly likely that different subunit and receptor types are under different expression mechanisms.

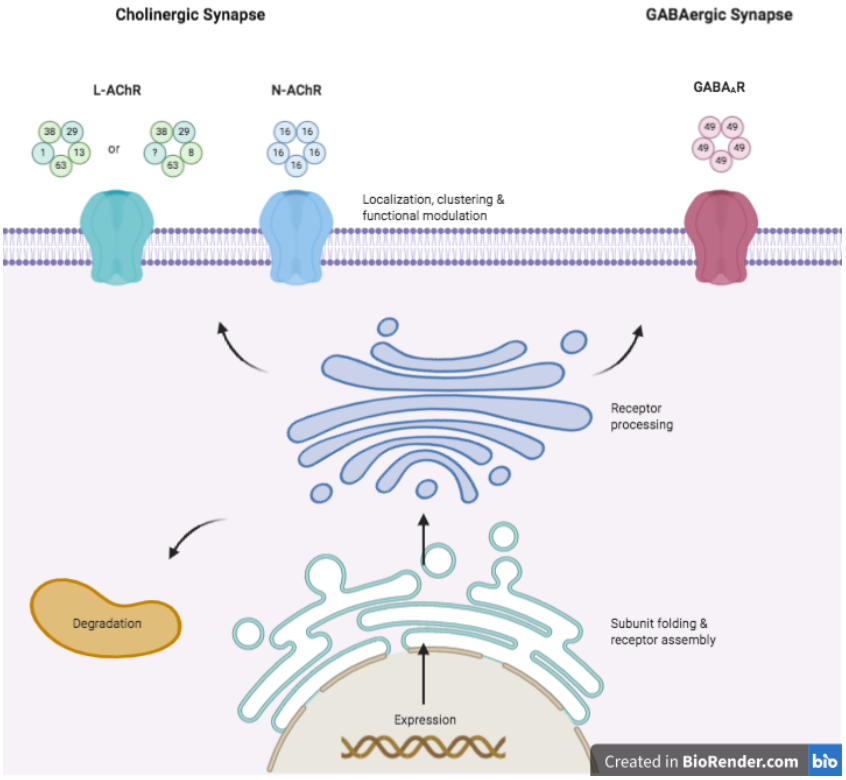

Figure 7. General expression and trafficking of nematode muscle receptors.

Subunit genes are transcribed in the nucleus and translated in the ER.Within the ER accessory proteins (RIC-3, NRA-2, NRA-4, EMC-6 & UNC-74) help fold nascent subunits and assemble them into pentamers. Receptors are then transported to the golgi for processing (accessory protein UNC-50 acts here) and finally sent to the membrane surface where they are acted upon by proteins that modulate their functional properties (MOLO-1). Misfolded subunits/ pentamers are degraded to the lysozyme. Accessory proteins relevant to this thesis are mentioned. Image made in BioRender.

1.6.1 Subunit folding, stability and assembly in the ER

Subunits are synthesized in the ER and must be stabilized and come together in a complex before leaving the ER. Many APs function at this level. Appropriate subunit folding within the ER is critical with misfolded proteins targeted for degradation (Green & Wanamaker,

1997). Disulfide bonds, formed in the ER, are important for pLGIC structure and function (Green, 1999). At least two disulfide bond isomerases assist in their formation. For the *C. elegans* L-AChR, these are UNC-74 and CRELD-1A (Ballivet et al., 1996; Boulin et al., 2008; D'alessandro et al., 2018; Haugstetter et al., 2005; Lewis et al., 1980b).

Newly synthesized proteins acquire their final, stabilized structure over time. During this period, RIC-3 plays a critical role in both invertebrate and vertebrate receptors (Halevi et al., 2002). *C. elegans* RIC-3 is an ER resident protein with two predicted transmembrane domains and an intracellular coiled-coil C-terminal domain (Halevi et al., 2003). Both of these regions physically interact with, and are required for, stabilizing immature nematode nematode AChR subunits (Ben-Ami et al., 2005, 2009; Yoav Biala et al., 2009). Apart from a short region in the ICL of serotonin receptors (Nishtala et al., 2014, 2016), no other regions have been identified that interact with RIC-3. RIC-3 is unique from other APs in its ability to regulate different pLGIC receptors types (serotonin vs ACh). Furthermore, different *ric-3* isoforms have been found to affect AChR responses differently (Bao et al., 2018) and show distinct subcellular localization (Cheng et al., 2007). RIC-3 binds to a pre-assembled subunit in a one-to-one ratio, and promotes assembly by participating in homotypic interactions with other RIC-3 that are also bound to subunits (Wang et al., 2009). EMC-6 is another ER transmembrane-associated protein involved in subunit stabilization during receptor maturation and assembly (Richard et al., 2013). Its knock-out in *C. elegans* led to decreased responses from all three NMJ receptor subtypes and is likely to have a broad function regulating the assembly of many receptor types (Richard et al., 2013). EMC-6 acts in a complex with multiple other proteins ensuring the appropriate folding and insertion into the membrane (Bai et al., 2020; Richard et al., 2013), the other proteins in this complex have not been explored in *C. elegans*.

Once folded, subunits are assembled into their pentameric forms in the ER over a period of several hours (Green & Claudio, 1993). Formation of pentameric heteromeric receptors is slow and inefficient. As little as 5% and as much 30% of individual subunits synthesized are incorporated into complete pentamers (Gu et al., 1991a; Gu et al., 1991b; Merlie & Lindstrom, 1983). The N-AChR and L-AChR in *C. elegans* are expressed in the same tissue and synapse and will therefore interact with a common pool of accessory proteins involved in this process (Ballivet et al., 1996; Lewis et al., 1980a; Lewis et al., 1980b; Touroutine et al., 2005, 2004). Indeed, RIC-3 that is required for both, is bound to subunits at least at the beginning of the

assembly process (Wang et al., 2009). Additional assembly proteins involved in nematode pLGICs include NRA-2 and NRA-4 that form direct interactions with subunits and create a "nucleation center" to promote subunit oligomerization (Almedom et al., 2009). In the absence of these proteins, receptors display altered kinetics and the homomeric ACR-16 formed heteromeric complexes with L-AChR subunits, and the L-AChR composition was changed (Almedom et al., 2009). They may act by preventing L-AChR subunits from forming heteromeric receptors with ACR-16 (Almedom et al., 2009). Recently, NRA-2 has been found to affect the subunit composition of L-AChR *in vivo* upon exposure to levamisole and is thus thought to play a role in the "plasticity" of receptor composition (Kashyap et al., 2021).

What determines subunit arrangement and compatibility? What makes a homomeric receptor versus a heteromeric receptor; is it simply direct structural incompatibilities in the subunits themselves, or is it a different synthesis pathway/interaction with APs that keep them separate? Or both? The L- and N-AChRs are good examples to study this process because both respond to the same ligand in the same synapse and share at least some of the same accessory proteins.

1.6.2 Receptor trafficking and modification through the Golgi and modulation at the synapse

Post-translational processing in the Golgi produces mature receptors that are sent to the surface membrane. UNC-50 is the only Golgi protein known to be involved in *C. elegans* body wall muscle receptors. UNC-50 is a large membrane protein with widespread conservation across eukaryotes that is required for expression of the L-AChR in both *X. laevis* oocytes and *C. elegans* (Boulin et al., 2008; Eimer et al., 2007). UNC-50 likely regulates cargo transport pathways and in its absence, receptors are sent to the lysosome for degradation (Eimer et al., 2007).

The intricate processing involved in synthesizing receptors is a means to an end, with the end goal of producing a protein complex that can quickly and efficiently transmit the neuron chemical signal into a muscle response. Once receptors have reached the synapse, they are still acted upon by auxiliary proteins that modulate their functional properties. MOLO-1 remains the identified auxiliary protein for these three receptors in *C. elegans* (Boulin et al., 2012). MOLO-1 is thought to increase the open probability of the L-AChR, thereby enhancing the response of the

muscle to a constant amount of neurotransmitter (Boulin et al., 2012), yet it has no effect on the ACR-16 receptor.

The pLGIC neurotransmitter receptors have been characterized in great detail, from their structure, ligand binding and gating mechanics. This has been based on research focusing primarily on the receptors of a few species leading to a relatively static picture of their properties. One aspect that has been little studied is the regulation of receptor composition and subunit position. The origin of diversity within the pLGIC family in early animals and the changes that occur within and between species of nematodes suggest that similar processes are involved in both phenomena.

1.7 Identification of *unc-29, acr-8, acr-13, unc-38* and *unc-63* duplications as models for subunit interactions and composition and the alpha- non-alpha switch

Three other nematode L-AChRs have been reconstituting in *Xenopus laevis* oocytes; *H. contortus, A. suum,* and *O. dentatum* (Boulin et al., 2011; Buxton et al., 2014; Williamson et al., 2009). The genomes of *H. contortus* and *O. dentatum* do not encode an ortholog of *acr-13* (Beech & Neveu, 2015; Boulin et al., 2011; Buxton et al., 2014; Coghlan et al., 2019). They do retain the closely related *acr-8*, that can form a functional L-AChR in combination with *unc-38, unc-63* and *unc-29* (Boulin et al., 2011; Buxton et al., 2014). This demonstrates flexibility in composition between closely related species. In fact, both these species can form functional L-AChRs with fewer subunit types within each species. This implies that at least one of the subunits must be present twice to produce a pentamer and they can therefore occupy more that one different position.

For example, the closely related *Trichonstrongylid H. contortus* L-AChR lacks a LEV-1 subunit (Boulin et al., 2011). Many recent duplications of the non-alpha *unc-29* are found in the *Strongyloid* worms (Duguet et al., 2016). *H. contortus* has four full length copies of the non-alpha subunit with each copy functionally diverging (Duguet et al., 2016). The first *H. contortus* (Hco) L-AChR (Hco-L-AChR) to be reconstituted in oocytes required subunits ACR-8, UNC-38, UNC-63, and UNC-29.1 and accessory proteins RIC-3, UNC-50, and UNC-74 (Boulin et al., 2011). This confirmed first, that the LEV-1 subunit does not contribute to the Hco-L-AChR in oocytes and that UNC-29.1 can function as the only non-alpha subunit in the receptor; a striking

difference to the Cel-LAChR (Figure 8) (Boulin et al., 2008). Second, this confirmed that both L-AChRs require the same three accessory proteins and are thus controlled by similar regulatory mechanisms. Further work on the *H. contortus* receptor showed that three of the four *unc-29* copies produced functional channels, but the UNC-29.2 copy did not (Duguet et al., 2016). When the Hco-unc-29.2 subunit replaced Cel-unc-29 in the Cel-L-AChR, a functional channel was measured (Figure 8C) (Duguet, 2017). Therefore the subunit is inherently functional, but cannot act as the only non-alpha subunit in the receptor. Substitution rates measured along the branches of the *unc-29* subunit family predicted this functional change of divergence occurring at each duplication event (Duguet et al., 2016). This represents an example of a non-alpha subunit meditating the requirement of another non-alpha subunit.

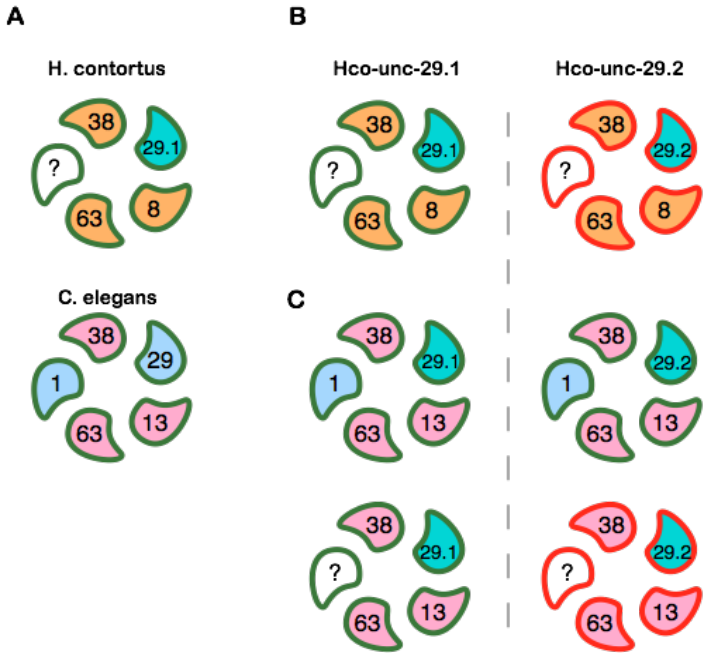

Figure 8. Functional divergence of *H. contortus unc-29* paralogs.

(A) The subunit arrangement proposed by T. Duguet for the *H. contortus* and *C. elegans* L-AChR. (B) In the *H. contortus* receptor, the non-alpha Hco-unc-29.1 subunit is able to contribute to a functional receptor and Hco-unc-29.2 subunit cannot.
(C) In the *C. elegans* receptor, Hco-unc-29.1 can form a functional receptor with and without LEV-1, but Hco-unc-29.2 needs LEV-1 to contribute to a functional receptor.
H. contortus alpha subunits in orange and non-alpha subunits in teal. *C. elegans* alpha subunits in pink and non-alpha subunits in blue. Red outline shows nonfunctional receptor, green outline shows functional receptor. Question mark indicates unknown subunit that replaces LEV-1. Adapted from Duguet, (2017); Duguet et al., (2016).

A second functional difference observed after a gene duplication event is that of *acr-8* and *acr-13*. The alpha-subunit *acr-13* has been lost from the *H. contortus* genome and is replaced by the paralogous *acr-8* in the Hco-L-AChR (Boulin et al., 2011). The Hco-LAChR does not require LEV-1 when it has ACR-8 a phenomenon shared by a *C. elegans* L-AChR where ACR-8 replaces ACR-13 (Figure 9) (Blanchard et al., 2018). Therefore the ability to produce a functional channel without LEV-1 is shared amongst ACR-8 subunits. This represents an alpha subunit regulating the requirement of a non-alpha subunit.

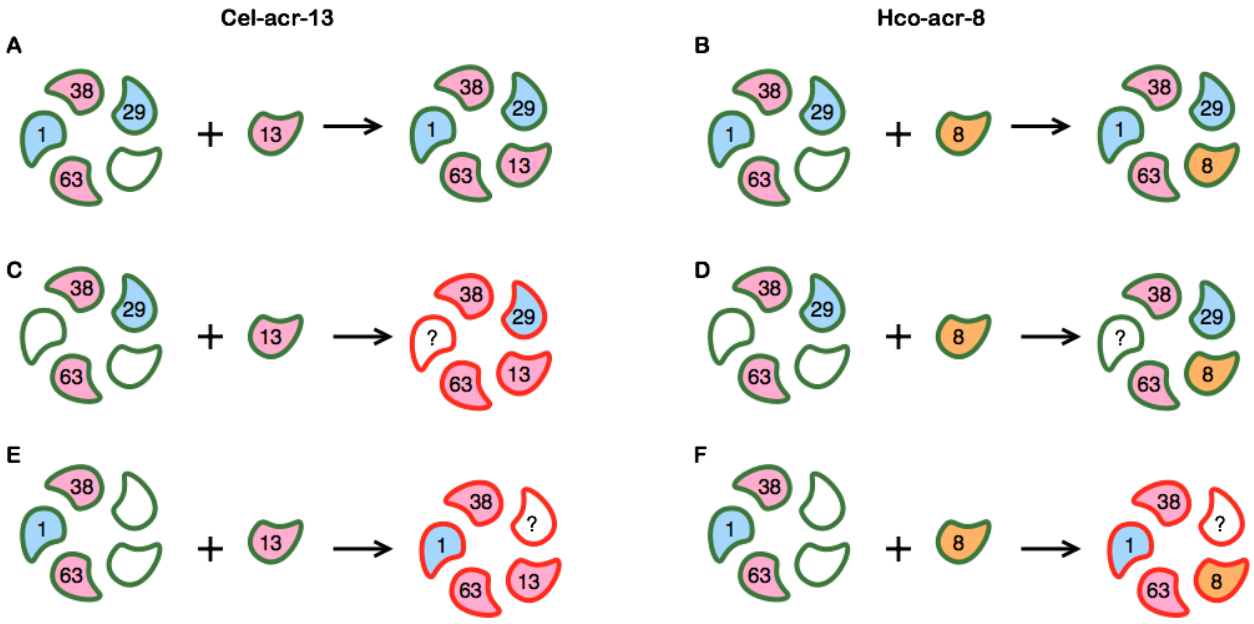

Figure 9. Functional divergence of *H. contortus acr-8* and *C. elegans acr-13* subunits.
(A) *C. elegans* acr-13 produces a functional receptor with unc-29 and lev-1. (B) *H. contortus* acr-8 can replace acr-13 in the *C. elegans* receptor to produce a functional receptor with both unc-29 and lev-1. (C) *C. elegans* acr-13 cannot produce a functional receptor when lev-1 is removed; (D) *H. contortus* acr-8 can produce a functional receptor when lev-1 is removed. (E) *C. elegans* acr-13 cannot produce a functional receptor when unc-29 is removed; (F) *H. contortus* acr-8 cannot produce a functional receptor when unc-29 is removed. *H. contortus* acr-8 subunit in orange and *C. elegans* subunits in blue and pink. Red outline depicts nonfunctional receptor, green outline depicts functional receptor. Adapted from Blanchard et al., (2018); Boulin et al., (2011); Boulin et al., (2008).

In vivo recordings from different *C. elegans* strains further explored functional diversity of this receptor. No levamisole-sensitive channel was recorded from *unc-29, unc-38*, or *unc-63*

knock-out strains (Culetto et al., 2004; Lewis et al., 1980a; Lewis et al., 1980b), evidence that they are essential to the L-AChR. *Acr-13* knock-out worms exhibited functional receptors but with severely altered kinetics, suggesting this subunit not essential but preferentially used in the native receptor (Hernando et al., 2012; Lewis et al., 1980a; Lewis et al., 1980b). *Acr-8* knock-out worms did not exhibit any loss of levamisole-sensitivity (Hernando et al., 2012; Touroutine et al., 2005; Towers et al., 2005), therefore it is not an essential component to the receptor. However, it is able to replace its paralog *acr-13* (Blanchard et al., 2018). *Lev-1* knock-out worms had measurable, but diminished, responses to LEV (Culetto et al., 2004). Taken together, these results indicate that the preferential Cel-L-AChR contains alpha subunits ACR-13, UNC-38, and UNC-63, and non-alpha subunits LEV-1 and UNC-29. However, this is not absolute, because ACR-8 can replace ACR-13, and LEV-1 can be omitted (and replaced with an unknown subunit) (Blanchard et al., 2018). This *in vivo* work, along with the *in vitro* oocyte expression studies stresses the dynamic nature of this channel. It is unclear what subunit replaces LEV-1 when it is omitted from these receptors, and, what regions in the UNC-29.1 allows it function without LEV-1. These examples provide a model where non-alpha subunits differ in their requirement for another non-alpha subunit and alpha-subunits also differ in their requirement for the same non-alpha subunit. Since we know that subunit interaction is essential for this phenomenon, they may represent the different sides of this interaction.

The L-AChR subunit genes from other worms have been explored. Interestingly, the Clade III nematodes have lost all non-alpha subunits (*lev-1, acr-2,* and *acr-3*) and only kept *unc-29* (Beech & Neveu, 2015; Coghlan et al., 2019; Williamson et al., 2007). They also share duplications of the two alpha subunits, *unc-38* and *unc-63*. In some *Onchocerca* species the second copy of each have lost the YXCC motif that defines an alpha subunit (Beech pers comm). This represents an experimental opportunity to investigate a potential alpha- non-alpha switch and accompanying change in position within the receptor. It would also allow a determination of what causes a non-alpha subunit to assume that functional role as opposed to the alpha subunit motif that appears to be only diagnostic.

In situ hybridization expression studies found expression of *unc-29, unc-38* and *unc-63* in body wall muscle of the Clade III *Brugia malayi* worm (Li et al., 2015), but which duplicate copy of *unc-38* or *unc-63* is not known since the authors were not aware two copies exist. As well *B. malayi* muscle recordings identified *in vivo* receptors sensitive to cholinergic compounds

(Kashyap et al., 2021; Verma et al., 2017). The exceptional quality of the *B. malayi* genome allows us to reliably identify all potential AChR subunit genes candidates for cloning (Howe et al., 2016, 2017). Therefore, *B. malayi* is an ideal worm to investigate the potential alpha to non-alpha subunit type change. As well, reconstituting the first filarial L-AChR in *X. laevis* oocytes would allow for the investigation of other filarial worm L-AChRs.

1.8 Remaining questions and common themes

Studying how pLGIC receptors change will reveal details of their interactions with each other and with their synthesis machinery. In order to achieve this, specific examples are needed which can be found by mining the genome data from the 50 HGI to identify subunit duplication events followed by functional characterization using electrophysiology (Coghlan et al., 2019; Howe et al., 2016, 2017). The focus of this thesis was to examine the regulation of subunit interactions within the *C. elegans* L-AChR as a model for this process in general. An evolutionary approach was used to reveal details of the mechanism by examining recent subunit duplications that have led to altered interaction between subunits and the accessory protein network that influences production and assembly of these receptors.

The first objective was to identify the subunit that replaces *lev-1* in the *C. elegans* L-AChR and identify the regions in the non-alpha (*unc-29.1*) subunit that allows it to contribute to a functional receptor without *lev-1*. A major objective at the outset was the characterization of the reconstituted *B. malayi* L-AChR. This proved, unexpectedly, to be impractical since no response to various expected agonists was observed. The examination of why this failed led to a change in focus for the thesis, a detailed investigation of changes of the N-AChR in the Clade III nematodes. During this analysis one of the Clade III N-AChRs no longer required any RIC-3 accessory protein. This was unexpected because all known N-AChRs require RIC-3 (Abongwa et al., 2016; Ballivet et al., 1996; Charvet et al., 2018; Choudhary et al., 2019; Hansen et al., 2021; Kaji et al., 2020). A final project was then undertaken to identify the sequence determining a subunits requirement for the accessory protein.

This work has shown that sequences within subunits influence their ability to combine with others into a functional receptor, they can also influence the compatibility of other subunits. The failure to reconstitute a functional *B. malayi* receptor lies in production of the receptor, likely through an altered interaction with the AP network since the addition of additional APs produced small currents. Finally, the identification of a single amino acid in an AChR that

determines RIC-3 requirement is novel and confirms that AP requirement can be both extreme and complex. In conclusion, the nematode pLGICs represent ideal models for studying receptor functional change. Although identifying subunit sequences is important, consideration should be given to the AP network since the receptors do not work in isolation and APs can completely determine receptor function.

Hypothesis and Specific Aims

My hypothesis is that non-alpha subunits within a heteromeric receptor play an essential structural role and at least two must be present. For instances where a non-alpha subunit is no longer required, another non-alpha subunit will take its place. Loss of non-alpha subunit genes may lead to duplication and functional adaptation of an alpha-subunit to become non-alpha. This regulation of receptor composition and arrangement will be influenced by the accessory protein network and these interactions may also change as a result.

Objective 1. Identification of the subunit replacing LEV-1 and sequences responsible.

Identification of the subunit that replaces the non-alpha lev-1 subunit, followed by identification of the regions that determine unc-29.1 ability to produce a functional levamisole-sensitive acetylcholine receptor (L-AChR) without lev-1. First, a series of dimers was carried out to identify the lev-1 replacing subunit. Second, identification of the regions in UNC-29.1 and UNC-29.2 subunits that determine their requirement for the LEV-1 subunit was achieved using chimeric exchange between the paralogs. Objective 1 is covered in Chapter 2.

Objective 2. Characterize changes in Clade III unc-38 and unc-63 duplications associated with a subunit switch to non-alpha.

Characterize the signature of selective pressure present in the filarial nematode UNC-38 and UNC-63 paralogous copies. First, a bioinformatic analysis of substitution rates was carried out on these two subunit genes. Second, efforts to reconstitute the L-AChR from *Brugia malayi* to evaluate the different functional properties of the UNC-38.1/UNC-63.1 subunits compared to the UNC-38.2/UNC63.2 subunits were attempted. Objective 2 is covered in Chapter 3.

Objective 3. Characterize the inability to reconstitute *B. malayi* AChRs in oocytes.

The inability to produce any *B. malayi* receptor in Objective 2 indicated a change occurred in later Clade III receptors preventing their *ex vivo* functional reconstitution. This problem was thus investigated further to identify and characterize the source of this change. ACR-16 was used because it is a homomeric receptor previously characterized from the earlier Clade III worm *Ascaris suum*. ACR-16 from intermediate species between *A. suum* and *B.*

malayi, *Dracunculus medinensis, Gonglyonema pulchrum,* and *Thelazia callipaeda* were used to track the changes. Pharmacological characterization and responses with different accessory protein mixtures was carried out. Objective 3 is covered in Chapters 4 & 5.

Objective 4. Identification of the sites mediating a RIC-3 requirement for ACR-16

The observation in Objective 3 that the intermediate species *D. medinensis* no longer requires RIC-3 for oocyte function was unexpected. The high sequence similarity between ACR-16s indicates it is determined by few amino acids. A fourth and final objective was included to identify the sequence mediating ACR-16 requirement for RIC-3. A series of chimeras and site-directed mutagenesis was used between *A. suum* and *D. medinensis acr-16.* Objective 4 is covered in Chapter 6.

Chapter 2: Clade V levamisole-sensitive acetylcholine receptor

2.1 Introduction

The levamisole-sensitive acetylcholine receptor (L-AChR) of the free-living model nematode *Caenorhadbitis elegans* has been the focus of research into development of neuromusculature for the past 40 years and is particularly suited as an ideal model for the study of functional change following gene duplication and loss events. The *C. elegans* L-AChR can exist in two forms, the first contains five different subunits ACR13, UNC-38, UNC-63, UNC-29 and LEV-1, the second can be formed by replacing ACR-13 with its paralog ACR-8, from either *C. elegans* or the closely related *Haemonchus contortus* (Figure 9) (Blanchard et al., 2018; Boulin et al., 2008). The second no longer requires LEV-1, demonstrating an evolved functional difference between these two subunits. The non-alpha subunit gene of the *C. elegans* L-AChR, *unc-29*, has duplicated within the closely related trichostrongylid parasites into four copies (Duguet et al., 2016). While their response to various agonists and antagonists are broadly similar, UNC-29.1, UNC-29.3 and UNC-29.4 can all contribute to reconstitute functional receptors, even when ACR-13 is present, acting as the only non-alpha subunit. UNC-29.2 cannot do this, another example of a functional change associated with duplication (Figure 8) (Duguet et al., 2016). In both of these cases, the functional characteristics of the receptors are broadly similar. The differences are seen in how their subunits interact. Two questions immediately arise from these observations. First, when ACR-8, replaces ACR-13 in the Cel-L-AChR, which subunit is present twice? Second, what sequence mediates the difference between UNC-29.1 and UNC-29.2 in terms of their requirement for LEV-1.

In vertebrate acetylcholine receptors (AChRs) that contain both alpha and non-alpha subunits, there are at least two alpha subunits separated by another subunit. This configuration is consistent with the asymmetrical binding of two acetylcholine (ACh) molecules in non-adjacent binding sites that is thought to promote channel opening (Mowrey et al., 2013). We have no reason to believe that nematode receptors are different in this regard. In the L-AChR subunit phylogeny, non-alpha and alpha subunits were the first functional types to diverge (Figure 2C) (Beech & Neveu, 2015; Dent, 2006), suggesting that this is, perhaps, the most important structural feature for heteromeric receptors. Later duplications led to further specialization within

each of these clades (for example Duguet et al., 2016). Based on this it seems most likely that LEV-1 is replaced by the other non-alpha subunit, UNC-29 in its absence.

A previous study found that the LEV-1 subunit occupies the space between UNC-38 and UNC-63 in the Cel-L-AChR (Duguet, 2017). This was achieved using subunits joined into a single polypeptide by removing the stop codon from the first subunit, the signal peptide from the second and then fusing the two into a single transcript. Using short amino acid sequences to link subunits together is commonly used to determine subunit placement or express channels in defined stoichiometry (Carbone et al., 2009; Groot-Kormelink et al., 2006; Zhou et al., 2003). The limitation with linkers is that its length must be optimized to ensure that it does not create structural constraints in the final receptor nor allow other subunits to "sit" between the two linked subunits (Liao et al., 2020, 2021). In this case, the linker between the two is sufficiently short that the subunits are required to be adjacent in the final receptor and produced receptors with robust responses (Duguet, 2017). The only dimers able to produce a functional receptor were UNC-38:LEV-1 and LEV-1:UNC-63 and only the trimer UNC-38:LEV-1:UNC-63 was functional. If UNC-29 is able to replace LEV-1 when ACR-8 is present, then a dimer of UNC-38:UNC-29 should produce a functional receptor only when ACR-8 is present. This would confirm that UNC-29 indeed replaces LEV-1.

To identify regions in UNC-29.1 and UNC-29.2 that mediate their different abilities to produce receptors without LEV-1, chimeras were used where specific regions were exchanged between subunits, a common technique in ion channel research (Duret et al., 2011; Ghosh et al., 2017; Martinez-Torres, 2000). The differences between these subunits' abilities to form functional receptors with and without LEV-1 likely involves large, variable structural regions since it must lead to dramatically different inter-subunit interactions. Therefore, the chimeras exchanged the most variable region in the subunit sequences, the intracellular loop (ICL) (Langlhofer & Villmann, 2016). If the ICL does mediate the differences in ability to produce functional receptors without LEV-1, then that phenotype would follow the loop when it is exchanged.

2.2 Results

2.2.1 Dimers

Representative recordings of the different dimer combinations in response to 100 μM ACh and levamisole (LEV) are shown in Figure 10. The UNC-38:LEV-1 dimer, in the presence of UNC-63, UNC-29 and ACR-13 as monomers produced a functional receptor (Figure 10A), reproducing the original result and confirming subunits as dimers remain functional. Replacing UNC-38:LEV-1 with UNC-38:UNC-29 (Figure 10C) produced no significant ACh induced current consistent with UNC-29 being unable to replace LEV-1 in the presence of ACR-13. Expectedly, removing free UNC-29 from this combination (Figure 10E) produced no response. UNC-38:UNC-29 in the presence of ACR-8 produced a functional receptor (Figure 10D) confirming that indeed, UNC-29 can physically replace LEV-1 in between UNC-38 and UNC-63. ACR-8 mediates this despite having no physical contact with the position that changes. In addition, no receptor was produced when the free UNC-29 was removed (Figure 10F), meaning that UNC-29 is the subunit that is present twice when ACR-8 is present. This also confirms that the UNC-29 subunit physically linked with UNC-38 is unable to function independently and contribute only the UNC-29 subunit to the receptor. Interestingly, UNC-38:LEV-1, with free UNC-29 in the presence of ACR-8 produced a robust ACh induced current (Figure 10B). This would imply that the specificity for LEV-1 in between UNC-38 and UNC-63 is relaxed in the presence of ACR-8, not that the requirement for that position changes to UNC-29.

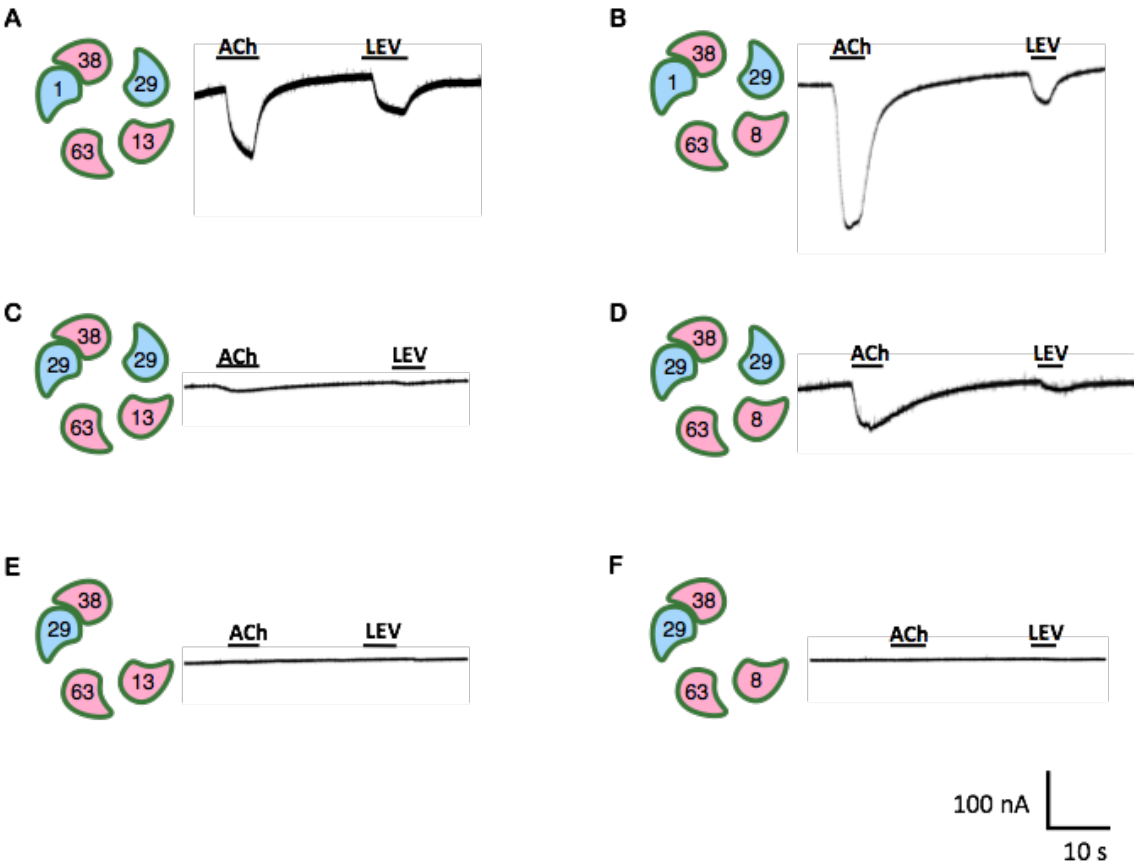

Figure 10. Unc-29 is present twice in the functional receptor without lev-1.

A series of dimers (two subunits physically linked with a short linker sequence) and monomer conditions were used to identify the subunit that replaces LEV-1 when ACR-8 is present. Representative recordings are shown with the respective dimer-monomer conditions to 100 µM ACh and LEV. Dimers are shown as two subunits touching each other and monomers are shown as individual subunits. Non-alpha subunits in dark blue and alpha subunits in light blue. (A) UNC-38:LEV-1 dimer positive control with ACR-13; (B) UNC-38:LEV-1 dimer positive control with ACR-8; (C) UNC-38:UNC-29 dimer with ACR-13 shows little to no response; (D) UNC-38:UNC-29 dimer with ACR-13 shows dampened but consistent responses; (E) UNC-38:UNC-29 dimer with ACR-13 but omitting UNC-29 has no response; (F) UNC-38:UNC-29 dimer with ACR-8 but omitting UNC-29 has no response. See Figure 11 for average responses. Subunit positioning inferred from, and dimers used from Duguet, (2017).

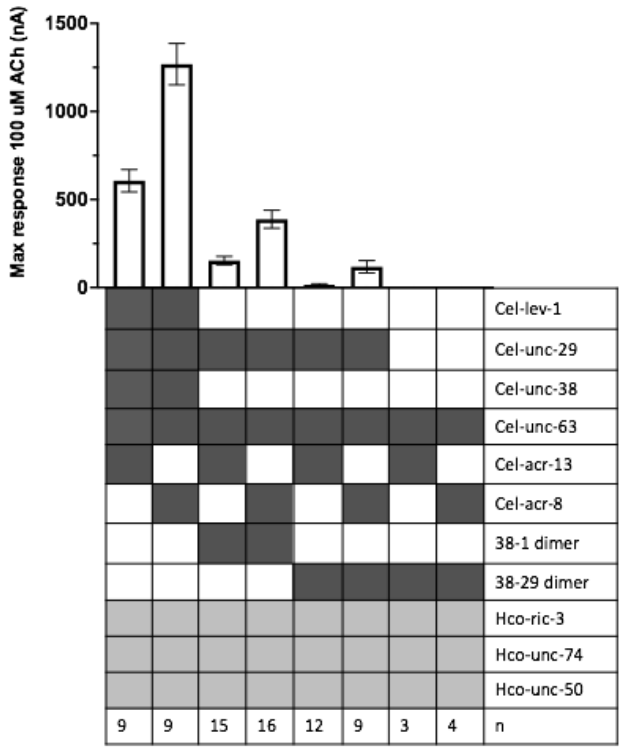

Figure 11. Unc-29 is present twice in the functional receptor without lev-1.
A series of dimers (two subunits physically linked with a short linker sequence) and monomer conditions were used to identify the subunit that replaces LEV-1 when ACR-8 is present. Responses to 100 µM ACh are shown. The UNC-38:UNC-29 dimer was functional without LEV-1 in the presence of ACR-8 but not ACR-13. The absence of response when the unc-29 monomer was omitted (rightmost column) confirms that unc-29 replaces LEV-1 and is present twice in the receptor. Example recordings shown in Figure 10. Error represents standard error. See Appendix Table 9 for values.

2.2.2 Non-alpha subunit sequence mediating position specificity

An L-AChR containing ACR-13 and Hco-UNC-29.2 requires LEV-1, whereas one containing Hco-UNC-29.1 does not (Figure 8) (Duguet, 2017; Duguet et al., 2016). The functional difference must have occurred since their duplication. In order to identify the region in UNC-29 that mediates its ability to occupy both non-alpha subunit positions within the receptor, chimeras exchanging the intracellular loop between *unc-29.1* and *unc-29.2* were made as shown in Figure 12. Chimera-1 has the *unc-29.1* sequence with the intracellular loop of *unc-29.2*, and Chimera-2 has the *unc-29.2* sequence with the intracellular loop of *unc-29*.

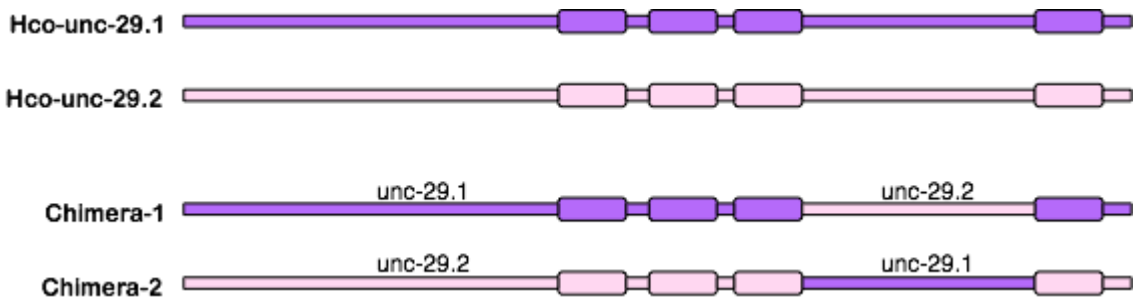

Figure 12. Chimeras for the Hco-unc-29 duplication.

Chimeras were made between *H. contortus* unc-29.1 and unc-29.2 by exchanging the intracellular loop to identify the region mediating the ability of unc-29.1 to function as the only non-alpha subunit in the receptor. Chimera-1 has the unc-29.1 sequence with the intracellular loop of unc-29.2, and Chimera-2 has the unc-29.2 sequence with the intracellular loop of unc-29.1. Responses of these chimeras are shown in Figures 13 & 14.

UNC-29 chimeras were expressed with combinations of other subunits to evaluate their requirement for LEV-1. Chimera-1 behaved as UNC-29.2, requiring LEV-1 in either the *C. elegans L-AChR* (Figure 13C) or the *H. contortus* L-AChR (Figure 13E). Chimera-2 behaved as UNC-29.1, not requiring LEV-1 in either the *C. elegans* L-AChR (Figure 13D) or the *H. contortus* L-AChR (Figure 13F). Select recordings of the chimera combinations are shown in Figure 13 and averaged responses in Figure 14. These results suggest the intracellular loop is responsible for a majority of the phenotype differences and is a region that is critical in determining subunit compatibility and positioning within a receptor.

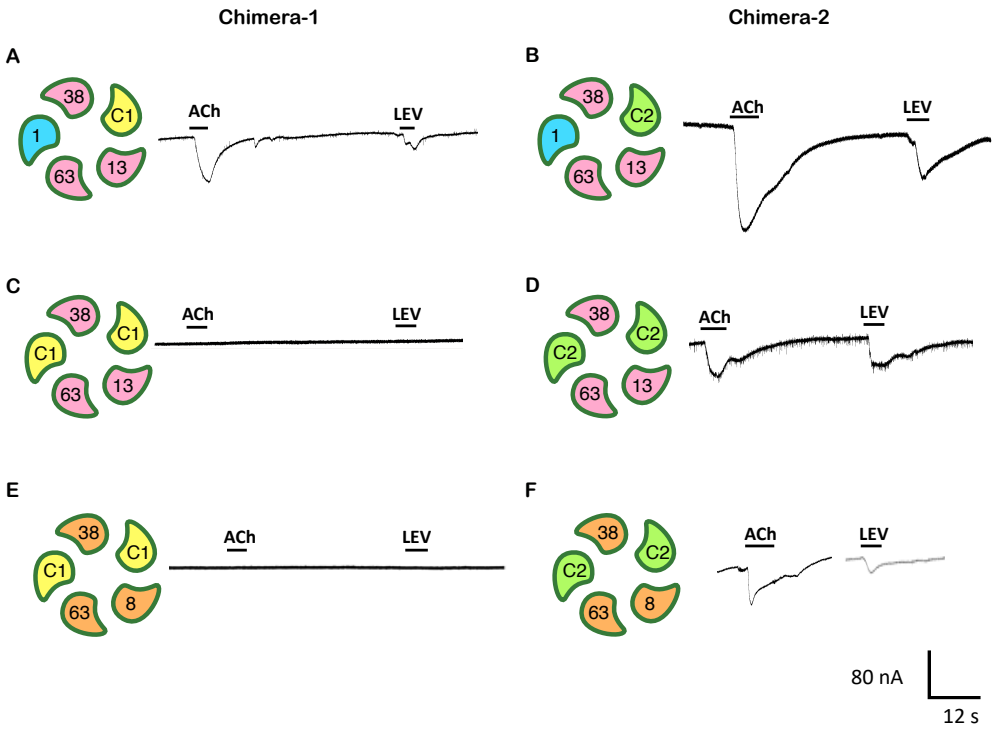

Figure 13. Unc-29 chimera responses in the L-AChR.

Representative recordings of unc-29 chimeras are shown in response to 100 µM ACh and LEV. Chimeras were made between *H. contortus unc-29.1* and *unc-29.2* by exchanging the intracellular loop to identify the region mediating the ability of unc-29.1 to function as the only non-alpha subunit in the receptor. C1 = Chimera-1, C2 = Chimera-2. (A, B) Both chimeras were functional in the L-AChR, confirming that the exchanged ICLs do not render the chimeras nonfunctional. (C) Chimera-1 was no longer functional without LEV-1. (D) Chimera-2 was functional without LEV-1. (E) Chimera-1 was not functional in the *H. contortus* L-AChR. (F) Chimera-2 was functional in the *H. contortus* L-AChR. The ICL, therefore, mediates the ability of unc-29.1 to function as the only non-alpha subunit. See Figure 12 for schematic of chimeras and Figure 14 for average responses, and Appendix Table 10 for values.

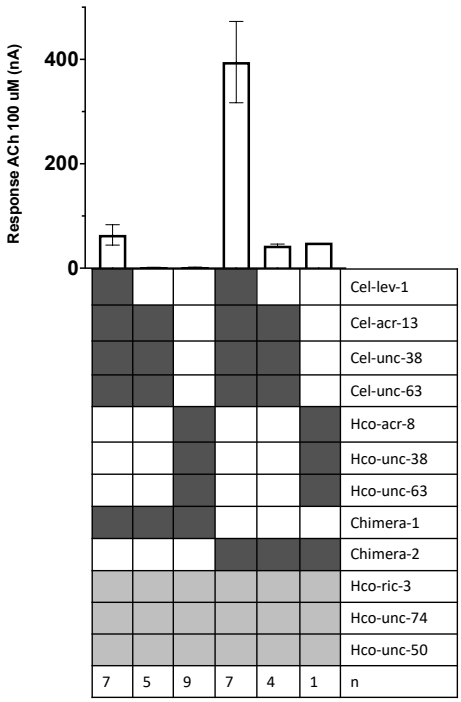

Figure 14. Chimera-1 and Chimera-2 responses in the L-AChR.

Responses of unc-29 chimeras in response to 100 µM ACh. Chimeras were made between *H. contortus unc-29.1* and *unc-29.2* by exchanging the intracellular loop to identify the region mediating the ability of unc-29.1 to function as the only non-alpha subunit in the receptor. Both chimeras were functional in the L-AChR, confirming that the exchanged ICLs do not render the chimeras nonfunctional. Chimera-001 was not functional in the *C. elegans* L-AChR without LEV-1 nor in the *H. contortus* L-AChR. Chimera-002 was functional in the *C. elegans* L-AChR without LEV-1 and in the *H. contortus* L-AChR. The ICL therefore mediates the ability of unc-29.1 to function as the only non-alpha subunit. See Figure 12 for schematic of chimeras and Figure 13 for representative recordings. See Appendix Table 10 for values. Error bars represent standard error.

2.3 Discussion

Two duplications producing four L-AChR subunit genes were investigated in this Chapter. These include the duplication of *H. contortus unc-29* and the duplication that gave rise to *acr-13* and *acr-8*. These duplication events represent different aspects of functional change that occur within a heteromeric receptor. The two different UNC-29 copies differ in their ability to occupy the space between the UNC-38 and UNC-63 subunits. The ACR-8 and ACR-13 subunits differ in their ability to relax specificity for the LEV-1 space. Interestingly, it achieves this without contacting LEV-1 directly in the mature receptor.

2.3.1 Unc-29 replaces lev-1 in the L-AChR

Previous work identified functional differences in ACR-8 and ACR-13 in their abilities to contribute to a functional receptor without LEV-1 (Blanchard et al., 2018; Boulin et al., 2008). Since only four subunits were required without LEV-1, it was not clear which of these was present twice. The fact that UNC-29 and LEV-1 are more closely related phylogenetically (Figure 2C) and the structural and functional importance associated with having two non-alpha subunits in the receptor suggests that UNC-29 is likely the subunit that is present twice and replaces LEV-1. In order to determine this, a series of combinations containing subunits fused together into a concatemer were used. The dimers used had been previously constructed and used to determine the relative positions of three subunits of the Cel-L-AChR in the order UNC-38:LEV-1:UNC-63 (Duguet, 2017). Results from these dimers confirm that receptors reconstituted with the UNC-38:LEV-1 dimer do not differ from receptors where all five individual subunits are present (Duguet, 2017). Receptors produced only very small responses when UNC-29 was physically linked to UNC-38 in the presence of ACR-13, but produced robust responses in the presence of ACR-8 (Figure 10 C & 10 D). In the presence of ACR-13, the small currents were reminiscent of some efforts to reconstitute the L-AChR with missing subunits and are likely an artefact of the *ex vivo* expression system. It may be that the physical link retaining UNC-29 with UNC-38 partly bypasses the normal assembly process. Previous work suggests that the subunits UNC-38, LEV-1 and UNC-63 co-assemble as a first step in receptor assembly and that the subunits ACR-13 and UNC-29 are then added sequentially to this complex (Duguet, 2017). If this is the case, then the specificity for LEV-1 is conferred only after the initial trimer is formed. The fact that the UNC-38:UNC-29 dimer produces smaller maximal currents than UNC-38:LEV-1 when ACR-8 is present may suggest an initial preference for the LEV-1 subunit in the initial trimer. The specificity conferred by ACR-13 may be either the production of a non-functional complex with two UNC-29 subunits present, or preferential degradation before localization to the cell surface. Regardless, the ACR-13 subunit achieves this without direct contact with the position of LEV-1 in the receptor. This mechanism is likely different from the ability of Hco-UNC-29.1 to remove the requirement for LEV-1. Further work using dimers that physically link Hco-UNC-38:Hco-UNC-29.1 would confirm this.

The use of linkers to ensure two subunits to occupy defined positions within a receptor is a commonly used, powerful tool to determine subunit stoichiometry (Carbone et al., 2009;

Groot-Kormelink et al., 2006; Zhou et al., 2003). However, some reports show that this may not be a reliable method because short linkers may induce steric hindrance that interferes with subunit folding whereas long linkers may allow others subunits to be inserted between the two linked subunits (Liao et al., 2020, 2021). Computer modelling suggested that the linker between subunit dimers here would not be compatible if their positions were reversed and were too short to allow a subunit to intervene (Dr. Beech pers comm). Here, dimers produced functional receptors, so the dimer did not block function by steric hindrance, however in some cases had dampened responses (Figure 11). Combinations that were functional with two copies of UNC-29 produced no response when the individual 29 was absent but the UNC-38:UNC-29 dimer was. This confirmed that when UNC-29 is in a dimer it cannot function as a single monomer. Other methods exist that could provide independent support for the conclusions here. These include, physically linking adjacent subunits with much shorter cysteine bridges (Hanson & Czajkowski, 2011) or single channel patch clamp recordings combined with conductance mutants to count the contributions from different subunits (Emlaw et al., 2021).

2.3.2 The ICL determines functional change in unc-29 subunits

The functional differences observed between Hco-UNC-29.1 and Hco-UNC-29.2 for their ability to contribute to a functional receptor without LEV-1 means that the sequence change responsible occurred since their duplication after divergence from *C. elegans* (Duguet et al., 2016). This represents about 25% of the UNC-29 sequence, the majority of which is within the ICL. Indeed, chimeras where the ICL was exchanged essentially reversed their phenotypes (albeit with dampened responses) and, therefore, the ICL mediates a majority of the requirement for LEV-1. It is not clear yet whether UNC-29.1 is present twice and can physically replace LEV-1, although this seems a likely explanation based on the results from the previous section. As mentioned, assessment of this would require the creation of UNC-38:UNC-29.1 dimers and similar experiments as those described above.

The structure and function of the intracellular loop is largely unknown due its high sequence variability and because structure prediction tools cannot predict any defined features. The only known structures are two alpha helices at each end of the ICL, the first is slightly wedged in the inner leaflet of the membrane and the second acts as an ion funnel for ions entering the cytoplasm (Unwin, 2005) (Figure 3). Known functions of the ICL include

involvement in receptor trafficking (Ren et al., 2005) and some contribution to receptor kinetics (McKinnon et al., 2012) and conductance (Hales et al., 2006; Peters et al., 2005). The results here indicate that the intracellular loop is critical for subunit stoichiometry and by extension may make important contacts with the other subunits mediating their compatibility (either positively or negatively), or even with the accessory proteins. The ICL may act as a "higher level" mechanism of receptor diversity since the minimum sequence length needed for the ICL in eukaryotes is 70 amino acids and the emergence of large diverse ICLs arose in the animal receptors (Baptista-Hon et al., 2013; Tasneem et al., 2005).

The results from this chapter suggest that the specificity of position for the LEV-1 subunit may depend on the specific nature of the non-alpha subunit and that other subunits within the complex can influence this specificity. The origin of the non-alpha subunit clade from the alpha-subunit clade was the first event at the base of the L-AChR subunit phylogeny. The change from a homomeric receptor, to one containing alpha and non-alpha subunits would be accompanied by the evolution of specificity for subunit position within the receptor. There are examples within the vertebrate heteromeric AChR of non-alpha subunits more closely related to alpha subunits from the same receptor. This suggests it is possible for an alpha subunits duplication to adapt and fulfill the role of a non-alpha subunit. The next chapter attempts to addresses this possibility using the L-AChR from Clade III nematode, *Brugia malayi*.

Chapter 3. Alpha to non-alpha subunit switch

3.1 Introduction

Chapter 2 explored the concept of subunit placement within the levamisole-sensitive acetylcholine receptor (L-AChR). The ability of one non-alpha subunit to replace the other depended on the presence of an alpha subunit that did not make contact with the position involved. When only a single non-alpha type subunit was present, two copies were present to maintain the alpha-, non-alpha composition and two alpha-, non-alpha subunit interfaces for ligand binding. The L-AChR subunit phylogeny shows that the alpha:non-alpha split occurred first, followed by further subunit specialization within each (Figure 2C). The division between alpha- and non-alpha subunit types appears to be fundamentally important for the receptor.

The L-AChR subunit gene family is particularly dynamic especially in nematodes. Many gene loss and duplication events have occurred. Three such events that are particularly interesting have occurred within the Clade III filarial parasites. Three of the four known non-alpha subunits, *acr-2*, *acr-3* and *lev*-1 have been lost while both alpha subunits *unc*-38 and *unc-63* have duplicated (Beech & Neveu, 2015; Coghlan et al., 2019; Williamson et al., 2007). In addition, in each case, one of the duplicate copies within the genus *Onchocercidae* has lost the vicinal cysteine motif that is a defining feature of alpha subunits (Howe et al., 2016, 2017). It is therefore possible that these duplicate alpha subunits have undergone a functional shift from alpha to non-alpha following duplication. If so, this would provide an excellent opportunity to investigate mechanisms that determined subunit subtype placement at the base of L-AChR clade. Estimates of codon substitution rate may indicate the types of evolutionary changes that have occurred and where functional change has occurred in the sequence (Beech et al., 2013; Duguet et al., 2016; Franchini & Elgoyhen, 2006; Thompson et al., 2018).

An ideal method for investigation of the functional characteristics of the L-AChR is through reconstitution of the receptor *ex vivo* using *Xenopus laevis* oocytes. This requires expression clones of the necessary subunits and accessory proteins for which the Clade III filarial parasite *Brugia malayi* may be the best candidate for a number of reasons. First, there is evidence of a functional L-AChR *in vivo*. Live muscle recordings measure acetylcholine and levamisole sensitive receptors and L-AChR subunits are found to be expressed in body wall muscle (Kashyap et al., 2021; Li et al., 2015; Verma et al., 2017). Second, the duplicate copies still

contain the vicinal cysteine motifs so it is possible they are still undergoing functional adaptation and we can study this process in progress. Third, the *B. malayi* genome is of exceptional quality allowing us to reliably identify and clone all acetylcholine receptor subunit genes for characterization (Howe et al., 2016, 2017). Finally, no *B. malayi* acetylcholine receptor (AChR) has been reconstituted *ex vivo*. Cloning all the *B. malayi* AChR subunit genes and testing them in oocytes would yield a plethora of information and lead to additional future projects characterizing the other receptors from *B. malayi*. It was expected that selection pressure analysis would show elevated substitution rates for the duplicate copies, indicative of functional change. This was indeed the case. In addition it was expected that the *B. malayi* L-AChR could be reconstituted *ex vivo*, as was routine for other nematodes (Boulin et al., 2011; Boulin et al., 2008; Buxton et al., 2014; Williamson et al., 2009). Unfortunately, this proved not to be the case.

Composition of the L-AChR in parasites closely related to *Caenorhabditis elegans* varies, with the requirement for LEV-1 being relaxed, allowing the other non-alpha subunit, UNC-29 to take its place. This replacement of one non-alpha subunit by another may be a common phenomenon based on the large number of duplications of the *unc*-29 subunit gene in the Clade V nematodes (Duguet et al., 2016). The origin of a heteromeric receptor must occur when gene duplication and divergence allows subunits to acquire specialized positions in the receptor. An alpha subunit may function as either the principal or complementary face of ligand binding pocket and a non-alpha subunit only as the complementary face (Corringer et al., 2000). The appearance of a non-alpha subunit may lead to the loss of its ability to function as a principal face and specialization to create the asymmetric ligand binding sites required for opening the channel (Mowrey et al., 2013). Subsequent duplication and divergence that leads to a maximally heteromeric receptor such as the Cel-L-AChR would involve subunits acquiring new positions within the receptor. It would seem more likely for an alpha subunit to become non-alpha than for the reverse, where functionality as the principal face would have to be reacquired. In fact the alpha- to non-alpha switch has occurred within the vertebrate equivalent of the L-AChR, when the CHRNB3 subunit is more closely related to the CHRNA5 subunit than any other non-alpha subunit (Pedersen et al., 2019). Subunits from the same receptor are more likely to replace one another because they are already appropriately expressed and are the most similar in sequence. Relaxation that allows subunits to occupy multiple positions within the receptor, as shown in the previous chapter followed by specific adaptation to a new position would underlie this process.

Duplication of the alpha *unc*-38 and *unc*-63 subunit genes within the Clade III nematodes appear to be ideal examples to study the possible switch of an alpha to non-alpha subunit because they are relatively recent duplications with minimal sequence change responsible and, therefore, the potential that the sequence responsible could be identified.

3.2 Results

3.2.1 Unc-38 and unc-63 duplication

Phylogeny and substitution rate analysis for both subunit genes were highly similar (Figure 15 & 17, Table 1). *Unc-38* and *unc-63* are widely conserved across nematodes, with duplications occurring in the Clade III worms after separation from *Ascaris suum* for *unc-38* (Figure 15) and *Dracunculus medinensis* for *unc-63* (Figure 17). For *unc*-38, after each *Gonglyonema pulchrum* copy, long branches leading to each duplicate cluster is observed followed by small branches within. The duplicate copies are similar, with the *B. malayi* copies having 74% amino acid sequence identity. For *unc*-63, a long branch separates the duplicate copies from *A. suum* followed by two distinct *unc*-63.1 and *unc*-63.2 clusters. A third *G. pulchrum unc-63.3* copy exists that might suggest several duplication events, of which only two genes survive in other related species. The duplicate *unc*-63 copies are similar, with the *B. malayi* copies sharing 68% amino acid sequence identity.

Interestingly, *unc-38.2* and *unc-62.3* within the *Onchocerca* genus have lost the YXCC motif characteristic of an alpha subunit (Howe et al., 2016, 2017). Predictors of subunit functional change has been previously done by measuring selection pressures acting on recently duplicated genes (Beech et al., 2013; Duguet et al., 2016; Franchini & Elgoyhen, 2006; Thompson et al., 2018). By measuring substitution rates, one can infer functional change associated with sequence change. PAML is a maximum likelihood phylogeny analysis that provides likelihood ratio tests on hierarchical nested models (Yang, 2007). The model that best fits the evolution of the phylogeny can be identified by comparing the likelihood of various models to the simplest/null model. For this analysis, earlier Clade III (prior to duplication) and Clade V substitution rates were used as background because these sequences have no evidence of duplication for these subunits and, therefore, provide a reference for selection on a single gene.

Appendix Tables 1 and 2 show PAML results. The M0 model had one rate class for all amino acids on all branches of the phylogeny, with a substitution rate of 0.05 (dN/dS) for *unc-38*

and 0.038 dN/dS for *unc-63*. For both subunits, the M3k2 model that has two different amino acid substitution rates and the M3k3 model that has three were significantly better than the M0 and M3k2 models respectively. In each case the three different rate classes accounted for approximately 2/3, 1/4 and 1/12 of the protein sequence For *unc-38* a majority of sites (65%) were highly conserved with a substitution rate of 0.005 dN/dS, 27% of sites with a rate of 0.088 dN/dS and 7% of sites with the highest rate of 0.42 dN/dS. For *unc-63*, these classes were61% with a rate of 0.004, by 29% with a rate of 0.058 and 10% with the highest rate of 0.20 dN/dS.

Model D, in which one of the three rate classes was allowed to differ on the branches leading to the *unc-38.1* and *unc-38.2* clades fit the data significantly better than the M3k3 model. For unduplicated, background *unc-38*, the rate was 0.035, for *unc-38.1* the rate was almost five times higher, at 0.174 and *unc-38.2* eight times higher at 0.280. For *unc-63*, the background rate for the middle rate class was 0.027, for the branch leading to *unc-63.1* was 0.068 and *unc-63.2* was 0.196. The higher rates for both subunit duplicate copies suggest that after the gene duplicate event selective constraint was reduced. The rate was not above 1 so this is inferred to be a relaxation of selection pressure. In the previous chapter, changes in subunit combination were associated with a relaxation of the ability of the UNC-29 subunit to occupy the position of LEV-1 in the receptor. The region responsible for a majority of the ability for UNC-29.1 to remove the requirement for LEV-1 was found to be the intracellular loop.

The probability of each codon position belonging to one of the three rate classes was mapped onto the linear subunit sequence (Figures 16 & 18). Both subunits had strikingly similar patterns of codon probability. A majority of the extracellular domain (ECD) and transmembrane domains (TMs) belong to the low rate class (Figures 16 & 18, red). The middle rate class (Figures 16 & 18, green), which represents the regions undergoing possible functional change, are found in a few select regions in the ECD and the intracellular loop (ICL) and also coincide with where the few high rate classes are found (Figures 16 & 18, blue). This coincides with the region associated with changes in subunit position in the previous chapter. In fact, one of the large regions of the middle and high rate class codons correspond to codon positions 150-200 in *unc-38* (Figure 16) and 130-150 in *unc-63* (Figure 18) which contain many of the binding pocket loops on both principle and complementary faces. This substitution rate analysis indicates that despite the largely conserved subunit sequence, elevated rates for both are observed in the middle rate class that corresponds to the ICL and binding pocket regions within the ECD.

Unc-38	Low rate class (63%)	Middle rate class (33%)	High rate class (4%)	**Unc-63**	Low rate class (58%)	Middle rate class (35%)	High rate class (7%)
Clade V	0.003	0.035	0.518	Clade V	0.003	0.027	0.198
Unc-38.1	0.003	0.174	0.518	Unc-63.1	0.003	0.068	0.198
Unc-38.2	0.003	0.280	0.518	Unc-63.2	0.003	0.196	0.198

Table 1. PAML substitution rates (dN/dS) of unc-38 and unc-63 subunits.

PAML identified three rate classes in both subunits, with the middle rate classes elevated in the Clade III copies. See Figures 15 & 17 for phylogeny and Appendix Tables 1 & 2 for PAML results.

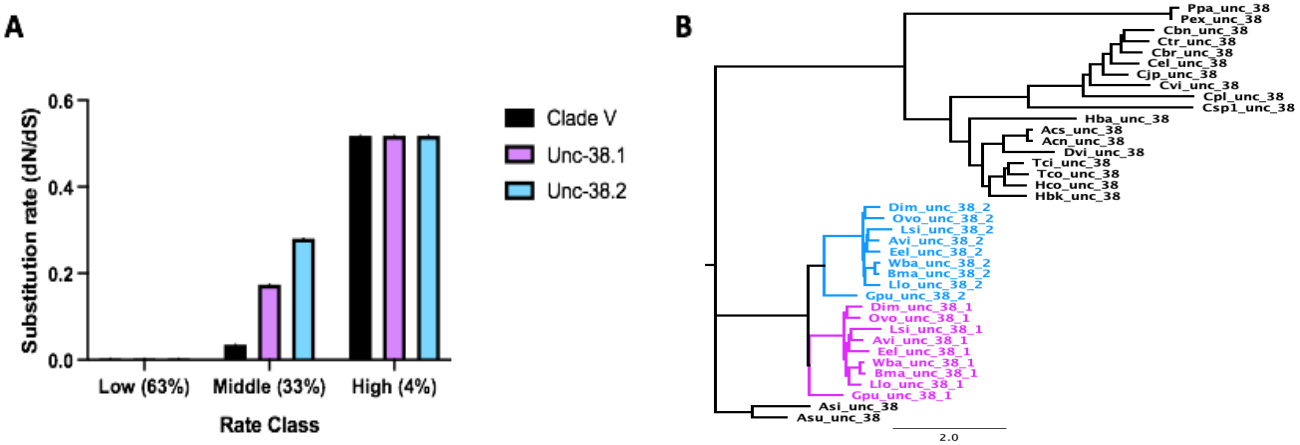

Figure 15. Maximum likelihood phylogeny of unc-38.

Substitution rate analysis was carried out on *unc-38*. (A) The best model had three substitution rate classes representing 63%, 4%, and 33% of codons (Table 1 & Appendix Table 1). The highest rate class, (63%), shows high conservation (0.003 dN/dS) in all branches. The least conserved rate class (4%) is 0.518 dN/dS across all branches. For the middle rate class (33%), Clade V has a rate of 0.035 dN/dS, *unc-38.1* a rate of 0.174 dN/dS, and *unc-38.2*, 0.280 dN/dS. (B) *Unc-38* duplication is observed in the Clade III nematodes. Purple branches indicate *unc-38.1*, blue branches indicate *unc-38.2*. See Table 1 and Appendix Table 1 for PAML analysis.

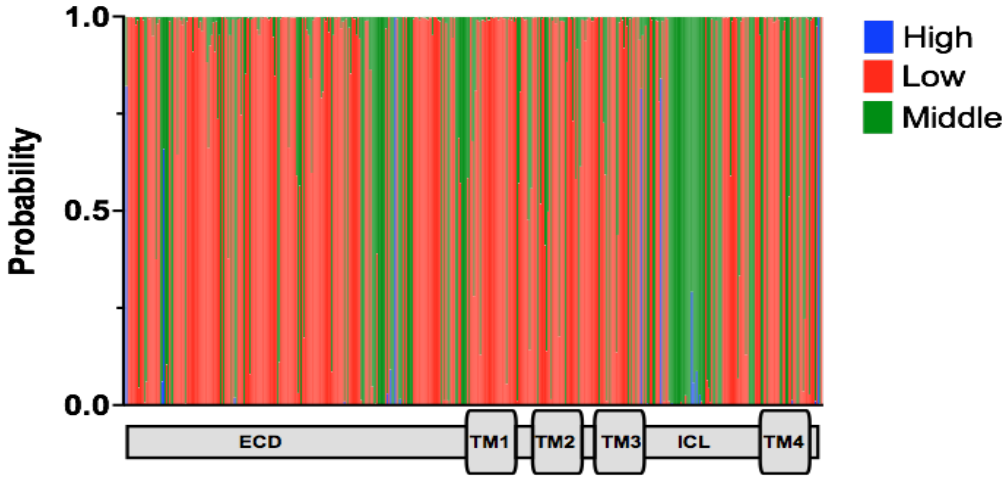

Figure 16. The ICL and ECD are changing in unc-38.

The probability of each codon site belonging to one of the three substitution rate classes is shown. The majority of the sequence is highly conserved belonging to the low rate class (red), in particular are the transmembrane domains and most of the ECD. Few sites are predicted to belong to the high rate class (blue). The ICL and two regions within the ECD are predicted to belong to the middle rate class (green), which is the rate class that is higher in duplicate copies, suggesting these regions may be involved in subunit type change. See Table 1, Figure 15 & Appendix Table 1 for rate classes.

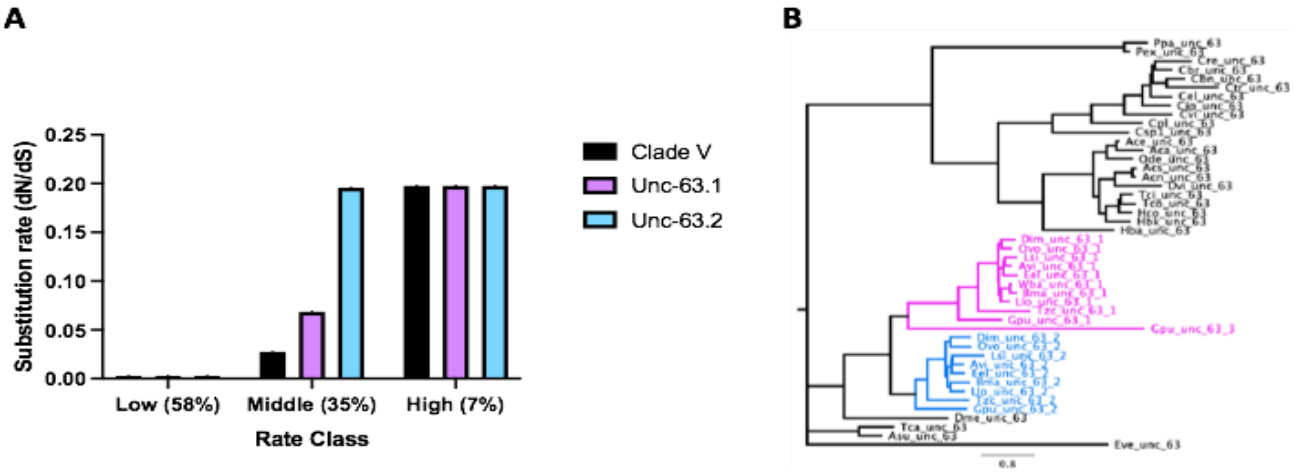

Figure 17. Maximum likelihood phylogeny of unc-63.

Substitution rate analysis was carried out on *unc-63*. (A) The best model had three rate classes representing 58%, 7%, and 35% of codons (Table 1 & Appendix Table 2). This model separates each of the duplicated *unc-63*. The highest rate class (58%), shows high evolutionary conservation (0.003 dN/ dS) over all branches. The least conserved class (7%) shows 0.198 dN/dS across all branches. For the middle rate class Clade V has a rate of 0.027 dN/dS, *unc-63.1* has a rate of 0.068, and *unc-63.2* a rate of 0.196 dN/dS. (B) Pink branches indicate *unc-63.1*, blue branches indicate *unc-63.2*. See Table 1 and Appendix Table 2 for PAML analysis.

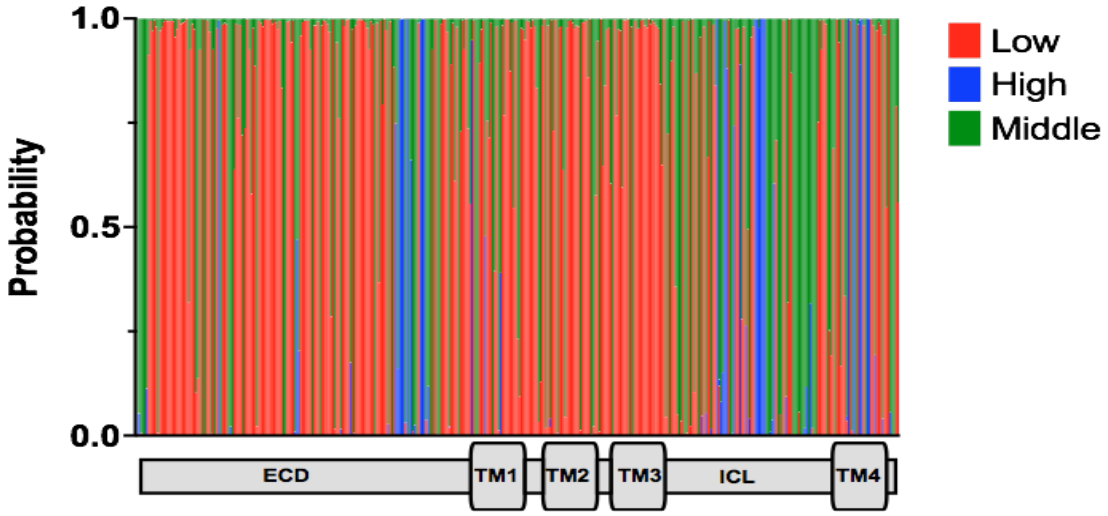

Figure 18. The ICL and ECD are changing in Unc-63.

The probability of each codon site belonging to one of the three substitution rate classes is shown. The majority of the sequence is highly conserved belonging to the low rate class (red), in particular are the transmembrane domains and most of the ECD. Few sites are predicted to belong to the high rate class (blue), mainly found in the ICL and one region in the ECD. The ICL and two regions within the ECD are predicted to belong to the middle rate class (green), which is the rate class that is higher in duplicate copies, suggesting these regions may be involved in subunit type change. See Table 1, Figure 17 & Appendix Table 2 for rate classes.

3.2.2 *B. malayi* L-AChR

Experimental verification that the functional change predicted by substitution rate analysis of duplicated Clade III *unc-38* and *unc-63* subunits would require reconstitution of a functional Bma-L-AChR *ex vivo.* Recordings from living *B. malayi* have shown both acetylcholine (ACh) and levamisole (LEV) produce cell depolarization characteristic of a functional L-AChR (Verma et al., 2017). All cationic pentameric ligand-gated ion channel (pLGIC) genes predicted from the *B. malayi* genome were, therefore, cloned into a *Xenopus laevis* oocyte expression vector for cRNA synthesis (Duguet, 2017). The exceptional quality of the *B. malayi* genome increases our confidence that all subunits have been identified and predicted correctly (Howe et al., 2016, 2017).

No response to ACh or other known agonists of the Cel-L-AChR was observed with the *B. malayi* subunits (Figure 19, second column). The *B. malayi* L-AChR subunits are expected to contribute to a heteromeric receptor; which means that if just one subunit is non-functional then the entire receptor complex would be non-functional and no response would be obtained.

Admixtures replacing one subunit from the *C. elegans* L-AChR with its ortholog from *B. malayi* were then evaluated to identify if any one of the *B. malayi* L-AChR subunits showed evidence for being specifically defective. None of these admixtures produced any measurable response suggesting a systemic issue rather than cloning artefacts (Figure 19 columns 3-8, and Figure 20).

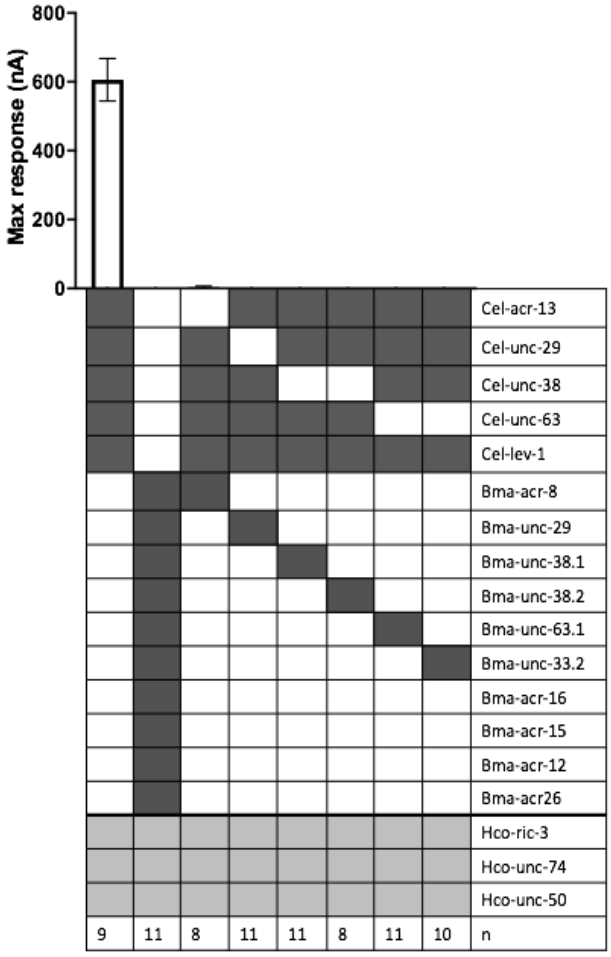

Figure 19. No *B. malayi* AChR was measured.

Responses to 100 μM ACh are shown. No response was measured from either the megamixture containing all predicted AChR subunit genes from the *B. malayi* genome nor the *C. elegans and B. malayi* admixtures. The currents obtained with the *C. elegans* L-AChR served as a positive control for the admixtures (leftmost column). See Figure 20 for representative recordings of admixtures.

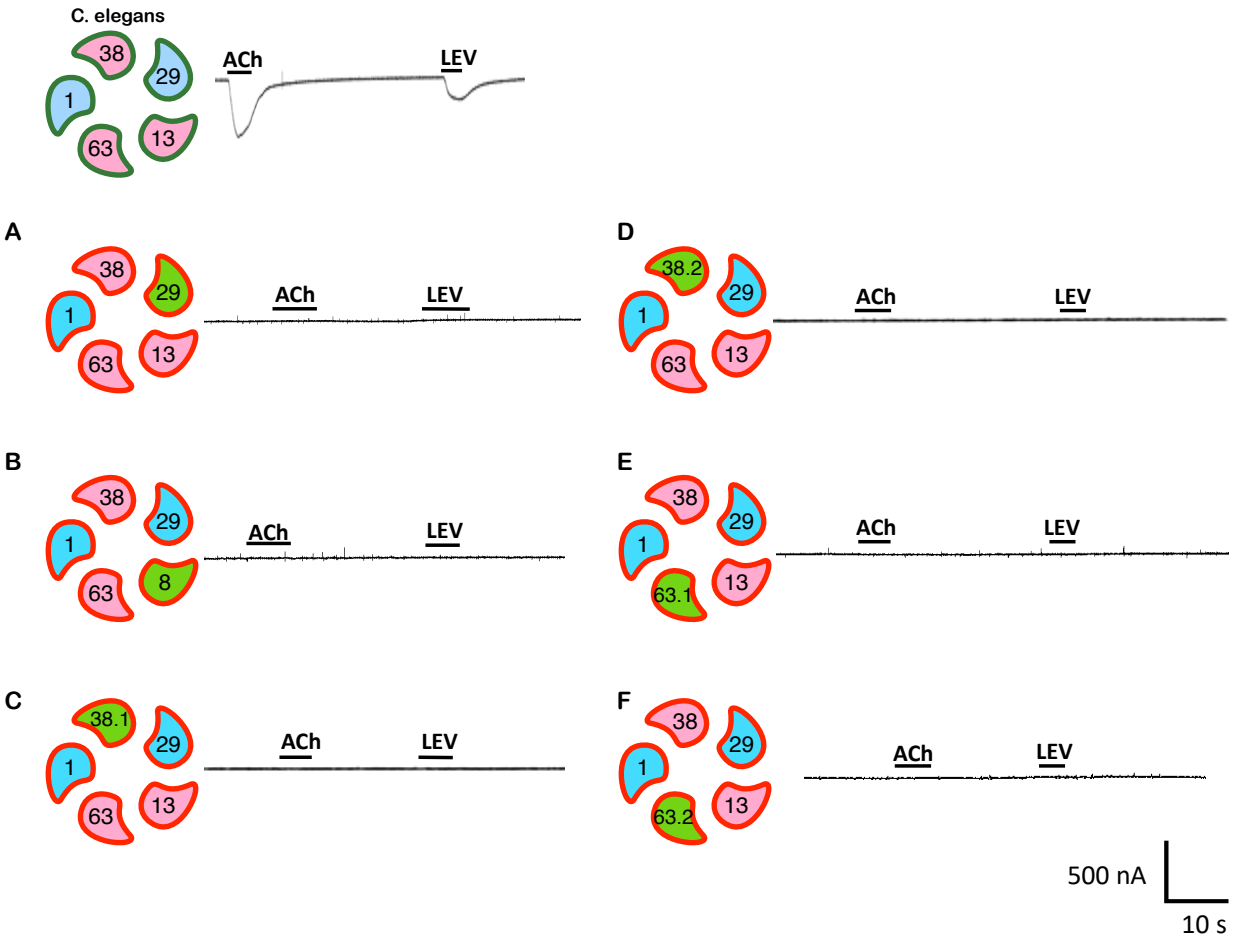

Figure 20. *B. malayi* and *C. elegans* L-AChR admixtures.

Admixtures were made between the *C. elegans* and *B. malayi* L-AChR subunits to identify if any of the *B. malayi* subunits can functionally replace their *C. elegans* orthologs. Admixtures were made by replacing individual subunits with the *B. malayi* ortholog and responses to 100 µM ACh and LEV recorded. Green subunits represent the *B. malayi* subunits for (A) *B. malayi* UNC-29; (B) *B. malayi* ACR-8; (C) *B. malayi* UNC-38.1; (D) *B. malayi* UNC-38.2; (E) *B. malayi* UNC-63.1; (F) *B. malayi* UNC-63.2. The *C. elegans* L-AChR (top) served as a positive control. Subunits were co-injected with Hco-ric-3, Hco-unc-50 and Hco-unc-74. None of the *B. malayi* subunits were able to replace their *C. elegans* orthologs. Green outline depicts functional receptor. Red outline depicts non-functional receptor. See Figure 19 for average responses.

3.3 Discussion

3.3.1 Clade III unc-38 and unc-63 duplications are under positive selection

The duplication of *unc*-38 and *unc*-63 in Clade III worms were associated with one copy in each case losing the vicinal cysteine motif in some filarial nematodes. This suggests a possible subunit-type change since the motif is essential for alpha-type subunits. To explore this,

substitute rates were measured in each set of duplicate genes, using the Clade V sequences as background reference rates. Substitution rates represent a measure of sequence change and can be used to predict functional change after ion channel subunit duplication (Beech et al., 2013; Duguet et al., 2016; Franchini & Elgoyhen, 2006; Thompson et al., 2018). PAML analysis identified three substitution rate classes in both *unc*-38 and *unc*-63. These classes are referred to here as the low-, middle- and high-rate classes based on their relative rates. In both genes, a majority of codons (63% of *unc-38* codons and 58% of *unc-63* codons) belonged to the low rate class. These rates of 0.003 for both genes, similar to others of the most highly conserved genes, including tubulins and histones (Nielsen et al., 2010). A small fraction of codons (4% of *unc-38* codons and 7% of *unc-63* codons) belonged to the high rate class, although still experiencing purifying selection, 0.518 for *unc-38* and 0.198 in *unc-63*). Finally, about a third of codons in both genes (33% of *unc-38* codons and 35% of *unc-63* codons) belonged to the middle rate class. This class was significantly different between the duplicate genes compared to unduplicated genes. Most conserved in the unduplicated genes, higher for the *unc-38.1* and *unc-63.1* copies and highest for the *unc-38.2* and *unc-63.2* copies. This is consistent with a general relaxation of specificity of subunit position for both copies and an additional reduced functional requirement for non-alpha subunits. The middle rate class codons are primarily found in the ICL and regions within the ECD including ligand binding loops on the principal face (Figures 16 & 18). The ICL of UNC-29 was shown in the previous chapter to mediate the requirement for the LEV-1. Multiple key regions clearly play a role in the mechanisms determining subunit position.

When a gene duplication event persists, an obvious question is why? Does duplication of one gene alleviate the requirement for another, in which case duplication would precede loss of other genes. In the reverse case, the loss of other genes may create an environment that favours diversification of remaining subunits to take on the functional characteristics of the lost genes, in which case loss would precede duplication. The phylogeny suggests that loss of the *acr-2, acr-3* and *lev-1* subunits preceded the duplication of *unc-63* and then later the duplication of *unc-38* (Beech & Neveu, 2015; Coghlan et al., 2019; Williamson et al., 2007). This may suggest a vacancy created by the loss of non-alpha subunits favoured retention of alpha-subunit duplicates and subsequent adaptation as non-alpha. However, both these duplications are of alpha subunits. Why not duplicate a non-alpha subunit since this might be more favourable and require fewer changes to refine the subunit adaptation, as was seen with the duplications of *unc-29* in *H.*

contortus (Duguet et al., 2016)? Gene duplication is a random process and it may be that we will not find a satisfactory answer for this. In order to investigate this, a functional *B. malayi* L-AChR would be needed.

3.3.2 No measurable *B. malayi* AChR receptor

Electrophysiology of living *B. malayi* body wall muscle reveals that LEV and ACh sensitive receptors are present *in vivo* (Verma et al., 2017). *In situ* hybridization confirms mRNA for subunits orthologous to those found in the *C. elegans* L-AChR are expressed in the muscle (Li et al., 2015). The high quality and well annotated genome means cloning cationic pLGIC subunits, including those of the L-AChR should be straightforward (Howe et al., 2016, 2017).

Reconstitution of a functional receptor using a mix of all *B. malayi* subunits combined was unsuccessful. This approach has been successful previously for other species, including *A. suum*, *Haemonchus contortus* and *Oesophagostomum dentatum* (Boulin et al., 2011; Boulin et al., 2008; Buxton et al., 2014; Williamson et al., 2009). The ACR-16, nicotine sensitive AChR has been successfully expressed from a variety of different nematodes (Abongwa et al., 2016; Boulin et al., 2008; Charvet et al., 2018; Hansen et al., 2021; Kaji et al., 2020; Touroutine et al., 2005) but after many attempts, no nicotine response could be detected for the combination of all *B. malayi* subunits with the accessory proteins normally required. This suggests some functional change has occurred for the later Clade III cationic receptors in general. The L-AChR is a heteromeric receptor where the absence of one subunit leads to no functional receptor. Admixtures (replacing one subunit from the *C. elegans* L-AChR with its ortholog from *B. malayi*) were then tested to identify if any of the *B. malayi* L-AChR subunits are causing the problem. This method has been used previously with other nematodes using the *C. elegans* L-AChR as the background receptor (Blanchard et al., 2018; Duguet, 2017). None of the *B. malayi* admixtures produced any measurable current and indicates changes in each Bma-L-AChR subunit, not just one (Figure 20). The *C. elegans* and *H. contortus* L-AChRs never produced significant responses until a combination of all required subunits and accessory proteins were combined (Boulin et al., 2011; Boulin et al., 2008). The genome of *B. malayi* is good quality, with the sequence of entire chromosomes available so it is very unlikely that the failure can be explained by subunits that remain to be identified (Howe et al., 2016, 2017).

The absence of a *B. malayi* ACR-16 receptor was unexpected because the Clade III *A. suum* ACR-16 receptor is robust and has been characterized in detail (Abongwa et al., 2016;

Zheng et al., 2016). It is unlikely an artefact of the Bma-acr-16 clone since a similar failure has been reported for the close relative, *Dirofilaria immitis* (Dr. Neveu pers comm). The explanation for the lack of receptor reconstitution is unknown. *A. suum* lies at the base of this nematode Clade. The parasites *D. medinensis, G. pulchrum,* and *Thelazia callipaeda*, diverge in this order from the Clade (Coghlan et al., 2019). In an attempt to find any insight into the problem of reconstituting ACR-16, it was decided to express ACR-16 from each of these parasites to study any progression between a fully functional ASU-ACR-16 and the non-functional Bma-ACR-16. This would identify when and what causes the inability to produce the homomeric channel and may provide insight into the inability to produce the more complex heteromeric L-AChR as well. This analysis is explored in Chapter 4 & 5.

Chapter 4: Clade III ACR-16 phylogeny characterization

4.1 Introduction

The cationic pentameric ligand-gated ion channel (pLGIC) subunits in the filarial parasite, *Brugia malayi*, present an interesting model system to investigate adaptive evolution of subunits that switch from alpha-type, that can occupy either the principal or complementary face of the ligand binding pocket, to a non-alpha type, that can function only as the complementary face. A duplication of subunits *unc-38* and *unc-63* from the levamisole-sensitive acetylcholine receptor (L-AChR) have produced, in each case, one copy that appears to have switched roles from alpha- to non-alpha. The previous chapter described the attempt to verify this experimentally. The failure to reconstitute any functional acetylcholine receptor (AChR) in *Xenopus levis* oocytes, despite including of all cationic subunits present in the *B. malayi* genome and the three accessory proteins normally required, suggests that there has been a functional change of these receptor subunits from those found in other nematodes, such as the free living *Caenorhabdtis elegans*. Admixtures of subunits of the L-AChR between *C. elegans* and the closely related parasitic nematode, *Haemonchus contortus* reconstitute functional receptors (Blanchard et al., 2018; Duguet, 2017). This is also true between *C. elegans* and the Clade III intestinal parasite, *Ascaris suum* (Blanchard et al., 2018). Those from *B. malayi* do not (Chapter 3). This suggests that individual subunits have changed in *B. malayi* preventing their ability to reconstitute functional receptors using our current techniques in *X. laevis* oocytes. To investigate this, the acr-16 subunit that encodes a homomeric nicotine-sensitive acetylcholine receptor (N-AChR) in *C. elegans* and several other nematodes was used as a representative model, as the most simple receptor of the family.

The *B. malayi* subunit, Bma-acr-16, is expected to form a homomeric nicotine sensitive channel in the presence of the accessory protein RIC-3, based on many examples from other species, including the most closely related *A. suum* (Abongwa et al., 2016). No nicotine dependent current was observed for the combination of subunits from *B. malayi* (Chapter 3). This was surprising because *B. malayi* are sensitive to nicotine and an N-AChR exists in body wall muscle (Kashyap et al., 2021; Li et al., 2015; Verma et al., 2017). The two most plausible reasons for the inability to reconstitute a nicotine sensitive N-AChR with *Bma-acr-16* are

changes in receptor function or in expression. After diverging from *A. suum,* the Clade III filarial nematodes lost many members of the cationic pLGIC receptor subunit family (Beech & Neveu, 2015; Williamson et al., 2007). It is possible that during this process, there were changes in agonist affinity, efficacy or channel conductance. There may also have been changes in the way subunits interact with the expression machinery. This could mean that *B. malayi* subunits have an increased dependence on accessory protein absent from the reconstitution experiments.

Since Asu-acr-16 reconstitutes an N-AChR and Bma-acr-16 does not, the question arises: at what point does this ability change and does it represent an all or nothing switch or a gradual change? To address this, ACR-16 was characterized from three species intermediate between *A. suum* and *B. malayi*, namely *Dracuculus medinensis*, *Gongylonema pulchrum* and *Thelazia callipaeda* (see phylogeny Figure 21). These intermediate ACR-16s each represent independent samples of the change at different timepoints in adaptation between *A. suum* and *B. malayi*. These different ACR-16s were characterized and the ability to reconstitute a functional receptor was shown to change gradually, suggesting a functional adaptation. In addition, the functional characteristics of the receptors produced were not substantially different from each other. This suggested that the difference may reflect an altered assembly and processing. The more derived species showed a delayed time of expression in oocytes consistent with this. Addition of other the accessory proteins NRA-2, NRA-4 and EMC-6 increased expression of the *G. pulchrum* and *T. callipaeda* N-AChR and was able to recover a receptor from Bma-ACR-16. The small response from Bma-ACR-16 suggests that expression of the N-AChR from *B. malayi* puts increased dependence on other accessory proteins besides these three.

4.2 Results

4.2.1 ACR-16 is conserved

ACR-16 is highly conserved within the helminths. Clade V and Clade III subunit genes have relatively short branches indicating their low sequence change. *A. suum* acr-16 is at the base of Clade III, with *B. malayi* being most derived. No unusually long branches were observed within this cluster that may have suggested a functional change. Phylogenetic reconstruction of orthologous ACR-16 sequences from the nematodes with the five species characterized here highlighted, *A. suum, D. medinensis, G. pulchrum,* and *T. callipaeda*, and *B. malayi* in order of divergence (Figure 21).

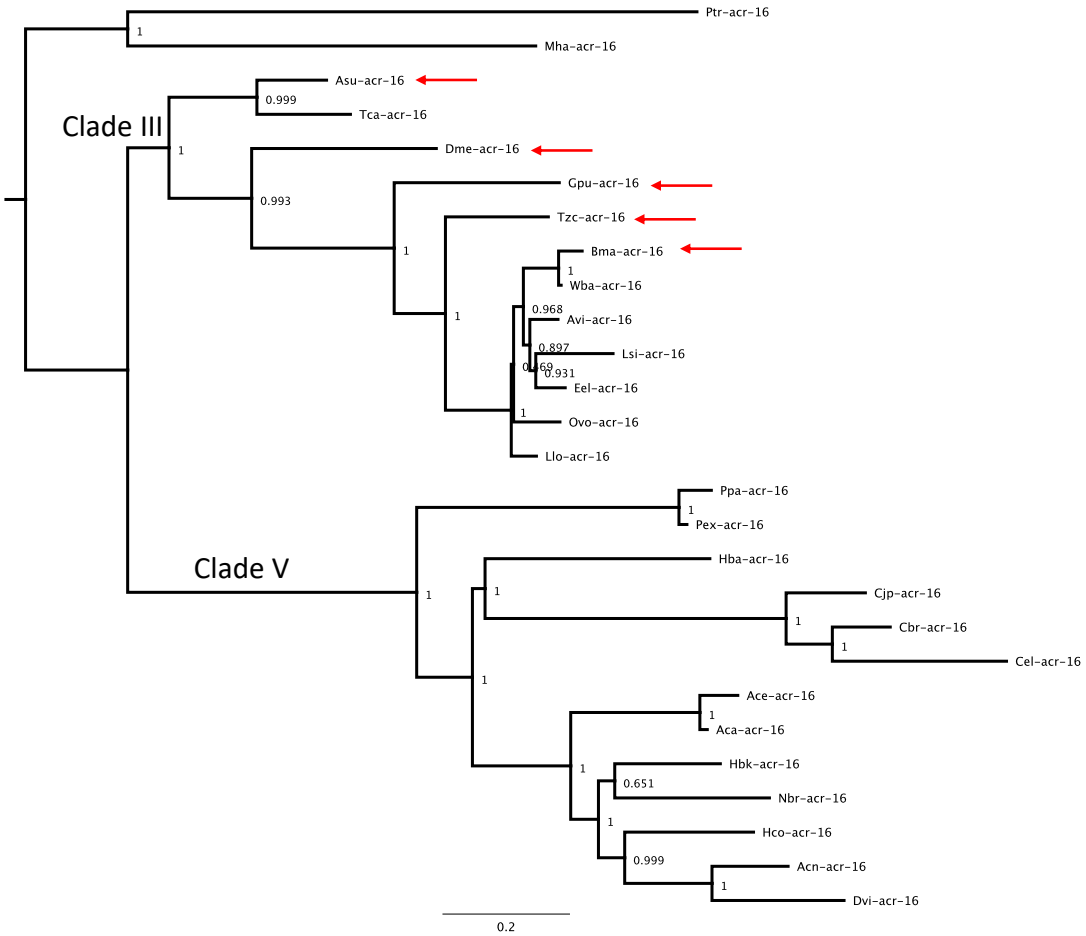

Figure 21. ACR-16 phylogeny.

ACR-16 is conserved across worms with short branches observed within the Clade III and Clade V worms. ACR-16 sequences used in this analysis indicated with red arrows. Nucleotide coding sequences were aligned as codons and phylogeny made using PhyML. SH-branch support values shown.

The multiple sequence alignment of the ACR-16 characterized shows largely conserved sequences with the majority of changes occurring within the intracellular loop (ICL) (Figure 22), this is to be expected as the ICL is the most variable region within cys-loop receptors (Langlhofer & Villmann, 2016). The transmembrane domains (blue annotations) have few changes, mainly confined to transmembrane domain 2 (TM2) and transmembrane domain 4 (TM4). The ion charge motif, located at the start of TM2, (GEK) is conserved throughout, as such all receptors are expected to be cation permeable (Cymesa & Grosman, 2016; Keramidas et

al., 2004). Although there are substitutions found within TM2, they are not extreme (I287V & E290D), therefore, ion conductance is not expected to be severely reduced down the receptor phylogeny (Unwin, 1995, 2005). Substitutions found within the six agonist binding loops (brown annotations) may affect agonist affinity, however, none are the residues that interact with cholinergic ligands (red annotations) so it is unlikely that the later Clade III receptors no longer respond to cholinergic ligands. Overall, no obvious sequences changes are observed in the alignment that would explain the inability of measuring a BMA-ACR-16 in oocytes. *A. suum, D. medinensis, G. pulchrum,* and *T. callipaeda* sequences were then injected into oocytes to measure their function.

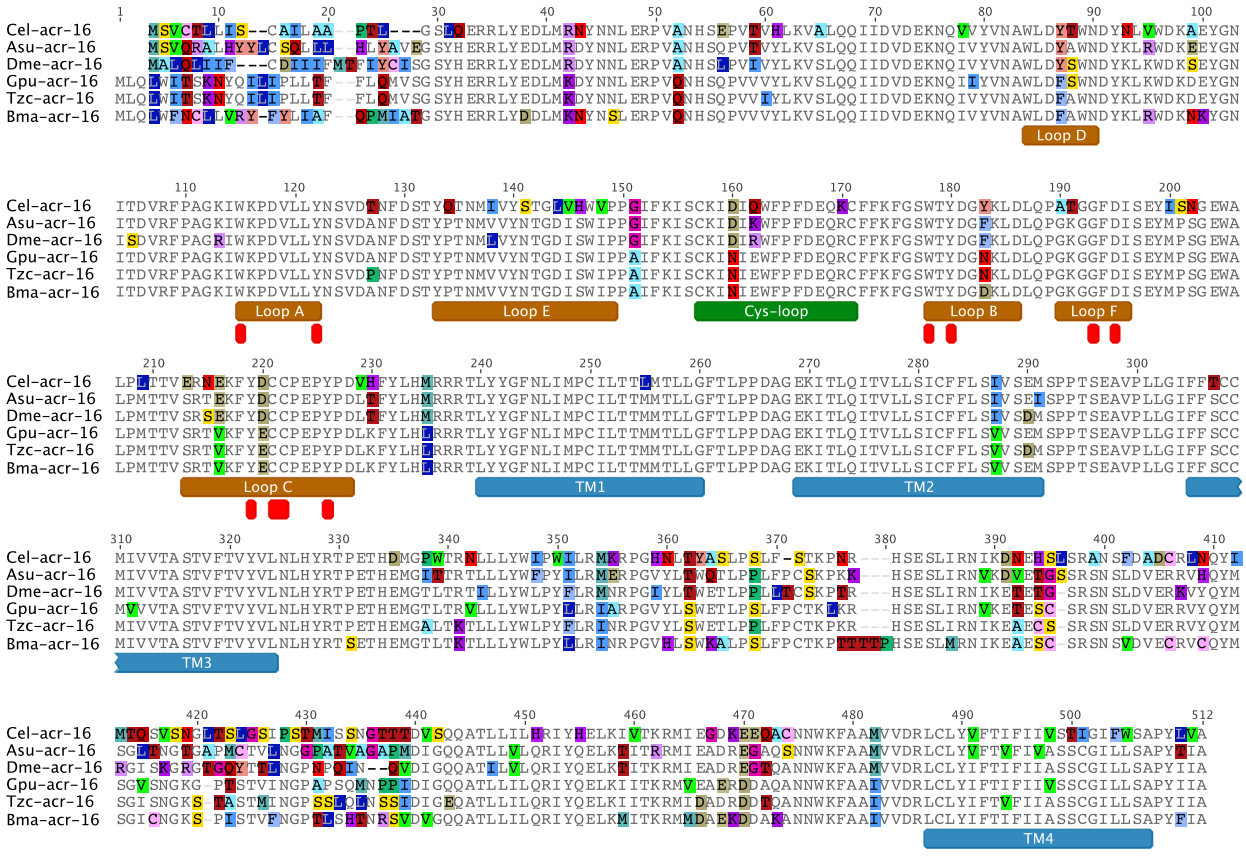

Figure 22. Clade III ACR-16 multiple sequence alignment.

ACR-16 is mostly conserved, with the majority of changes occurring within the intracellular loop. Transmembrane domains are shown in blue, acetylcholine binding loops shown in brown, cys-loop shown in green and residues that interact with agonist in red (Bisson et al., 2008).

4.2.2 Maximal response of ACR-16 in *X. laevis* oocytes

ACR-16 receptors were successfully reconstituted, in combination with Hco-ric-3, from *A. suum, D. medinensis, G. pulchrum*, and *T. callapaeda* but not *B. malayi*. Asu-ACR-16 served as the reference receptor because it is at the base of the Clade and has been previously characterized (Figure 21) (Abongwa et al., 2016). The maximal current in response to 100 µM acetylcholine (ACh) (Figure 23A) and nicotine (NIC) (Figure 23B) decreased progressively in order of divergence in the phylogeny between *D. medinensis* and *B. malayi* (values shown in Appendix Table 3). The change is not discrete as might be expected from a single event, but gradual, suggesting the accumulation of multiple changes over time are responsible. The maximal current reflects the aggregate current through a number of individual receptors. The decrease could, therefore, be in the function of individual receptors or in the total number of receptors present. To address the first of these, various functional characteristics of the reconstituted receptors were evaluated.

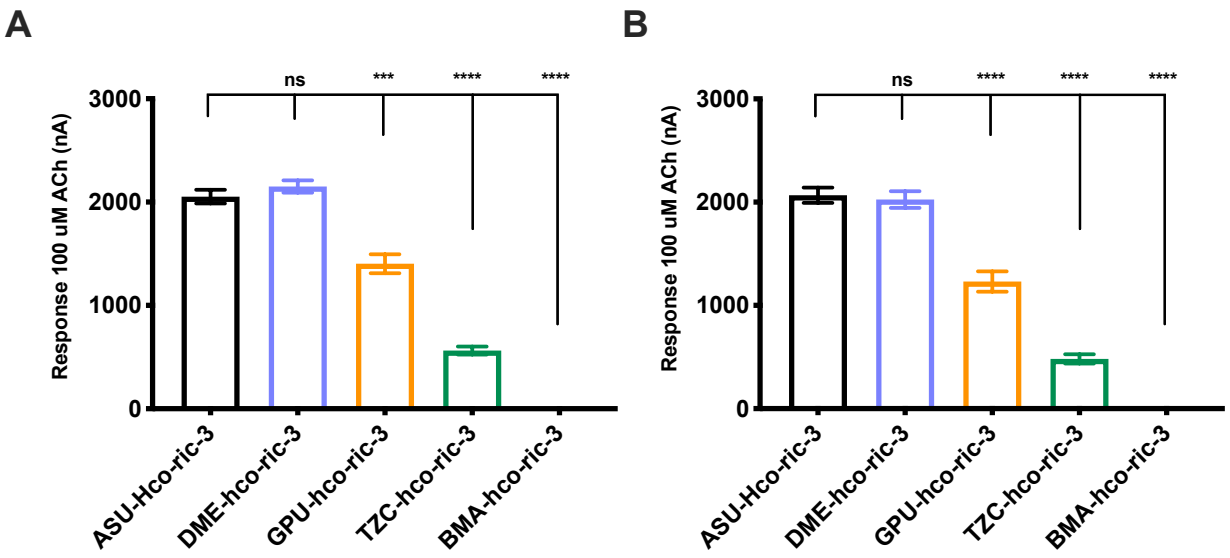

Figure 23. Clade III ACR-16s show phylogenetic decline in response.

Response of Clade III ACR-16 receptors co-injected with Hco-ric-3 are shown to 100 µM (A) acetylcholine and (B) nicotine. In order of phylogeny, *A. suum* in black, *D. medinensis* in blue, *G. pulchrum* in orange, *T. callipaeda* in green, *B. malayi* in grey. The declining response indicates a slow, phylogenetic change has occurred in the Clade III receptor in its ability to produce currents. Error bars represent standard error. ***p<0.0002; ****p<0.0001. See Appendix Table 3 for values.

4.2.3 ACR-16 EC_{50}

Ligand affinity, as reflected in the concentration of ligand that produces half maximal opening, is a sensitive measure of the interaction between ligand and receptor. To explore this, the concentration dependent relative current was determined for both ACh and NIC. There were no significant differences in EC_{50} between the receptors (Figure 24 & Table 2). A slightly lower EC_{50} was observed for NIC than ACh and all receptors reached maximal response, consistent with published characterization of the N-AChR of other related species (Abongwa et al., 2016; Choudhary et al., 2019; Hansen et al., 2021; Kaji et al., 2020).

	ACETYLCHOLINE			NICOTINE		
	EC_{50} (µM)	**Hill coefficient**	**n**	**EC_{50} (µM)**	**Hill coefficient**	**n**
Asu-acr-16	8.9 ± 0.3	1.8 ± 0.1	11	5.1 ± 0.2	2.0 ± 0.1	13
Dme-acr-16	12.8 ± 0.4	1.7 ± 0.1	11	3.8 ± 0.2	1.6 ± 0.1	14
Gpu-acr-16	10.5 ± 0.5	2.1 ± 0.2	15	2.1 ± 0.1	2.3 ± 0.2	13
Tzc-acr-16	17.4 ± 0.8	2.1 ± 0.2	10	4.9 ± 0.4	1.9 ± 0.2	14

Table 2. Clade III ACR-16 show similar agonist affinities.

Dose-response curves were measured to determine if declining maximal response is due to decreasing ligand affinity. No difference in EC_{50} confirms the declining response in Figure 23 is not due to changes in agonist affinity. $EC_{50.}$ curves and representative recordings are shown in Figure 24. Error represents standard error.

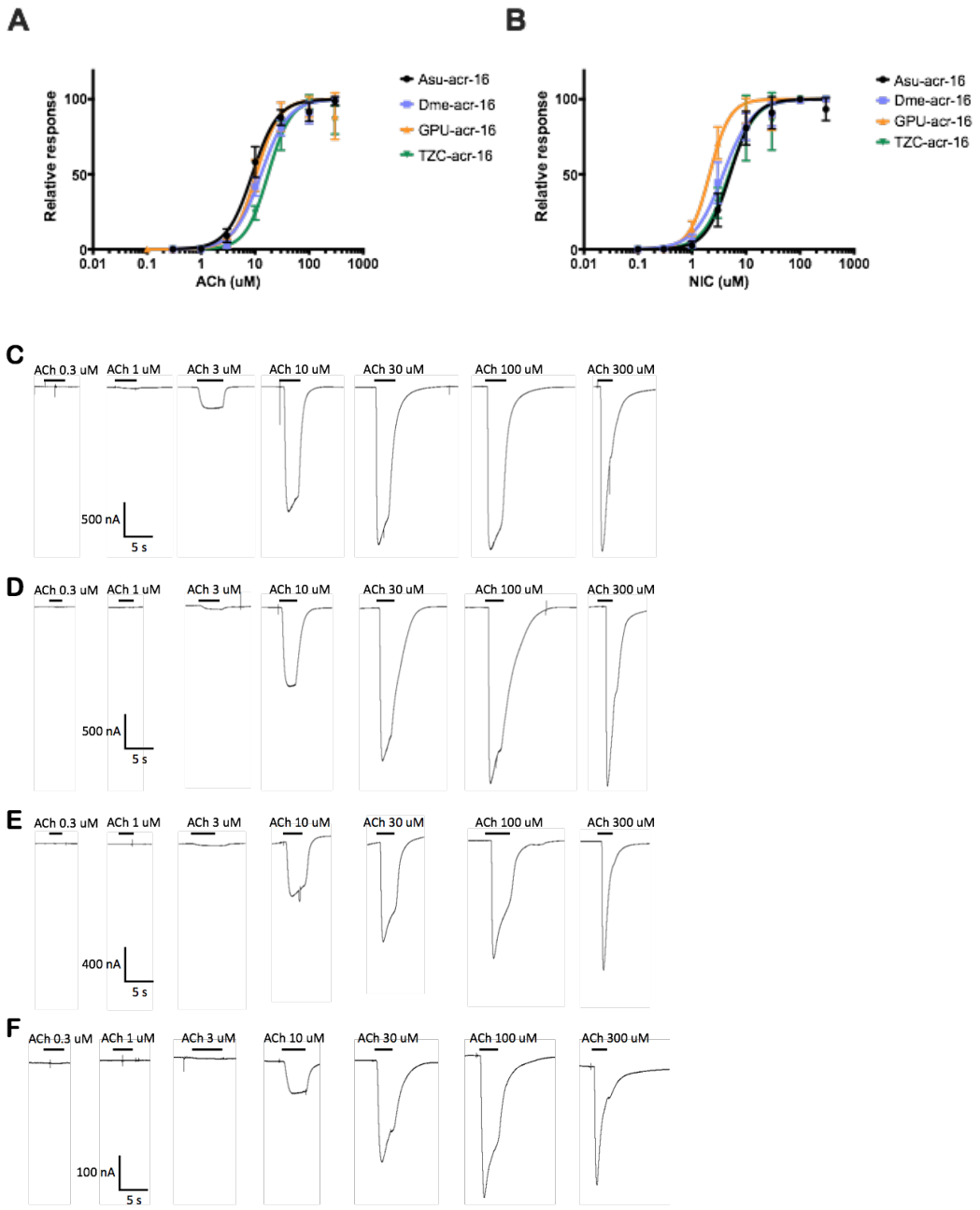

Figure 24. Clade III ACR-16 show similar agonist affinities.

Dose- response curves were measured to determine if declining maximal response is due to decreasing ligand affinity. EC_{50} curves for Clade III ACR-16 receptors for (A) acetylcholine and (B) nicotine. In order of phylogeny, *A. suum* in black, *D. medinensis* in blue, *G. pulchrum* in orange, *T. callipaeda* in green, *B. malayi* in grey. Representative recordings to acetylcholine for (C) *A. suum*. (D) *D. medinensis,* (E) *G. pulchrum* and (F) *T. callipaeda* are shown. No difference in EC_{50} confirms the declining response in Figure 23 is not due to changes in agonist affinity. Error bars represent standard deviation. See Table 2 for values.

4.2.4 Agonist response profile

Four classes of nematode AChR exist; L-, N-, M-, and B- AChRs named for their preferential response to levamisole (LEV), NIC, morantel (MOR) or bephenium (BEPH), respectively (Courtot et al., 2015; Qian et al., 2006). The response to these, along with other known pLGIC agonists, were determined. The profiles of response relative to ACh were similar across species; large responses to NIC, small responses to dimethylphenylpiperazinium (DMPP) and oxantel (OXA), and minimal responses to MOR and pyrantel (PYR). No responses were measured for any receptor to LEV, epinephrine (EPI), norepinephrine (NOR), dopamine (DA), tyramine (TYR), betaine (BET), or BEPH (Figure 25 & Appendix Table 4).

It seems clear that the N-AChR reconstituted from each species, with the exception of *B. malayi* do not differ in their functional characteristics in any meaningful way. This leaves the possibility that the decrease in maximal current could be due to a decrease in the number of receptors present on the oocyte surface. The use of *X. laevis* oocytes has been instrumental for the functional characterization of ion channels. However, early experiments to reconstitute the L-AChR produced only minimal currents until five subunits and three accessory proteins were combined (Boulin et al., 2008). Removal of any one greatly reduced observed currents. It seems unlikely that there remain cationic pLGIC subunits that have not been identified in the *B. malayi* genome since the genome and annotation are good quality (Howe et al., 2016, 2017). The most likely candidate to explain the decrease in maximal current here is, therefore, that there may be missing, or less efficient interaction with accessory proteins.

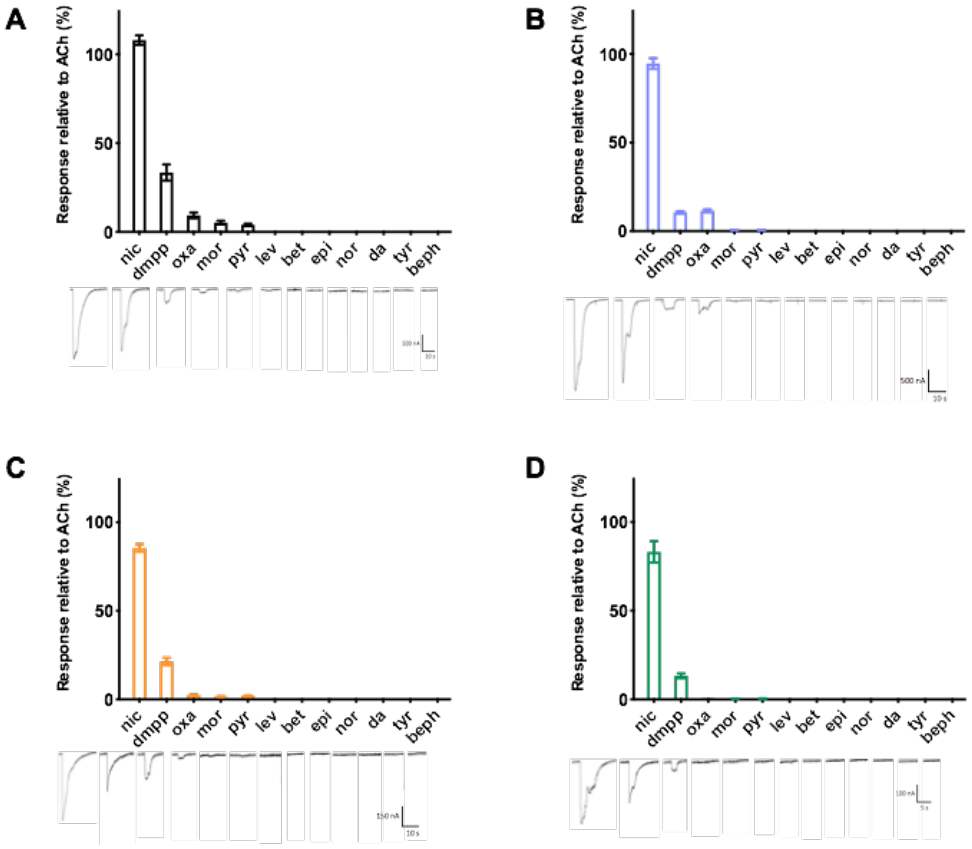

Figure 25. No change in ligand response profile is observed in Clade III ACR-16.
Responses to different agonists were measured to determine if declining maximal response is due to changing ligand preference. Responses to 100 µM are shown relative to acetylcholine for (A) *A. suum*, (B) *D. medinensis*, (C) *G. pulchrum*, (D) *T. callipaeda*. ACR-16 responses to different ligands show no change in ligand response down receptor phylogeny. Error bars represent Standard error. N>6 See Appendix Table 4 for values.

4.2.5 Expression analysis

An inefficient receptor assembly and processing might be expected to cause expression to take longer. The experiments above were recorded currents two days after oocyte injection. To determine if receptor expression was maximal after two days, responses to ACh and NIC were recorded every day, for three consecutive days post-injection and shown in Figure 26 and Table 3. Responses were normalized to Day 3, with each step down the phylogeny of ACR-16 took progressively longer to reach maximal response. After day 1, both Asu-acr-16 and Dme-acr-16 had nearly 50% of their maximal response that was reached on day 2, which had plateaued by day 3. On day 1, Gpu-acr-16 had less than 20% of its maximal response that was reached by day

3. Tzc-acr-16 had 8% of its maximal response on day 1 and by day 2 had only reached 50% of its maximal response that was reached by day 3. No response was observed from Bma-acr-16 even after 5 days post-injection (data not shown).

Both ASU-ACR-16 and DME-ACR-16 reached maximal responses before GPU-ACR-16 and TZC-ACR-16 suggesting that it takes longer to functionally express ACR-16 closer to *B. malayi*. This could be explained if other components of the accessory protein network besides RIC-3 play a progressively larger role in N-AChR assembly down the phylogeny. A literature search of nematode pLGIC accessory proteins (reviewed in Chapter 1) identified accessory proteins known to regulate *C. elegans* L- and N-AChRs as likely candidates. These were co-injected to determine their effects on maximal response of the reconstituted receptor. Accessory proteins included were UNC-50, UNC-74, MOLO-1, EAT-18, EMC-6, NRA-2 and NRA-4 (Almedom et al., 2009; Boulin et al., 2008, 2012; Choudhary et al., 2020; Richard et al., 2013).

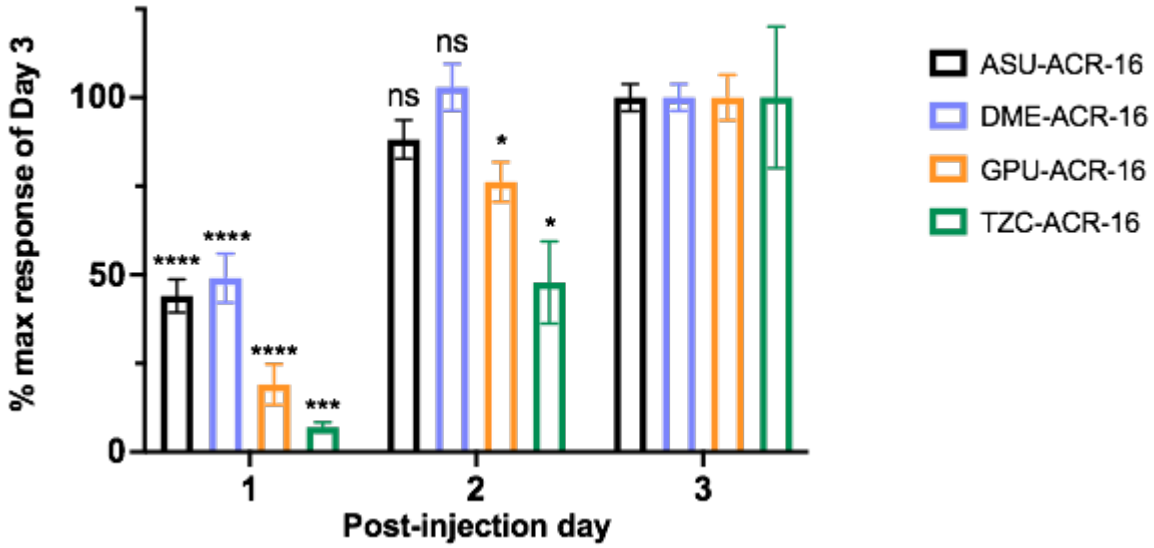

Figure 26. ACR-16 shows delayed expression from later Clade III worms.

Response to 100 µM ACh was recorded for three consecutive days post-injection to measure the time taken to reach maximal responses. Responses are shown as a percent using Day 3 as reference. In order of phylogeny, *A. suum* in black, *D. medinensis* in blue, *G. pulchrum* in orange, *T. callipaeda* in green. *A. suum* and *D. medinensis reach* 50% response after one day and full response by Day 2 that is not significantly different from Day3. *G. pulchrum* and *T. callipaeda* have small responses on day 1 and only reach maximal response by Day 3. No response was measured with *B. malayi* even after 5 days (data not shown). Error bars represent standard error. *$p<0.05$; ***$p<0.0002$; ****$p<0.0001$. Percent maximal response values shown in Table 3.

	Day 1	Day 2	Day 3
ASU-ACR-16	44 ± 5 (n=12) ****	88 ± 5 (n=10) ns	100 ± 4 (n=12)
DME-ACR-16	49 ± 7 (n=10) ****	102 ± 7 (n=10) ns	100 ± 4 (n=11)
GPU-ACR-16	19 ± 6 (n=17) ****	76 ± 6 (n=14) *	100 ± 4 (n=17)
TZC-ACR-16	7 ± 1 (n=11) ***	47 ± 12 (n=10) *	100 ± 20 (n=11)

Table 3. ACR-16 shows delayed expression from later Clade III worms.

Response to 100 μM ACh was recorded for three consecutive days post-injection to measure the time taken to reach maximal responses. Responses are shown as a percent using Day 3 as maximal response. In order of phylogeny, *A. suum* and *D. medinensis* reach 50% response after one day and full response by Day 2 that is not significantly different from Day3. *G. pulchrum* and *T. callipaeda* have small responses on day 1 and only reach maximal response by Day 3. No response was measured with *B. malayi* even after 5 days (data not shown). *p<0.05; p<***0.0002; ****p<0.0001

4.2.6 Expression of Clade III ACR-16 with different accessory proteins

In order to assess the effect of accessory proteins (APs) on maximal response, different accessory protein combinations were co-injected with each of the subunits. Combinations of accessory protein mixtures included: BMA-RIC-3; BMA-RIC-3+ BMA-UNC-50 + BMA-UNC-74; BMA-RIC-3 + BMA-MOLO-1; BMA-RIC-3 + BMA-EAT-18; BMA-RIC-3 + BMA-UNC-50 + BMA-UNC-74 + BMA-EAT-18; BMA-RIC-3 + EMC-6; BMA-RIC-3 + NRA-2 + NRA-4; and no accessory protein. Individual APs were first co-injected with RIC-3 to observe any individual effects on receptor response. If no inhibitory affect was observed, then it was included in the accessory protein "megamix" to determine if a combination of known accessory proteins was missing. Unc-50 and unc-74 were co-injected with RIC-3 together because of their joint need to be included in L-AChR oocyte expression (Boulin et al., 2011; Thomas et al., 2008; Buxton et al., 2014; Williamson et al., 2009). NRA-2 and NRA-4 were also co-injected with RIC-3 together because they work in tandem during subunit assembly (Almedom et al., 2009).

In general, the same progressive decline was observed, regardless of accessory protein combination, however some combinations induced significant deviations from the RIC-3 reference condition (Figure 27, Appendix Figure1 & Appendix Table 3). No difference was observed when using *B. malayi* RIC-3 (Figure 27) versus *H. contortus* RIC-3 (Figure 23), therefore all future conditions will be compared to the BMA-RIC-3 condition. When MOLO-1 was co-injected ASU-ACR-16 maximal response was decreased compared to just RIC-3

(Appendix Figure 1B). The co-injection of EAT-18 significantly increased the maximal response for ASU-ACR-16 and DME-ACR-16, but not for GPU-ACR-16 or TZC-ACR-16 (Appendix Figure 1). There increased responses for the earlier receptors, but not later receptors, suggest accessory protein effects can be observed using this system and do occur down ACR-16 phylogeny.

Interesting changes to maximal responses were observed when either EMC-6 or NRA-2 + NRA-4 were included. Co-injection with EMC-6 did not increase response of ASU-, DME-, GPU-, or TZC-ACR-16, but small currents were measured with BMA-ACR-16 (Figure 27). Co-injection with NRA-2 and NRA-4 increased the maximal responses of GPU-ACR-16 those of ASU- and DME-ACR-16 (Figure 27). TZC-ACR-16 was significantly higher with responses above 1000nA, comparable to those of GPU-ACR-16 + RIC-3. BMA-ACR-16 produced small (<20nA) but measurable responses with the addition of these two APs. These findings indicate that there is a phylogenetic change in the requirement of APs down the receptor phylogeny and is discussed in the discussion.

Interestingly, when no accessory protein was included, DME-ACR-16 had large, measurable responses, ASU-ACR-16 has minimal to no responses, whereas the other receptors showed no response (Figure 27). This was unexpected because previous ACR-16 receptors have been reported to require co-injection of RIC-3 (Abongwa et al., 2016; Boulin et al., 2008; Charvet et al., 2018; Choudhary et al., 2019; Hansen et al., 2021; Kaji et al., 2020). Identifying the region(s) responsible for this change in requirement would provide novel insight into regions that determine accessory proteins, this is investigated in Chapter 6.

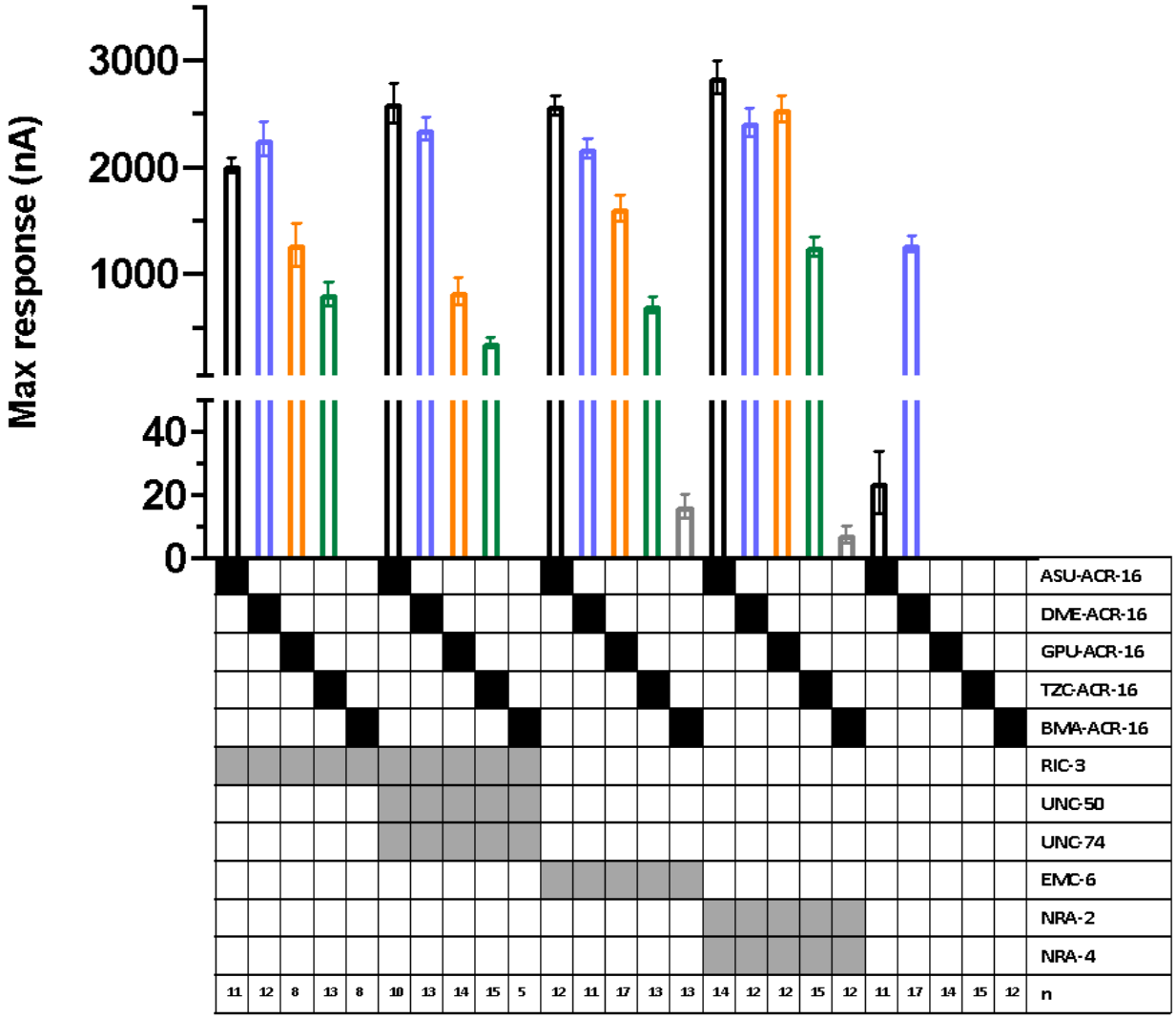

Figure 27. Clade III ACR-16 receptors exhibit phylogenetic decreasing responses.

Response of Clade III ACR-16 receptors co-injected with various accessory proteins are shown to 100 µM acetylcholine. In order of phylogeny, *A. suum* in black, *D. medinensis* in blue, *G. pulchrum* in orange, *T. callipaeda* in green, *B. malayi* in grey. The declining response indicates a slow, phylogenetic change has occurred in the Clade III receptor in its ability to produce currents. *B. malayi* responses were only measured with co-injection of RIC-3+EMC-6 or RIC-3 + NRA-2 + NRA-4. *Acr-16* subunits in black, accessory proteins in grey. Error bars represent standard error. Additional accessory protein conditions shown in Appendix Figure 1 and values in Appendix Table 3. Error bars represent standard error.

4.3 Discussion

Five Clade III ACR-16 receptors were used to track functional change that had occurred in ACR-16; *A. suum*, *B. malayi*, and three intermediates between them; *D. medinensis, G. pulchrum* and *T. callipaeda*. These intermediate species of ACR-16 represent independent time points of the receptors change along Clade III worm phylogeny and would allow for the approximation of when ACR-16 lost its ability to be reconstituted in oocytes. *A. suum* was used as a positive reference point because it has been previously characterized using oocytes and is at the base of Clade III worms (Figure 21) (Abongwa et al., 2016). All ACR-16s, except for *B. malayi*, produced measurable currents in oocytes with the addition of *H. contortus* RIC-3. Interestingly, a progressive phylogenetic decline in maximal responses to ACh and NIC was observed. *A. suum* and *D. medinensis* ACR-16 produced the highest responses with ≈ 2000nA. *G. pulchrum,* the next ACR-16, produced significantly lower responses with ≈ 1200nA, and the next ACR-16 after that, *T. callipaeda*, produced even smaller responses with about ≈ 500nA. The finding that the intermediate species *G. pulchrum* and *T. callipaeda* show intermediate success in reconstitution of the ACR-16 suggests that the basis for the change is experimentally tractable and is not an all or nothing response. This provided us with the opportunity to investigate in detail how ACR-16 has changed.

This progressive decline is not due to changing pharmacology of the receptors as they had similar response profiles to agonists and no obvious changes to ligand affinity. This indicates that down ACR-16 phylogeny there is a gradual decrease in the efficiency of functional expression within the heterologous expression system. The expression analysis further supported this idea. With each “step” down ACR-16 phylogeny, it took increasingly longer to reach maximal response, and therefore maximal functional expression. Even 24 hours after injection, a clear efficiency in % response was observed (Figure 26). Since accessory proteins regulate expression of the channels, it is likely that there could be changes in the requirements of accessory proteins. AP characterization in the nematode body wall muscle neuromuscular junction (NMJ) has primarily focused on the L-AChR of *C. elegans*. However, since the N-AChR and the L-AChR are expressed in the same tissue, in *C. elegans* and other nematodes (Lewis et al., 1980a; Lewis et al., 198b0; Li et al., 2015; Qian et al., 2006; Touroutine et al., 2005, 2004), if new APs were being required in later ACR-16s it is likely they would utilize ones

already being expressed. The addition of accessory proteins known to be involved in L-AChR *in vivo* synthesis were then included.

The *B. malayi* RIC-3 produced the same trend as *H. contortus* RIC-3, therefore the decline is not due to different clade APs. The first other APs included were UNC-50 and UNC-74 because they are required for L-AChR *ex vivo* expression (Boulin et al., 2011; Boulin et al., 2008; Buxton et al., 2014; Williamson et al., 2009). They did not produce a functional *B. malayi* ACR-16 and did not increase the responses of intermediate species. The addition of MOLO-1 or EAT-18 also did not produce functional *B. malayi* ACR-16 nor did combinations of UNC-50, UNC-74 with EAT-18. It was only when EMC-6 or NRA-2 and NRA-4 were included with RIC-3 where *B. malayi* ACR-16 produced measurable currents.

These findings indicate that there is a phylogenetic change in the requirement of accessory proteins down this receptor's phylogeny for three reasons. First, changes in the effects that some of the accessory proteins had were phylogenetic. Specifically, EAT-18 increased responses for the first two species *A. suum* and *D. medinensis*, but not for the later more derived species *G. pulchrum, T. callipaeda* or *B. malayi*. Second, the increased responses for the "intermediate" receptors, when NRA-2 and NRA-4 were included, indicate that a gradual change has occurred in the receptors' ability to functionally express in *X. laevis* oocytes. This change can be reversed by including NRA-2 and NRA-4, because only later Clade III receptors' responses are increased. Third, the small currents obtained with BMA-ACR-16 confirm that it is indeed a functional homomeric channel, however, changes occurred in it that cause it to require the addition of at least three additional accessory proteins that the other receptors do not need. The responses obtained with BMA-ACR-16 are very small in comparison to those of the other ACR-16s, it is likely that there is at least one other unidentified accessory protein that is required. Considering receptor synthesis machinery is complex and might involve over 200 proteins (Gottschalk et al., 2005), what else is missing has likely yet to be identified.

EMC-6, NRA-2 and NRA-4 are all ER-resident proteins involved in subunit stabilization and pentamer assembly (Almedom et al., 2009; Kashyap et al., 2021; Richard et al., 2013). It is therefore possible that the changes that have occurred down ACR-16 phylogeny have affected the stability of pre-assembled subunits and/or the assembly process. EMC-6 is one protein within an entire ER membrane protein complex (EMC). EMC is conserved throughout the eukaryotes and is estimated to contain 8 – 10 different proteins (Wideman, 2015). EMC functions as an

insertase by directing the appropriate insertion of transmembrane domains through the membrane. Little is known about its exact mechanism, but recent structures suggest the EMC proteins form a grove within the membrane that guides the transmembrane domain of another protein (Bai et al., 2020; O'donnell et al., 2020). The *C. elegans* characterization of EMC-6 found at least 5 other EMC genes predicted within its genome and RNAi of each decreased L-AChR responses in muscle (Richard et al., 2013). It is possible that their addition would produce higher *B. malayi* ACR-16 receptors.

NRA-2 is a nicalin-like homolog but contains an additional calcium sensing EF hand motif. NRA-4 is a NOMO-like homolog. In *B. malayi*, NRA-2 is thought to sense intracellular influx of calcium and regulate the levels of the different L-AChR subunits to produce receptors with different subunit combinations (Kashyap et al., 2021). In *C. elegans,* NRA-2 and NRA-4 KO worms had reduced L-and N- AChR responses and the L-AChR had altered properties. It was proposed that they function together by determining the subunits that form a channel and exit the ER (Almedom et al., 2009). However, in another study, NRA-2 was found to act as a quality control check to retain mutant DEG/ENaC channels in the ER, preventing cell death (Kamat et al., 2014). In vertebrates, nicalin and NOMO proteins function by regulating the expression of transforming growth factor beta receptors (Haffner et al., 2007) and may also catalyze signal peptide cleavage (Dettmer et al., 2010). Therefore, precise function and mechanism of nematode ion channel regulation of NRA-2 and NRA-4 remains unclear and may differ from those of their vertebrate homolog. Based on the proposed functions of EMC-6, NRA-2 and NRA-4, it is clear their ER stages of receptor synthesis has changed. Focusing future efforts onto proteins involved in stages within ER stages of synthesis may uncover which other accessory protein is missing and specifically how later Clade III receptors have changed.

To confirm the decrease in receptor expression at the surface of the oocyte, tagging each subunit with a short tag followed by chemiluminescence measurement would provide relative amounts of membrane surface receptor. This technique has been previously carried out to identify signal sequences for appropriate receptor folding and was able to correlate maximal responses with surface expression (Etxeberria et al., 2004; Maue, 2007; Zerangue et al., 1999). Furthermore, patch clamp electrophysiology would exclude that the decrease in response is not due to changes in the transmembrane domain 2 that affect ion conductance through the channel pore (Emlaw et al., 2021).

The changes in ACR-16 may explain why other later Clade III worm receptors have yet to be reconstituted *ex vivo*. The use of an evolutionary approach to follow functional change in accessory protein requirement is novel. At least part of the mechanism preventing successful filarial acetylcholine receptors (AChRs) in oocytes has been identified. This will have a major impact, not only in the successful reconstitution of drug target receptors in the filarial nematodes with a view to understanding anthelmintic action, but on possibly allowing reconstitution of native AChRs from other organisms that have yet to be reconstituted. One other notable finding from this chapter was that *D. medinensis* ACR-16 no longer requires any RIC-3 for expression in oocytes. This was unexpected because all ACR-16 receptors need RIC-3 (Abongwa et al., 2016; Boulin et al., 2008; Charvet et al., 2018; Choudhary et al., 2019; Hansen et al., 2021; Kaji et al., 2020) and indicates specific changes occurred in this receptor mediating its ability to not require any additional accessory protein. This is interesting because it is currently not known what structural regions or sequences determine RIC-3 requirement for expression and the minimal sequence change between *D. medinensis* ACR-16 and *A. suum* ACR-16 provides the opportunity to identify it. This was investigated in Chapter 6. Now that a *B. malayi* acr-16 receptor can be recorded in oocytes, a number of questions remain. What region of the receptor is responsible for this change in AP requirement? Has the receptors pharmacology differed from other ACR-16 receptors? And finally, can these new APs also allow the measurement of a *B. malayi* L-AChR? These questions are investigated in Chapter 5.

Chapter 5: *B. malayi* nicotine-sensitive acetylcholine receptor characterization

5.1 Introduction

Now that a *Brugia malayi* receptor can be reconstituted, several questions remain. First, in Chapter 2 I reviewed the fact that nematode levamisole-sensitive acetylcholine receptors (L-AChRs) differ in their subunit composition between species as subunits are lost or duplicated. Characterization of duplicate *unc-29* showed that pharmacological properties were largely unaffected between the different copies but the interaction and ability to produce a functional receptor were (Duguet et al., 2016). In the literature review I also reviewed the role of accessory proteins (APs) in receptor production and the fact that they have been found to regulate receptor composition. In Chapter 4 I found a similar phenomenon where the pharmacological properties of the nicotine-sensitive acetylcholine receptor (N-AChR) were consistent between species of Clade III nematodes, but their requirement for APs changed progressively. The co-injection of accessory proteins involved in subunit stabilization and assembly within the ER (EMC-6, NRA-2 and NRA-4) produced measurable *B. malayi* ACR-16 currents. ACR-16 provides an ideal opportunity to investigate the basis for interactions with the AP network, something that appears to be a major aspect of pentameric ligand-gated ion channel (pLGIC) evolution. How receptors evolve requirements for accessory proteins, and why, is not known. ACR-16 is an opportunity to provide the first report and investigation of what regions undergo evolutionary change for accessory protein requirement. The sites identified in this example can be used to understand how subunits interact with accessory proteins in the ER allowing them to be stabilized pre-assembly and to potentially predict the AP requirement for other receptors. This would provide novel information on receptor change and synthesis. To address this, a series of chimeras will be made, exchanging each of the three main regions between *Ascaris suum* and *Thelazia callipaeda*. *T. callipaeda* will be used, as opposed to *B. malayi*, because it is the closest relative to *B. malayi* that produces large consistent results.

Second, characterizing the *B. malayi* receptor would answer if the acquired accessory protein (AP) requirement coincides with pharmacology changes. Based on the receptor characterization from Chapter 4, it is expected that the change in accessory protein requirement does not affect receptor pharmacology. To characterize the BMA-ACR-16 receptor, first, a

combination of different accessory protein combinations using the three new APs will be co-injected with it to identify which combination best expresses the receptor. Using the accessory protein combination that produces the highest and most consistent BMA-ACR-16 receptor response, ligand affinity and agonist response profiles will be measured. This will not only confirm if AP requirements occurs independently of receptor pharmacology, but it will also be the first *ex vivo* characterization of a *B. malayi* acetylcholine receptor (AChR).

Finally, knowing that ACR-16 has changed in its accessory protein requirement, applying this to the L-AChR would confirm if the heteromeric receptor has also undergone the same accessory protein changes that prevent functional reconstitution in oocytes. To investigate this the *B. malayi* subunits from Chapter 2 will be combined with the accessory proteins from Chapter 3 & 4 and responses measured. The work in this Chapter will identify the regions that regulate changing in accessory protein requirements, characterize *B. malayi* ACR-16, and investigate if AP changes is also causing the difficulty in *B. malayi* L-AChR expression.

5.2 Results

5.2.1 Changes in the ECD and ICL regulate ACR-16 AP requirement

Chimeras were made between *A. suum* and *T. callipaeda* to identify the general structural region mediating the change in ACR-16 AP requirement. *T. callipaeda* was used in the place of *B. malayi* because if no response was obtained with the chimeras, then we would not know if it is because of the act of making the chimera or because it is the region that mediates new AP requirement. *A. suum* -*T. callipaeda* chimera nomenclature is shown in Figure28A. Coding sequences were first modified to introduce multiple complementary restriction enzyme sites (termed REM), these would be used to construct chimeras with restriction enzyme digestion reactions. Responses of REMs compared to unmodified sequences (Appendix Figure 2) show that the modifications did not affect receptor response. The three main structural regions (extracellular domain ECD, intracellular loop ICL, & transmembrane domains TMs) were exchanged between the two receptors, and reversal of maximal response compared to the native receptors was used to determine if the region contributes to the AP requirement change.

Exchanging the ECDs completely reversed maximal response. TZC-ECD (Asu-acr-16 with the *T. callipaeda* ECD) inhibited nearly all response to ACh (42 ± 9 nA, $p<0.0001$) whereas the ASU-ECD chimera (TZC-ACR-16 with the *A. suum* ECD) significantly increased responses

(1819 ± 115 nA, $p<0.0001$) (Figure 28B). Exchanging the TMs had no effect on reversing the responses. In fact, replacing the TZC-ACR-16 with the ASU TMs severely decreased maximal response (24 ± 8 nA, $p<0.0001$). This may reflect specific co-evolution of regions within the *T. callipaeda* TM and ECD & ICL that need to coincide together for efficient expression. Interestingly, both ICL chimeras produced large responses. ASU-ACR-16 with the *T. callipaeda* ICL (TZC-ICL) responses were not significantly different from native ASU-ACR-16 (1959 ± 78 nA), which suggests the ICL is not involved. However, TZC-ACR-16 with the *A. suum* ICL significantly increased responses compared to TZC-ACR-16 (2237 ± 98 nA, $p<0.0001$), which suggests the ICL is involved because its removal from tzc-acr-16 increased responses. Maximal responses of the chimeras compared to those of their native full-length receptors suggests two regions have changes that regulate AP requirement with different levels of contribution to this effect. The ECD has the most contribution to maximal responses followed by the ICL, and the effect of the ECD can overshadow the effect of the ICL.

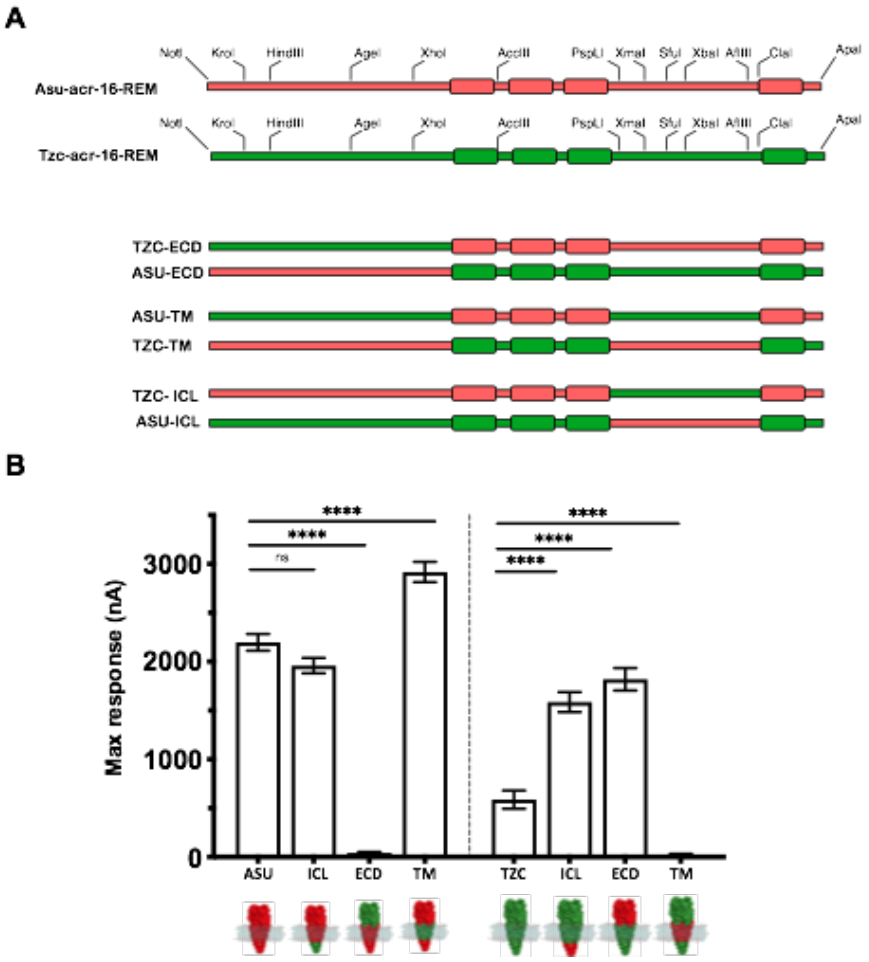

Figure 28. *A. suum* and *T. callipaeda* ACR-16 chimeras.

The three main structural regions (ECD, ICL & TM) were exchanged between the two receptors to identify the regions mediating the declining responses in later Clade III ACR-16 receptors. *A. suum* shown in red and *T. callipaeda* in green.
(A) *A. suum* and *T. callipaeda* acr-16 coding sequences were modified to introduce restriction enzyme sites to constrict chimeras. The three main structural regions (ECD, ICL, TMs) were exchanged between the two receptors. (A) the modified sequences introduced complementary restriction enzyme sites termed ACR-16-REM. TZC-ECD contains the *A. suum* sequence with the *T. callipaeda* ECD. ASU-ECD contains the *T. callipaeda* sequence with the *A. suum* ECD. ASU-TM contains the *T. callipaeda* sequence with the *A. suum* TM. TZC-TM contains the *A. suum* sequence with the *T. callipaeda* TM. TZC-ICL contains the *A. suum* sequence with the *T. callipaeda* ICL. ASU-ICL contains the *T. callipaeda* sequence with the *A. suum* ICL.
(B) Increased responses were obtained when the ICL or ECD of *A. suum* were introduced into the *T. callipaeda* receptor, and conversely decreased responses were obtained when the ICL or ECD of *T. callipaeda* were introduced into the *A. suum* receptor. Indicating the ICL and ECD govern the declining response. The greatest differences in responses observed with the ECD compared to the ICL exchanges suggest the ECD contributes more than the ICL. Error bars represent standard error. ****$p<0.0001$. See Appendix Table 5 for values.

5.2.2 Accessory proteins

Although BMA-ACR-16 currents were finally measured with additional accessory proteins in Chapter 3, they were still very small, which would make measuring receptor pharmacology difficult. The receptor was thus co-injected with various accessory protein mixtures to identify the combination that produces the highest response, which would then be used for receptor characterization. A chimera was made between BMA-ACR-16 and ASU-ACR-16 in the event that the responses would still be too small with all AP combinations tried. This chimera design would have to enhance expression while still containing the main *B. malayi* receptor pharmacology regions. Therefore, based on the results of the *A. suum- T. callipaeda* chimeras (Figure 28), it exchanged the ICL between *B. malayi* and *A. suum* ACR-16. This allows the chimera to contain the major pharmacology-related region (the ECD and TM) and exchange one of the regions contributing to the dampened response (the ICL) (Figure 29 Chimera-4). Basic receptor pharmacology can be inferred from ICL chimeras because major ligand-interacting and receptor gating regions are found in the ECD and TM regions (Corringer et al., 2012; Dacosta & Baenziger, 2013; Smart & Paoletti, 2012; Thompson et al., 2010). ICL chimeras have been used previously and shown to not affect receptor pharmacology (Eiselé et al., 1993; Mnatsakanyan et al., 2015). A control of the reverse chimera (*A. suum* acr-16 with the *B. malayi* ICL, Figure 29 Chimera-3) was included to ensure the exchanged ICL did not affect receptor properties. Chimera-3 and Chimera-4 were characterized alongside the *B. malayi* ACR-16.

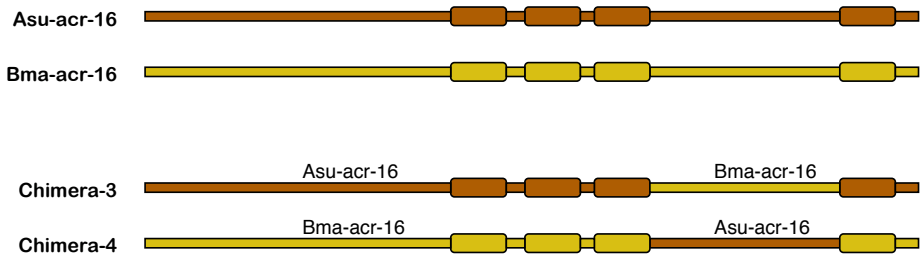

Figure 29. *A. suum* and *B. malayi* acr-16 chimeras.

Chimeras were made between *A. suum* and *B. malayi* acr-16 to characterize *B. malayi* acr-16 in the event that the unmodified *B. malayi* acr-16 did not produce robust enough responses for characterization. The intracellular loop was exchanged since it is one of the regions thought to contribute to the declining responses observed in Clade III acr-16 and it does not contain the ligand-binding regions. Chimera-3 contains the *A. suum* acr-16 extracellular domains and transmembrane domains with the *B. malayi* intracellular loop. Chimera-4 contains the *B. malayi* acr-16 extracellular domains and transmembrane domains with the *A. suum* intracellular loop. See Figure 30 for responses, Figure 31 for EC_{50}, and Figure 32 for ligand panel analysis.

BMA-ACR-16 responses were small regardless of AP condition (Figure 30 black bars & Appendix Table 7). The highest responses obtained when it was co-injected with RIC-3 + NRA-2 or RIC-3 + EMC-6. Smaller responses were observed when more APs were added, and in some cases abolishing response entirely. Inhibited responses with adding accessory proteins has been previously recorded for other ACR-16 receptors (Abongwa et al., 2016; Boulin et al., 2008; Choudhary et al., 2019). Chimera-4 responses were still quite small, but under some conditions larger than BMA-ACR-16, specifically RIC-3, RIC-3 + NRA-2, RIC-3 + NRA-2 + NRA-4, and RIC-3 + EMC-6 (Figure 30 teal bars). As with Bma-acr-16, the RIC-3 + NRA-2 + NRA-4 + EMC-6 conditions dampened responses. Based on these results, receptor characterization was done with RIC-3+ NRA-2. Chimera-3 produced large responses both with RIC-3 and with RIC-3 + NRA-2 (Figure 30 purple bars).

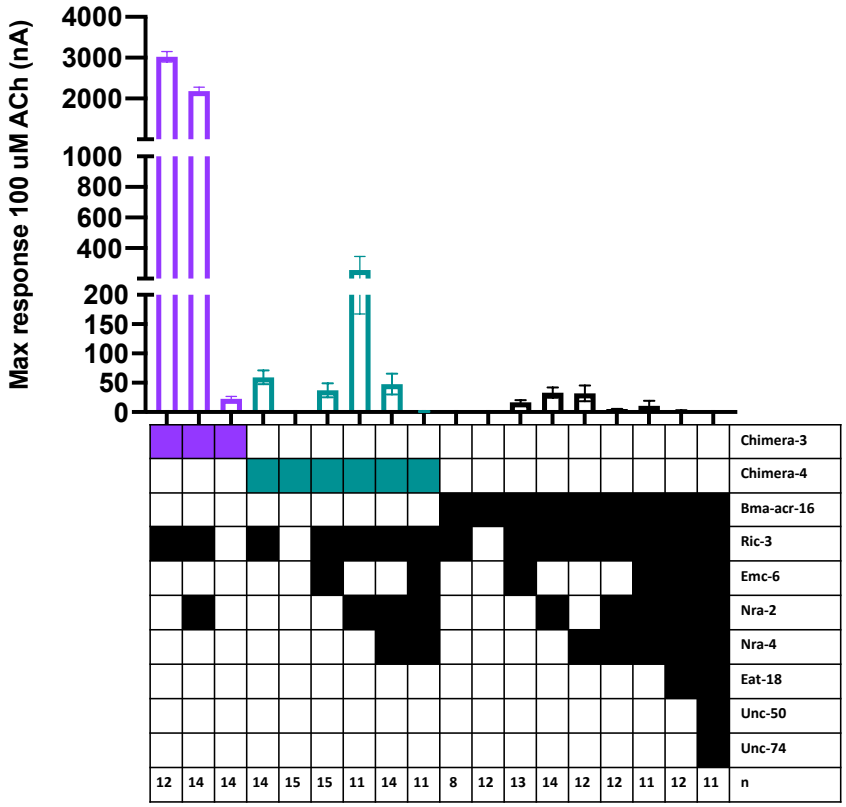

Figure 30. Effect of accessory protein combinations on *B. malayi* acr-16.
The effect of different accessory protein mixtures were included to identify the combination that produces the highest *B. malayi* acr-16 response. Chimera-4 was included as a back-up in case *B. malayi* responses were still too small for further pharmacology characterization. Chimera-3 in purple, chimera-4 in teal, *B. malayi* acr-16 in black. Error bars represent standard error. See Appendix Table 7 for values.

5.2.3 *B. malayi* ACR-16 pharmacology characterization

In order to confirm that the *B. malayi* ACR-16 receptor has undergone changes to its functional expression and not receptor pharmacology, EC_{50} and agonist response profiles were measured. Based on the accessory protein responses from Figure 30, RIC-3 and NRA-2 were included with each of the BMA-ACR-16, Chimera-4 and Chimera-3 receptors. This AP combination was chosen to best ensure the largest and most consistent BMA-ACR-16 responses. Despite this, the BMA-ACR-16 responses were not consistent enough and too small to obtain reliable EC_{50} and ligand panel analysis (data not shown). With each agonist exposure, responses diminished until none were obtained. Therefore Chimera-4 and Chimera-3 EC_{50} were measured. EC_{50} to both ACh and nicotine (NIC) are shown in Figure 31 and Appendix Table 6. Chimera-3 served as a control and its EC_{50} would be compared to the EC_{50} of the full length ASU-ACR-16. Chimera-3 EC_{50} to acetylcholine was 4.3 ± 0.5 μM which is lower than the asu-acr-16 EC_{50} (8.9± 0.3 μM) but within range of the other Clade III ACR-16 ACh EC_{50} (Figure 24 & Table 2). The Chimera-3 EC_{50} to nicotine was 4.3 ± 0.5 μM which is very similar to the Asu-acr-16 EC_{50} (5.1 ± 0.2 μM). The similarity in these EC_{50} confirm the intracellular loop chimeras will provide accurate measurements of the Bma-acr-16 receptor pharmacology. Chimera-4 EC_{50} to acetylcholine was 15.7 ± 2 μM and 2.1 ± 0.3 μM to nicotine. Like other Clade III ACR-16 receptors (Abongwa et al., 2016; Charvet et al., 2018), the affinity for nicotine was higher compared to acetylcholine, and they were both within range of the other Clade III nicotine EC_{50} (Chapter 4 Table 2 and Figure 24). The similarity in the EC_{50} confirm that the BMA-ACR-16 receptor agonist affinities have not drastically changed, and that its change in the requirement for additional accessory proteins did not coincide with any changes to receptor-ligand interactions or response.

Responses to a panel of ligands was, with two exceptions, as expected. Both chimeras responded to NIC, dimethylphenylpiperazinium (DMPP), oxantel (OXA), morantel (MOR), and pyrantel (PYR), and had no responses to NOR, dopamine (DA), betaine (BET), bephenium (BEPH) or tyramine (TYR) (Figure 32 and Appendix Table 4). However Chimera-3 response to DMPP was increased compared to Asu-acr-16 (Chapter 4 Figure 25) and Chimera-4 response to NIC was lower relative to ACh, compared to the other ACR-16s (Chapter 4 Figure 25). Possible explanation for this is in the Discussion.

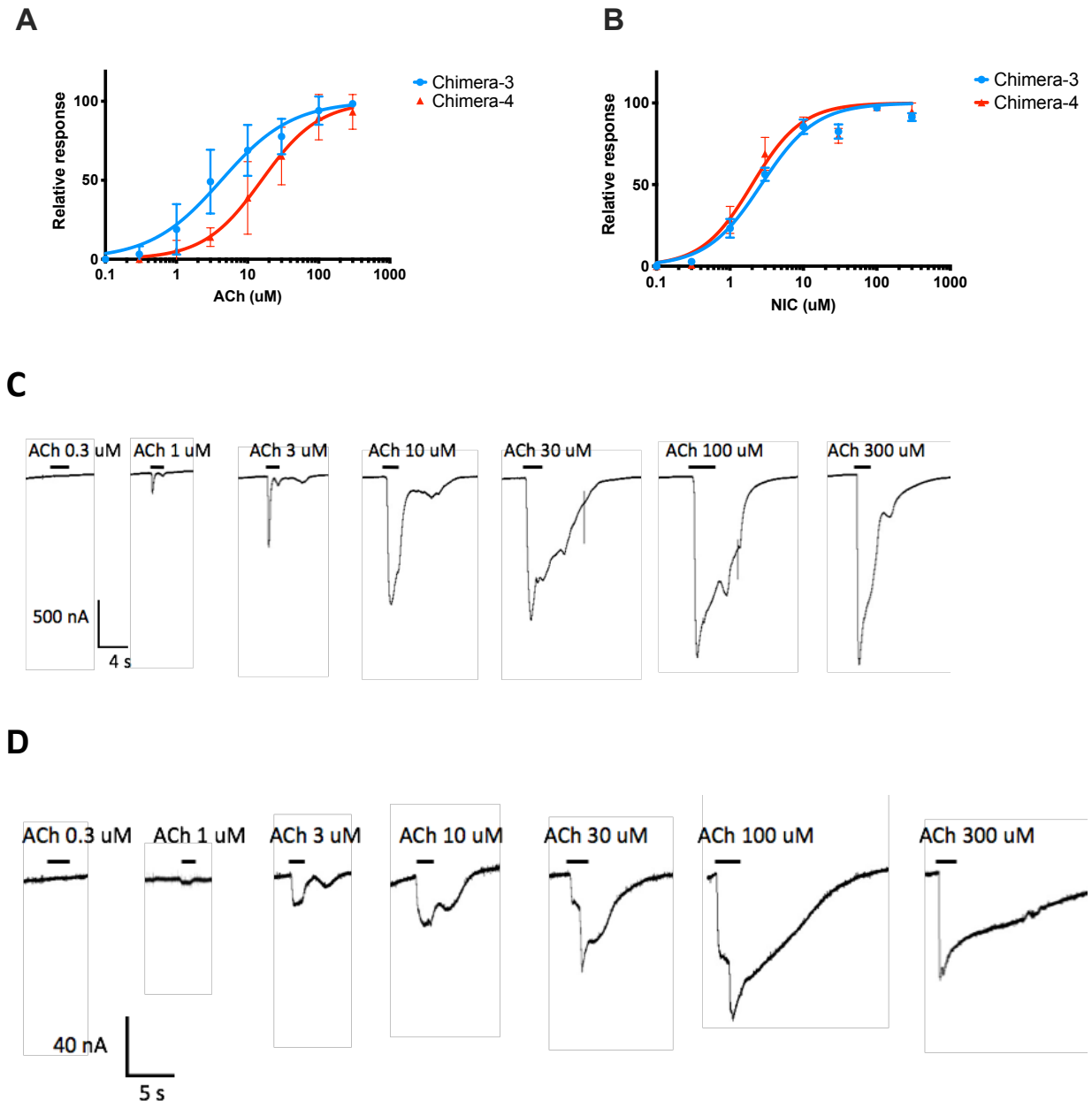

Figure 31. *B. malayi* ACR-16 has unchanged agonist affinity.

Dose-response curves were measured to compare Bma-acr-16 agonist affinity to other ACR-16 receptors. Dose-response curves for acetylcholine (A) and Nicotine (B) are shown. Representative recordings of responses to ACh for (C) Chimera-3 and (D) Chimera-4. Agonist affinity for *B. malayi* acr-16 chimera was not different from other ACR-16 receptors. *A. suum* acr-16 chimera (chimera-3) served as a control. See Appendix Table 6 for values. Error bars represent standard error.

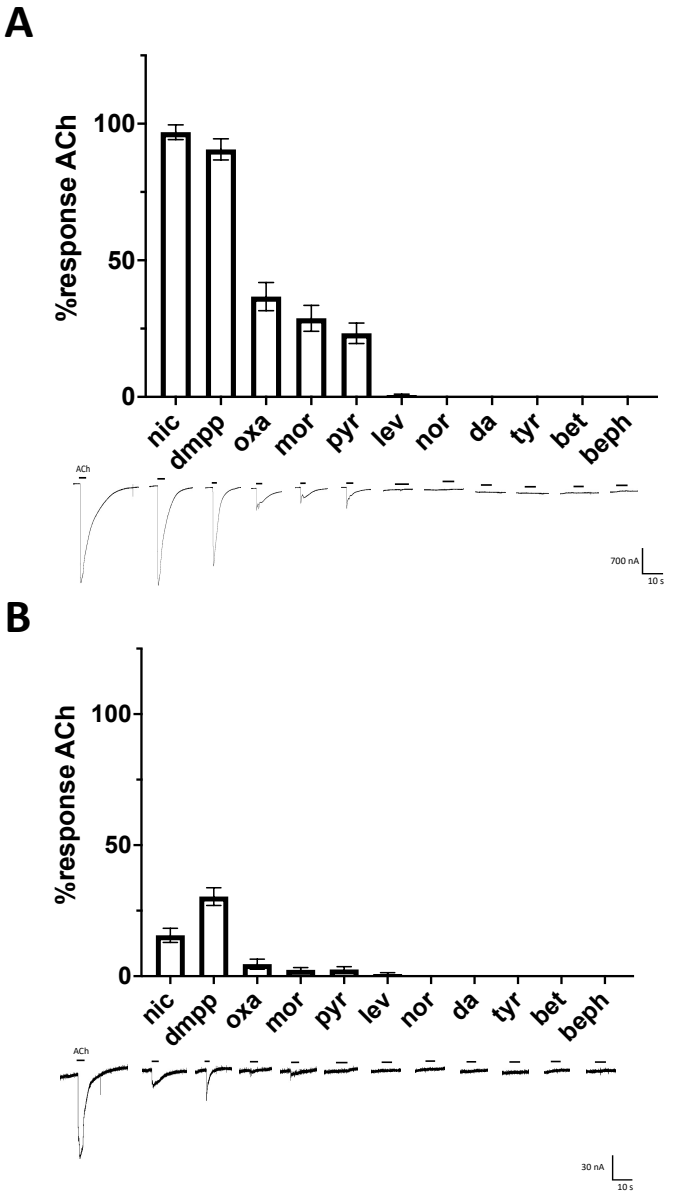

Figure 32. *B. malayi* ACR-16 has unchanged agonist response profile.

Responses to agonists relative to ACh (100 μM) were measured to compare to other ACR-16 receptors. Dose-response curves for (A) Chimera-3 (B) Chimera-4. Except for smaller responses to NIC, the *B. malayi* chimera responded to the same panel of ligands. Chimera-3 served as a control. See Appendix Table 4 for values.

5.2.4 *B. malayi* subunits and accessory protein combinations

The addition of NRA-2, NRA-4 or EMC-6 restored part of the inability to produce a *B. malayi* ACR-16 receptor in oocytes. ACR-16 was used as a model to understand why the L-AChR was not reconstituted in oocytes. To confirm if the three APs that gave BMA-ACR-16 currents also produce an L-AChR, the *B. malayi* subunits from Chapter 2 Figure 19 were combined with them. Since some of the AP conditions in Figure 30 completely abolished all BMA-ACR-16 responses, different AP combinations were considered. These included all APs that did not show any current inhibition or any of the channels (i.e. all APs except MOLO-1) and combinations of NRA-2, NRA-4 and EMC-6 on their own or in combination. All of these mixtures also include UNC-50 and UNC-74 because they are required for other worm L-AChR (Boulin et al., 2011; Boulin et al., 2008; Buxton et al., 2014; Williamson et al., 2009). Unfortunately, no measurable current to ACh, LEV, NIC, OXA, MOR, PYR or BEPH was obtained from any of the injection combinations (Figure 33 shows combinations tried).

■	■	■	■	■	■	Bma-acr-8
■	■	■	■	■	■	Bma-unc-29
■	■	■	■	■	■	Bma-unc-38.1
■	■	■	■	■	■	Bma-unc-38.2
■	■	■	■	■	■	Bma-unc-63.1
■	■	■	■	■	■	Bma-unc-33.2
■	■	■	■	■	■	Bma-acr-16
■	■	■	■	■	■	Bma-acr-15
■	■	■	■	■	■	Bma-acr-12
■	■	■	■	■	■	Bma-acr-26
■	■	■	■	■	■	Bma-ric-3
■	■	■	■	■	■	Bma-unc-74
■	■	■	■	■	■	Bma-unc-50
■	■			■		Cel-emc-6
■		■		■	■	Cel-nra-2
■			■	■	■	Cel-nra-4
■						Bma-eat-18
10	11	12	10	10	11	n

Figure 33. *B. malayi* subunits with all accessory protein conditions produced no responses.
B. malayi subunits were co-injected with various accessory protein combinations to determine if they can produce receptors. Combinations included RIC-3, NRA-2, NRA-4, EMC-6, UNC-50, UNC-74 and EAT-18. No responses were measured to any of the ligands used; ACh, LEV, NIC, OXA, MOR, PYR or BEPH.

5.3 Discussion

5.3.1. Changes in the ECD and ICL regulate ACR-16 AP requirement

Chimeras are a common tool when identifying receptor functional regions (Duret et al., 2011; Martinez-Torres, 2000; Tillman et al., 2014). In this case, chimeras were made between *A. suum* and *T. callipaeda* to identify the general structural region mediating the change in ACR-16 AP requirement. *T. callipaeda* was used in the place of *B. malayi* because if no response was obtained with the chimeras, then we would not know if it is because of the act of making the chimera or because it is the region that mediates new AP requirement. These results of these chimeras were not as straightforward as hoped, likely because *A. suum* and *T. callipaeda* have diverged, therefore more sequence change has occurred that obscures specific region identification.

The chimeras suggest two regions contribute to the change in maximal responses, the ECD and the ICL, and that the ECD has greater contribution and can "override" the effect of the ICL. In other words, if the sequence has the *T. callipaeda* ICL, it also requires the *T. callipaeda* ECD to have inhibited responses, however if it has the *T. callipaeda* ECD, it does not require the ICL. The TMs have no effect on the decline observed, however replacing the *T. callipaeda* TMs with the *A. suum* TMs severely decreased maximal response. This might be explained by specific changes in the TM regions that have coevolved with other regional changes required for efficient expression.

The ECD and ICL may be the regions in the channels that physically interact with the accessory proteins that are now required in later Clade III receptors. Indeed, NRA-2 and NRA-4 are both single-pass transmembrane proteins with large luminal regions (Almedom et al., 2009; Kashyap et al., 2021), and EMC-6 contains two transmembrane domains with two short regions within both luminal and cytoplasmic regions (Richard et al., 2013). The ECD effect on maximal response coincides with the fact that the ECD is the region that contains major assembly and folding sequences (Eertmoed & Green, 1999; Sumikawa & Nishizaki, 1994). Therefore if drastic changes to receptor synthesis were to occur, it would likely be within the ECD.

Interestingly, relatively few amino acid changes are found within the ACR-16 ECD (Chapter 4 Figure 22). The BMA-ACR-16 ECD is 96% similar to the TZC-ACR-16 ECD, and both are 92% similar to ASU-ACR-16. A follow up study could investigate if all, some, or just

one of those amino changes are responsible for the functional expression changes. Identifying the specific changes in the ICL would be more challenging because it is highly variable and its effects on receptor maximal response is small compared to the effects of the ECD.

5.3.2 *B. malayi* ACR-16 with accessory protein combinations

A number of accessory protein mixtures were used to identify the combination that best expresses BMA-ACR-16. Maximal responses showed that EMC-6, NRA-2 and NRA-4, individually with RIC-3, all produce measurable currents. Any combinations that include more APs began to dampen responses. This was also observed with Chimera-4. The addition of more accessory proteins abolished responses altogether. This has been observed previously with other ACR-16 receptors (Abongwa et al., 2016; Boulin et al., 2008; Choudhary et al., 2019) and may be explained by either the cell being injected with too much RNA or the APs interacting with one another and affecting their ability to efficiently express the channel. Since these proteins are not endogenous to the oocytes it is possible that there are other proteins in the muscle cells that regulate the inter-AP interaction network to ensure they do not interfere with the expression of channels. Two observations support the *A. suum* and *T. callipaeda* chimera conclusions that the ECD is the region that has changed. First, Chimera-4 still produced small responses under all AP conditions and second the Chimera-3 produced large responses when RIC-3 was included. If the *B. malayi* ICL was the only problem, Chimera-3 would have severely lower responses while Chimera-4 would produce large responses. These confirm that the *B. malayi* ICL is not the region inhibiting receptor expression (or at the very least not the only region on its own), further validating the *A. suum/T. callipaeda* chimera results. Based on these accessory protein conditions, RIC-3 + NRA-2 were used for BMA-ACR-16 characterization, however RIC-3 + EMC-6 or RIC-3 + NRA-4 could have also been used.

Two observations further confirm that the *B. malayi* receptor has undergone changes to its interactions with accessory proteins. First, NRA-2 + NRA-4 enhanced the other Clade III receptor responses (Chapter 4 Figure 27) but dampened *B. malayi* (Figure 30), and second, Emc-6 did not increase maximal responses for the other ACR-16s (Chapter 4 Figure 27) but it did for *B. malayi* (Figure 30). All three APs act within the ER, therefore it is likely that the changes in Bma-acr-16 have affected its either subunit stability, folding or assembly and now require additional protein chaperones. Considering the BMA-ACR-16 responses are still very small and inconsistent, it is highly likely that a critical accessory protein that acts in the ER that has yet to

be identified is missing. It is also possible that all the missing APs are included, but not in the right ratio. AP ratios have been known to affect receptor kinetics RIC-3 (Ben-David et al., 2016; Bennett et al., 2012). Investigating this would require altering the relative ratios of the APs and measuring any changes to maximal response.

What do these accessory proteins do? NRA-2 and NRA-4 work in tandem to ensure only the appropriately assembled subunits exit the ER (Almedom et al., 2009). In their absence the L-AChR and ACR-16 receptors contained subunits in altered ratios or the wrong subunits entirely (Almedom et al., 2009). Recently NRA-2 it has been found to regulate the "plasticity" in *B. malayi* AChR subunit composition upon exposure to levamisole (Kashyap et al., 2021). NRA-2 has also been implicated in controlling the subunit composition of other ion channel families in *C. elegans* (Kamat et al., 2014). Therefore it may function broadly regulating the general receptor composition and stoichiometry. NRA-2 is homologous to the human nicalin protein (another ER associated protein involved in the stability and assembly of ER protein complexes) and NRA-4 is also an ortholog of this membrane complex (Almedom et al., 2009). Why would the addition of NRA-2 or NRA-4 produce measurable currents? It could be that in their absence, improperly folded/assembled channels exit the ER and the cell exhausts its resources on non-functional channels, but when included, they prevent misfolded/assembled proteins from exiting the ER (thus getting sent for degradation) and the cell can then use its resources on the (very few) channels that are properly assembled. Measuring receptor levels at the oocyte membrane surface would provide insight into relative levels at the surface, however it would not provide insight into their functional form. Further studies testing the subunit composition of receptors at the membrane surface with and without the NRA accessory proteins would confirm if there is a problem in subunit composition. However ACR-16 is homomeric, so this may be more realistic using a heteromeric receptor.

EMC-6 is an ER transmembrane protein whose knock-out in *C. elegans* led to decreased responses from all three body wall muscle receptors (L-AChR, ACR-16 and UNC-49) and decreased expression of at least the L-AChR (Richard et al., 2013). Vertebrate orthologs of EMC-6 function in an ER complex with other proteins (ER membrane protein complex termed EMC) regulating the appropriate insertion and orientation of transmembrane proteins in the membrane (Bai et al., 2020; Shurtleff et al., 2018). It is thus involved in the processing of many proteins. The widespread expression profile of *C. elegans* EMC-6 coupled with knock-out

phenotypes other than the traditional LEV resistance behaviour further supports a potential broad function for this complex (Richard et al., 2013). Co-injection of EMC-6 may promote the appropriate folding and processing of BMA-ACR-16, thus increasing the amount of functional protein at the membrane surface. In its absence is it possible that BMA-ACR-16 is not inserted into the membrane properly, which would target it for degradation. Five other EMC-6 paralogs are predicted in the *C. elegans* genome (Richard et al., 2013), and it is possible their coinjection with BMA-ACR-16 may further increase responses in oocytes. Investigating the relationship and details of the entire EMC complex as a whole would provide specific insight into not only ion channel folding but insight into the general mechanisms of protein folding as a whole.

Although the functions of NRA-2 & NRA-4 and EMC-6 are different, they all act within ER stages of protein synthesis (Almedom et al., 2009; Bai et al., 2020; Kamat et al., 2014; Richard et al., 2013). It is therefore possible that it is not one specific stage of receptor synthesis that has changed within Clade III worms but rather early receptor synthesis as a whole. The obvious next question is why did this change occur? Did the pLGIC gene loss and gene duplication events in Clade III worms create an instability in ion channels that resulted in changes to the expression machinery as well? Or were there changes in the expression machinery, for reasons unrelated to pLGICs, which then created an environment that favoured pLGIC subunit gene loss/duplication events. Answering these questions is difficult because it occurred millions of years ago, nevertheless investigating the Clade III receptors' need for additional accessory proteins and what regions mediate is fundamental for understanding basic channel biology. Although many questions remain unanswered with how the interaction has changed between the receptor and its accessory proteins, the present results indicate that it is indeed receptor change that has occurred along the ACR-16 phylogeny because maximal response changes to the same AP can be different depending on the receptor.

5.3.3. *B. malayi* ACR-16 pharmacology

EC_{50} and ligand panel analysis to BMA-ACR-16 were carried out to confirm the change in AP requirement occurs independently of receptor pharmacology. Attempts to characterize the full length BMA-ACR-16 proved unsuccessful. Although currents were obtained with Bma-acr-16 (<35 nA) after a couple exposure to ligands responses were noticeably diminished which would make any characterization unrealistic. This is likely because the responses were so small to begin with that after time egg quality decreases and affects receptor response. To overcome

this a chimera was made containing the *B. malayi acr-16* sequence with the ICL of *A. suum* (Chimera-4). This chimera was made based on the chimera results earlier in this Chapter. The ICL contributes in part to the decreased responses, therefore by exchanging the ICL between *A. suum* and *B. malayi, B. malayi* current would be increased while leaving the major ligand-response regions (ECD and TMs) intact (Corringer et al., 2012; Dacosta & Baenziger, 2013; Smart & Paoletti, 2012; Thompson et al., 2010). In case the ICL exchanges affect receptor properties, the reverse chimera of *A. suum acr-16* sequence with the ICL of *B. malayi* was included as a control to compare to the native *A. suum* receptor (Chimera-3).

Overall both chimeras had responses comparable to ACR-16s from Chapter 4, with slight exceptions. Chimera-3 had a higher affinity for ACh and higher relative responses to DMPP compared to *A. suum*. Chimera-4 had lower responses to NIC compared to the other ACR-16s. The lower responses of Chimera-4 to NIC may be explained by the small currents. Although this chimera produced larger responses compared to BMA-ACR-16, responses were still small, therefore after multiple drug exposures any changes to oocyte viability will have noticeable effects on ligand responses. The lower EC_{50} and increased response to DMPP of Chimera-3 may be explained by the introduction of the B. *malayi* ICL. Although all major and well-studied ligand-binding and gating domains were preserved in the chimera, the ICL has been found to contribute to receptor function. Chimeric receptors changing the ICL or inducing mutations within it have been attributed to affect ion permeability, desensitization, maximal responses and reduced agonist efficacy (O'Toole & Jenkins, 2011). Other reports show ICL chimeras do not affect receptor pharmacology (Eiselé et al., 1993; Mnatsakanyan et al., 2015), therefore it may depend on the details of the receptors being studied. In our case, the ICL may contribute to some aspects of receptor pharmacology. However, despite these changes, receptor function was largely preserved in Chimera-3, validating Chimera-4 pharmacology.

Considering these minor changes to the expected Chimera-3 and Chimera-4 pharmacology, additional pharmacological characterization to further confirm the receptors have not changed in response include measuring responses to cholinergic antagonists and measuring EC_{50} to other agonists (such as DMPP or OXA as they give large responses) could also be carried out. Regardless, this represents the first *ex vivo* characterization of a *B. malayi* AChR and confirms no large changes to BMA-ACR-16 pharmacology coincide with the change in accessory protein requirement.

5.3.4. *B. malayi* AChR subunit and accessory protein combinations

The goal of characterizing the change in BMA-ACR-16 was to apply it to the L-AChR in the hopes of obtaining a *B. malayi* L-AChR. Different combinations of the APs were included with all *B. malayi* subunits. AP included RIC-3, UNC-74, UNC-50, EMC-6, NRA-2, NRA-4 and EAT-18 and various combinations of them. Despite these different combinations, no responses to ACh, LEV, NIC, OXA, MOR, PYR or BEPH were obtained. As mentioned, is it likely the "critical" accessory proteins that are missing are not presently known. It is possible that since ACR-16 is homomeric and "simpler" the changes to the heteromeric L-AChR receptor may be even more extreme and depend on even more APs. This is true for the *C. elegans* and *A. suum* ACR-16 and L-AChRs (Boulin et al., 2008; Williamson et al., 2009). However, if there is an accessory protein that is so crucial to receptor synthesis, why has it not yet been identified? It is possible that the accessory protein is unique to invertebrates or that it is only slightly involved in receptor synthesis in other worms but increasingly involved in later Clade III worms, and since AP research has been done on *C. elegans*, it would not be easily identified. However, whatever the missing protein is, based on the work in this chapter, it is likely involved in the ER, makes critical interactions with regions in the receptors ECD and involved in both ACR-16 and L-AChR processing. One place to start would be accessory proteins related to NRA-2, NRA-4 or EMC-6, in particular the other proteins in the EMC (Bai et al., 2020; Richard et al., 2013). The conclusions drawn in this Chapter and the previous Chapter 4 highlight that the effects of accessory proteins cannot be overstated on receptor characterization. In Chapter 4 it was found that *D. medinensis* ACR-16 no longer requires RIC-3 for functional expression in oocytes. This was unexpected finding and provided the opportunity to identify the regions determining this change. Chapter 6 investigated this further.

Chapter 6. Site-determination of RIC-3 requirement

6.1 Introduction

The *Xenopus laevis* oocyte expression system allows for transient and specific expression of cRNA that has been injected into the oocyte (Bianchi & Driscoll, 2006; Dascal & Aviv, 1987). If essential components cannot be provided by the existing translation and protein processing machinery of *X. laevis* functional protein complexes will fail to be produced (Martínez-Torres & Miledi, 2006). In the case of nematode pentameric ligand-gated ion-channels missing components may include subunits required for the receptor or accessory proteins required for functional assembly and/or transport of channels to the surface membrane (Boulin et al., 2008; Choudhary et al., 2020; Halevi et al., 2002). Of particular interest is the RIC-3 accessory protein that was first identified in *Caenorhabditis elegans* as required for correct expression of several nematode cationic pentameric acetylcholine receptors (Ben-Ami et al., 2009; Castelán et al., 2008; Halevi et al., 2002). RIC-3 has since been studied as a requirement for both invertebrate and vertebrate receptors (Millar, 2008). RIC-3 is an ER resident protein with sequence analysis predicting 1 to 2 N-terminal transmembrane domains and an intracellular coiled-coil C-terminal domain (Halevi et al., 2003). Both of these regions physically interact with and are required for stabilizing immature nematode acetylcholine receptor (AChR) subunits (Ben-Ami et al., 2005, 2009). Few have studies identified the regions in the receptors themselves that interact with RIC-3. Residues within the transmembrane domain 1 (TM1) helix of vertebrate receptor may interact with RIC-3 and be involved in the transport arrest observed in some receptors types (Castillo et al., 2005). More recently, the first 24 amino acids in the intracellular loop (ICL) of a mouse serotonin receptor have been found to interact with RIC-3 (Nishtala et al., 2014, 2016). In Chapter 4 I found that expression of an N-AChR as a homomer of ACR-16 subunits from *Dracunculus medinensis* is possible in the absence of RIC-3. All other Clade III ACR-16 receptors studied in that Chapter, and all other characterized ACR-16s, require RIC-3 (Abongwa et al., 2016; Boulin et al., 2008; Charvet et al., 2018; Choudhary et al., 2019; Hansen et al., 2021; Kaji et al., 2020). The same RIC-3 was used for all ACR-16 receptors in Chapter 4, therefore the difference must be in the subunit protein itself. *Ascaris suum* ACR-16 and *D. medinensis* have similar pharmacology and response sizes with RIC-3 (Chapter 4 Figures 24 &

25), and therefore present an ideal example to identify specific sequence differences between the two that confer this requirement for RIC-3. Doing so, may help to reveal how nascent subunits interact physically with RIC-3.

In order to identify the sequence regions that mediate ACR-16 RIC-3 requirement, a series of chimeras were made between *A. suum* and *D. medinensis*. To generate many chimeras quickly and easily, the nucleotide coding sequences of *A. suum* and *D. medinensis* were modified, like in Chapter 5, to introduce restriction enzyme recognition sites in such a way to not alter the protein product. The introduced restriction enzyme sites were put in the same positions in both sequences and allowed for chimera creation using simple restriction enzyme digestion. Restriction enzyme modified sequences (referred to as REMs) and the chimeras generated in this chapter are shown in Figure 34 & 38.

6.2 Results

The modified sequence responses (REMs) were measured and compared to those of the "native" coding sequence to ensure the changes made in the nucleotide sequences do not affect functional expression of the receptors. Receptor responses expressed from the engineered sequence were indistinguishable from their unmodified counterparts (Appendix Figure 2, Appendix Figure 5).

Chimeras were first made by exchanging each one of the three main domains (ECD, TMs and ICL) followed by measured responses to ACh and NIC. This first set of chimeras was used to identify the general domain(s) responsible for the RIC-3 requirement phenotype. Once identified, more chimeras were made exchanging smaller regions within them to narrow down the sequence of interest. Because the C-terminal tail was too small to introduce any restriction enzyme sites within it, its sequence follows that of the transmembrane domain 4 (TM4) species sequence, (i.e. if a chimera has the *A. suum* TM4 then it has the *A. suum* C-terminal tail as well) (Appendix Figure 5). *Ric-3* co-injection with each chimera served as a control to ensure the chimera in question was functional. All chimera and point mutation responses, with and without *ric-3*, are shown in Appendix Figures3 & 4. Nearly all chimeras had maximal responses identical to those of ASU-ACR-16 and DME-ACR-16 when co-injected with RIC-3. However, a few chimeras exhibited higher or lower responses, therefore in order to control for innate differences in functional expression, chimeras expressed without RIC-3 are shown as a percent of its expression with RIC-3. A possible explanation for this is described in the Discussion.

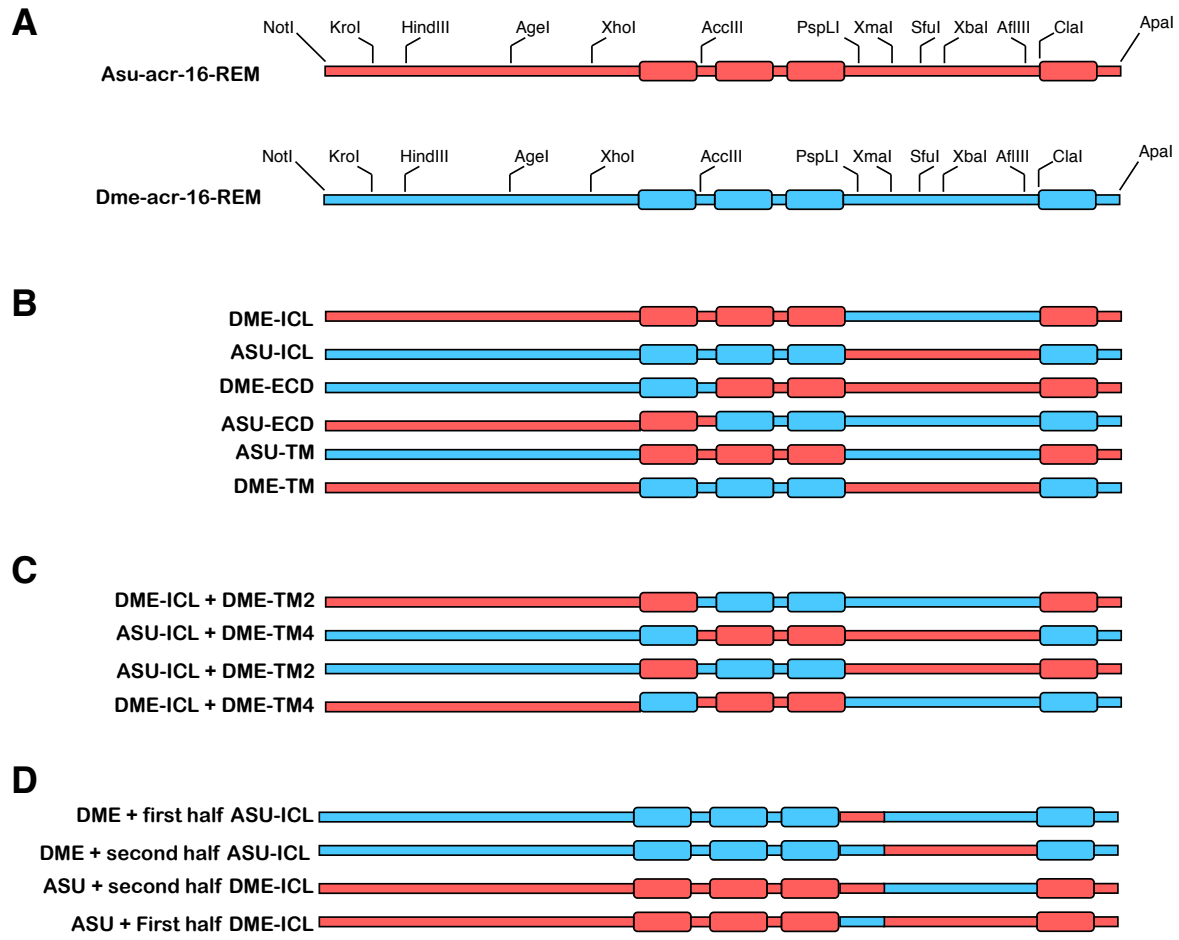

Figure 34. Schematic of *A. suum* and *D. medinensis*.

Chimeras were made to identify the regions contributing to RIC-3 requirement in ACR-16. (A) *A. suum* and *D. medinensis* coding sequences were modified to introduce complementary restriction enzyme sites (labelled ACR-16-REM) to generate the chimeras shown in (B-D). (B) Chimeras were first made exchanging the three main structural regions ECD, TM and ICL. See Figure 35 for results. (C) Chimeras were made exchanging each TM2 or TM4 along with the ICL. See Figure 36 for results. (D) Chimeras were made cutting the ICL in half with either *D. medinensis* or *A. suum* TM4. See Figure 37 and Appendix Table 8 for Results. TM4 and C-terminal tail point mutants shown in Figure 38.

6.2.1 The intracellular loop, transmembrane domain regions and C-terminal tail mediate RIC-3 requirement

Chimeras were compared to their reference receptor and shown as a % response without RIC-3 compared to with RIC-3. The requirement for RIC-3 is not determined by the ECD, based on chimeras in which this region was exchanged (Figure 35). The *A. suum* receptor with the *D.*

medinensis ECD was still unable to produce responses without RIC-3 (0 ± 0 %), while the *D. medinensis* receptor with the *A. suum* ECD produced large responses in the absence of RIC-3 (69 ± 5 %). The ICL contributes to some of the RIC-3 requirement, this exchange reversed some, but not all, of the RIC-3 requirement. Both pairs in this chimera swap responded minimally without RIC-3 (14.9 ± 2 % & 11.3 ± 5 %). The TMs and C-terminal tail contribute the most to RIC-3 requirement. This chimera exchange nearly completely reversed the RIC-3 requirement. The ASU-ACR-16 receptor with the *D. medinensis* transmembrane domains (and C-terminal tail) had large responses (38 ± 3 %) compared to those of the ASU-ACR-16 receptor (0.6 ± 0.2 %). The DME-ACR-16 with the *A. suum* transmembrane domains (and C-terminal tail) now had greatly reduced responses (2.0 ± 0.4 %) compared to the DME-ACR-16 receptor (52.6 ± 3 %). Taken together these chimeras indicate that the intracellular loop, transmembrane domain regions and C-terminal tail mediate acetylcholine receptor requirements for the RIC-3 accessory protein, with the transmembrane regions and tail having higher contribution compared to the ICL. The next set of chimeras therefore exchanged sequences within these two regions to narrow the sequence of interest.

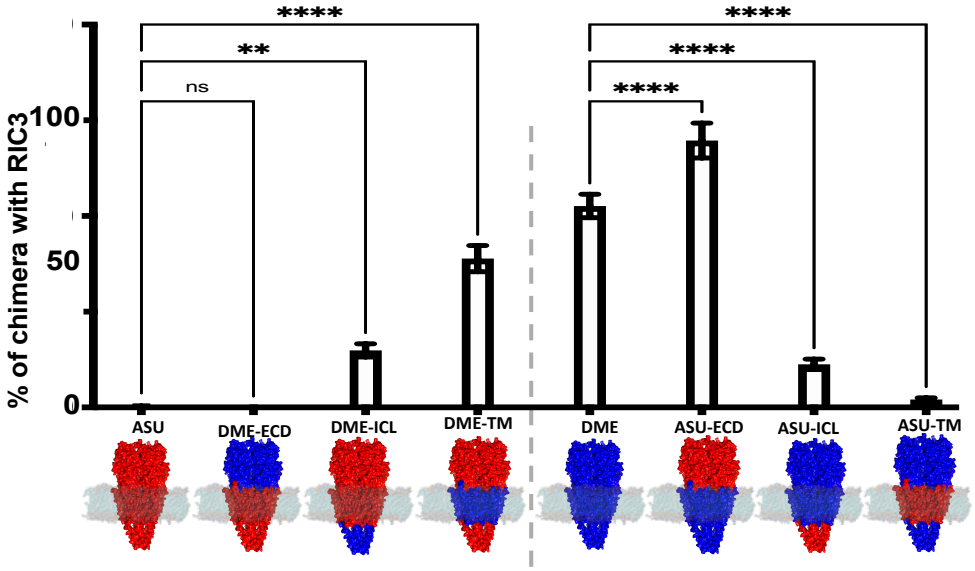

Figure 35. Main structural region chimeras show the intracellular loop, transmembrane domains and C-terminal tail mediate RIC-3 requirement.

Chimeras were made exchanging each of the three main structural regions (ECD, ICL or TM) to identify which regions mediate RIC-3 requirement. Percent response of the chimeras with RIC-3 compared to response without RIC-3 are shown. *A. suum* responses increased upon addition of *D. medinensis* ICL or TM + C-terminal tail. *D. medinensis* responses decreased upon addition of *A. suum* ICL or TM + C-terminal tail. *A. suum* in red, *D. medinensis* in blue. Error bars represent standard error. **p<0.005; ****p<0.0001

6.2.2 The fourth transmembrane domain and the C-terminal tail mediate RIC-3 requirement

Based on the results from Figure 35, the transmembrane domains and C-terminal tail contain a large contribution of the receptor requirement for RIC-3. The *A. suum* and *D. medinensis* transmembrane domain sequences are highly conserved, with substitutions observed in only the second (TM2) and fourth (TM4) domains (Chapter 4 Figure 22, Appendix Figure 5). The C-terminal tail sequences only contain one amino acid difference. Chimeras exchanging each transmembrane domain were made in order to identify if one or both of the TM2/4 regions contribute to the requirement for RIC-3. Two pairs of TM2 and TM4 chimeras were made; with and without the *D. medinensis* ICL since the ICL was found to contribute to the requirement for RIC-3. This allowed to measure the effect of each transmembrane domain individually, and in conjunction with the *D. medinensis* ICL. The TM2 does not contribute to the requirement for RIC-3 based on the chimeras that only had the *D. medinensis* TM2 (Figure 36; DME-ICL+DME-TM2 5.8 ± 0.7% & ASU-ICL+DME-TM2 0 ± 0%). TM4 and the C-terminal mediate RIC-3 requirement based on the chimeras that only had these *D. medinensis* regions (Figure 36; DME-ICL+DME-TM4 94 ± 3% & ASU-ICL+DME-TM4 49 ± 3%). This set of chimeras rules out the possibility that TM2 is involved and indicates that it is entirely within the TM4 the C-terminal tail sequences.

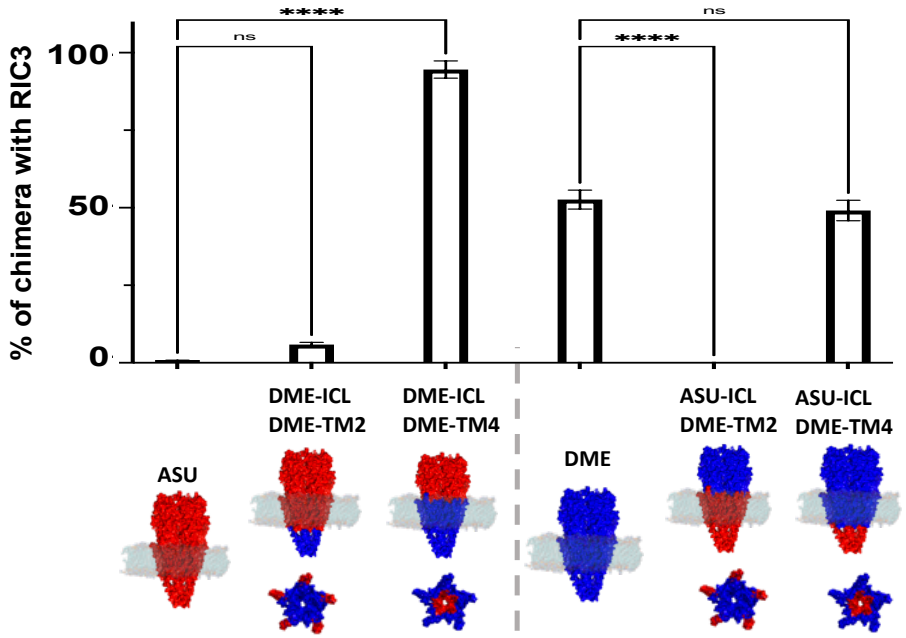

Figure 36. The fourth transmembrane domain and C-terminal tail mediate RIC-3 requirement.

Chimeras were made exchanging individually TM2 or TM4 along with the ICL to identify if one or both of those transmembrane domains mediate RIC-3 requirement. Percent response of the chimera without RIC-3 compared to response with RIC-3 are shown. Only chimeras that contained the *D. medinensis* TM4 and C-terminal (DME-TM4) produced robust responses without RIC-3. Therefore the TM4 and C-terminal, and not the TM2, determine RIC-3 requirement. Error bars represent standard error. ****p<0.0001.

6.2.3 The entire ICL contributes to RIC-3 requirement

Based on the results from Figure 35, the ICL domains contributes a small part of the receptor requirement for RIC-3. The cys-loop receptor ICL is highly variable in both sequence and structure (Langlhofer & Villmann, 2016). Studies have only identified two alpha helices at either end of the loop (Unwin, 1995, 2005). The ICL has been implicated in many functions including receptor kinetics, interactions with intracellular components and assembly (Haeger et al., 2010; Kracun et al., 2008; Lo et al., 2008; O'Toole & Jenkins, 2011; Rudell et al., 2020; Thompson et al., 2010). The precise details of how the ICL interacts with other subunits in the pentamer and with chaperone proteins is not known. Identifying the precise sequence(s) that regulate RIC-3 requirement is not straightforward because of the widespread range of the sequence differences between the *A. suum* and *D. medinensis* ICL. The first 24 amino acids of a

mouse serotonin receptor ICL have been found to interact with RIC-3 (Nishtala et al., 2014, 2016). Due to the longer length of AChR ICLs, sequence alignment indicates that these 24 amino acids correspond to the first 50 amino acids in AChRs and provides us with a reference with which to compare to. Chimeras were therefore made exchanging the first 50 amino acids of the ICL to see if it is the same region in an AChR that determines RIC-3 requirement as it is in the serotonin receptor. These chimeras were constructed under both *A. suum* or *D. medinensis* TM4 + C-terminal tail.

Neither half of the ICL contains the region that confers RIC-3 requirement. ICL chimeras with *D. medinensis* TM4 were compared to DME-ACR-16 and ASU-ICL (Figure 37A). If the region was confined to only one of these halves, these chimeras would be expected to have responses comparable to DME-ACR-16, and significantly higher than the ASU-ICL chimera. Both chimeras produced responses that were significantly smaller than DME-ACR-16 and one was significantly larger than ASU-ICL (first half 26 ± 4% & second half 18 ± 2%). This was further confirmed with the second paid of chimeras that split the ICL in half (Figure 37B). The requirement for RIC-3 could not be conferred by either segment of the ICL alone (first half 0 ± 0% and second half 0 ± 0%), suggesting the requirement was distributed between both parts. Therefore, the region within the ICL that mediates an ACR-16 receptors requirement for RIC-3 is not confined to the first half, as it is in serotonin receptors, but is spread out.

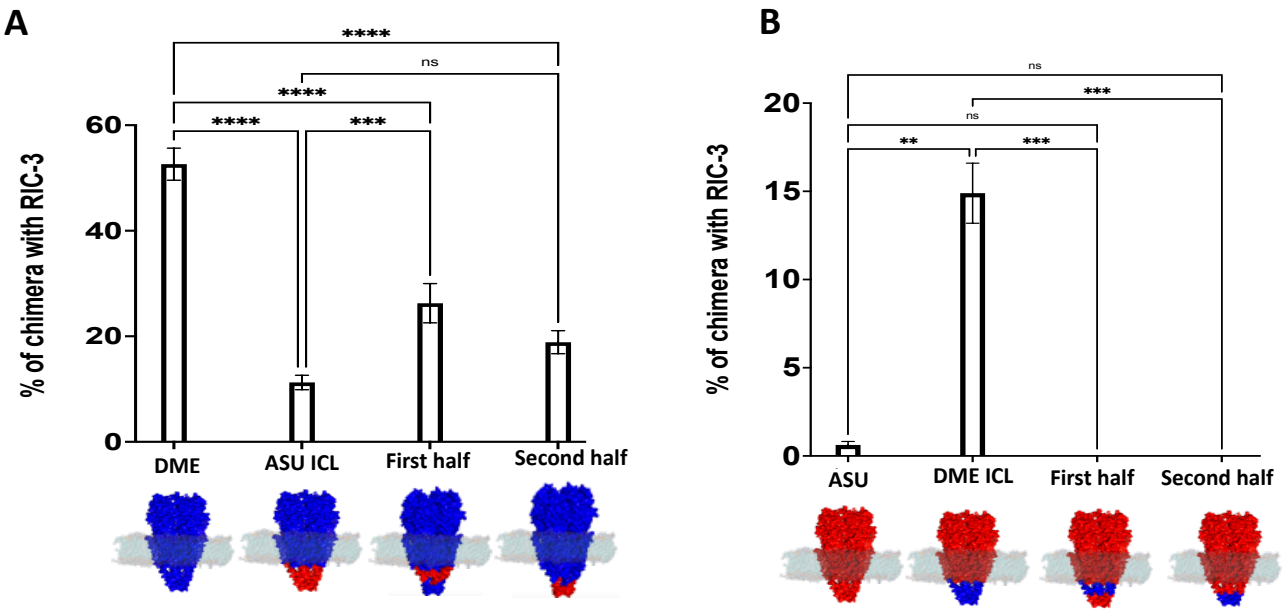

Figure 37. The entire intracellular loop contributes to RIC-3 requirement.

Chimeras were made cutting the ICL in half to see if either region determines RIC-3 requirement. Percent response of the chimera response without RIC-3 compared to response with RIC-3 are shown. (A) Intracellular loop chimeras in the *D. medinensis* receptor have intermediate responses between the ASU-ICL chimera and *D. medinensis* receptor indicating both halves contribute to RIC-3 requirement. (B) Intracellular loop chimeras in the *A. suum* receptor have no responses without RIC-3 indicating both halves are needed together for RIC-3 requirement. **p<0.005; ***p<0.0005; ****p<0.0001.

6.2.4 The C-terminal tail and transmembrane domain mediate ric-3 requirement

The TM4 and C-terminal tail were found to mediate most of the RIC-3 requirement (Figure 36). There are only three amino acid differences between *A. suum* and *D. medinensis* ACR-16 TM4 and one amino acid change in the tail (Chapter 4 Figure 22, Appendix Figure 5). DME-ACR-16 has all isoleucines, and ASU-ACR-16 has three valines in the TM4 and a threonine in the C-terminal tail. In order to determine the combination of these substitutions that mediate RIC-3 requirement, a series of point mutations were made mutating the sites in *A. suum* to those in *D. medinensis*, and vice versa. These chimeras were made testing all possible combinations of TM4 mutations between both *A. suum* and *D. medinensis,* and two tail mutations. Point mutation nomenclature is shown in Figure 38 A & B.

The substitution of Thr for Ile alone at position 509 in the C-terminal tail of *A. suum* was able to explain the difference between *A. suum* and *D. medinensis* entirely (Figure 38C). All single, double, and triple point mutations in the *A. suum* TM4 (V→I) had small (1-6% of the chimera with RIC-3) currents that were not significantly different from *A. suum* acr-16. The C-terminal tail + TM4 mutations combined produced larger percent responses compared to the C-terminal tail alone (95 ± 3% vs 64 ± 4%) (Figure 38C). Therefore, the three TM4 sites do contribute to RIC-3 requirement but need the Ile in the tail to exhibit their effect.

The *A. suum* TM4 point mutations indicate that all three TM4 positions play a minor role in the requirement for RIC-3, but that the C-terminal tail mutation was able to reverse the requirement entirely. This would predict that all of the single, double and triple point mutations of the *D. medinensis* TM4 region would function with responses below those of the native sequence, and that the two tail mutants would induce the lowest responses. This was observed (Figure 38D). The C-terminal tail mutation on its own nearly abolished all response without RIC-3 (2.6 ± 0.3%) and the tail + three TM4 mutations combined also had very little response (1.5 ± 0.5%). The single, double and triple TM4 point mutations produced responses that were significantly smaller than DME-ACR-16 (20-41%) (except for DME-ACR-16-TM4-2 point mutation that is not significantly different, 47 ± 3%).

Homology models reveal that the three TM4 sites are lined up in the helix and exposed to the membrane environment in a position where they could potentially interact with RIC-3 (Figure 39). Side chains between valine and isoleucine are similar, however the added methyl group on isoleucines makes the *D. medinensis* helix bulkier. The tail changes (Figure 39 B & D) show much overlap between the side chains however the hydroxyl group on the *A. suum* threonine create a polar side chain. It is important to note that the tail is a very short sequence and it did not have a complete template structure with which to build the homology model on, therefore the tail prediction may not be accurate.

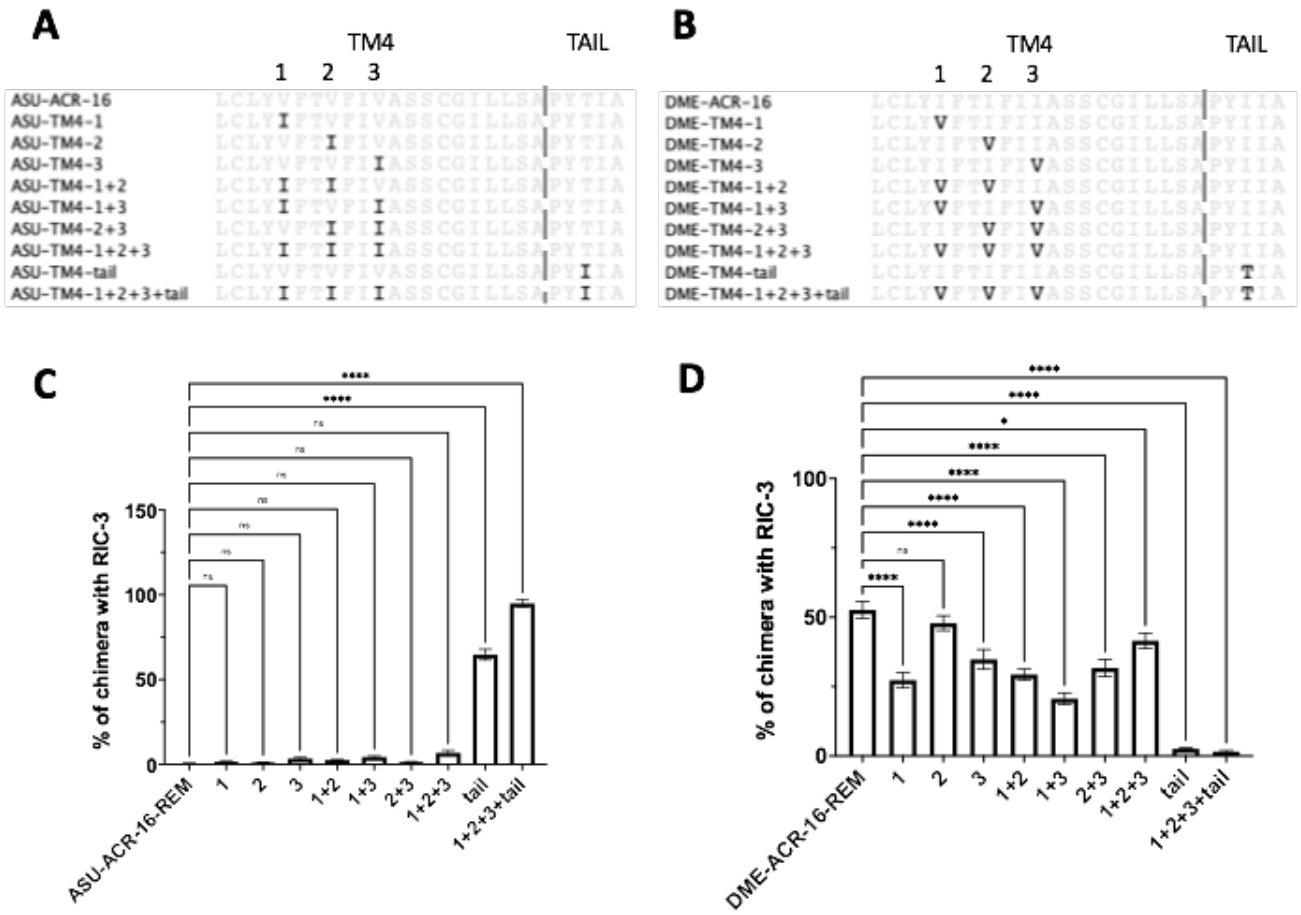

Figure 38. A single amino acid in the C-terminal tail determines RIC-3 requirement in ACR-16.

Point mutations were made in Asu-acr-16 and Dme-acr-16 TM4 and the C-terminal tail to identify the amino acids that determine RIC-3 requirement. (A) point mutations in Asu-acr-16 shown in bold. (B) point mutations in Dme-acr-16 shown in bold; (C) Percent response of Asu-acr-16 point mutations of response without RIC-3 compared to response with RIC-3; (D) Percent response of Dme-acr-16 point mutations of response without RIC-3 compared to response with RIC-3. The single C-terminal tail residue determines RIC-3 requirement. Mutating T509I in Asu-acr-16 no longer needed RIC-3, while I509T mutation in Dme-acr-16 needed RIC-3. Error bars represent standard error. *p<0.05; ****p<0.0001.

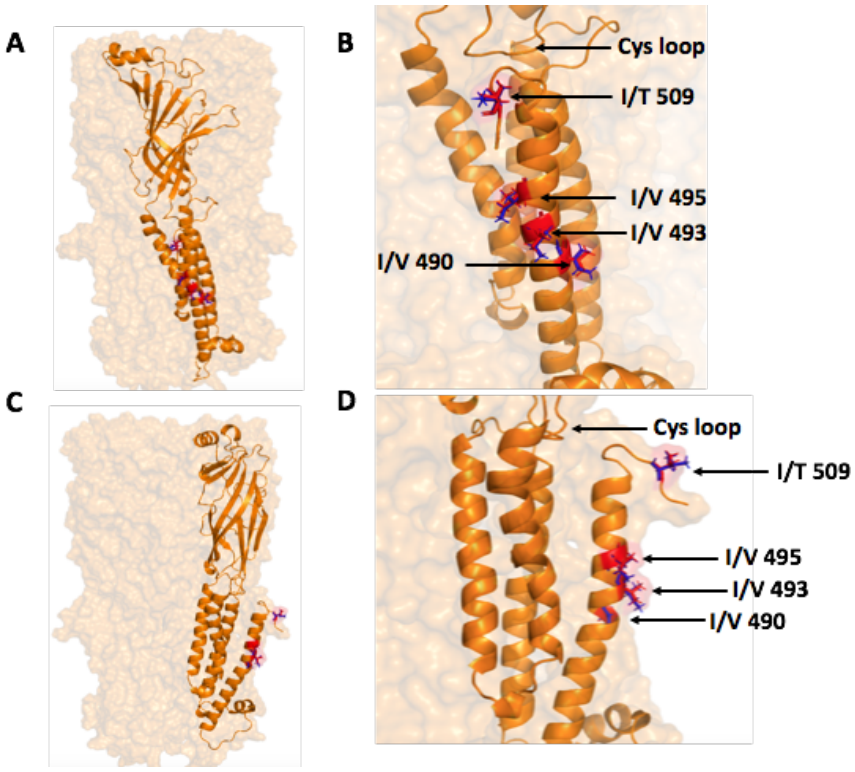

Figure 39. The C-terminal tail and transmembrane domain 4 substitutions are located on the outside of the receptor.

The four TM4 and C-terminal tail point mutation substitutions were mapped onto homology models in order to visualize their location. (A) front view of one subunit in the receptor complex with four residues circled. (B) Zoomed-in front view of the four residues show they are lined in and the C-terminal tail residue could make interactions with the neighbouring cSys-loop. (C) side-view of one subunit in the receptor complex with the four residues circled. (D) Zoomed-in side view of the four residues show the three helix sites point out and can interact with the membrane environment. *D. medinensis* residues in blue, *A. suum* residues in red.

6.3 Discussion

The complex and largely uncharacterized assembly and trafficking of pLGICs means that when channels cannot be expressed in heterologous systems, it is difficult to pinpoint why. Many AChRs require co-injection of specific accessory proteins enabling their functional expression (Boulin et al., 2008; Choudhary et al., 2020),

To ensure the changes created in the restriction enzyme modified nucleotide sequences do not affect functional expression of ACR-16s, the modified sequence maximal responses were measured and compared to those of the native coding sequence. No significant difference was

measured between native and restriction modified sequences, or for their requirements for RIC-3. REMs are a versatile method to create receptor chimeras and identify specific functional regions within them. However, the caveat is that the sequences must be homologous to allow for enough sequence similarity in the amino acid sequence to create nucleotide modifications.

One of the most well-studied pLGIC accessory proteins is RIC-3. While there has been much work done that has identified the regions in RIC-3 that are required for its function (Ben-Ami et al., 2005, 2009; Yoav Biala et al., 2009), little is known about the regions in the receptors themselves that interact (either directly or indirectly) with RIC-3. *A. suum* and *D. medinensis* ACR-16 receptors have identical pharmacology and maximal responses when expressed in oocytes, with dramatically different requirements for RIC-3 (Chapter 4 Figures 24, 25 & 27). With a sequence similarity of ~84%, these receptors are ideal candidates to identify structural regions that regulate RIC-3 requirement. By using chimeras and point mutation studies, three regions were identified that confer a requirement for RIC-3 for functional expression in oocytes. One amino acid in the C-terminal tail was enough to completely determine RIC-3 requirement, with three sites in TM4 and the ICL contributing as well.

RIC-3 was first identified in *C. elegans* and has since been extensively studied for its involvement for both vertebrate and invertebrate receptors. Sequence-structure predictions predict that RIC-3 has 1-2 transmembrane domains followed by an intracellular coiled-coil region and a disordered region (Halevi et al., 2002, 2003). The function of RIC-3 has been proposed by (Wang et al., 2009), and is thought to act in the ER by binding directly to nascent subunits using the transmembrane domains, in a one-to-one ratio (Figure 40). Once bound, the intracellular coiled-coil region of RIC-3 participates in homotypic interactions that binds to another RIC-3 coiled-coil region (that is also bound to a subunit). This coiled-coil binding brings the two attached subunits within proximity of each other, promoting their dimerization. One RIC-3 dissociates from this intermediate complex and the process continues until a pentamer is formed. Thus, direct physical interactions to both the subunits and to other RIC-3 proteins are critical for this process to occur (Bao et al., 2018; Ben-Ami et al., 2005, 2009; Castelán et al., 2008; Nishtala et al., 2014, 2016; Yoav Biala et al., 2009). Other reports suggest RIC-3 may also inhibit certain subunit types from exiting the ER thereby altering subunit composition in the receptors that do get sent to the surface (Bao et al., 2018; Ben-Ami et al., 2009; Castillo et al., 2005). It is clear that RIC-3 is a critical component for receptor expression and must bring the

right subunits together (and in the right stoichiometry in the case of heteromeric receptors) to promote the assembly, and perhaps subunit composition, of a functional receptor.

For the nematode receptors, both the RIC-3 TM and intracellular coiled-coil regions physically interact with and are required for its functional expression (Ben-Ami et al., 2005, 2009; Yoav Biala et al., 2009). This agrees with two of the regions identified here that mediate RIC-3 requirement (the ICL and TM). However, for the mouse alpha7 receptor, the intracellular coiled-coil region is not required (Wang et al., 2009). In the vertebrate serotonin receptor, the first 24 amino acids of the ICL were found to physically interact with RIC-3 and be required for functional expression (Nishtala et al., 2014, 2016). This is in contrast to what we find here where it is the entire ICL in the nematode AChR that requires RIC-3. This difference can be explained by the fact that RIC-3 has different effects depending on the receptor type (Dau et al., 2013), the host expression cell (Lansdell et al., 2005, 2008), its concentration (Ben-David et al., 2016; Bennett et al., 2012) and its isoform (Bao et al., 2018; Cheng et al., 2007). For the most part, RIC-3 enhances AChRs but inhibits serotonin receptors (Castillo et al., 2005; Gee et al., 2007). There are, however, specific cases where the effect of RIC-3 diverges from this general trend (Ben-Ami et al., 2009; Cheng et al., 2005). For the AChRs, RIC-3 preferentially enhances DEG-3 expression but inhibits DES-2 expression (Ben-Ami et al., 2005, 2009). For the serotonin receptors, RIC-3 preferentially enhances the expression of the homomeric receptors (Walstab et al., 2010). The relative contribution of the different regions in RIC-3 are also subunit-dependent (Ben-Ami et al., 2005, 2009; Yoav Biala et al., 2009). Therefore, when subunits belong to different classes, they could be interacting with RIC-3 under different mechanisms. Finally, although the regions identified in our study mediate RIC-3 requirement, they may not necessarily be the regions that physically interact with RIC-3. All of these reasons may account for the different ICL effects found here versus the serotonin receptor.

The finding that one amino acid in the C-terminal tail mediated nearly all of RIC-3 requirement was unexpected because the tail is often overlooked in structure—function studies. Hoes does this residue, along with the three sites in TM4 and the ICL mediate RIC-3 requirement? One explanation could be that these regions physically interact with RIC-3 and the specific sequences in DME-ACR-16 allow it to more efficiently interact with the *X. laevis* RIC-3 that is expressed in oocytes (Bennett et al., 2012; Nishtala et al., 2016). Another possibility is that these regions do not interact with RIC-3, but with some other unknown accessory protein

endogenous to the oocyte, and that the DME-ACR-16 sequence enables its ability to interact with it, no longer requiring RIC-3. Finally, it is also possible that the DME-ACR-16 sequence at these regions stabilizes the subunit and promotes receptor assembly no longer requiring RIC-3.

Although we did not investigate if the ICL, TM and C-terminal tail physically interact with RIC-3, they do mediate its requirement and are good candidates to start with when studying this. Identifying the regions in both receptor and accessory protein that interact with each other would provide invaluable insight into understanding receptor stability and assembly within the ER. Furthermore, this information could provide understanding into why some receptors need RIC-3 while others don't. If these are the regions of interaction, then knowing the precise details of how they interact may also help understand how RIC-3 has such different effects on closely related subunits and what interactions mediate those differences. However, caution must be taken when interpreting the results presented here because this is not representative *in vivo* and heterologous expression host cell types have been known to affect RIC-3 function (Lansdell et al., 2005, 2008). If these three regions do not interact with RIC-3, additional studies would have to investigate what they are doing.

Relating the work presented here to nematodes receptors is just as complex considering the TM of RIC-3 was found to be required for regulation for the DEG/DES receptor (Ben-Ami et al., 2009), while the RIC-3 intracellular coiled-coils were found to be required for functional regulation of the L-AChR and ACR-16 (Yoav Biala et al., 2009). Relating to the vertebrate receptors is just as complex. In vertebrate serotonin receptors a single residue near the receptors TM1 was found to determine RIC-3 requirement (Castillo et al., 2005), while others have found that the receptor ICL determines RIC-3 function (Nishtala et al., 2014, 2016) and can make prokaryotic receptors gain an inhibition of expression by RIC-3 with ICL chimeras (Mnatsakanyan et al., 2015). In the vertebrate AChRs, one study found series of residues within the distal alpha helix of the ICL determines RIC-3 requirement (Castillo et al., 2005), while another found the ECD and TMs interacts with RIC-3 (Wang et al., 2009). One reason to these discrepancies could be that some studies identify the regions for function while others identify the regions of interaction, and these may be not the same.

The results of the present work identified one amino acid in the tail that mediates RIC-3 requirement. If the receptor had a threonine it required RIC-3, whereas if it had an isoleucine it did not require RIC-3. The finding that the C-terminal tail mutation mediated nearly all of the

RIC-3 requirement was unexpected because the tail is not known to be involved in major receptor synthesis, however it has been reported to be involved in receptor gating by interacting with residues in the ECD cys-loop (Alcaino et al., 2017). A major limitation with this work is that the other ACR-16 receptors studied here also have the isoleucine at that position, yet still required RIC-3 (Chapter 4 Figure 22 *Gonglyonema pulchrum* & *Thelazia callipaeda*). Three reasons could account for this observation. First, this residue, along with the three amino acids identified in TM4, are all located on the outside of the receptor interacting with the membrane environment. It is possible that it is this region in general, opposed to those four specific sites, that is critical for receptor expression. This region could be acting as a "hot spot' for subunit-accessory protein interactions or subunit stability. This would mean that the other residues in this region also contribute to RIC-3 requirement and could be tested with further mutations to sites in that region. Second, the relative importance/contribution of different regions in RIC-3 depends on the subunit it is interacting with (Ben-Ami et al., 2005, 2009). This could mean that different regions in the *G. pulchrum* & *T. callipaeda* receptors as well have different levels of contribution for RIC-3. Considering the ICL was found to also mediate some of the RIC-3 requirement, a second explanation could be that in later Clade III ACR-16 receptors, the ICL has more importance for RIC-3 requirement compared to the tail/TM4 regions. A third reason may be that it is the interaction of the C-terminal tail residue with other residues in the ECD that stabilize the assembly process (the tail sticks out from the membrane on the extracellular side). In other words, *D. medinensis* could have residues in the ECD that interacts with the tail isoleucine in a way promoting its functional expression without the need of RIC-3. Previous work proposed that the more hydrophobic the tail is, the more it could interact with the ECD, in particular with residues within the cys-loop (Alcaino et al., 2017). Furthermore, the cys-loop is a critical region in regulating subunit assembly and needs to undergo large structural change otherwise assembly is halted at intermediate stages (Green & Wanamaker, 1997). Therefore, it is possible that the C-terminal tail hydrophobic isoleucine interacts with residues within the cys-loop in such a way to facilitate this structural change and subunit assembly, thus no longer requiring RIC-3. Amino acids position 162 & 164 (Figure 22 & 39) are in the cys-loop and differ between *D. medinensis* and the other ACR-16s that also have an isoleucine and still require RIC-3(Alcaino et al., 2017; daCosta & Baenziger, 2009). *D. medinensis* has oppositely charged residues, whereas these other ACR-16s have a charged residue and a polar residue. A series of point mutations exchanging

each of these residues individually and in combination would answer if they interact with the tail to mediate RIC-3 requirement.

In addition to identifying the regions that mediate AP requirement, two other conclusions can be made based on the observation that some chimeras had significantly higher or lower maximal responses with RIC-3. First, the chimeras that contained the *A. suum* ECD had higher responses compared to the same chimera but with the *D. medinensis* ECD. This suggests that the receptors may have two levels of expression without RIC-3; an absolute all-or-nothing requirement for RIC-3 mediated by the ICL, TM4 and C-terminal tail, and an "enhancement" level of expression observed when the *A. suum* ECD is included. This coincides with the fact that the ECD contains many of the subunits' signal sequences of expression (Eertmoed & Green, 1999; Neveu et al., 2010; Sumikawa & Nishizaki, 1994; Verrall & Hall, 1992). It is possible that the ECD interacts with other unknown APs endogenous to the oocyte, and the *A. suum* sequence enables more efficient expression, and this effect would only be observed if the receptor is already being functionally expressed without RIC-3. Second, chimeras that split the ICL into two halves (that contained the *A. suum* TM4 but not the *D. medinensis* TM4) had severely decreased responses compared to their non-split chimeras (Figure 37B). This suggests that since the split from their last common ancestor, sequence changes occurred across the entire ICL in these receptors that absolutely must coincide together with the *A. suum* TM4 in order for complete functional expression. The largely unknown structure and exact function of the ICL makes interpreting these results challenging. These findings provide an opportunity for further site-specific identification and understanding of regions that co-evolve for functional assembly and transport to the membrane surface.

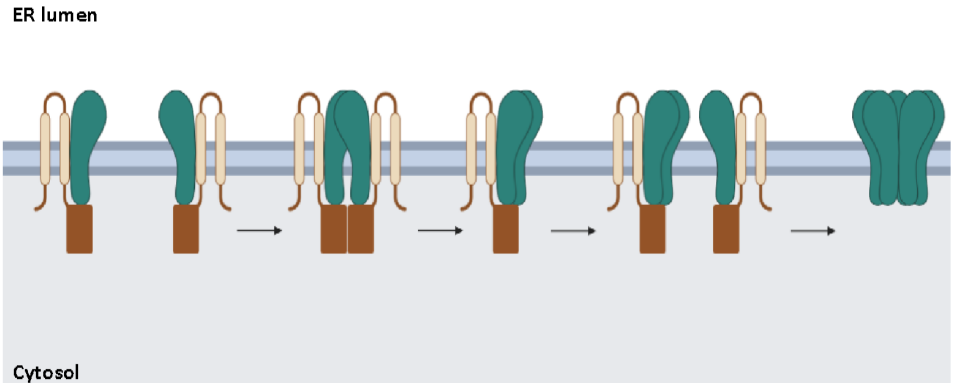

Figure 40. Proposed function of RIC-3 in the ER.
Within the ER, RIC-3 binds to a subunit in a one-to-one ratio via its second transmembrane domain and coiled-coil domain. The coiled-coil domain of RIC-3 partakes in homotypic interactions with other RIC-3 coiled-coil domains (also bound to a subunit) and brings subunits within close proximity to each other, promoting their assembly. One RIC-3 disassociates from this intermediate complex and another RIC-3 (bound to a subunit) joins, allowing a third subunit to join the complex. This process continues until a pentamer is formed. Image made in BioRender, adapted from Wang et al., (2009).

Expressing AChRs in heterologous expression systems can be challenging when accessory proteins are needed. The subunits that form the receptor can be known but the lack of including specific accessory proteins can prevent the measurement of a receptor (Boulin et al., 2008; Lewis et al., 1980a; Lewis et al., 1980b). Current understanding of the extent to which accessory proteins are involved in receptor synthesis and how they interact with subunits is limited. To our knowledge this is the first identification of a single amino acid in AChRs that regulate requirements for RIC-3 for functional expression. Future work would have to confirm if these regions directly interact with RIC-3 and how they are involved in receptor synthesis. However, given that they coincide with the regions in RIC-3 that are required for its function, it is possible that they do interact with it. These regions could also be used to understand how receptors change their "needs" for accessory proteins, and how evolution acts on these regions to mediate this diversity in AP requirement.

CHAPTER 7. General Discussion

Neurotransmission is fundamental to animals and marks the difference from the other major kingdoms of life. Fast synaptic signaling through the release and response to neurotransmitters is central to this and is thought to have developed from ion-channels that allowed the single celled ancestors of prokaryotes and eukaryotes to sense their environment (Tasneem et al., 2005). These pentameric ligand-gated ion-channels (pLGICs) are composed of five subunits encoded by members of a diverse gene family that has arisen from a presumed single ancestral subunit gene inherited by the multicellular eumetazoans. (Ortells & Lunt, 1995; Tasneem et al., 2005; Unwin, 1995, 2005). Gene duplication is central to this diversity where the two essentially identical genes create a redundancy that allows selection pressure to change the functional characteristics of the two products. (Beech & Neveu, 2015; Ohno, 1970; Pedersen et al., 2019; Thompson et al., 2018). Prior to the Cambrian explosion this process led to a family of genes that encode both anionic and cationic channel classes and within these, channels that respond to the major neurotransmitters known today (Ortells & Lunt, 1995; Tasneem et al., 2005). Channels may be homomeric, where five copies of a single subunit type combine or heteromeric, where different, related genes encode subunits that combine into the final channel (Corringer et al., 2000). This same process continues in the present with an expansion of pLGIC subunit genes within the nematodes associated with the switch from anionic to cationic, recognition of new neurotransmitters and diversification of subunits to create heteromeric channels. (Beech & Neveu, 2015; Dent, 2006, 2010; Jaiteh et al., 2016; Ortells & Lunt, 1995; Tasneem et al., 2005). Recent events are associated with minimal sequence change and so could provide insight into the specific mechanisms and sequences responsible for these events more generally.

The cationic pLGICs typically respond to acetylcholine (ACh) that binds at the interface between two adjacent subunits, one providing the principal face with the C-loop that encloses the bound neurotransmitter and one the complementary face that provides a more static framework for ligand binding (Corringer et al., 2000). Homomeric channels are composed of alpha-type subunits, where the C-loop contains a YXCC motif essential for ACh binding (Corringer et al., 2000). Heteromeric receptors have subunits with fixed relative positions, determined from CryoEM solved structures (ex. PDB: 2BG9). They also typically have subunits that lack the

YXCC C-loop motif, known as non-alpha, that specifically contribute the complementary face of the neurotransmitter binding site. The subunit organization invariably creates two dedicated ACh binding sites two subunits apart, an asymmetry that computer modelling has shown is essential for the transition of the channel from closed to the open state (Mowrey et al., 2013). This functional dedication of non-alpha subunits to the complementary face appears primarily important for heteromeric receptors since the division from alpha-type subunits is the first to appear in reconstructed phylogenies (Beech & Neveu, 2015; Dent, 2006; Jones et al., 2007).

The model system developed in this thesis is that of the levamisole sensitive acetylcholine receptor (L-AChR) of the body musculature in the free living, model nematode *C. elegans* (Lewis et al., 1980a; Lewis et al., 1980b). This pLGIC is maximally heteromeric, requiring the contribution from five different subunit genes, three alpha- and two non-alpha (Boulin et al., 2008). It has been characterized extensively as a significant antiparasitic drug target and orthologous receptors identified in closely related parasitic nematodes (Boulin et al., 2011; Buxton et al., 2014; Williamson et al., 2009). Reconstitution of a functional channel *ex vivo* in the *Xenopus laevis* frog oocyte system requires the addition of accessory proteins that function during the assembly and maturation of the channel, highlighting the importance of a network of regulatory proteins beyond the simple presence of channel subunits (Boulin et al., 2008; Lewis et al., 1980a; Lewis et al., 1980b). A surprising feature of these related channels is that they require only four, three or even two different subunits to make up a functional pentamer (Blanchard et al., 2018; Boulin et al., 2011; Buxton et al., 2014; Williamson et al., 2009). This immediately raises important questions that include the following. What process limits subunits to specific defined positions within a pentamer? When fewer than five subunits are present, which ones are present more than once and how is the replacement regulated? What steps occur when an alpha subunit becomes a non-alpha subunit? What role do the accessory proteins play in coordinating the interaction between subunits? The research presented addressed each of these questions in turn.

7.1 Subunit positioning

The *C. elegans* L-AChR is composed of three alpha-subunits: ACR-13, UNC-38, and UNC-63 and two non-alpha subunits: LEV-1, UNC-29 subunits, removing any one of those subunits fails to reconstitute a functional receptor in *X. laevis* oocytes (Boulin et al., 2008).

ACR-13 can be replaced by a closely related subunit, ACR-8, in which case only three other subunits are required: UNC-38, UNC-63 and UNC-29. LEV-1 is no longer essential (Blanchard et al., 2018). ACR-8 is present in the genomes of parasitic nematodes closely related to *C. elegans*. ACR-13 has been lost in many species and in each case, LEV-1 is either absent from the genome or appears to be nonfunctional, as is the case for the parasite of sheep, *Haemonchus contortus* (Boulin et al., 2011; Duguet et al., 2016). In Chapter 2 a series of experiments were carried out using UNC-38 fused into a single dimeric protein with either LEV-1 or UNC-29, to be certain of the location of the non-alpha subunit and to ensure that LEV-1 was physically replaced by UNC-29. This technique has been used routinely for pLGIC analysis (Carbone et al., 2009; Groot-Kormelink et al., 2006; Liao et al., 2020, 2021; Zhou et al., 2003).

Subunit combinations replacing ACR-13 with ACR-8 were able to demonstrate that indeed, the UNC-29 subunit was present twice and that the non-alpha UNC-29 specifically was able to replace the other non-alpha LEV-1. The presence of ACR-8 did not produce a new requirement for UNC-29 in this position, only relaxed the specificity since either LEV-1 or UNC-29 in this position could produce a functional channel. Previous work suggests that assembly of the Cel-L-AChR occurs by formation of a complex containing UNC-38:LEV-1:UNC-63 before ACR-13 and UNC-29 join as individual subunits (Duguet, 2017). In the case where ACR-8 is present and LEV-1 is not, a complex of UNC-38:UNC-29:UNC-63 presumably forms first followed by addition of ACR-8, then UNC-29 as individual subunits. The effect of ACR-13 to require LEV-1 could then be due to a selective inability of ACR-13 to join a trimer containing UNC-29 or production of a non-functional channel if it did. ACR-8 may be less restricted. The fact that smaller currents were observed when the positions of LEV-1 and UNC-29 were exchanged in the presence of ACR-8 suggests that the initial trimer may, in addition, show a preference for LEV-1 over UNC-29.

The non-alpha *unc-29* subunit has duplicated multiple times in *H. contortus*, producing four copies; *unc29.1* to *unc-29.4*. Each copy is functional and produces a receptor with highly similar pharmacology (Duguet et al., 2016). The *C. elegans* L-AChR containing Hco-UNC-29.1 does not require LEV-1, whereas LEV-1 is required with UNC-29.2 (Duguet, 2017). This is similar to the effect of replacing ACR-13 by ACR-8, but in this case is mediated by the non-alpha subunit itself. This could be explained if the two Hco-UNC-29 subunits differed in their ability to form the initial trimeric complex. A dimer of UNC-38 and UNC-29.1 was not available

and so confirmation that UNC-29.1 directly replaces LEV-1 has not yet been made. Chimeric exchange of the intracellular loop (ICL) between *unc-29.1* and *unc-29.2* suggests that the requirement for LEV-1 is mediated by the intracellular loop of these subunits (Chapter 2).

7.2 Transition from alpha- to non-alpha type subunit

Reconstructed phylogenies of the cationic pLGIC subunit genes find that the division between alpha and non-alpha type subunits within heteromeric receptors is the first to appear (Beech & Neveu, 2015; Blanchard et al., 2018; Coghlan et al., 2019; Pedersen et al., 2019). This suggests that the functional difference between alpha- and non-alpha subunits is fundamental to heteromeric receptors. The Clade III nematodes have lost three of the four non-alpha subunits related to *unc-29*, present in other related parasites. Following this, the *unc-63* and then *unc-38* genes duplicated and in the most derived *Onchocerca* species one of each gene has lost the YXCC motif characteristic of the alpha-type subunits. An analysis of the codon-substitution rates of these duplicate genes in comparison to the unduplicated *unc-38* and *unc-63* of related species found a significant accelerated rate of evolution of both duplicate copies (Chapter 3). It is possible that this is a result of changing subunit composition in the filarial L-AChR and possibly a specialization of *unc-63.2* and *unc-38.2* as non-alpha subunits even before the loss of the YXCC motif.

The *unc-38* and *unc-63* subunits have amino acid positions that can be divided into three general categories: those that are highly conserved, intermediate and less conserved. These make up approximately 65 %, 25 % and 10% of the protein respectively. When the branches leading to the duplicate gene copies were assigned their own substitution rate, the middle rate class showed a significant difference in each case, with *unc-38.1* and *unc-63.1* evolving some three to five times faster than unduplicated genes and *unc-38.2* and *unc-63.*2 evolving some seven to eight times faster. These rates did not approach a value of one and so are considered a relaxation of purifying selection and not directional positive selection for some new function. This is entirely consistent with the relaxation of constraint for the position of UNC-29 in the Cel-L-AChR described in Chapter 2.

Amino acids that fall into the middle rate class are found primarily in the ligand binding regions within the extracellular domain and in the intracellular loop. The ligand binding region is precisely that which is characteristic of the difference between alpha- and non-alpha subunits and an accelerated change here is expected if subunits were changing from one type to the other. The

intracellular loop was shown in Chapter 2 to be the principal region of UNC-29 that determined the ability to replace the LEV-1 subunit in the Cel-L-AChR. An elevated substitution rate for both these regions strongly suggests that there has been a change in subunit composition of the later Clade III L-AChR consistent with the appearance of *unc-38.2* and *unc-63.2* as new non-alpha type subunits and that the characteristic of being non-alpha more fundamental than simply loss of the YXCC motif.

The goal of reconstituting an L-AChR *ex vivo* from *Brugia malayi* to characterize functional changes associated with the accelerated subunit substitution rate was unfortunately unsuccessful. A functional L-AChR has been demonstrated in living *B. malayi* (Kashyap et al., 2021; Verma et al., 2017). The genome is very high quality, so the likelihood of missing subunits was remote (Howe et al., 2016, 2017). Comparison of the cloned subunit sequences with the other known sequences from related nematodes did not indicate any substitutions likely to make the subunits non-functional. The same approach has been used with *C. elegans*, *H. contortus, A. suum* and *Oesophagostomum dentatum* with success (Boulin et al., 2011; Boulin et al., 2008; Buxton et al., 2014; Williamson et al., 2009), and yet even replacing *B. malayi* subunits one-by-one into the Cel-L-AChR produced no ACh response. One possible explanation for this was that something fundamental had changed for these pLGIC subunits within the filarial nematodes.

The ACR-16 subunit of many nematodes has been used to reconstitute a functional, homomeric nicotine sensitive AChR (N-AChR) (Abongwa et al., 2016; Ballivet et al., 1996; Charvet et al., 2018; Choudhary et al., 2019; Hansen et al., 2021; Kaji et al., 2020). This requires the accessory protein RIC-3, whereas the L-AChR typically requires RIC-3, UNC-50 and UNC-73. Living *B. malayi* express a characteristic nicotine sensitive channel but no reconstituted nicotine response with *B. malayi* subunits was observed *ex vivo* (Kashyap et al., 2021; Verma et al., 2017). As a receptor that shares characteristics with the L-AChR but requires many fewer components to reconstitute, it was chosen as a representative model with which to investigate changes within the Clade III nematodes.

7.3 A change in accessory protein requirement for Clade III nematodes

An underlying premise for the work presented here is that evolutionary change in protein sequence is constrained by the proteins they interact with. Investigating changes will reveal those constraints and therefore details of those protein interactions. Functional nicotine sensitive N-AChRs have been reconstituted for a variety of different nematodes, including *C. elegans* and

Ascaris suum, a Clade III nematode at the base of the Clade III diversification (Abongwa et al., 2016; Ballivet et al., 1996). Since *B. malayi* subunits reconstituted no nicotine response there must have been a change between *Ascaris suum* and *B. malayi* responsible for this. Intermediate species that diverged between *A. suum* and *B. malayi* would each carry an independent example of ACR-16. Characterizing the properties of any N-AChR they produced would be an indirect evaluation of ACR-16 at the point when they diverged from each other. The species investigated were *Dracunculus medinensis*, *Gonglyonema pulchrum* and *Thelazia callipaeda* that diverge, in this order from the lineage from *A. suum* down to *B. malayi* (Coghlan et al., 2019).

The maximal response to ACh of each receptor produced from coexpression of ACR-16 and RIC-3 decreased progressively from a maximum with *A. suum* to nothing for *B. malayi*. The change was not discrete from all to nothing that would indicate a single event was responsible. Rather, the change suggested a gradual evolutionary adaptation. Receptor pharmacology was essentially unchanged for all species, except *B. malayi*, which could not be measured, with EC_{50} for both acetylcholine and nicotine and the response to a panel of different agonists and antagonists being similar. Interestingly, expression took progressively longer for each to reach maximal response. This suggested a progressive decrease in expression efficiency rather than a change in channel function was responsible.

Assembly and transport of receptors to the surface membrane involves many accessory proteins that stabilize individual subunits, promote assembly into a pentameric complex and maturation through the golgi and transport to the cell surface (Crespi et al., 2018; Millar & Harkness, 2008). Reconstitution of the *C. elegans* L-AChR was never fully achieved until three different accessory proteins were co-expressed, RIC-3, UNC-50 and UNC-74 (Boulin et al., 2008; Fleming et al., 1997). Other proteins certainly play a role *in vivo*, but these three proved essential for expression *ex vivo*. One possible explanation for the failure of Bma-ACR-16 to reconstitute a functional N-AChR *ex vivo* when one is observed *in vivo* is an increased dependence on accessory proteins not normally included in the oocyte expression experiments. Addition of endoplasmic reticulum resident accessory proteins EMC-6, NRA-2 or NRA-4 successfully recovered a nicotine and acetylcholine induced current *ex vivo* (Almedom et al., 2009; Richard et al., 2013). This demonstrated that the Bma-ACR-16 was indeed a functional subunit and that the hypothesis that an increased dependence on accessory proteins likely explained the failure to observe a response previously. In fact, co-expression ACR-16 from the

other species with EMC-6, NRA-2 or NRA-4 increased their response significantly. This was particularly apparent for *T. callipaeda* that had the smallest detectable response with only RIC-3. The small, but measurable response of BMA-ACR-16 with additional accessory proteins suggests that there are others, yet to be identified, that are required for full reconstitution of the Bma-N-AChR.

One question that remains is why did this change in AP requirement occur? The Clade III worms have seen many gene loss events, and this coincides with a changing AP requirement. It is possible that when dramatic changes to the subunits occur, for example many gene loss events, this creates an instability in the receptor system. As seen in Chapter 3, the Clade III subunits are undergoing relaxed selection pressure with higher rates of sequence change. The changes in the subunit sequences and numbers may lead to increased chances of errors occurring during folding and assembly, which would then lead to non-functional receptors. This could be overcome by having an increased dependence on accessory proteins. This means there exists a dynamic and inter-dependent relationship between receptors and their synthesis machinery.

One objective for this investigation was to use ACR-16 as a model for the more complex L-AChR. A combination of all the *B. malayi* subunits, together with EMC-6, NRA-2 or NRA-4 produced no response to ACH, LEV or NIC. Given the very small currents observed for the BMA-ACR-16 alone, it is likely that there was insufficient expression from the mix to produce a detectable current. Considering over 200 associated proteins are involved in receptor synthesis in the *C. elegans* (Gottschalk et al., 2005), identifying any critical missing accessory proteins would not be straightforward.

Overall, the strategy of using evolutionary change proved successful in that it was possible to show that the loss of ability to reconstitute a receptor was due to a progressive change, rather than a discrete event and that the reason was a decreased production of functional receptor at the cell surface, rather than a change in the physical properties of the receptor itself. Ultimately, this led to what we believe is the first *ex vivo* characterization of a filarial N-AChR.

7.4 Sequence interaction with accessory proteins.

Details of the subunit sequence that has changed within the filarial nematodes to alter their assembly and processing requirements may provide details useful in the ultimate identification of required components for reconstitution *ex vivo*. In Chapter 5 a series of chimeras were made between the ACR-16 of *A. suum* and *T. callipaeda* to identify the structural region(s)

involved in the requirement for new accessory proteins. The rationale for choosing these two species was that both produced a measurable response to ACh but were the most different in maximal response. Chimeras could therefore be classified as similar to either of the two original subunits. If *B. malayi* had been chosen one expected phenotype would have been no response to ACh and it would have been impossible to distinguish this from an artefactual, non-functional chimera. Results indicated that the extracellular domain (ECD) and ICL contribute to the requirement, but to varying degrees. The ECD was sufficient to determine significant functional expression. The ICL also contributed, but to a much lesser extent. The 95% similarity between *B. malayi* and *A. suum* in the ECD means that only these few amino acids exhibit a large effect on receptor functional expression. More finely divided chimeras followed by site directed mutagenesis could further narrow down the specific amino acids involved.

An accidental observation made while characterizing the Clade III ACR-16 receptors found that *D. medinensis* ACR-16 could produce large ACh induced currents, even in the absence of RIC-3 co-injection. Evidence suggested that the failure to reconstitute an N-AChR from BMA-ACR-16 was due to a change in its interaction with the accessory protein network. DME-ACR-16 provided dramatic evidence that the requirement for an accessory protein can change rapidly. All known ACR-16s require RIC-3 for functional expression in *X. laevis* oocytes (Abongwa et al., 2016; Ballivet et al., 1996; Charvet et al., 2018; Choudhary et al., 2019; Hansen et al., 2021; Kaji et al., 2020), therefore specific changes in the DME-ACR-16 must regulate this difference. While extensive work has been previously carried out on the regions in RIC-3 that interact with subunits and are required for its function (Ben-Ami et al., 2005, 2009; Yoav Biala et al., 2009), very little is known about the regions in the receptor subunits that interact with RIC-3 (Nishtala et al., 2014, 2016). Using a series of chimeras and point mutations between *A. suum* and *D. medinensis acr-16,* in Chapter 6 I was able to narrow down this effect to a single residue in the C-terminal tail. Other sequences in the ICL and transmembrane domain 4 (TM4) region also contributed to the RIC-3 requirement, but to a much lesser extent.

These results highlight the complex relationship between receptors and accessory proteins. On one hand, regions in the ECD and ICL appear to have changed progressively to mediate their need for EMC-6, NRA-2 and NRA-4, whereas a single residue in the C-terminal tail of DME-ACR-16 could completely determine its requirement for RIC-3. The interplay between receptors and accessory proteins is therefore both complex, determined by multiple

regions that contribute to different degrees and sensitive to changes in a single amino acid. However, care must be taken when interpreting the results from these chimeras because the regions identified may not physically interact with accessory proteins directly, but only influence subunit stability and other interactions, as was the case in Chapter 2 of ACR-13 influencing the requirement for LEV-1 without contact.

This research set out to determine how interactions between subunits within the L-AChR and with the accessory protein network could influence receptor composition and specificity for subunit position within the receptor. A novel approach of using evolutionary information to provide evidence of these interactions proved very successful. The principal challenge proved to be that while the process of cloning all subunits thought to play a role in the L-AChR from a new species has worked many times previously, on this occasion it did not. Rather than abandoning the model system, several different approaches were used to determine if there were cloning artefacts that could render the subunits non-functional. In the absence of any confirmation of a problem, the conclusion remaining was that a functional adaptation had occurred. The decision was taken to develop a new focus on the N-AChR as a simpler model and with this it was possible to show that the functional characteristics of the receptor did not change to any great extent, but that interactions involving the assembly and processing of receptors changed more fundamentally and progressively rather than in a single event.

This work provides an explanation for how parasitic nematode species related to *C. elegans* can produce an L-AChR with variable composition and specifically why the genes *acr-13* and *lev-1* often are lost together. Knowing that loss of a non-alpha subunit is often replaced by another non-alpha and this is accompanied by a reduced restriction of subunit position can now explain similar events seen in other species including vertebrates. These ideas may also be used in the search to find an explanation for the regulation of important drug target receptor composition in humans. The similarities between nematodes and vertebrates suggest that investigation of nematodes, and especially the use of evolutionary ideas, should play a more prominent role in this field of research.

CHAPTER 8: Methods

8.1 *Xenopus laevis*

Xenopus laevis are used in this study under Animal Use Protocol AUP-2015-7758. Adult female frogs were obtained from Xenopus1 (Dexter, USA) and housed in the Xenoplus Housing System (Technoplast, Italy). Each frog had a maximum of four oocyte extraction surgeries, before sacrifice in 0.45% MS-222 for 4 hours, followed by heart removal.

8.2 Subunit and accessory protein cloning

Subunit and accessory protein sequences were either cloned from worm complimentary deoxyribonucleic acid (cDNA) or synthesized from predicted coding sequences, depending on the availability of worm cDNA. *Caenorhabditis elegans, Haemonchus contortus* & *Brugia malayi* cDNA subunit library cDNA clones used throughout the study were inserted in the *X. laevis* expression plasmid pTB207 that contains the beta-globin 3' UTR, or the modified pTD2 that also contain the beta-globin 5' UTR (Dr. T. Duguet, pers comm). *C. elegans lev-1*, *unc-29*, *unc-38*, *unc-73*, and *acr-13* were obtained from Dr. Thomas Boulin (Boulin et al., 2008). *H. contortus* cDNA subunit and ancillary protein clones *lev-1*, *acr-8*, *unc-38*, *unc-63*, *unc-50*, *unc-73*, *ric-3.1*, *unc-29.1*, and *unc-29.2* were obtained from Dr. Cédric Neveu, (Boulin et al., 2011) . *B. malayi* subunits and accessory protein cDNA clones (*acr-8, acr-11, acr-12, acr-15, acr-16, acr-26, acr-27, unc-29, unc-38.1, unc-38.2, unc-63.1*, *unc-63.2, acr-26, unc-54, unc-70, ric-3,* and *molo-1*) were cloned by Dr. Thomas Duguet and Sophia Bertolussi or myself. *C. elegans* dimers were obtained from previous work in this lab (Duguet, 2017). *C. elegans* accessory proteins *nra-2, nra-4 and emc-6* and Clade III acr-16s were synthesized from Gene Universal Inc (USA).

8.2.1 B. malayi ric-3, unc-50, unc-74, molo-1 and eat-18

unc-50, ric-3, unc-74, and *molo-1* were cloned from adult female *B. malayi* cDNA. Two rounds of PCR were carried out. The first round, using "outer" primers amplified the gene of interest from the cDNA. The second round, using "inner" primers amplified the first round PCR products and introduced a Not1 restriction enzyme site at the 5' end of the gene and an ApaI restriction enzyme site on the 3' end of the gene. Primers are shown in Table 4. The *Bma-eat-18* coding sequence was identified from the annotated genome of *B. malayi*. The short sequence of

Bma-eat-18 enabled it to be synthesized in two halves with long, overlapping oligos. The first half primers introduced the Not1 restriction enzyme site at the 5' end and the SphI restriction enzyme site at the 3' end. The second half primers introduced the SphI restriction enzyme site at the 5' end and the ApaI restriction enzyme site at the 3' end (Figure 4).

	Outer Forward primer (5'-'3)	**Outer Reverse primer (5'-'3)**	**Inner Forward primer (5'-'3)**	**Inner Reverse primer (5'-'3)**
Ric-3	GAAGGCTTGCTCTCTCTTGGT	TTGGGTCCATAAGTTGTTGATGT	GCGGCCGCCGTTGAATGTCAGCGGAACC	GGGCCCTTAGATTCTTAACTTTTTCCACG
Unc-50	CTGACGATTGATCAGCTACTGC	TCAGAAGCATATGCATATCACT	GCGGCCGCCTACTGCAGCTGTTTCACA	GGGCCCGCAAATATTCTATTCTCAACTTCCTCT
Unc-74	GCAAGGATTTTGAATATCCGTAATTT	ACGCTTCTGCTGGATTTCATC	GCGGCCGCTGTGAATGTGGTTATTTAATTGTTGC	GGGCCCCACATCCAACTTTTACTCCTCCT
Molo-1	CTCGTTAATAATAATTCAAATAATGGC	ACAATAATCAATTTATGAAATTATACA	GCGGCCGCTGTAAAATGAGCCTAACACATTGG	GGGCCCTTTTTGAATCAAACAAATGTTGCAT
eat-18 first half	GCGGCCGCATGGCACAAATGCGCACATTGGAAAATGTATTAGAAGCACGGATTAATTTATTAATTAATGAAGAAAAAGCTAATGCAAAAGA		GCATGCAATAATACAGGTAAATAATAATGCAAAAAGAATATCACAATCCAAACTACGACAAAATGCGCAATCGTCTTTTGCATTAGCTTTTTCT	
eat-18 second half	GCGGCCGCATGGCACAAATGCGCACATTGGAAAATGTATTAGAAGCACGGATTAATTTATTAATTAATGAAGAAAAAGCTAATGCAAAAGA		GCATGCAATAATACAGGTAAATAATAATGCAAAAAGAATATCACAATCCAAACTACGACAAAATGCGCAATCGTCTTTTGCATTAGCTTTTTCT	

Table 4. *Brugia malayi* accessory protein primers.

B. malayi accessory proteins were cloned from adults cDNA using the following primers. Cloning procedure is described above in Section 8.2.1. The accessory proteins are used in Chapters 5 & 6.

PCR products were ran on a 0.8% agarose gel, and the bands extracted, purified (ZymoResearch, USA), ligated into pGEM-T (Promega, USA) and transformed into D-H5α *Escherichia coli* (ThermoFisher Scientific, USA) grown on LB-X-gal plates with 100 μM Ampicilin (ThermoFisher Scientific, USA). Plasmids were purified from white colonies (BioBasic, USA) and successful clones identified by sequencing (Genome Quebec Sequencing, Canada). Genes were then transferred to the pTD2 expression vector by digesting the 5' end with Not1 and the 3' end with ApaI at 37°C for 2 hours (Fast Digest, ThermoFisher Scientific, USA). For the two halves of the *eat-18* sequence, they were transferred to the pTD2 expression vector

by digesting the 5' end with Not1 and SphI and the 3' end with Apa1and SphI at 37 °C for 2 hours (Fast Digest, ThermoFisher Scientific, USA). Digestions were ran on a 0.8% agarose gel to confirm digestion, the appropriate bands extracted, purified (Zymo Research, USA) and ligated (T4 DNA ligase, Promega, USA) into pTD2 at 4°C overnight, followed by transformation into D-H5α. Successful digestion and ligation was confirmed with sequencing (Genome Quebec Sequencing, Canada).

8.2.2 Clade III ACR-16, *C. elegans* Nra-2, nra-4, emc-6

Clade III *acr-16* coding sequences were identified from the annotated genomes of *Aascaris suum, Gongylonema pulchrum, Dracunculus medinensis, and Thelazia callapaeda,* accessory proteins *emc-6, nra-2* and *nra-4* coding sequences were identified from the *C. elegans* genome. cDNA clones in the pTD2 expression vector were purchased from Gene Universal Inc. (USA). Plasmids were transformed into D-H5α and verified with sequencing (McLab, USA).

8.2.3 Chimeras

Chimeras, in the pTD2 expression vector, were purchased from Gene Universal Inc. (Newark, USA). Sequences were designed as shown in Figure 41 exchanging the intracellular loop between *Hco-unc-29.1* and *Hco-unc-29.2*, and between *Asu-acr-16* and *Bma-acr-16*.

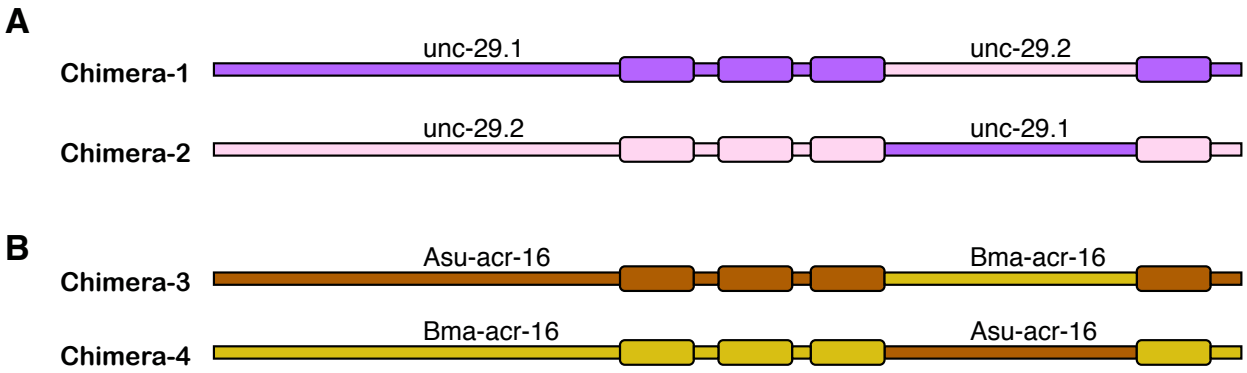

Figure 41. Chimeras.
Chimeras were made exchanging the intracellular loops
(A) Chimeras for the *H. contortus unc-29* duplication. Chimera-1 has the *unc-29.1* subunit with the intracellular loop of *unc-29.2*, and Chimera-2 has the *unc29.2* subunit with the intracellular loop of *unc-29.1*.
(B) Chimeras for the *A. suum* and *B. malayi acr-16s.* Chimera-3 has the *Asu-acr-16* subunit with the intracellular loop of *Bma-acr-16*, and Chimera-4 has the Bma-*acr-63* subunit with the intracellular loop of *Bma-acr-16*. Chimeras 1 & 2 are used in Chapter 2, Chimeras 3 & 4 are used in Chapter 5.

8.2.4 *Ascarus suum, Dracunculus medinensis & Thelazia callipaeda* ACR-16 Chimeras

Predicted coding sequences of *A. suum D. medinensis and T. callipaeda acr-16* were obtained from their respective genomes available at Wormbase Parasite. The high sequence similarity between the *acr-16* genes allowed for the nucleotide sequences to be modified to insert restriction enzyme recognized sites between the three sequences without altering the protein product. The restriction enzyme modified sequences are termed REM (Figure 42, Appendix Figure 5). This allowed for the generation of many chimeras exchanging regions between the introduced restriction enzyme sites. ACR-16-REM genes were synthesized from Gene Universal (USA) in the pTD2 vector.

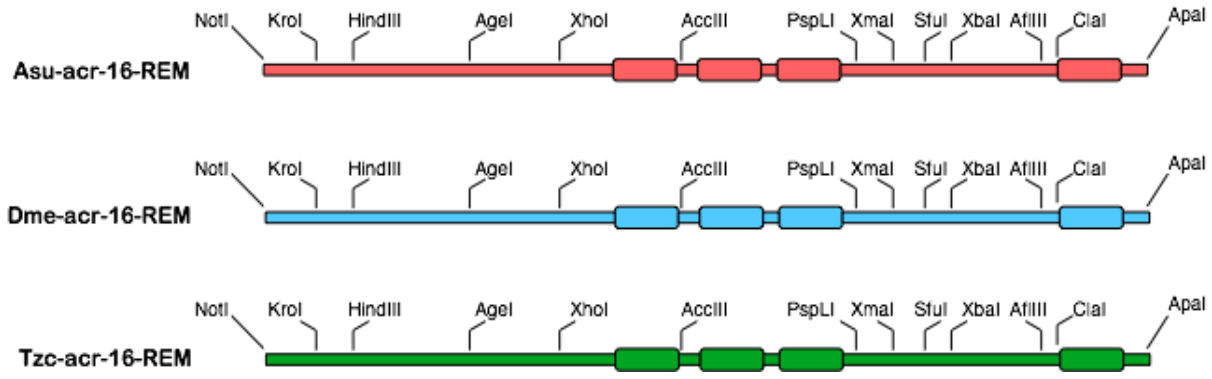

Figure 42. ACR-16 REM schematic.
Nucleotide sequences were modified to introduce complementary restriction enzyme sites (ACR-16-RAM). These sequences were then used to generate the acr-16 chimeras used in Chapters 5 and 6 (see Table 5). Cloning protocol is described in Chapter 8.2.4.

In order to construct the chimeras, plasmids were digested with the appropriate restriction enzymes (Fast Digest, ThermoFisher Scientific, USA) at 37°C for two hours and ran on a 0.8% agarose gel (see Table 5). The appropriately sized bands were extracted, purified (Zymo Research, USA) and ligated overnight at 4°C (T4 DNA ligase, Promega, USA). Ligated products were transformed into D-H5α and positive clones were confirmed with sequencing (McLab, USA). Chimera digestion and ligation combinations are shown in Table 5.

The TM4 and C-terminal tail point mutation chimeras were made by digesting ASU-ACR-16-REM and DME-ACR-16-REM with FastDigest Bsu15I and ApaI (ThermoScientific, USA). Digest were ran on an 0.8% agarose gel and the band extracted and purified (Zymo Research, USA). The oligo inserts, containing primers with the point mutations of interest (see Table 6), were made following the Sigma - oligo anneal protocol. Briefly, the primers were suspended in annealing buffer (10 mM Tris, pH 7.5 - 8.0, 50 mM NaCl, 1 mM EDTA) to a final concentration of 100 µM. Equal volumes of complementary primers then were combined and annealed by heating at 95°C for 3 min followed by a gradual decline to 25°C over 45 minutes. Oligos were then ligated to the appropriate digested ASU-ACR-16-REM and DME-ACR-16-REM using T4 ligase (Promega, USA) and transformed into DH5α. Clones were confirmed with sequencing (McLab, USA).

	"Background" digestion	**"Insert" Digestion**	**Restriction enzymes**
DME-ICL	ASU-ACR-16-REM	DME-ACR-16-REM	PspLI + ClaI
ASU-ICL	DME-ACR-16-REM	ASU-ACR-16-REM	PspLI + ClaI
DME-ECD	ASU-ACR-16-REM	DME-ACR-16-REM	NotI + AccIII
ASU-ECD	DME-ACR-16-REM	ASU-ACR-16-REM	NotI + AccIII
DME-TM	ASU-ECD	DME-ECD	PspLI + ClaI
ASU-TM	DME-ECD	ASU-ECD	PspLI + ClaI
ASU + first half DME ICL	DME-ICL	ASU-ICL	Not1 + SfuI
ASU + second half DME ICL	ASU-ACR-16-REM	DME-ACR-16-REM	Not1 + SfuI
DME + first half ASU ICL	DME-ACR-16-REM	ASU-ICL	Not1 + SfuI
DME + second half ASU ICL	ASU-ICL	DME-ACR-16-REM	Not1 + SfuI
ASU-ICL +DME-TM2	ASU-TM	DME-TM	AccIII + ClaI
DME-ICL + DME-TM2	ASU-ACR-16	DME-ACR-16	AccIII + ClaI
ASU-ICL + DME-TM4	DME-ACR-16	ASU-ACR-16	AccIII + ClaI
DME-ICL + DME-TM4	DME-TM	ASU-TM	AccIII + ClaI
ASU-TZCICL	ASU-ACR-16-REM	TZC-ACR-16-REM	PspLI + ClaI
TZC-ASUICL	TZC-ACR-16-REM	ASU-ACR-16-REM	PspLI + ClaI
ASU-TZCECD	ASU-ACR-16-REM	TZC-ACR-16-REM	NotI + AccIII
TZC-ASUECD	TZC-ACR-16-REM	ASU-ACR-16-REM	NotI + AccIII
ASU-TZCTM	TZC-ASUECD	ASU-TZCECD	PspLI + ClaI
TZC-ASUTM	ASU-TZCECD	TZC-ASUECD	PspLI + ClaI

Table 5. *A. suum* and *D. medinensis* point mutation restriction enzyme combinations.
ACR-16 chimeras were made by digesting the ACR-16-REM sequences (Figure 42) using the designated restriction enzymes. The cloning protocol is detailed in Chapter 8.2.4. These chimeras were used in Chapter 5 & 6.

Parent plasmid	Point mutation name	Forward primer (5'-3')	Reverse primer (5'-3')	Desired Point Mutation(s)
Dme-acr-16-REM	DME-ACR-16-TM 1	CGATTGTGCTTATATGTCTT TACAATATTTATTATAGCAT CCTCTTGCGGAATATTACTA TCAGCGCCTTACATTATAGC ATAAGGGCC	CTTATGCTATAATGTAAGG CGCTGATAGTAATATTCCG CAAGAGGATGCTATAATA AATATTGTAAAGACATAT AAGCACAAT	LCLY**V**FTIFIIASSCGILLSAPYII A
	DME-ACR-16-TM 2	CGATTGTGCTTATATATATT TACAGTCTTTATTATAGCAT CCTCTTGCGGAATATTACTA TCAGCGCCTTACATTATAGC ATAAGGGCC	CTTATGCTATAATGTAAGG CGCTGATAGTAATATTCCG CAAGAGGATGCTATAATA AAGACTGTAAATATATAT AAGCACAAT	LCLYIFT**V**FIIASSCGILLSAPYII A
	DME-ACR-16-TM 3	CGATTGTGCTTATATATATT TACAATATTTATTGTAGCAT CCTCTTGCGGAATATTACTA TCAGCGCCTTACATTATAGC ATAAGGGCC	CTTATGCTATAATGTAAGG CGCTGATAGTAATATTCCG CAAGAGGATGCTACAATA AATATTGTAAATATATATA AGCACAAT	LCLYIFTIFI**V**ASSCGILLSAPYII A
	DME-ACR-16-TM 1+2	CGATTGTGCTTATATGTCTT TACAGTCTTTATTATAGCAT CCTCTTGCGGAATATTACTA TCAGCGCCTTACATTATAGC ATAAGGGCC	CTTATGCTATAATGTAAGG CGCTGATAGTAATATTCCG CAAGAGGATGCTATAATA AAGACTGTAAAGACATAT AAGCACAAT	LCLY**V**FT**V**FIIASSCGILLSAPYII A
	DME-ACR-16-TM 1+3	CGATTGTGCTTATATGTCTT TACAATATTTATTGTAGCAT CCTCTTGCGGAATATTACTA TCAGCGCCTTACATTATAGC ATAAGGGCC	CTTATGCTATAATGTAAGG CGCTGATAGTAATATTCCG CAAGAGGATGCTACAATA AATATTGTAAAGACATAT AAGCACAAT	LCLY**V**FTIFI**V**ASSCGILLSAPYII A
	DME-ACR-16-TM 2+3	CGATTGTGCTTATATATATT TACAGTCTTTATTGTAGCAT CCTCTTGCGGAATATTACTA TCAGCGCCTTACATTATAGC ATAAGGGCC	CTTATGCTATAATGTAAGG CGCTGATAGTAATATTCCG CAAGAGGATGCTACAATA AAGACTGTAAATATATAT AAGCACAAT	LCLYIFT**V**FI**V**ASSCGILLSAPYII A
	DME-ACR-16-TM 1+2+3	CGATTGTGCTTATATGTCTT TACAGTCTTTATTGTAGCAT CCTCTTGCGGAATATTACTA TCAGCGCCTTACATTATAGC ATAAGGGCC	CTTATGCTATAATGTAAGG CGCTGATAGTAATATTCCG CAAGAGGATGCTACAATA AAGACTGTAAAGACATAT AAGCACAAT	LCLY**V**FT**V**FI**V**ASSCGILLSAPYI IA
	DME-ACR-16-tail	CGATTGTGCTTATATATATT TACAATATTTATTATAGCAT CCTCTTGCGGAATATTACTA TCAGCGCCTTACACCATAGC ATAAGGGCC	CTTATGCTATGGTGTAAGG CGCTGATAGTAATATTCCG CAAGAGGATGCTATAATA AATATTGTAAATATATATA AGCACAAT	LCLYIFTIFIIASSCGILLSAPY**T**I A
	DME-ACR-16-TM 1+2+3+tail	CGATTGTGCTTATATGTCTT TACAGTCTTTATTGTAGCAT CCTCTTGCGGAATATTACTA TCAGCGCCTTACACCATAGC ATAAGGGCC	CTTATGCTATGGTGTAAGG CGCTGATAGTAATATTCCG CAAGAGGATGCTACAATA AAGACTGTAAAGACATAT AAGCACAAT	LCLY**V**FT**V**FI**V**ASSCGILLSAPY **T**IA
Asu-acr-16-REM	ASU-ACR-16-TM 1	CGATTGTGTCTGTACATCTT CACGGTCTTCATTGTAGCTT CTTCATGTGGAATACTGCTC TCTGCGCCTTACACCATCGC ATAGGGGCC	CCTATGCGATGGTGTAAG GCGCAGAGAGCAGTATTC CACATGAAGAAGCTACAA TGAAGACCGTGAAGATGT ACAGACACAAT	LCLY**I**FTVFIVASSCGILLSAPYT IA
	ASU-ACR-16-TM 2	CGATTGTGTCTGTACGTCTT CACGATCTTCATTGTAGCTT CTTCATGTGGAATACTGCTC TCTGCGCCTTACACCATCGC ATAGGGGCC	CCTATGCGATGGTGTAAG GCGCAGAGAGCAGTATTC CACATGAAGAAGCTACAA TGAAGATCGTGAAGACGT ACAGACACAAT	LCLYVFT**I**FIVASSCGILLSAPYT IA
	ASU-ACR-16-TM 3	CGATTGTGTCTGTACGTCTT CACGGTCTTCATTATAGCTT CTTCATGTGGAATACTGCTC	CCTATGCGATGGTGTAAG GCGCAGAGAGCAGTATTC CACATGAAGAAGCTATAA	LCLYVFTVFI**I**ASSCGILLSAPYT IA

	TCTGCGCCTTACACCATCGC ATAGGGGCC	TGAAGACCGTGAAGACGT ACAGACACAAT	
ASU-ACR-16-TM 1+2	CGATTGTGTCTGTACATCTT CACGATCTTCATTGTAGCTT CTTCATGTGGAATACTGCTC TCTGCGCCTTACACCATCGC ATAGGGGCC	CCTATGCGATGGTGTAAG GCGCAGAGAGCAGTATTC CACATGAAGAAGCTACAA TGAAGATCGTGAAGATGT ACAGACACAAT	LCLY**I**FT**I**FIVASSCGILLSAPYTI A
ASU-ACR-16-TM 1+3	CGATTGTGTCTGTACATCTT CACGGTCTTCATTATAGCTT CTTCATGTGGAATACTGCTC TCTGCGCCTTACACCATCGC ATAGGGGCC	CCTATGCGATGGTGTAAG GCGCAGAGAGCAGTATTC CACATGAAGAAGCTATAA TGAAGACCGTGAAGATGT ACAGACACAAT	LCLY**I**FTVFI**I**ASSCGILLSAPYTI A
ASU-ACR-16-TM 2+3	CGATTGTGTCTGTACGTCTT CACGATCTTCATTATAGCTT CTTCATGTGGAATACTGCTC TCTGCGCCTTACACCATCGC ATAGGGGCC	CCTATGCGATGGTGTAAG GCGCAGAGAGCAGTATTC CACATGAAGAAGCTATAA TGAAGATCGTGAAGACGT ACAGACACAAT	LCLYVFT**I**FI**I**ASSCGILLSAPYTI A
ASU-ACR-16-TM 1+2+3	CGATTGTGTCTGTACATCTT CACGATCTTCATTATAGCTT CTTCATGTGGAATACTGCTC TCTGCGCCTTACACCATCGC ATAGGGGCC	CCTATGCGATGGTGTAAG GCGCAGAGAGCAGTATTC CACATGAAGAAGCTATAA TGAAGATCGTGAAGATGT ACAGACACAAT	LCLY**I**FT**I**FI**I**ASSCGILLSAPYTI A
ASU-ACR-16-tail	CGATTGTGTCTGTACGTCTT CACGGTCTTCATTGTAGCTT CTTCATGTGGAATACTGCTC TCTGCGCCTTACATTATCGC ATAGGGGCC	CCTATGCGATAATGTAAG GCGCAGAGAGCAGTATTC CACATGAAGAAGCTACAA TGAAGACCGTGAAGACGT ACAGACACAAT	LCLYVFTVFIVASSCGILLSAPY **I**IA
ASU-ACR-16-TM 1+2+3+tail	CGATTGTGTCTGTACATCTT CACGATCTTCATTATAGCTT CTTCATGTGGAATACTGCTC TCTGCGCCTTACATTATCGC ATAGGGGCC	CCTATGCGATAATGTAAG GCGCAGAGAGCAGTATTC CACATGAAGAAGCTATAA TGAAGATCGTGAAGATGT ACAGACACAAT	LCLY**I**FT**I**FI**I**ASSCGILLSAPY**I**I A

Table 6. *A. suum* and *D. medinensis* point mutation primers.

Point mutations were introduced into the fourth transmembrane domain and C-terminal tail of *A. suum* and *D. medinensis* ACR-16. The cloning protocol is detailed in Chapter 8.2.4. Desired point mutations are shown with the mutated residues in bold. These point mutations were used in Chapter 6.

8.3 *In vitro* RNA transcription

A PCR of all genes using forward primer pTD2F (5'-TTGGCACCAAAATCAACGGG – 3') and reverse primer SP6 (5'- ATTTAGGTGACACTATAG -3') was carried out with the SuperFi DNA Polymerase (ThermoFischer Scientific, USA). This PCR amplifies the gene of interest, the T7 promoter sequence, the poly-A tail, and 5' and 3' beta-globin UTRs. PCR products were ran on a 0.8% agarose gel and the band extracted, purified (Zymo Research, USA) and used for the *in vitro* transcription reaction.

In vitro transcription using the mMESSAGE mMACHINE T7 kit (Ambion, USA) was carried out following manufacturers protocol. cRNA was precipitated with lithium chloride and dissolved in RNase- free water. Purified cRNA concentration was measured using a Nanodrop

spectrophotometer (ThermoFisher Scientific, USA) and quality determined with a 0.8% agarose gel. Each subunit and accessory protein cRNA was diluted in nuclease-free water. Desired subunit combinations with associated ancillary proteins were mixed and diluted with nuclease-free water to a final concentration of 250ng/uL of each construct in the injection mixture.

8.4 *Xenopus laevis* oocyte extraction and preparation

Adult female *X. leavis* were anaesthetized in 0.15% MS-222. A < 1 cm incision was made on the side of the abdomen and ovarian lobes containing oocytes extracted. The incision was sutured and the frog place in a recovery holding tank. When recovered (approximately 7 days) the frog was returned to the colony housing tank. Extracted oocytes were prepared according to standard protocol (Goldin, 1991). Briefly, the lobes were placed in a Ca2+-free OR2 solution and manually divided into clusters of <10 oocytes with thin tweezers. A 90 minute incubation in 10 mg/mL collagenase type II (Sigma-Aldrich, USA) was necessary to further separate the oocytes and digest the follicular envelope layer. Oocytes were washed five times in Ca2+-free OR2 and finally placed ND96 solution (NaCl 96 mM, KCl 2 mM, $CaCl_2$ 1.8 mM, $MgCl_2$ 1 mM and HEPES 5 mM, pH 7.3) supplemented with sodium pyruvate 2.5 mM (Forrester et al., 2003) and incubated at 18°C until cRNA injection.

8.5 Oocyte injection

Oocytes were injected with 50 nL (12.5 ng per injected gene) of the desired cRNA subunit and accessory combination mix. Oocytes were placed on a plastic mesh sheet immersed in ND96 solution and injected via Nanoject (Drummond Scientific, USA). Pulled glass capillaries (World Precision Instruments, USA) were back filled with oil and used for injections. Following injection, oocytes were incubated in ND96 buffer at 18°C until electrophysiology. Unless otherwise stated, ACR-16 receptors and chimeras were measured 2 days after injection and levamisole-sensitive acetylcholine receptors (L-AChRs) and chimeras were measured 4-5 days after injection.

8.6 Pharmacological compounds

Receptor ligands acetylcholine (ACh), levamisole (LEV), nicotine (NIC), bephenium (BEPH), betaine (BET), norepinephrine (NOR), epinephrine (EPI), oxantel (OXA), morantel

(MOR), Pyrantel (PYR), dopamine (DA) used for electrophysiology characterization of ion channels were obtained from Sigma-Aldrich (USA).

All drugs were dissolved in recording solution (NaCl 100 mM, KCl 2.5 mM, $CaCl_2$ 1 mM, HEPES 5 mM, pH 7.3) to a stock concentration of 10mM and diluted to their final recording concentrations. OXA, BEPH, and BET were first dissolved in dimethyl suloxide (DMSO) to ensure a final recording concentration contained less than 0.1% DMSO. All compounds were adjusted to a final recording pH of 7.3. For agonist profiling, all drugs were diluted to a concentration of 100 μM. For EC_{50}, NIC and ACh were diluted to concentrations between 0.1 and 300 μM. For ACR-16 maximum response measurements, 100 μM NIC and ACh was used. For L-AChR response measurements, 100 μM LEV and ACh was used.

8.7 Two-electrode voltage-clamp electrophysiology (TEVC)

Oocytes were placed individually in an RC3Z chamber (Harvard Apparatus, USA), submerged in recording solution. The RC3Z chamber was connected to a perfusion system which itself was connected to a flat RC-1Z chamber (Harvard Apparatus, USA). Pulled glass capillaries (World Precision Instruments, USA) were filled with 3M KCl and the tips clipped and checked for appropriate resistance (between 0.5 and 3 MΩ). A 3M KCl agar bridge connected the oocyte bath chamber to the ground. Measurements were made using a Geneclamp 500B amplifier with Digidata1322M (Axon instruments, USA). Oocytes were voltage-clamped at -60 mV while exposed to drug solutions. Oocytes with holding potentials less than -400nA were not considered for analysis due to poor membrane condition. Data was analyzed using Clampex 9.2 (Axon Instruments, USA) and graphs made in Prism (version 9.0).

8.8 Manual Gene Curation

Sequences of the pentameric ligand-gated ion channel (pLGIC) family were identified in the genome data from nematode species available in the WBPS13 release of the WormBase ParaSite database (Coghlan et al., 2019). Manual curation of annotations was based on the strong structural conservation of the pLGIC subunits. Multiple sequence alignment of orthologs from all species was used to make final corrections. Manual gene curation was graciously carried out by Dr. Robin Beech.

8.9 Subunit Phylogeny

Nucleotide sequences were aligned as codons in Geneious (v 9.0.5, Biomatters Ltd) using the MAFFT plugin (v7.017) (Katoh et al., 2002). Highly variable regions including the signal peptide sequence, the TM4 C-terminal tail, and the TM3–TM4 intracellular loop were removed. PhyML (v3.0) was used to produce a maximum likelihood phylogeny and SH branch support statistics used to determine branch reliability (Guindon et al., 2010). Resulting subunit trees were overlaid onto the species tree (Coghlan et al., 2019) in order to confirm accuracy of branching topology.

8.10 Subunit substitution rates

CodeML (PAML) was used to estimate relative non-synonymous:synonymous substitution rates (dN/dS) in all branches of the phylogenetic tree (Yang, 2007). A number of nested models were used with 1 to 3 amino acid rate class categories. Model 0 had a single substitution rate across all branches. Model 3k2 has two substitution rates across all branches. Model 3k3 had three substitution rates across all branches. Nested Model D has three rate classes across all branches with a single class that could vary in marked branches and clades. Analysis was carried out with the same species for both *unc-38* and *unc-63* and the translated MSA and phylogeny files used for substitution rate analysis. Branches leading to the *unc-63.2* and *unc-38.2* subclades were allowed a different rate to the rest of the tree. A probability of less than 0.1 was considered significant.

8.11 *In Silico* Homology Modelling

Homology modelling was carried out using the default hm_build.mcr macro of YASARA (v.16.3.8, YASARA Biosciences) (Krieger & Vriend, 2014). The YASARA quality Z-score, that depends on the average distance away from the high-resolution template structure, was used to assess each model (Krieger & Vriend, 2014). The top scoring model was used for subsequent analysis. For the homomeric ACR-16 receptors of *A. suum* and *D. medinensis*, a sequencing alignment to the alpha subunit (Mol A) of the human alpha4beta2 nicotine receptor (PDB: 6CNK) as a template was used for structural prediction.

Appendix

Model	Test	Likelihood	2d	df	Prob		Rate classes		
M0		-23322.59317				p	1		
						w	0.05015		
M3k2	3k2 - M0	-22479.73945	1685.707448	2	0	p	0.77114	0.22886	
						w	0.1109	0.20060	
M3k3	3k3 - M0	-22335.19114	1974.804066	2	0	p	0.65001	0.27641	0.07358
						w	0.00459	0.08760	0.42047
M3k3	3k3 - M3k2	-22335.19114	289.096618	2	0	p	0.65001	0.27641	0.07358
						w	0.00459	0.08760	0.42047
MDA	DA - M3k3	-22316.16615	38.049968	2	$5.46E^{-09}$	p	0.65784	0.06274	0.27941
						w	0.00468	0.45093	0.07777
						w	0.00468	0.45093	0.17263
MDB	DB - M3k3	-22248.25275	173.876776	2	0	p	0.59438	0.08661	0.31901
						w	0.00255	0.36398	0.04659
						w	0.00255	0.36398	0.22708
MDC	MDC - M3k3	-22190.61484	289.152594	2	0	p	0.6262	0.0448	0.3290
						w	0.00262	0.51769	0.03545
						w	0.00262	0.51769	0.17383
						w	0.00262	0.51769	0.2804
MDa	Da -M3K3	-22334.47788	1.426506	2	0.49	p	0.07327	0.27287	0.65386
						w	0.42153	0.08760	0.00470
						w	0.42153	0.08760	977.64340
MDb	MDb - M3k3	-22331.64679	7.088696	2	0.0288	p	0.07066	0.65043	0.27891
						w	0.43021	0.00462	0.08622
						w	0.43021	0.00462	0.37224
MDc	MDc - M3k3	-22331.61285	7.156564	2	0.0279	p	0.07066	0.64959	0.27975
						w	0.43033	0.00458	0.08599
						w	0.43033	0.00458	68.33349
						w	0.43033	0.00458	0.34847

Appendix Table 1. Substitution rate analysis of unc-38 duplications.

Chi squared analysis of PAML substitution rate models for unc-38. Model MDC was the best fitting Model with a likelihood of -22190.61484 and prob. of 0. This model sets three amino acid rate classes; with the middle substitution rate class varying between subclades unc-38.1, unc-38.2, and Clade V background; 0.17383, 0.2804, and 0.03545 respectively.

Model	Test	Likelihood	2d	d.f.	Prob		Rate classes		
M0		-24131.60634				p	1		
						w	0.03757		
M3k2	M3k2 - M0	-23559.16852	1144.875642	2	0	p	0.72211	0.27789	
						w	0.00856	0.11791	
M3k3	M3k3 - M0	-23483.21485	1296.782992	2	0	p	0.60695	0.29385	0.09920
						w	0.00410	0.05793	0.20482
M3k3	M3k3 - M3k2	-23483.21485	151.90735	2	0	p	0.60695	0.29385	0.09920
						w	0.00410	0.05793	0.20482
MDA	MDA - M3k3	-23480.8922	4.645286	2	0.098	p	0.61110	0.29523	0.09367
						w	0.00418	0.05938	0.22314
						w	0.00418	0.05938	0.15777
MDB	MDB - M3k3	-23387.96443	190.500838	2	0	p	0.06960	0.59692	0.33348
						w	0.20865	0.00327	0.03815
						w	0.20865	0.00327	0.20423
MDC	MDC - M3k3	-23370.46038	225.508934	2	0	p	0.58	0.07	0.35
						w	0.00281	0.19757	0.0274
						w	0.00281	0.19757	0.06839
						w	0.00281	0.19757	0.19569
MDa	MDa - M3K3	-23481.55552	3.318662	2	0.1902	p	0.60653	0.29362	0.09985
						w	0.00408	0.05754	0.20590
						w	0.00408	0.05754	0.0000
MDb	MDb - M3k3	-23482.30451	1.820666	2	0.4023	p	0.09989	0.60707	0.29304
						w	0.20397	0.00410	0.05795
						w	0.20397	0.00410	0.04770
MDc	MDc - M3k3	-23480.55296	5.323766	2	0.0698	p	0.29279	0.60470	0.10251
						w	0.05716	0.00406	0.20165
						w	0.05716	0.00406	0.0000
						w	0.05716	0.00406	0.43134

Appendix Table 2. Substitution rate analysis of unc-63 duplications.

Chi squared analysis of PAML substitution rate models for unc-63. Model MDC was the best fitting Model with a likelihood of -23370.46038 and prob. of 0.001. This model sets three amino acid rate classes; with the middle substitution rate class varying between subclades unc-63.1, unc-63.2, and Clade V background; 0.06839, 0.19569, and 0.0274 respectively.

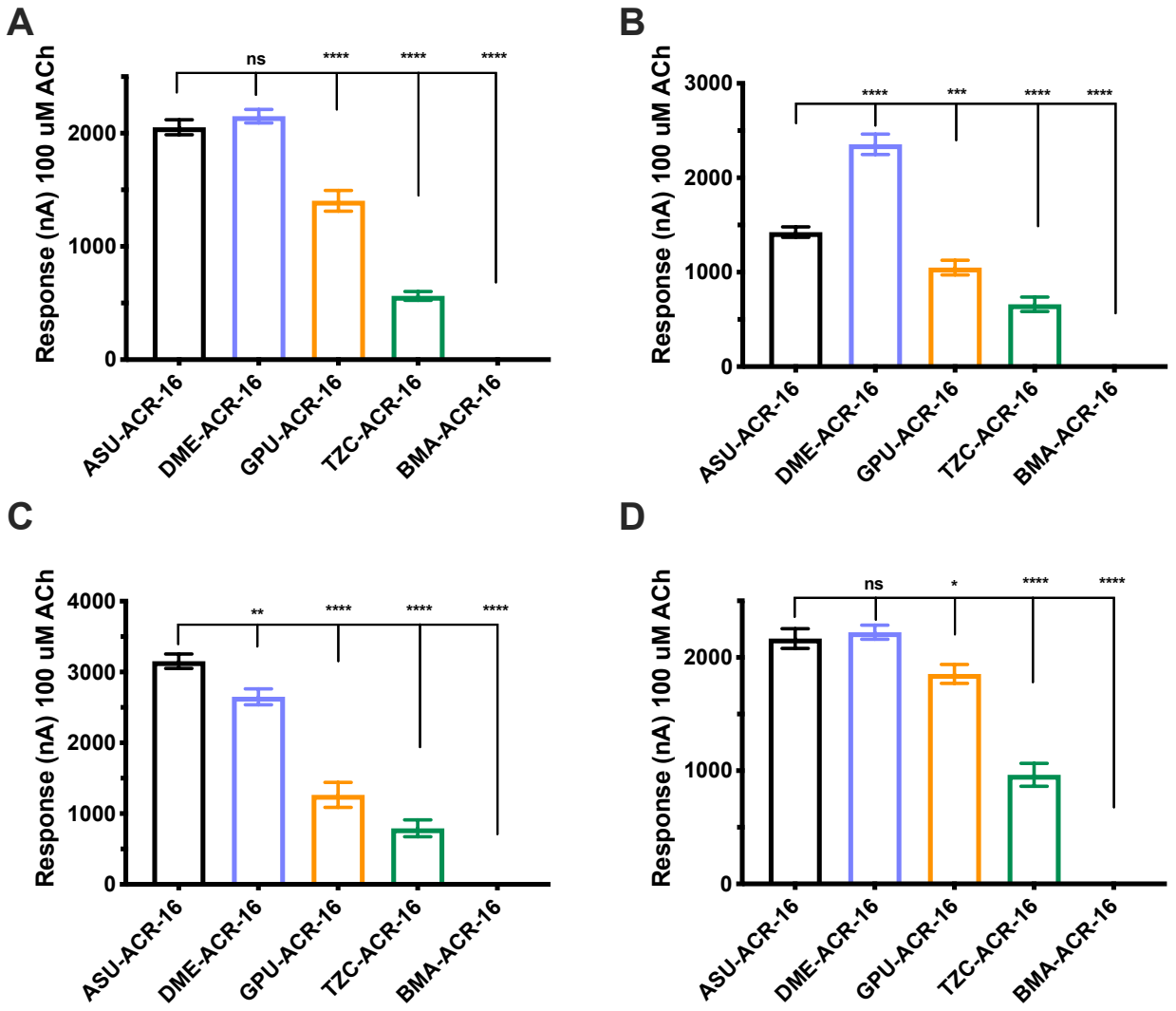

Appendix Figure 1. Responses of ACR-16 with different accessory proteins show declining phylogenetic responses.

Responses of *A. suum* (black), *D. medinensis* (purple), *G. pulchrum* (orange), *T. callipaeda* (green) and *B. malayi* (grey) to 100 µM ACh with accessory proteins.
(A) *H. contortus* RIC-3;
(B) *B. malayi* RIC-3 + MOLO-1;
(C) *B. malayi* RIC-3 + EAT-18;
(D) *B. malayi* RIC-3 + EAT-18 + UNC-50 + UNC-74.
See Appendix Table 3 for values and Chapter 4. Error bars represent standard error.
n>8, *p<0.05. ***p<0.0005; ****p<0.0001.

	ASU-ACR-16	DME-ACR-16	GPU-ACR-16	TZC-ACR-16	BMA-ACR-16
Hco-ric-3	2052 ± 66 (n=13)	2150 ± 59 (n=15)	1403 ± 91 (n=14)	563 ± 39 (n=13)	± 0 (n=12)
Bma-ric-3	2023 ± 68 (n=11)	2275 ± 157 (n=12)	1281 ± 197 (n=8)	818 ± 112 (n=13)	0 ± 0 (n=8)
Bma-ric-3 Bma-unc-50 Bma-unc-74	2606 ± 183 (n=10)	2368 ± 105 (n=13)	847 ± 124 (n=14)	367 ± 43 (n=15)	0 ± 0 (n=5)
Bma-ric-3 Bma-molo-1	1425 ± 55 (n=15)	2354 ± 108 (n=13)	1049 ± 77 (n=16)	660 ± 76 (n=15)	0 ± 0 (n=16)
Bma-ric-3 Bma-eat-18	3152 ± 102 (n=13)	2649 ± 112 (n=11)	1264 ± 177 (n=10)	791 ± 119 (n=8)	0± 0 (n=10)
Bma-ric-3 Bma-unc-50 Bma-unc-74 Bma-eat-18	2166 ± 87 (n=12)	2222 ± 62 (n=15)	1854 ± 83 (n=14)	964 ± 101 (n=15)	0 ± 0 (n=13)
Bma-ric-3 Cel-emc-6	2582 ± 89 (n=12)	2183 ± 87 (n=11)	1628 ± 123 (n=17)	720 ± 70 (n=13)	17 ± 4 (n=13)
Bma-ric-3 Cel-nra-2 Cel-nra-4	2849 ± 152 (n=14)	± (n=12)	2553 ±123 (n=12)	1263 ± 88 (n=15)	4 ± 2 (n=12)
No accessory protein	24 ± 9 (n=11)	1290 ± 70 (n=17)	0 ± 0 (n=14)	0± 0 (n=15)	0± 0 (n=12)

Appendix Table 3. ACR-16 response to 100 µM acetylcholine with various accessory protein combinations.

Clade III ACR-16 responses (nA) to 100 µM acetylcholine with various accessory protein combinations. See Figure 23 & 26 and Appendix Figure 1. See Chapter 4 for discussion of this project. Error represents standard error.

	ASU-ACR-16	DME-ACR-16	GPU-ACR-16	TZC-ACR-16	Chimera-3 (*A. suum* with *B. malayi* ICL)	Chimera-4 (*B. malayi* with A. suum ICL)
100 µM ACh	100	100	100	100	100	100
100 µM NIC	108 ± 3	95 ± 3	86 ± 2	83 ± 5	96 ± 6	16 ± 3
100 µM DMPP	33 ± 5	11 ± 1	21 ± 2	15 ± 1.0	91 ± 4	30 ± 3
100 µM OXA	9 ± 2	12 ± 1	2 ± 0.4	0.3 ± 0.1	36 ± 5	5 ± 2
100 µM MOR	5 ± 1	0.5 ± 0.1	1.5 ± 0.2	0.3 ± 0.1	29 ± 5	2 ± 1
100 µM PYR	4 ± 1	0.5 ± 0.2	1.9 ± 0.3	0.3 ± 0.1	23± 4	3 ± 1
100 µM LEV	0 ± 0	0 ± 0	0 ± 0	0 ± 0	0.6 ± 0.3	0.8 ± 0.5
100 µM EPI	0 ± 0	0 ± 0	0 ± 0	0 ± 0	0 ± 0	0 ± 0
100 µM NOR	0 ± 0	0 ± 0	0 ± 0	0 ± 0	0 ± 0	0 ± 0
100 µM DA	0 ± 0	0 ± 0	0 ± 0	0 ± 0	0 ± 0	0 ± 0
100 µM TYR	0 ± 0	0 ± 0	0 ± 0	0 ± 0	0 ± 0	0 ± 0
100 µM BET	0 ± 0	0 ± 0	0 ± 0	0 ± 0	0 ± 0	0 ± 0
100 µM BEPH	0 ± 0	0 ± 0	0 ± 0	0 ± 0	0 ± 0	0 ± 0

Appendix Table 4. ACR-16 ligand response profiles relative to acetylcholine.

ACR-16 receptor responses to various ligands are shown as a percent relative to acetylcholine. See Figures 25 & 32 and Chapters 4 & 5. N >6 for all. Error represents standard error.

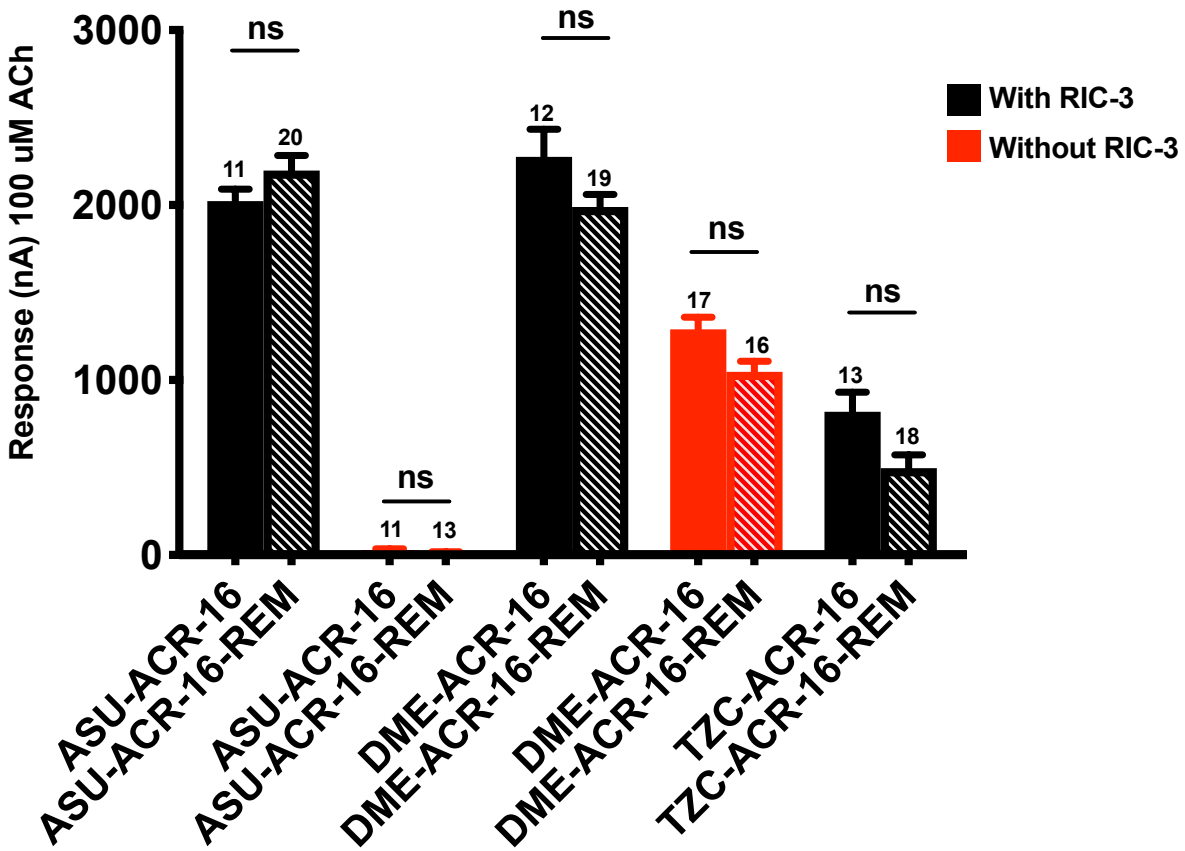

Appendix Figure 2. Responses of ACR-16 restriction enzyme modified sequences (REM) with and without RIC-3.

ACR-16 REM sequences were made to generate chimeras between *A. suum* and *D. medinensis* and *A. suum* and *T. callipaeda*. Responses were compared to the native unmodified sequences to confirm the changes did not affect receptor responses. Responses to 100 µM ACh are shown with RIC-3 (black bars) and without RIC-3 (red bars). Native sequences in solid bars, REM sequences in striped bars. Raw values shown in Appendix Table 5 & 8. Error represents standard error. N values shown on top of bars.

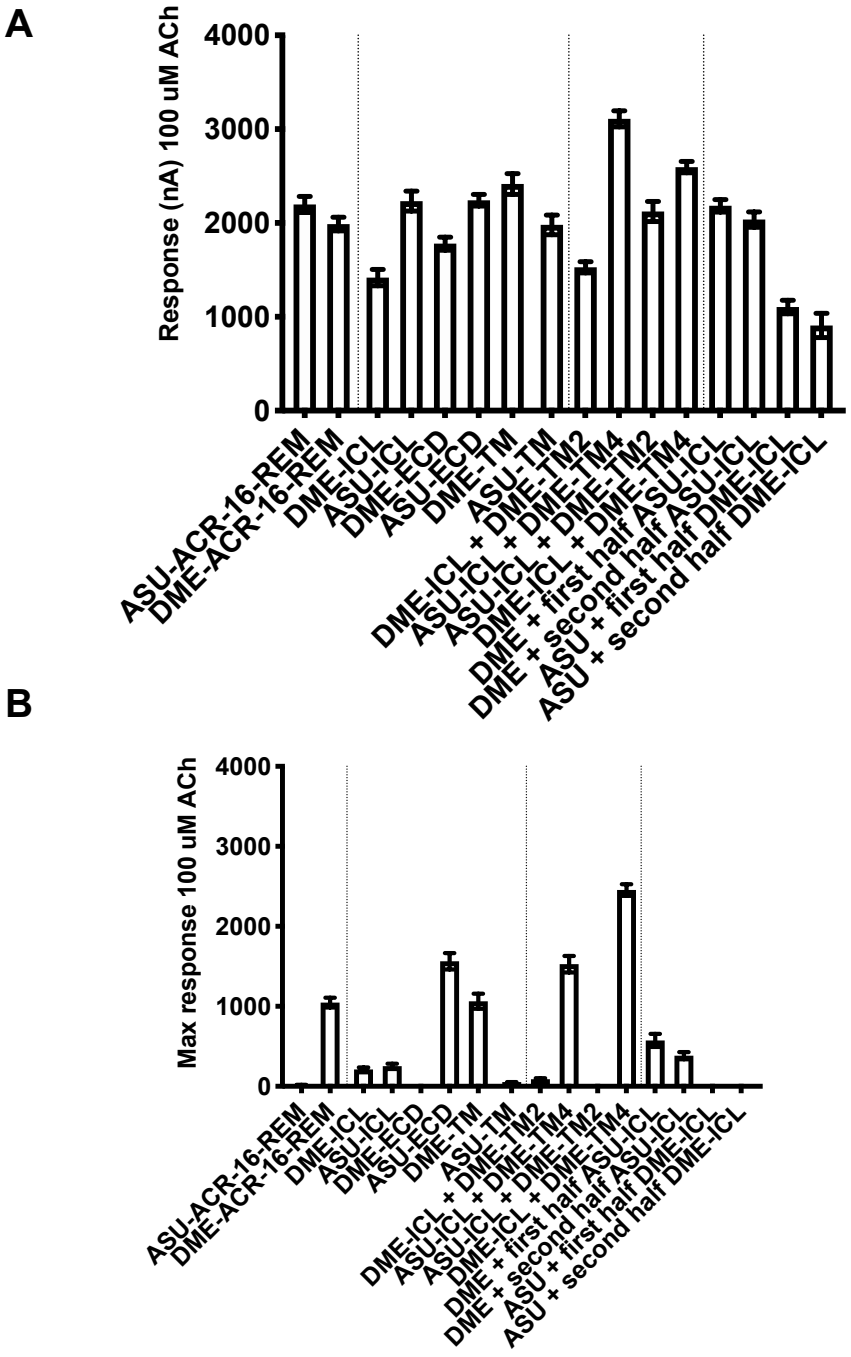

Appendix Figure 3. Responses of *A. suum* and *D. medinensis* ACR-16 chimeras with and without RIC-3.

Chimeras were made exchanging regions between *A. suum* and *D. medinensis* acr-16 to identify the residues determining ric-3 requirement. Responses to 100 μM ACh are shown in (A) with RIC-3; (B) without RIC-3. Schematic of chimeras is shown in Figure 34. Calculated percent responses (response without RIC-3 relative to with RIC-3) are shown in Figures 35 - 37. See Chapter 6 for overview of this work. Raw values shown in Appendix Table 8. Error represents standard error.

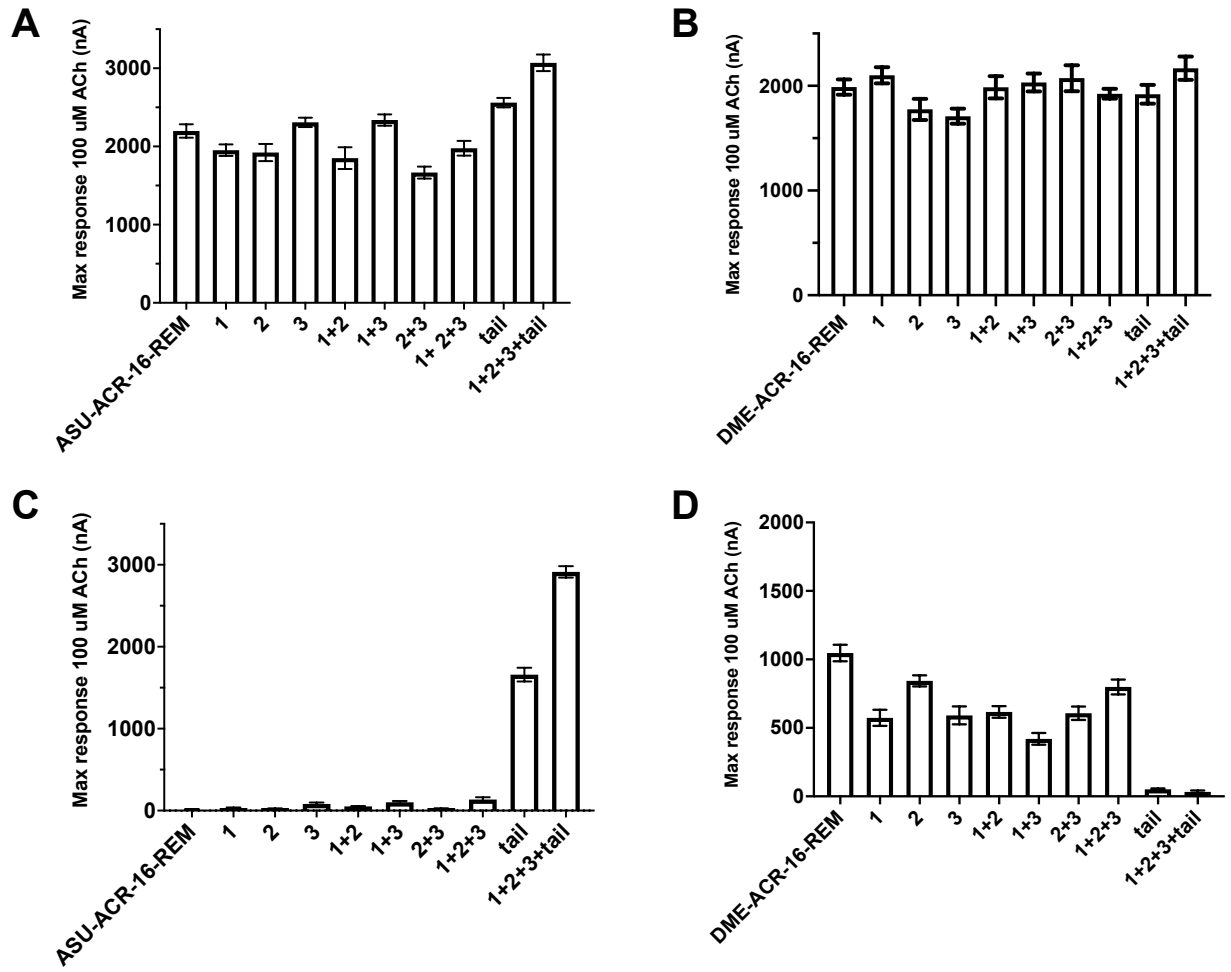

Appendix Figure 4. Responses of *A. suum* and *D. medinensis* ACR-16 TM4 and C-terminal tail point mutation mutants with and without RIC-3.

Point mutations were made in *A. suum* and *D. medinensis acr-16* to identify the residues determining ric-3 requirement. Mutations were made in the fourth transmembrane domain and/or C-terminal tail. Mutant nomenclature is shown in Figure 38. Responses to 100 μM ACh are shown for

(A) *A. suum* mutations with RIC-3;
(B) *D. medinensis* mutations with RIC-3;
(C) *A. suum* mutations without RIC-3;
(D) *D. medineneis* mutations without RIC-3.

Calculated percent responses (response without RIC-3 relative to with RIC-3) are shown in Figure 38. See Chapter 6. Raw values shown in Appendix Table 8. Error represents standard error.

	Response (nA)
ASU-ACR-16-REM	2197 ± 383 (n=20)
TZC-ICL	1959 ± 78 (n=14) ns
TZC-ECD	42 ± 9 (n=13) ****
TZC-TM	2917 ± 104 (n=16)****
TZC-ACR-16-REM	587 ± 415 (n=20)
ASU-ICL	2237 ± 98 (n=14)****
ASU-ECD	1819 ± 115 (n=17) ****
ASU-TM	24 ± 8 (n=12) ****

Appendix Table 5. *A. suum* and *T. callipaeda* ACR-16 chimera responses.

Chimeras were made between *A. suum* and *T. callipaeda* acr-16 to identify the regions mediating the declining responses in oocytes. Responses are shown in response to 100 μM ACh both with co-injection of *B. malayi ric-3*. See Chapter 5 for overview of this work. Schematic of the chimeras shown in Figure 28. Error represents standard error. Significance compared to response of reference receptor. ****p<0.0001.

	Acetylcholine		**Nicotine**	
	EC_{50} (μM)	Hill coefficient	EC_{50} (μM)	Hill coefficient
Chimera-3	4.3 ± 0.5 (n=8)	0.8 ± 0.1 (n=8)	2.7 ± 0.3 (n=10)	1.2 ± 0.1 (n=10)
Chimera-4	15.7 ± 2 (n=6)	1 ± 0.1 (n=6)	2.1 ± 0.3 (n=8)	1.2 ± 0.1 (n=8)

Appendix Table 6. *B. malayi* and *A. suum* ACR-16 chimera agonist affinities.

Dose-response curves were measured to compare to the ACR-16 receptors. Chimera-3 was the *A. suum* acr-16 sequence with the *B. malayi* ICL. Chimera-4 was the *B. malayi* acr-16 sequence with the *A. suum* ICL. Chimera-3 served as a control. See Figure 29 & 31. Error represents standard error.

	Bma-acr-16	Chimera-3	Chimera-4
No AP	0 ± 0 (n=12)	22 ± 15 (n=14)	0 ± 0 (n=15)
RIC-3	0 ± 0 (n=8)	3021 ± 444 (n=12)	59 ± 43 (n=14)
RIC-3 + NRA-2	33 ± 32 (n=14)	2181 ± 369 (n=14)	256 ± 295 (n=11)
RIC-3 + NRA-4	31 ± 46 (n=12)	NA	NA
RIC-3 + EMC-6	17 ± 4 (n=13)	NA	37 ± 46 (n=15)
RIC-3 + NRA-2 + NRA-4	4 ± 2 (n=12)	NA	47 ± 66 (n=14)
RIC-3 + NRA-2 + NRA-4 + EMC-6	11 ± 9 (n=11)	NA	1 ± 2 (n=11)
RIC-3 + NRA-2 + NRA-4 + EMC-6 + EAT-18	2 ± 1 (n=12)	NA	NA
RIC-3 + NRA-2 + NRA-4 + EMC-6 + EAT-18 + UNC-50 + UNC-74	0 ± 0 (n=11)	NA	NA

Appendix Table 7. Effect of different accessory protein combinations on *B. malayi* acr-16 responses.

B. malayi ACR-16, chimera-3 & chimera-4 responses to acetylcholine were measured in response to different accessory protein combinations in order to identify the mixture that elicits the highest response. *B. malayi* RIC-3 + NRA-2 combination was used for further pharmacological characterization of chimera-3 and chimera-4. See Figure 30 and Chapter 5.
Error represents standard error.

	Response with RIC-3 (nA)	Response without RIC-3 (nA)	% without RIC-3
ASU-ACR-16-REM	2197 ± 86 (n=20)	13 ± 4 (n=13)	0.6 ± 0.2 (n=13)
DME-ACR-16-REM	1989 ± 73 (n=19)	1047 ± 60 (n=16)	52.6 ± 3 (n=16)
DME-ICL	1418 ± 87 (n=18)	211 ± 24 (n=15)	14.9 ± 2 (n=15)
ASU-ICL	2233 ± 105 (n=14)	251 ± 30 (n=14)	11.3 ± 5 (n=14)
DME-ECD	1779 ± 69 (n=14)	0 ± 0 (n=14)	0 ± 0 (n=14)
ASU-ECD	2242 ± 62 (n=13)	1563 ± 102 (n=22)	69 ± 5 (n=22)
DME-TM	2415 ± 111 (n=13)	1064 ± 93 (n=15)	38 ± 3 (n=15)
ASU-TM	1979 ± 104 (n=16)	43 ± 9 (n=11)	2.0 ± 0.4 (n=11)
ASU + first half DME-ICL	1104 ± 72 (n=14)	0 ± 0 (n=14)	0 ± 0 (n=14)
ASU + second half DME-ICL	907 ± 129 (n=13)	0 ± 0 (n=13)	0 ± 0 (n=13)
DME + first half ASU-ICL	2183 ± 66 (n=16)	573 ± 81 (n=15)	26 ± 4 (n=15)
DME + second half ASU-ICL	2036 ± 81 (n=12)	383 ± 44 (n=14)	18 ± 2 (n=14)
ASU-ICL +DME-TM2	2123 ± 106 (n=16)	0 ± 0 (n=13)	0 ± 0 (n=13)
DME-ICL + DME-TM2	1528 ± 69 (n=16)	89 ± 11 (n=14)	5.8 ± 0.7 (n=14)
ASU-ICL + DME-TM4	3110 ± 85 (n=14)	1527 ± 102 (n=17)	49 ± 3 (n=17)
DME-ICL + DME-TM4	2595 ± 60 (n=15)	2454 ± 72 (n=15)	94 ± 3 (n=15)
ASU-ACR-16-TM 1	1952 ± 73 (n=14)	31 ± 7 (n=14)	1.5 ± 0.4 (n=14)
ASU-ACR-16-TM 2	1923 ± 109 (n=14)	23 ± 4 (n=12)	1.2 ± 0.2 (n=12)
ASU-ACR-16-TM 3	2309 ± 60 (n=14)	80 ± 18 (n=14)	3.4 ± 0.7 (n=14)
ASU-ACR-16-TM 1+2	1851 ± 139 (n=15)	48 ± 7 (n=14)	2.5 ± 0.3 (n=14)
ASU-ACR-16-TM 1+3	2338 ± 73 (n=13)	101 ± 16 (n=13)	4.3 ± 0.7 (n=13)
ASU-ACR-16-TM 2+3	1666 ± 76 (n=18)	24 ± 3 (n=16)	1.4 ± 0.2 (n=16)
ASU-ACR-16-TM 1+2+3	1977 ± 95 (n=13)	134 ± 29 (n=20)	6.8 ± 1.4 (n=20)
ASU-ACR-16-tail	2560 ± 60 (n=14)	1659 ± 84 (n=18)	64 ± 4 (n=18)
ASU-ACR-16-TM 1+2+3+tail	3070 ± 106 (n=13)	2914 ± 70 (n=13)	95 ± 3 (n=13)
DME-ACR-16-TM 1	2100 ± 76 (n=13)	573 ± 59 (n=13)	27 ± 3 (n=13)
DME-ACR-16-TM 2	1776 ± 101 (n=13)	843 ± 40 (n=14)	47 ± 3 (n=14)
DME-ACR-16-TM 3	1710 ± 71 (n=15)	591 ± 65 (n=14)	34 ± 4 (n=14)
DME-ACR-16-TM 1+2	1987 ± 106 (n=16)	616 ± 42 (n=18)	29 ± 2 (n=18)
DME-ACR-16-TM 1+3	2033 ± 86 (n=14)	419 ± 43 (n=12)	20 ± 2 (n=12)
DME-ACR-16-TM 2+3	2074 ± 123 (n=15)	606 ± 49 (n=13)	31 ± 3 (n=13)
DME-ACR-16-TM 1+2+3	1925 ± 47 (n=16)	789 ± 54 (n=14)	41 ± 3 (n=14)
DME-ACR-16-tail	1920 ± 90 (n=15)	51 ± 7 (n=14)	2.6 ± 0.3 (n=14)
DME-ACR-16-TM 1+2+3+tail	2169 ± 110 (n=12)	32 ± 10 (n=11)	1.5 ± 0.5 (n=11)

Appendix Table 8. *A. suum* and *D. medinensis* ACR-16 chimeras and point mutations.

Chimeras and point mutations were made between *A. suum* and *D. medinensis* acr-16 to identify the regions determining RIC-3 requirement. Raw responses are shown in response to 100 μM ACh both with and without co-injection of *B. malayi ric-3*. Calculated percent responses (response without RIC-3 relative to with RIC-3) are shown in the rightmost column. See Chapter 6. Schematic of the chimeras are shown in Figure 34, and graphs depicting these responses are shown in Figures 35 - 38 and Appendix Figures 3 & 4.

	Response (nA)
UNC-38:LEV-1 dimer + UNC-63 + ACR-13 + UNC-29	152 ± 24 (n=15)
UNC-38:UNC-29 dimer + UNC-63 + ACR-13 + UNC-29	16 ± 5 (n=12)
UNC-38:UNC-29 dimer + UNC-63 + ACR-13	0 ± 0 (n=3)
UNC-38:LEV-1 dimer + UNC-63 + ACR-8 + UNC-29	388 ± 51 (n=16)
UNC-38:UNC-29 dimer + UNC-63 + ACR-8 + UNC-29	117 ± 35 (n=9)
UNC-38:UNC-29 dimer + UNC-63 + ACR-8	0 ± 0 (n=4)

Appendix Table 9. UNC-29 is present twice in the receptor without LEV-1

A series of dimers (two subunits physically linked with a short linker sequence) and monomer conditions were used to identify the subunit that replaces LEV-1 when ACR-8 is present. Responses to 100 μM ACh are shown. The UNC-38:UNC-29 dimer was functional without LEV-1 in the presence of ACR-8 but not ACR-13. The absence of response when the unc-29 monomer was omitted (rightmost column) confirms that unc-29 replaces LEV-1 and is present twice in the receptor. Example recordings shown in Figure 10. Error represents standard error. See figures 10 and 11.

	Response (nA)
Chimera-1 + Cel: ACR-13, UNC-38, UNC-63, LEV-1	63 ± 20 (n=7)
Chimera-1 + Cel: ACR-13, UNC-38, UNC-63	1 ± 1 (n=5)
Chimera-1 + Hco: ACR-8, UNC-38, UNC-63	1 ± 1(n=9)
Chimera-2 + Cel: ACR-13, UNC-38, UNC-63, LEV-1	394 ± 78 (n=7)
Chimera-2 + Cel: ACR-13, UNC-38, UNC-63	43 ± 3 (n=4)
Chimera-2 + Hco: ACR-8, UNC-38, UNC-63	49 (n=1)

Appendix Table 10. Chimera-1 and chimera-2 responses in L-AChRs

Responses of unc-29 chimeras in response to 100 μM ACh. Chimeras were made between *H. contortus unc-29.1* and *unc-29.2* by exchanging the intracellular loop to identify the region mediating the ability of unc-29.1 to function as the only non-alpha subunit in the receptor. Both chimeras were functional in the L-AChR, confirming that the exchanged ICLs do not render the chimeras nonfunctional. Chimera-1 was not functional in the *C. elegans* L-AChR without LEV-1 nor in the *H. contortus* L-AChR. Chimera-2 was functional in the *C. elegans* L-AChR without LEV-1 and in the *H. contortus* L-AChR. The ICL therefore mediates the ability of unc-29.1 to function as the only non-alpha subunit. See Figure 13 and 14. Error bars represent standard error. These conditions will need to be repeated for reproducibility.

Appendix Figure 5. ***A. suum*** **and** ***D. medinensis*** **restriction enzyme modified** ***acr-16***

Coding and translated sequences shown for the restriction enzyme modified for *A. suum* and *D. medinensis acr-16.*

References

Abad, P., Gouzy, J., Aury, J. M., Castagnone-Sereno, P., Danchin, E. G. J., Deleury, E., Perfus-Barbeoch, L., Anthouard, V., Artiguenave, F., Blok, V. C., Caillaud, M. C., Coutinho, P. M., Dasilva, C., De Luca, F., Deau, F., Esquibet, M., Flutre, T., Goldstone, J. V., Hamamouch, N., … Wincker, P. (2008). Genome sequence of the metazoan plant-parasitic nematode *Meloidogyne incognita*. *Nature Biotechnology*, *26*(8), 909–915. https://doi.org/10.1038/nbt.1482

Abongwa, M., Buxton, S. K., Courtot, E., Charvet, C. L., Neveu, C., McCoy, C. J., Verma, S., Robertson, A. P., & Martin, R. J. (2016). Pharmacological profile of *Ascaris suum* ACR-16, a new homomeric nicotinic acetylcholine receptor widely distributed in Ascaris tissues. *British Journal of Pharmacology*, 2463–2477. https://doi.org/10.1111/bph.13524

Alcaino, C., Musgaard, M., Minguez, T., Mazzaferro, S., Faundez, M., Iturriaga-Vasquez, P., Biggin, P. C., & Bermudez, I. (2017). Role of the cys loop and transmembrane domain in the allosteric modulation of α4β2 nicotinic acetylcholine receptors. *Journal of Biological Chemistry*, *292*(2), 551–562. https://doi.org/10.1074/jbc.M116.751206

Almedom, R. B., Liewald, J. F., Hernando, G., Schultheis, C., Rayes, D., Pan, J., Schedletzky, T., Hutter, H., Bouzat, C., & Gottschalk, A. (2009). An ER-resident membrane protein complex regulates nicotinic acetylcholine receptor subunit composition at the synapse. *EMBO Journal*, *28*(17), 2636–2649. https://doi.org/10.1038/emboj.2009.204

Bai, L., You, Q., Feng, X., Kovach, A., & Li, H. (2020). Structure of the ER membrane complex, a transmembrane-domain insertase. *Nature*, *584*(7821), 475–478. https://doi.org/10.1038/s41586-020-2389-3

Ballivet, M., Alliod, C., Bertrand, S., & Bertrand, D. (1996). Nicotinic acetylcholine receptors in the nematode *Caenorhabditis elegans*. *Journal of Molecular Biology*, *258*(2), 261–269. https://doi.org/10.1006/jmbi.1996.0248

Bao, H., Xu, X., Liu, W., Yu, N., & Liu, Z. (2018). Dual effects of insect nAChR chaperone RIC-3 on hybrid receptor: Promoting assembly on endoplasmic reticulum but suppressing transport to plasma membrane on Xenopus oocytes. *Neurochemistry International*, *115*, 24–30. https://doi.org/10.1016/j.neuint.2017.10.007

Baptista-Hon, D. T., Deeb, T. Z., Lambert, J. J., Peters, J. A., & Hales, T. G. (2013). The minimum M3-M4 loop length of neurotransmitteractivated pentameric receptors is critical for the structural integrity of cytoplasmic portals. *Journal of Biological Chemistry*, *288*(30), 21558–21568. https://doi.org/10.1074/jbc.M113.481689

Beech, R. N., Callanan, M. K., Rao, V. T. S., Dawe, G. B., & Forrester, S. G. (2013). Characterization of cys-loop receptor genes involved in inhibitory amine neurotransmission in parasitic and free living nematodes. *Parasitology International*, *62*(6), 599–605. https://doi.org/10.1016/j.parint.2013.03.010

Beech, R. N., & Neveu, C. (2015). The evolution of pentameric ligand-gated ion-channels and the changing family of anthelmintic drug targets. *Parasitology*, *142*(2), 303–317. https://doi.org/10.1017/S003118201400170X

Beech, R. N., Wolstenholme, A. J., Neveu, C., & Dent, J. A. (2010). Nematode parasite genes: What's in a name? *Trends in Parasitology*, *26*(7), 334–340. https://doi.org/10.1016/j.pt.2010.04.003

Beg, A. A., & Jorgensen, E. M. (2003). EXP-1 is an excitatory GABA-gated cation channel.

Nature Neuroscience, *6*(11), 1145–1152. https://doi.org/10.1038/nn1136
Ben-Ami, H. C., Biala, Y., Farah, H., Elishevitz, E., Battat, E., & Treinin, M. (2009). Receptor and subunit specific interactions of RIC-3 with nicotinic acetylcholine receptors. *Biochemistry*, *48*(51), 12329–12336. https://doi.org/10.1021/bi901234a
Ben-Ami, H. C., Yassin, L., Farah, H., Michaeli, A., Eshel, M., & Treinin, M. (2005). RIC-3 affects properties and quantity of nicotinic acetylcholine receptors via a mechanism that does not require the coiled-coil domains. *Journal of Biological Chemistry*, *280*(30), 28053–28060. https://doi.org/10.1074/jbc.M504369200
Ben-David, Y., Mizrachi, T., Kagan, S., Krisher, T., Cohen, E., Brenner, T., & Treinin, M. (2016). RIC-3 expression and splicing regulate nAChR functional expression. *Molecular Brain*, *9*(1). https://doi.org/10.1186/s13041-016-0231-5
Bennett, H. M., Lees, K., Harper, K. M., Jones, A. K., Sattelle, D. B., Wonnacott, S., & Wolstenholme, A. J. (2012). *Xenopus laevis* RIC-3 enhances the functional expression of the *C. elegans* homomeric nicotinic receptor, ACR-16, in Xenopus oocytes. *Journal of Neurochemistry*, *123*(6), 911–918. https://doi.org/10.1111/jnc.12013
Bianchi L, Driscoll M. Heterologous expression of C. elegans ion channels in Xenopus oocytes. WormBook. 2006 Aug 1:1-16. doi: 10.1895/wormbook.1.117.1. PMID: 18050441; PMCID: PMC4781024.
Bisson, W. H., Westera, G., Schubiger, P. A., & Scapozza, L. (2008). Homology modeling and dynamics of the extracellular domain of rat and human neuronal nicotinic acetylcholine receptor subtypes α4β2 and α7. *Journal of Molecular Modeling*, *14*(10), 891–899. https://doi.org/10.1007/s00894-008-0340-x
Blanchard, A., Guégnard, F., Charvet, C. L., Crisford, A., Courtot, E., Sauvé, C., Harmache, A., Duguet, T., O'Connor, V., Castagnone-Sereno, P., Reaves, B., Wolstenholme, A. J., Beech, R. N., Holden-Dye, L., & Neveu, C. (2018). Deciphering the molecular determinants of cholinergic anthelmintic sensitivity in nematodes: When novel functional validation approaches highlight major differences between the model *Caenorhabditis elegans* and parasitic species. *PLoS Pathogens*, *14*(5), 1–28. https://doi.org/10.1371/journal.ppat.1006996
Blaxter, M., & Koutsovoulos, G. (2015). The evolution of parasitism in Nematoda. *Parasitology*, *142*, S26–S39. https://doi.org/10.1017/S0031182014000791
Blaxter, M. L., De Ley, P., Garey, J. R., Llu, L. X., Scheldeman, P., Vierstraete, A., Vanfleteren, J. R., Mackey, L. Y., Dorrls, M., Frisse, L. M., Vida, J. T., & Thomas, W. K. (1998). A molecular evolutionary framework for the phylum Nematoda. *Nature*, *392*(6671), 71–75. https://doi.org/10.1038/32160
Bolt, B. J., Rodgers, F. H., Shafie, M., Kersey, P. J., Berriman, M., & Howe, K. L. (2018). Using WormBase ParaSite: An integrated platform for exploring helminth genomic data. *Methods in Molecular Biology*, *1757*, 471–491. https://doi.org/10.1007/978-1-4939-7737-6_15
Boulin, T., Fauvin, A., Charvet, C. L., Cortet, J., Cabaret, J., Bessereau, J. L., & Neveu, C. (2011). Functional reconstitution of *Haemonchus contortus* acetylcholine receptors in *Xenopus* oocytes provides mechanistic insights into levamisole resistance. *British Journal of Pharmacology*, *164*(5), 1421–1432. https://doi.org/10.1111/j.1476-5381.2011.01420.x
Boulin, Thomas, Gielen, M., Richmond, J. E., Williams, D. C., Paoletti, P., & Bessereau, J. L. (2008). Eight genes are required for functional reconstitution of the *Caenorhabditis elegans* levamisole-sensitive acetylcholine receptor. *Proceedings of the National Academy of Sciences of the United States of America*, *105*(47), 18590–18595.

https://doi.org/10.1073/pnas.0806933105
Boulin, Thomas, Rapti, G., Briseño-Roa, L., Stigloher, C., Richmond, J. E., Paoletti, P., & Bessereau, J. L. (2012). Positive modulation of a Cys-loop acetylcholine receptor by an auxiliary transmembrane subunit. *Nature Neuroscience*, *15*(10), 1374–1381. https://doi.org/10.1038/nn.3197
Boulter, J., O'Shea-Greenfield, A., Duvoisin, R. M., Connolly, J. G., Wada, E., Jensen, A., Gardner, P. D., Ballivet, M., Deneris, E. S., McKinnon, D., Heinemann, S., & Patrick, J. (1990). α3, α5, and β4: Three members of the rat neuronal nicotinic acetylcholine receptor-related gene family form a gene cluster. *Journal of Biological Chemistry*, *265*(8), 4472–4482. https://doi.org/10.1016/S0021-9258(19)39588-2
Brenner S. The genetics of Caenorhabditis elegans. Genetics. 1974;77(1):71-94.
Buxton, S. K., Charvet, C. L., Neveu, C., Cabaret, J., Cortet, J., Peineau, N., Abongwa, M., Courtot, E., Robertson, A. P., & Martin, R. J. (2014). Investigation of Acetylcholine Receptor Diversity in a Nematode Parasite Leads to Characterization of Tribendimidine- and Derquantel-Sensitive nAChRs. *PLoS Pathogens*, *10*(1). https://doi.org/10.1371/journal.ppat.1003870
Campos-Caro, A., Sala, S., Ballesta, J. J., Vicente-Agulló, F., Criado, M., & Sala, F. (1996). A single residue in the M2-M3 loop is a major determinant of coupling between binding and gating in neuronal nicotinic receptors. *Proceedings of the National Academy of Sciences of the United States of America*, *93*(12), 6118–6123. https://doi.org/10.1073/pnas.93.12.6118
Carbone, A. L., Moroni, M., Groot-Kormelink, P. J., & Bermudez, I. (2009). Pentameric concatenated (α4) 2(β2) 3 and (α4) 3(β2) 2 nicotinic acetylcholine receptors: Subunit arrangement determines functional expression. *British Journal of Pharmacology*, *156*(6), 970–981. https://doi.org/10.1111/j.1476-5381.2008.00104.x
Castelán, F., Castillo, M., Mulet, J., Sala, S., Sala, F., Domínguez Del Toro, E., & Criado, M. (2008). Molecular characterization and localization of the RIC-3 protein, an effector of nicotinic acetylcholine receptor expression. *Journal of Neurochemistry*, *105*(3), 617–627. https://doi.org/10.1111/j.1471-4159.2007.05169.x
Castillo, M., Mulet, J., Gutiérrez, L. M., Ortiz, J. A., Castelán, F., Gerber, S., Sala, S., Sala, F., & Criado, M. (2005). Dual role of the RIC-3 protein in trafficking of serotonin and nicotinic acetylcholine receptors. *Journal of Biological Chemistry*. https://doi.org/10.1074/jbc.M503746200
Changeux, J. P., Kasai, M., & Lee, C. Y. (1970). Use of a snake venom toxin to characterize the cholinergic receptor protein. *Proceedings of the National Academy of Sciences of the United States of America*, *67*(3), 1241–1247. https://doi.org/10.1073/pnas.67.3.1241
Changeux, Jean Pierre. (2018). The nicotinic acetylcholine receptor: A typical 'allosteric machine.' *Philosophical Transactions of the Royal Society B: Biological Sciences*, *373*(1749). https://doi.org/10.1098/rstb.2017.0174
Charvet, C. L., Guégnard, F., Courtot, E., Cortet, J., & Neveu, C. (2018). Nicotine-sensitive acetylcholine receptors are relevant pharmacological targets for the control of multidrug resistant parasitic nematodes. *International Journal for Parasitology: Drugs and Drug Resistance*, *8*(3), 540–549. https://doi.org/10.1016/j.ijpddr.2018.11.003
Cheng, A., Bollan, K. A., Greenwood, S. M., Irving, A. J., & Connolly, C. N. (2007). Differential subcellular localization of RIC-3 isoforms and their role in determining 5-HT3 receptor composition. *Journal of Biological Chemistry*, *282*(36), 26158–26166. https://doi.org/10.1074/jbc.M703899200

Cheng, A., McDonald, N. A., & Connolly, C. N. (2005). Cell surface expression of 5-hydroxytryptamine type 3 receptors is promoted by RIC-3. *Journal of Biological Chemistry*, *280*(23), 22502–22507. https://doi.org/10.1074/jbc.M414341200

Choudhary, S., Buxton, S. K., Puttachary, S., Verma, S., Mair, G. R., McCoy, C. J., Reaves, B. J., Wolstenholme, A. J., Martin, R. J., & Robertson, A. P. (2020). EAT-18 is an essential auxiliary protein interacting with the non-alpha nAChR subunit EAT-2 to form a functional receptor. *PLoS Pathogens*, *16*(4), 1–23. https://doi.org/10.1371/journal.ppat.1008396

Choudhary, S., Tipton, J. G., Abongwa, M., Brewer, M. T., Chelladurai, J. J., Musselman, N., Martin, R. J., & Robertson, A. P. (2019). Pharmacological characterization of a homomeric nicotinic acetylcholine receptor formed by *Ancylostoma caninum* ACR-16. *Invertebrate Neuroscience*, *19*(4), 1–10. https://doi.org/10.1007/s10158-019-0231-0

Coghlan, A., Tyagi, R., Cotton, J. A., Holroyd, N., Rosa, B. A., Tsai, I. J., Laetsch, D. R., Beech, R. N., Day, T. A., Hallsworth-Pepin, K., Ke, H. M., Kuo, T. H., Lee, T. J., Martin, J., Maizels, R. M., Mutowo, P., Ozersky, P., Parkinson, J., Reid, A. J., … Berriman, M. (2019). Comparative genomics of the major parasitic worms. *Nature Genetics*, *51*(1), 163–174. https://doi.org/10.1038/s41588-018-0262-1

Corringer, P.-J., Le Novere, N., & Changeux, J.-P. (2000). Nicotinic receptors at the amino acid level. *Annu. Rev. Pharmacol. Toxicol*, *40*, 431–458.

Corringer, P. J., Bertrand, S., Galzi, J. L., Devillers-Thiéry, A., Changeux, J. P., & Bertrand, D. (1999). Mutational analysis of the charge selectivity filter of the α7 nicotinic acetylcholine receptor. *Neuron*, *22*(4), 831–843. https://doi.org/10.1016/S0896-6273(00)80741-2

Corringer, P. J., Poitevin, F., Prevost, M. S., Sauguet, L., Delarue, M., & Changeux, J. P. (2012). Structure and pharmacology of pentameric receptor channels: From bacteria to brain. *Structure*, *20*(6), 941–956. https://doi.org/10.1016/j.str.2012.05.003

Courtot, E., Charvet, C. L., Beech, R. N., Harmache, A., Wolstenholme, A. J., Holden-Dye, L., O'Connor, V., Peineau, N., Woods, D. J., & Neveu, C. (2015). Functional Characterization of a Novel Class of Morantel-Sensitive Acetylcholine Receptors in Nematodes. *PLoS Pathogens*, *11*(12), 1–29. https://doi.org/10.1371/journal.ppat.1005267

Crespi, A., Colombo, S. F., & Gotti, C. (2018). Proteins and chemical chaperones involved in neuronal nicotinic receptor expression and function: an update. *British Journal of Pharmacology*, *175*(11), 1869–1879. https://doi.org/10.1111/bph.13777

Culetto, E., Baylis, H. A., Richmond, J. E., Jones, A. K., Fleming, J. T., Squire, M. D., Lewis, J. A., & Sattelle, D. B. (2004). The *Caenorhabditis elegans unc-63* gene encodes a levamisole-sensitive nicotinic acetylcholine receptor α subunit. *Journal of Biological Chemistry*, *279*(41), 42476–42483. https://doi.org/10.1074/jbc.M404370200

Cymesa, G. D., & Grosman, C. (2016). Identifying the elusive link between amino acid sequence and charge selectivity in pentameric ligand-gated ion channels. *Proceedings of the National Academy of Sciences of the United States of America*, *113*(45), E7106–E7115. https://doi.org/10.1073/pnas.1608519113

D'alessandro, M., Richard, M., Stigloher, C., Gache, V., Boulin, T., Richmond, J. E., & Bessereau, J. L. (2018). CRELD1 is an evolutionarily-conserved maturational enhancer of ionotropic acetylcholine receptors. *ELife*, *7*, 1–29. https://doi.org/10.7554/eLife.39649

daCosta, C. J. B., & Baenziger, J. E. (2009). A lipid-dependent uncoupled conformation of the acetylcholine receptor. *Journal of Biological Chemistry*, *284*(26), 17819–17825. https://doi.org/10.1074/jbc.M900030200

Dacosta, C. J. B., & Baenziger, J. E. (2013). Gating of pentameric ligand-gated ion channels:

Structural insights and ambiguities. *Structure*, *21*(8), 1271–1283. https://doi.org/10.1016/j.str.2013.06.019

Dascal, N., & Aviv, R. (1987). The use of *Xenopus* oocytes for the study of ion channels. *22*(4).

Dau, A., Komal, P., Truong, M., Morris, G., Evans, G., & Nashmi, R. (2013). RIC-3 differentially modulates α4β2 and α7 nicotinic receptor assembly, expression, and nicotine-induced receptor upregulation. *BMC Neuroscience*, *14*, 1–18. https://doi.org/10.1186/1471-2202-14-47

De Planque, M. R. R., Rijkers, D. T. S., Liskamp, R. M. J., & Separovic, F. (2004). The αM1 transmembrane segment of the nicotinic acetylcholine receptor interacts strongly with model membranes. *Magnetic Resonance in Chemistry*, *42*(2), 148–154. https://doi.org/10.1002/mrc.1326

Dent, J. A. (2006). Evidence for a diverse Cys-loop ligand-gated ion channel superfamily in early bilateria. *Journal of Molecular Evolution*, *62*(5), 523–535. https://doi.org/10.1007/s00239-005-0018-2

Dent, J. A. (2010). The evolution of pentameric ligand-gated ion channels. *Advances in Experimental Medicine and Biology*, *683*, 11–23. https://doi.org/10.1007/978-1-4419-6445-8_2

Dettmer, U., Kuhn, P. H., Abou-Ajram, C., Lichtenthaler, S. F., Krüger, M., Kremmer, E., Haass, C., & Haffner, C. (2010). Transmembrane protein 147 (TMEM147) is a novel component of the Nicalin-NOMO protein complex. *Journal of Biological Chemistry*, *285*(34), 26174–26181. https://doi.org/10.1074/jbc.M110.132548

Droser, M. L., & Gehling, J. G. (2015). *The advent of animals : The view from the Ediacaran*. *112*(16), 4865–4870. https://doi.org/10.1073/pnas.1403669112

Duguet, T. (2017). *Subunit Diversity of the Nematode Levamisole-sensitive Acetylcholine Receptor*. McGill University.

Duguet, T. B., Charvet, C. L., Forrester, S. G., Wever, C. M., Dent, J. A., Neveu, C., & Beech, R. N. (2016). Recent Duplication and Functional Divergence in Parasitic Nematode Levamisole-Sensitive Acetylcholine Receptors. *PLoS Neglected Tropical Diseases*, *10Alan L.*(7), 1–26. https://doi.org/10.1371/journal.pntd.0004826

Duret, G., Van Renterghem, C., Weng, Y., Prevost, M., Moraga-Cid, G., Huon, C., Sonner, J. M., & Corringer, P. J. (2011). Functional prokaryotic-eukaryotic chimera from the pentameric ligand-gated ion channel family. *Proceedings of the National Academy of Sciences of the United States of America*, *108*(29), 12143–12148. https://doi.org/10.1073/pnas.1104494108

Eertmoed, A. L., & Green, W. N. (1999). Nicotinic receptor assembly requires multiple regions throughout the γ subunit. *Journal of Neuroscience*, *19*(15), 6298–6308. https://doi.org/10.1523/jneurosci.19-15-06298.1999

Eimer, S., Gottschalk, A., Hengartner, M., Horvitz, H. R., Richmond, J., Schafer, W. R., & Bessereau, J. L. (2007). Regulation of nicotinic receptor trafficking by the transmembrane Golgi protein UNC-50. *EMBO Journal*, *26*(20), 4313–4323. https://doi.org/10.1038/sj.emboj.7601858

Eiselé, J. L., Bertrand, S., Galzi, J. L., Devillers-Thiéry, A., Changeux, J. P., & Bertrand, D. (1993). Chimaeric nicotinic-serotonergic receptor combines distinct ligand binding and channel specificities. *Nature*, *366*(6454), 479–483. https://doi.org/10.1038/366479a0

Emlaw, J. R., Tessier, C. J. G., McCluskey, G. D., McNulty, M. S., Sheikh, Y., Burkett, K. M., Musgaard, M., & daCosta, C. J. B. (2021). A single historical substitution drives an increase

in acetylcholine receptor complexity. *Proceedings of the National Academy of Sciences of the United States of America*, *118*(7). https://doi.org/10.1073/pnas.2018731118
Etxeberria, A., Santana-Castro, I., Regalado, M. P., Aivar, P., & Villarroel, A. (2004). Three mechanisms underlie KCNQ2/3 heteromeric potassium M-channel potentiation. *Journal of Neuroscience*, *24*(41), 9146–9152. https://doi.org/10.1523/JNEUROSCI.3194-04.2004
Fleming, J. T., Squire, M. D., Barnes, T. M., Tornoe, C., Matsuda, K., Ahnn, J., Fire, A., Sulston, J. E., Barnard, E. A., Sattelle, D. B., & Lewis, J. A. (1997). *Caenorhabditis elegans* levamisole resistance genes lev-1, unc-29, and unc-38 encode functional nicotinic acetylcholine receptor subunits. *Journal of Neuroscience*, *17*(15), 5843–5857. https://doi.org/10.1523/jneurosci.17-15-05843.1997
Forrester, S. G., Prichard, R. K., Dent, J. A., & Beech, R. N. (2003). *Haemonchus contortus:* HcGluCla expressed in *Xenopus* oocytes forms a glutamate-gated ion channel that is activated by ibotenate and the antiparasitic drug ivermectin. *Molecular and Biochemical Parasitology*, *129*(1), 115–121. https://doi.org/10.1016/S0166-6851(03)00102-6
Franchini, L. F., & Elgoyhen, A. B. (2006). Adaptive evolution in mammalian proteins involved in cochlear outer hair cell electromotility. *Molecular Phylogenetics and Evolution*, *41*(3), 622–635. https://doi.org/10.1016/j.ympev.2006.05.042
Gee, V. J., Kracun, S., Cooper, S. T., Gibb, A. J., & Millar, N. S. (2007). Identification of domains influencing assembly and ion channel properties in α7 nicotinic receptor and 5-HT 3 receptor subunit chimaeras. *British Journal of Pharmacology*, *152*(4), 501–512. https://doi.org/10.1038/sj.bjp.0707429
Ghosh, B., Tsao, T. W., & Czajkowski, C. (2017). A chimeric prokaryotic-eukaryotic pentameric ligand gated ion channel reveals interactions between the extracellular and transmembrane domains shape neurosteroid modulation. *Neuropharmacology*, *125*, 343–352. https://doi.org/10.1016/j.neuropharm.2017.08.007
Gielen, M., & Corringer, P. J. (2018). The dual-gate model for pentameric ligand-gated ion channels activation and desensitization. *Journal of Physiology*, *596*(10), 1873–1902. https://doi.org/10.1113/JP275100
Goldin, A. L. (1991). mRNA into *Xenopus Oocytes*. *36*.
Gottschalk, A., Almedom, R. B., Schedletzky, T., Anderson, S. D., Yates, J. R., & Schafer, W. R. (2005). Identification and characterization of novel nicotinic receptor-associated proteins in *Caenorhabditis elegans*. *EMBO Journal*, *24*(14), 2566–2578. https://doi.org/10.1038/sj.emboj.7600741
Goyal, R., Salahudeen, A. A., & Jansen, M. (2011). Engineering a prokaryotic Cys-loop receptor with a third functional domain. *Journal of Biological Chemistry*, *286*(40), 34635–34642. https://doi.org/10.1074/jbc.M111.269647
Green, W. N. (1999). Perspective: Ion channel assembly: Creating structures that function. *Journal of General Physiology*, *113*(2), 163–169. https://doi.org/10.1085/jgp.113.2.163
Green, W. N., & Claudio, T. (1993). Acetylcholine receptor assembly: Subunit folding and oligomerization occur sequentially. *Cell*, *74*(1), 57–69. https://doi.org/10.1016/0092-8674(93)90294-Z
Green, W. N., & Wanamaker, C. P. (1997). The role of the cystine loop in acetylcholine receptor assembly. *Journal of Biological Chemistry*, *272*(33), 20945–20953. https://doi.org/10.1074/jbc.272.33.20945
Groot-Kormelink, P. J., Broadbent, S., Beato, M., & Sivilotti, L. G. (2006). Constraining the expression of nicotinic acetylcholine receptors by using pentameric constructs. *Molecular*

Pharmacology, *69*(2), 558–563. https://doi.org/10.1124/mol.105.019356
Grosman, C., Salamone, F. N., Sine, S. M., & Auerbach, A. (2000). The extracellular linker of muscle acetylcholine receptor channels is a gating control element. *Journal of General Physiology*, *116*(3), 327–339. https://doi.org/10.1085/jgp.116.3.327
Gu, S., Matta, J. A., Lord, B., Harrington, A. W., Sutton, S. W., Davini, W. B., & Bredt, D. S. (2016). Brain α7 Nicotinic Acetylcholine Receptor Assembly Requires NACHO. *Neuron*, *89*(5), 948–955. https://doi.org/10.1016/j.neuron.2016.01.018
Gu, Y., Forsayeth, J. R., Verrall, S., Yu, X. M., & Hall, Z. W. (1991a). Assembly of the mammalian muscle acetylcholine receptor in transfected COS cells. *Journal of Cell Biology*, *114*(4), 799–807. https://doi.org/10.1083/jcb.114.4.799
Gu, Yong, Camacho, P., Gardner, P., & Hall, Z. W. (1991b). Identification of two amino acid residues in the ϵ subunit that promote mammalian muscle acetylcholine receptor assembly in COS cells. *Neuron*, *6*(6), 879–887. https://doi.org/10.1016/0896-6273(91)90228-R
Guindon, S., Dufayard, J. F., Lefort, V., Anisimova, M., Hordijk, W., & Gascuel, O. (2010). New algorithms and methods to estimate maximum-likelihood phylogenies: Assessing the performance of PhyML 3.0. *Systematic Biology*, *59*(3), 307–321. https://doi.org/10.1093/sysbio/syq010
Haeger, S., Kuzmin, D., Detro-Dassen, S., Lang, N., Kilb, M., Tsetlin, V., Betz, H., Laube, B., & Schmalzing, G. (2010). An intramembrane aromatic network determines pentameric assembly of Cys-loop receptors. *Nature Structural and Molecular Biology*, *17*(1), 90–99. https://doi.org/10.1038/nsmb.1721
Haffner, C., Dettmer, U., Weiler, T., & Haass, C. (2007). The nicastrin-like protein nicalin regulates assembly and stability of the Nicalin-Nodal modulator (NOMO) membrane protein complex. *Journal of Biological Chemistry*, *282*(14), 10632–10638. https://doi.org/10.1074/jbc.M611033200
Hales, T. G., Dunlop, J. I., Deeb, T. Z., Carland, J. E., Kelley, S. P., Lambert, J. J., & Peters, J. A. (2006). Common determinants of single channel conductance within the large cytoplasmic loop of 5-hydroxytryptamine type 3 and α4β 2 nicotinic acetylcholine receptors. *Journal of Biological Chemistry*, *281*(12), 8062–8071. https://doi.org/10.1074/jbc.M513222200
Halevi, S., McKay, J., & Palfreyman, M. (2002). The *C.elegans ric-3* gene is required for maturation of nicotinic acetylcholine receptors. *EMBO Journal*, *21*(5), 1012–1020. https://doi.org/10.1093/emboj/21.5.1012
Halevi, S., Yassin, L., Eshel, M., Sala, F., Sala, S., Criado, M., & Treinin, M. (2003). Conservation within the RIC-3 gene family: Effectors of mammalian nicotinic acetylcholine receptor expression. *Journal of Biological Chemistry*, *278*(36), 34411–34417. https://doi.org/10.1074/jbc.M300170200
Hansen, T. V. A., Cirera, S., Neveu, C., Courtot, E., Charvet, C. L., Calloe, K., Klaerke, D. A., & Martin, R. J. (2021). The narrow-spectrum anthelmintic oxantel is a potent agonist of a novel acetylcholine receptor subtype in whipworms. *PLoS Pathogens*, *17*(2), 1–26. https://doi.org/10.1371/JOURNAL.PPAT.1008982
Hanson, S. M., & Czajkowski, C. (2011). Disulphide trapping of the GABA A receptor reveals the importance of the coupling interface in the action of benzodiazepines. *British Journal of Pharmacology*, *162*(3), 673–687. https://doi.org/10.1111/j.1476-5381.2010.01073.x
Haugstetter, J., Blicher, T., & Ellgaard, L. (2005). Identification and characterization of a novel thioredoxin-related transmembrane protein of the endoplasmic reticulum. *Journal of*

Biological Chemistry, *280*(9), 8371–8380. https://doi.org/10.1074/jbc.M413924200
Hénault, C. M., Sun, J., Therien, J. P. D., DaCosta, C. J. B., Carswell, C. L., Labriola, J. M., Juranka, P. F., & Baenziger, J. E. (2015). The role of the M4 lipid-sensor in the folding, trafficking, and allosteric modulation of nicotinic acetylcholine receptors. *Neuropharmacology*, *96*(PB), 157–168. https://doi.org/10.1016/j.neuropharm.2014.11.011
Hernando, G., Bergé, I., Rayes, D., & Bouzat, C. (2012). Contribution of subunits to *Caenorhabditis elegans* levamisole-sensitive nicotinic receptor function. *Molecular Pharmacology*, *82*(3), 550–560. https://doi.org/10.1124/mol.112.079962
Holden Dye, L. and R. Walker (2007). Anthelmintic drugs. WormBook: 1-13. Jorgensen, E. M. N., M.L. (1995). Neuromuscular junctions in the nematode C. elegans. Seminars in Developmental Biology
Holland, P. W. H. (2015). Did homeobox gene duplications contribute to the Cambrian explosion? *Zoological Letters*, *1*(1), 1–8. https://doi.org/10.1186/s40851-014-0004-x
Holterman, M., Van Der Wurff, A., Van Den Elsen, S., Van Megen, H., Bongers, T., Holovachov, O., Bakker, J., & Helder, J. (2006). Phylum-wide analysis of SSU rDNA reveals deep phylogenetic relationships among nematodes and accelerated evolution toward crown clades. *Molecular Biology and Evolution*, *23*(9), 1792–1800. https://doi.org/10.1093/molbev/msl044
Howe, K. L., Bolt, B. J., Cain, S., Chan, J., Chen, W. J., Davis, P., Done, J., Down, T., Gao, S., Grove, C., Harris, T. W., Kishore, R., Lee, R., Lomax, J., Li, Y., Muller, H. M., Nakamura, C., Nuin, P., Paulini, M., … Sternberg, P. W. (2016). WormBase 2016: Expanding to enable helminth genomic research. *Nucleic Acids Research*, *44*(D1), D774–D780. https://doi.org/10.1093/nar/gkv1217
Howe, K. L., Bolt, B. J., Shafie, M., Kersey, P., & Berriman, M. (2017). WormBase ParaSite − a comprehensive resource for helminth genomics. *Molecular and Biochemical Parasitology*, *215*, 2–10. https://doi.org/10.1016/j.molbiopara.2016.11.005
Huganir, R. L., Delcour, A. H., Greengard, P., & Hess, G. P. (1986). Phosphorylation of the nicotinic acetylcholine receptor regulates its rate of desensitization. *Nature*, *321*(6072), 774–776. https://doi.org/10.1038/321774a0
Innan, H., & Kondrashov, F. (2010). The evolution of gene duplications: Classifying and distinguishing between models. *Nature Reviews Genetics*, *11*(2), 97–108. https://doi.org/10.1038/nrg2689
Jaiteh, M., Taly, A., & Hénin, J. (2016). Evolution of pentameric ligand-gated ion channels: Pro-loop receptors. *PLoS ONE*, *11*(3), 1–24. https://doi.org/10.1371/journal.pone.0151934
Jensen, M. L., Schousboe, A., & Ahring, P. K. (2005). Charge selectivity of the Cys-loop family of ligand-gated ion channels. *Journal of Neurochemistry*, *92*(2), 217–225. https://doi.org/10.1111/j.1471-4159.2004.02883.x
Jha, A., Cadugan, D. J., Purohit, P., & Auerbach, A. (2007). Acetylcholine receptor gating at extracellular transmembrane domain interface: The Cys-Loop and M2-M3 linker. *Journal of General Physiology*, *130*(6), 547–558. https://doi.org/10.1085/jgp.200709856
Jin, X., & Steinbach, J. H. (2015). Potentiation of Neuronal Nicotinic Receptors by 17β-Estradiol: Roles of the Carboxy-Terminal and the Amino-Terminal Extracellular Domains. *PLoS ONE*, *10*(12), 1–18. https://doi.org/10.1371/journal.pone.0144631
Jobson, M. A., Valdez, C. M., Gardner, J., Garcia, L. R., Jorgensen, E. M., & Beg, A. A. (2015). Spillover transmission is mediated by the excitatory GABA receptor LGC-35 in *C. elegans*. *Journal of Neuroscience*, *35*(6), 2803–2816. https://doi.org/10.1523/JNEUROSCI.4557-

14.2015
Johnson, J. R., Jenn, R. C., Barclay, J. W., Burgoyne, R. D., & Morgan, A. (2010). *Caenorhabditis elegans*: A useful tool to decipher neurodegenerative pathways. *Biochemical Society Transactions*, *38*(2), 559–563. https://doi.org/10.1042/BST0380559
Jones, A. K., Davis, P., Hodgkin, J., & Sattelle, D. B. (2007). The nicotinic acetylcholine receptor gene family of the nematode *Caenorhabditis elegans*: An update on nomenclature. *Invertebrate Neuroscience*, *7*(2), 129–131. https://doi.org/10.1007/s10158-007-0049-z
Jones, A. K., & Sattelle, D. B. (2008). The cys-loop ligand-gated ion channel gene superfamily of the nematode, *Caenorhabditis elegans*. *Invertebrate Neuroscience*, *8*(1), 41–47. https://doi.org/10.1007/s10158-008-0068-4
Jones, M. V., & Westbrook, G. L. (1996). The impact of receptor desensitization on fast synaptic transmission. *Trends in Neurosciences*, *19*(3), 96–101. https://doi.org/10.1016/S0166-2236(96)80037-3
Jospin, M., Qi, Y. B., Stawicki, T. M., Boulin, T., Schuske, K. R., Horvitz, H. R., Bessereau, J. L., Jorgensen, E. M., & Jin, Y. (2009). A neuronal acetylcholine receptor regulates the balance of muscle excitation and inhibition in *Caenorhabditis elegans*. *PLoS Biology*, *7*(12). https://doi.org/10.1371/journal.pbio.1000265
Kaji, M. D., Geary, T. G., & Beech, R. N. (2020). A Functional Comparison of Homopentameric Nicotinic Acetylcholine Receptors (ACR-16) Receptors From *Necator americanus* and *Ancylostoma ceylanicum*. *Frontiers in Molecular Neuroscience*, *13*(November), 1–19. https://doi.org/10.3389/fnmol.2020.601102
Kamat, S., Yeola, S., Zhang, W., Bianchi, L., & Driscoll, M. (2014). NRA-2, a nicalin homolog, regulates neuronal death by controlling surface localization of toxic *caenorhabditis elegans* DEG/ENaC channels. *Journal of Biological Chemistry*, *289*(17), 11916–11926. https://doi.org/10.1074/jbc.M113.533695
Kandel, E. R., J. H. Schwartz and T. M. Jessell (2000). Principles of neural science. New York, McGraw-Hill, Health Professions Division
Kashyap, S. S., Verma, S., McHugh, M., Wolday, M., Williams, P. D., Robertson, A. P., & Martin, R. J. (2021). Anthelmintic resistance and homeostatic plasticity (*Brugia malayi*). *Scientific Reports*, *11*(1), 1–17. https://doi.org/10.1038/s41598-021-93911-4
Katoh, K., Misawa, K., Kuma, K. I., & Miyata, T. (2002). MAFFT: A novel method for rapid multiple sequence alignment based on fast Fourier transform. *Nucleic Acids Research*, *30*(14), 3059–3066. https://doi.org/10.1093/nar/gkf436
Keramidas, A., & Lynch, J. W. (2013). An outline of desensitization in pentameric ligand-gated ion channel receptors. *Cellular and Molecular Life Sciences*, *70*(7), 1241–1253. https://doi.org/10.1007/s00018-012-1133-z
Keramidas, A., Moorhouse, A. J., Schofield, P. R., & Barry, P. H. (2004). Ligand-gated ion channels: Mechanisms underlying ion selectivity. In *Progress in Biophysics and Molecular Biology* (Vol. 86, Issue 2). https://doi.org/10.1016/j.pbiomolbio.2003.09.002
Kinde, M. N., Chen, Q., Lawless, M. J., Mowrey, D. D., Xu, J., Saxena, S., Xu, Y., & Tang, P. (2015). Conformational Changes Underlying Desensitization of the Pentameric Ligand-Gated Ion Channel ELIC. *Structure*, *23*(6), 995–1004. https://doi.org/10.1016/j.str.2015.03.017
Kneussel, M., & Betz, H. (2000). Clustering of inhibitory neurotransmitter receptors at developing postsynaptic sites: The membrane activation model. *Trends in Neurosciences*, *23*(9), 429–435. https://doi.org/10.1016/S0166-2236(00)01627-1

Kracun, S., Harkness, P. C., Gibb, A. J., & Millar, N. S. (2008). Influence of the M3-M4 intracellular domain upon nicotinic acetylcholine receptor assembly, targeting and function. *British Journal of Pharmacology*, *153*(7), 1474–1484. https://doi.org/10.1038/sj.bjp.0707676

Krieger, E., & Vriend, G. (2014). YASARA View - molecular graphics for all devices - from smartphones to workstations. *Bioinformatics (Oxford, England)*, *30*(20), 2981–2982. https://doi.org/10.1093/bioinformatics/btu426

Langlhofer, G., & Villmann, C. (2016). The intracellular loop of the glycine receptor: It's not all about the size. *Frontiers in Molecular Neuroscience*, *9*(JUNE), 1–14. https://doi.org/10.3389/fnmol.2016.00041

Lansdell, S. J., Collins, T., Yabe, A., Gee, V. J., Gibb, A. J., & Millar, N. S. (2008). Host-cell specific effects of the nicotinic acetylcholine receptor chaperone RIC-3 revealed by a comparison of human and Drosophila RIC-3 homologues. *Journal of Neurochemistry*, *105*(5), 1573–1581. https://doi.org/10.1111/j.1471-4159.2008.05235.x

Lansdell, S. J., Gee, V. J., Harkness, P. C., Doward, A. I., Baker, E. R., Gibb, A. J., & Millar, N. S. (2005). RIC-3 enhances functional expression of multiple nicotinic acetylcholine receptor subtypes in mammalian cells. *Molecular Pharmacology*, *68*(5), 1431–1438. https://doi.org/10.1124/mol.105.017459

Lee, D.L. (Ed.). (2002). The Biology of Nematodes (1st ed.). CRC Press.

Lee, W. Y., & Sine, S. M. (2005). Principal pathway coupling agonist binding to channel gating in nicotinic receptors. *Nature*, *438*(7065), 243–247. https://doi.org/10.1038/nature04156

Lewis, J. A., Wu, C. H., Berg, H., & Levine, J. H. (1980a). The genetics of levamisole resistance in the nematode *Caenorhabditis elegans*. *Genetics*, *95*(4), 905–928.

Lewis, J. A., Wu, C. H., Levine, J. H., & Berg, H. (1980b). Levamisole-resitant mutants of the nematode *Caenorhabditis elegans* appear to lack pharmacological acetylcholine receptors. *Neuroscience*, *5*(6), 967–989. https://doi.org/10.1016/0306-4522(80)90180-3

Li, B. W., Rush, A. C., & Weil, G. J. (2015). Expression of five acetylcholine receptor subunit genes in *Brugia malayi* adult worms. *International Journal for Parasitology: Drugs and Drug Resistance*, *5*(3), 100–109. https://doi.org/10.1016/j.ijpddr.2015.04.003

Liao, V. W. Y., Chebib, M., & Ahring, P. K. (2021). Efficient expression of concatenated α1β2δ and α1β3δ GABAA receptors, their pharmacology and stoichiometry. *British Journal of Pharmacology*, *178*(7), 1556–1573. https://doi.org/10.1111/bph.15380

Liao, V. W. Y., Kusay, A. S., Balle, T., & Ahring, P. K. (2020). Heterologous expression of concatenated nicotinic ACh receptors: Pros and cons of subunit concatenation and recommendations for construct designs. *British Journal of Pharmacology*, *177*(18), 4275–4295. https://doi.org/10.1111/bph.15188

Lo, W. Y., Botzolakis, E. J., Tang, X., & Macdonald, R. L. (2008). A conserved Cys-loop receptor aspartate residue in the M3-M4 cytoplasmic loop is required for GABAA receptor assembly. *Journal of Biological Chemistry*, *283*(44), 29740–29752. https://doi.org/10.1074/jbc.M802856200

Lustigman, S., Prichard, R. K., Gazzinelli, A., Grant, W. N., Boatin, B. A., McCarthy, J. S., & Basáñez, M. G. (2012). A research agenda for helminth diseases of humans: The problem of helminthiases. *PLoS Neglected Tropical Diseases*, *6*(4). https://doi.org/10.1371/journal.pntd.0001582

Lynagh, T., Beech, R. N., Lalande, M. J., Keller, K., Cromer, B. A., Wolstenholme, A. J., & Laube, B. (2015). Molecular basis for convergent evolution of glutamate recognition by

pentameric ligand-gated ion channels. *Scientific Reports*, *5*, 1–8. https://doi.org/10.1038/srep08558
Lynch, J. W., Rajendra, S., Pierce, K. D., Handford, C. A., Barry, P. H., & Schofield, P. R. (1997). Identification of intracellular and extracellular domains mediating signal transduction in the inhibitory glycine receptor chloride channel. *EMBO Journal*, *16*(1), 110–120. https://doi.org/10.1093/emboj/16.1.110
Markaki, M., & Tavernarakis, N. (2010). Modeling human diseases in *Caenorhabditis elegans*. *Biotechnology Journal*, *5*(12), 1261–1276. https://doi.org/10.1002/biot.201000183
Martin, R. J., Robertson, A. P., Buxton, S. K., Beech, R. N., Charvet, C. L., & Neveu, C. (2012). Levamisole receptors: A second awakening. *Trends in Parasitology*, *28*(7), 289–296. https://doi.org/10.1016/j.pt.2012.04.003
Martinez-Torres, A. (2000). GABArho 1/GABAAalpha 1 receptor chimeras to study receptor desensitization. *Proceedings of the National Academy of Sciences*, *97*(7), 3562–3566. https://doi.org/10.1073/pnas.050582397
Martínez-Torres, A., & Miledi, R. (2006). Expression of *Caenorhabditis elegans* neurotransmitter receptors and ion channels in Xenopus oocytes. *Proceedings of the National Academy of Sciences of the United States of America*, *103*(13), 5120–5124. https://doi.org/10.1073/pnas.0600739103
Maue, R. (2007). Understanding Ion Channel Biology Using Epitope Tags: Progress, Pitfalls, and Promise. *Journal Cellular Physiology*, *211(3)*, 618–625. https://doi.org/10.1002/JCP
McKinnon, N. K., Bali, M., & Akabas, M. H. (2012). Length and amino acid sequence of peptides substituted for the 5-HT3a receptor M3M4 loop may affect channel expression and desensitization. *PLoS ONE*, *7*(4). https://doi.org/10.1371/journal.pone.0035563
Merlie, J. P., & Lindstrom, J. (1983). Assembly in vivo of mouse muscle acetylcholine receptor: Identification of an α subunit species that may be an assembly intermediate. *Cell*, *34*(3), 747–757. https://doi.org/10.1016/0092-8674(83)90531-7
Millar, N. S. (2008). RIC-3: A nicotinic acetylcholine receptor chaperone. *British Journal of Pharmacology*, *153*(SUPPL. 1), 177–183. https://doi.org/10.1038/sj.bjp.0707661
Millar, Neil S., & Gotti, C. (2009). Diversity of vertebrate nicotinic acetylcholine receptors. *Neuropharmacology*, *56*(1), 237–246. https://doi.org/10.1016/j.neuropharm.2008.07.041
Millar, Neil S., & Harkness, P. C. (2008). Assembly and trafficking of nicotinic acetylcholine receptors (Review). *Molecular Membrane Biology*, *25*(4), 279–292. https://doi.org/10.1080/09687680802035675
Mitreva, M., Blaxter, M. L., Bird, D. M., & McCarter, J. P. (2005). Comparative genomics of nematodes. *Trends in Genetics*, *21*(10), 573–581. https://doi.org/10.1016/j.tig.2005.08.003
Miyazawa, A., Fujiyoshi, Y., & Unwin, N. (2003). Structure and gating mechanism of the acetylcholine receptor pore. *Nature*, *423*(6943), 949–955. https://doi.org/10.1038/nature01748
Mnatsakanyan, N., Nishtala, S. N., Pandhare, A., Fiori, M. C., Goyal, R., Pauwels, J. E., Navetta, A. F., Ahrorov, A., & Jansen, M. (2015). Functional chimeras of GLIC obtained by adding the intracellular domain of anion- and cation-conducting Cys-loop receptors. *Biochemistry*, *54*(16), 2670–2682. https://doi.org/10.1021/acs.biochem.5b00203
Mongan, N. P., Jones, A. K., Smith, G. R., Sansom, M. S. P., & Sattelle, D. B. (2002). Novel α7-like nicotinic acetylcholine receptor subunits in the nematode *Caenorhabditis elegans* . *Protein Science*, *11*(5), 1162–1171. https://doi.org/10.1110/ps.3040102
Mowrey, D., Cheng, M. H., Liu, L. T., Willenbring, D., Lu, X., Wymore, T., Xu, Y., & Tang, P.

(2013). Asymmetric ligand binding facilitates conformational transitions in pentameric ligand-gated ion channels. *Journal of the American Chemical Society*, *135*(6), 2172–2180. https://doi.org/10.1021/ja307275v

Neveu, C., Charvet, C. L., Fauvin, A., Cortet, J., Beech, R. N., & Cabaret, J. (2010). Genetic diversity of levamisole receptor subunits in parasitic nematode species and abbreviated transcripts associated with resistance. *Pharmacogenetics and Genomics*, *20*(7), 414–425. https://doi.org/10.1097/FPC.0b013e328338ac8c

Nielsen, M. G., Gadagkar, S. R., & Gutzwiller, L. (2010). Tubulin evolution in insects: Gene duplication and subfunctionalization provide specialized isoforms in a functionally constrained gene family. *BMC Evolutionary Biology*, *10*(1). https://doi.org/10.1186/1471-2148-10-113

Nishtala, S. N., Mnatsakanyan, N., & Jansen, M. (2014). Direct Interaction of RIC-3 with the Intracellular Domain of Eukaryotic Cationic Pentameric Ligand-Gated Ion Channels. *Biophysical Journal*, *106*(2), 342a. https://doi.org/10.1016/j.bpj.2013.11.1954

Nishtala, S. N., Mnatsakanyan, N., Pandhare, A., Leung, C., & Jansen, M. (2016). Direct interaction of the resistance to inhibitors of cholinesterase type 3 protein with the serotonin receptor type 3A intracellular domain. *Journal of Neurochemistry*, *137*(4), 528–538. https://doi.org/10.1111/jnc.13578

O'donnell, J. P., Phillips, B. P., Yagita, Y., Juszkiewicz, S., Wagner, A., Malinverni, D., Keenan, R. J., Miller, E. A., & Hegde, R. S. (2020). The architecture of EMC reveals a path for membrane protein insertion. *ELife*, *9*, 1–56. https://doi.org/10.7554/eLife.57887

O'Toole, K. K., & Jenkins, A. (2011). Discrete M3-M4 intracellular loop subdomains control specific aspects of γ-aminobutyric acid type A receptor function. *Journal of Biological Chemistry*, *286*(44), 37990–37999. https://doi.org/10.1074/jbc.M111.258012

Ohno, S. (1970). Evolution by Gene Duplication. In *Evolution by Gene Duplication*. https://doi.org/10.1007/978-3-642-86659-3

Ortells, M. O. (2016). Structure and function development during evolution of pentameric ligand gated ion channels. *Neurotransmitter*, 1–12. https://doi.org/10.14800/nt.1273

Ortells, M. O., & Lunt, G. G. (1995). Evolutionary history of the ligand-gated ion-channel superfamily of receptors. *Trends in Neurosciences*, *18*(3), 121–127. https://doi.org/10.1016/0166-2236(95)93887-4

Paradiso, K., Zhang, J., & Steinbach, J. H. (2001). The C terminus of the human nicotinic α4β2 receptor forms a binding site required for potentiation by an estrogenic steroid. *Journal of Neuroscience*, *21*(17), 6561–6568. https://doi.org/10.1523/jneurosci.21-17-06561.2001

Parkinson, J., Mitreva, M., Whitton, C., Thomson, M., Daub, J., Martin, J., Schmid, R., Hall, N., Barrell, B., Waterston, R. H., McCarter, J. P., & Blaxter, M. L. (2004). A transcriptomic analysis of the phylum Nematoda. *Nature Genetics*, *36*(12), 1259–1267. https://doi.org/10.1038/ng1472

Pedersen, J. E., Bergqvist, C. A., & Larhammar, D. (2019). Evolution of vertebrate nicotinic acetylcholine receptors. *BMC Evolutionary Biology*, *19*(1), 1–21. https://doi.org/10.1186/s12862-018-1341-8

Peters, J. A., Hales, T. G., & Lambert, J. J. (2005). Molecular determinants of single-channel conductance and ion selectivity in the Cys-loop family: Insights from the 5-HT3 receptor. *Trends in Pharmacological Sciences*, *26*(11), 587–594. https://doi.org/10.1016/j.tips.2005.09.011

Putrenko, I., Zakikhani, M., & Dent, J. A. (2005). A family of acetylcholine-gated chloride

channel subunits in *Caenorhabditis elegans*. *Journal of Biological Chemistry*, *280*(8), 6392–6398. https://doi.org/10.1074/jbc.M412644200

Qian, H., Martin, R. J., Robertson, A. P., Qian, H., Martin, R. J., & Robertson, A. P. (2006). Pharmacology of N -, L -, and B -subtypes of nematode nAChR resolved at the single-channel level in *Ascaris suum* . *The FASEB Journal*, *20*(14), 2606–2608. https://doi.org/10.1096/fj.06-6264fje

Ren, X. Q., Cheng, S. Bin, Treuil, M. W., Mukherjee, J., Rao, J., Braunewell, K. H., Lindstrom, J. M., & Anand, R. (2005). Structural determinants of α4β2 nicotinic acetylcholine receptor trafficking. *Journal of Neuroscience*, *25*(28), 6676–6686. https://doi.org/10.1523/JNEUROSCI.1079-05.2005

Richard, M., Boulin, T., Robert, V. J. P., Richmond, J. E., & Bessereau, J. L. (2013). Biosynthesis of ionotropic acetylcholine receptors requires the evolutionarily conserved ER membrane complex. *Proceedings of the National Academy of Sciences of the United States of America*, *110*(11). https://doi.org/10.1073/pnas.1216154110

Richmond, J. E., & Jorgensen, E. M. (1999). One GABA and two acetylcholine receptors function at the *C. elegans* neuromuscular junction. *Nature Neuroscience*, *2*(9), 791–798. https://doi.org/10.1038/12160

Roeber, F., Jex, A. R., & Gasser, R. B. (2013). Impact of gastrointestinal parasitic nematodes of sheep, and the role of advanced molecular tools for exploring epidemiology and drug resistance - An Australian perspective. *Parasites and Vectors*, *6*(1), 1–13. https://doi.org/10.1186/1756-3305-6-153

Rudell, J. C., Borges, L. S., Yarov-Yarovoy, V., & Ferns, M. (2020). The MX-Helix of Muscle nAChR Subunits Regulates Receptor Assembly and Surface Trafficking. *Frontiers in Molecular Neuroscience*, *13*(March), 1–13. https://doi.org/10.3389/fnmol.2020.00048

Sauguet, L., Poitevin, F., Murail, S., Van Renterghem, C., Moraga-Cid, G., Malherbe, L., Thompson, A. W., Koehl, P., Corringer, P. J., Baaden, M., & Delarue, M. (2013). Structural basis for ion permeation mechanism in pentameric ligand-gated ion channels. *EMBO Journal*, *32*(5), 728–741. https://doi.org/10.1038/emboj.2013.17

Sharma, P., Li, L., Liu, H., Tikiyani, V., Hu, Z., & Babu, K. (2018). The claudin-like protein HPO-30 is required to maintain lachrs at the *C. Elegans* neuromuscular junction. *Journal of Neuroscience*, *38*(32), 7072–7087. https://doi.org/10.1523/JNEUROSCI.3487-17.2018

Shurtleff, M. J., Itzhak, D. N., Hussmann, J. A., Schirle Oakdale, N. T., Costa, E. A., Jonikas, M., Weibezahn, J., Popova, K. D., Jan, C. H., Sinitcyn, P., Vembar, S. S., Hernandez, H., Cox, J., Burlingame, A. L., Brodsky, J. L., Frost, A., Borner, G. H. H., & Weissman, J. S. (2018). The ER membrane protein complex interacts cotranslationally to enable biogenesis of multipass membrane proteins. *ELife*, *7*, 1–23. https://doi.org/10.7554/eLife.37018

Sine, S. M. (2002). The nicotinic receptor ligand binding domain. *Journal of Neurobiology*, *53*(4), 431–446. https://doi.org/10.1002/neu.10139

Smart, T. G., & Paoletti, P. (2012). Synaptic neurotransmitter-gated receptors. *Cold Spring Harbor Perspectives in Biology*, *4*(3). https://doi.org/10.1101/cshperspect.a009662

Smith, M. P., & Harper, D. A. T. (2013). Causes of the Cambrian explosion. *Science*, *341*(6152), 1355–1356. https://doi.org/10.1126/science.1239450

Sulston, J. E., Schierenberg, E., White, J. G., & Thomson, J. N. (1983). The embryonic cell lineage of the nematode *Caenorhabditis elegans*. *Developmental Biology*, *100*(1), 64–119. https://doi.org/10.1016/0012-1606(83)90201-4

Sumikawa, K., & Nishizaki, T. (1994). The amino acid residues 1-128 in the α subunit of the

nicotinic acetylcholine receptor contain assembly signals. *Molecular Brain Research*, *25*(3–4), 257–264. https://doi.org/10.1016/0169-328X(94)90161-9

Taly, A., Corringer, P. J., Guedin, D., Lestage, P., & Changeux, J. P. (2009). Nicotinic receptors: Allosteric transitions and therapeutic targets in the nervous system. *Nature Reviews Drug Discovery*, *8*(9), 733–750. https://doi.org/10.1038/nrd2927

Tasneem, A., Iyer, L. M., Jakobsson, E., & Aravind, L. (2005). Identification of the prokaryotic ligand-gated ion channels and their implications for the mechanisms and origins of animal Cys-loop ion channels. *Genome Biology*, *6*(1), 1–12. https://doi.org/10.1186/gb-2004-6-1-r4

Thompson, A., Infield, D. T., Smith, A. R., Smith, G. T., Ahern, C. A., & Zakon, H. H. (2018). Rapid evolution of a voltage-gated sodium channel gene in a lineage of electric fish leads to a persistent sodium current. *PLoS Biology*, *16*(3). https://doi.org/10.1371/journal.pbio.2004892

Thompson, A. J., Lester, H. A., & Lummis, S. C. R. (2010). The structural basis of function in Cys-loop receptors. In *Quarterly Reviews of Biophysics* (Vol. 43, Issue 4). https://doi.org/10.1017/S0033583510000168

Tillman, T. S., Seyoum, E., Mowrey, D. D., Xu, Y., & Tang, P. (2014). ELIC-α7 nicotinic acetylcholine receptor (α7nAChR) chimeras reveal a prominent role of the extracellular-transmembrane domain interface in allosteric modulation. *Journal of Biological Chemistry*, *289*(20), 13851–13857. https://doi.org/10.1074/jbc.M113.524611

Touroutine, D., Fox, R. M., Von Stetina, S. E., Burdina, A., Miller, D. M., & Richmond, J. E. (2005). acr-16 encodes an essential subunit of the levamisole-resistant nicotinic receptor at the *Caenorhabditis elegans* neuromuscular junction. *Journal of Biological Chemistry*, *280*(29), 27013–27021. https://doi.org/10.1074/jbc.M502818200

Touroutine, D. V, Fox, R. M., III, D. M. M., & Richmond, J. E. (2004). acr-16 mutants eliminate the non-levamisole acetylcholine response in *C. elegans* body wall muscles. In *West Coast Worm Meeting*.

Towers, P. R., Edwards, B., Richmond, J. E., & Sattelle, D. B. (2005). The *Caenorhabditis elegans lev-8* gene encodes a novel type of nicotinic acetylcholine receptor α subunit. *Journal of Neurochemistry*, *93*(1), 1–9. https://doi.org/10.1111/j.1471-4159.2004.02951.x

Treinin, M., & Jin, Y. (2020). Cholinergic transmission in *C. elegans*: Functions, diversity, and maturation of ACh-activated ion channels. *Journal of Neurochemistry*, *June*, 1–18. https://doi.org/10.1111/jnc.15164

Unwin, N. (1995). Acetylcholine receptor channel imaged in the open state. In *Nature* (Vol. 373, Issue 6509, pp. 37–43). https://doi.org/10.1038/373037a0

Unwin, N. (2005). Refined structure of the nicotinic acetylcholine receptor at 4 Å resolution. *Journal of Molecular Biology*, *346*(4), 967–989. https://doi.org/10.1016/j.jmb.2004.12.031

Verma, S., Kashyap, S. S., Robertson, A. P., & Martin, R. J. (2017). Functional genomics in *Brugia malayi* reveal diverse muscle nAChRs and differences between cholinergic anthelmintics. *Proceedings of the National Academy of Sciences of the United States of America*, *114*(21), 5539–5544. https://doi.org/10.1073/pnas.1619820114

Verrall, S., & Hall, Z. W. (1992). The N-terminal domains of acetylcholine receptor subunits contain recognition signals for the initial steps of receptor assembly. *Cell*, *68*(1), 23–31. https://doi.org/10.1016/0092-8674(92)90203-O

Walstab, J., Hammer, C., Lasitschka, F., Möller, D., Connolly, C. N., Rappold, G., Brüss, M., Bönisch, H., & Niesler, B. (2010). RIC-3 exclusively enhances the surface expression of human homomeric 5-hydroxytryptamine type 3A (5-HT3A) receptors despite direct

interactions with 5-HT3A, -C, -D, and -E subunits. *Journal of Biological Chemistry*, *285*(35), 26956–26965. https://doi.org/10.1074/jbc.M110.122838
Wang, J. M., Zhang, L., Yao, Y., Viroonchatapan, N., Rothe, E., & Wang, Z. Z. (2002). A transmembrane motif governs the surface trafficking of nicotinic acetylcholine receptors. *Nature Neuroscience*, *5*(10), 963–970. https://doi.org/10.1038/nn918
Wang, Y., Yao, Y., Tang, X. Q., & Wang, Z. Z. (2009). Mouse RIC-3, an endoplasmic reticulum chaperone, promotes assembly of the α7 acetylcholine receptor through a cytoplasmic coiled-coil domain. *Journal of Neuroscience*, *29*(40), 12625–12635. https://doi.org/10.1523/JNEUROSCI.1776-09.2009
Wideman, J. G. (2015). The ubiquitous and ancient ER membrane protein complex (EMC): Tether or not? *F1000Research*, *4*(May), 1–12. https://doi.org/10.12688/f1000research.6944.2
Williams, M. E., Burton, B., Urrutia, A., Shcherbatko, A., Chavez-Noriega, L. E., Cohen, C. J., & Aiyar, J. (2005). Ric-3 promotes functional expression of the nicotinic acetylcholine receptor α7 subunit in mammalian cells. *Journal of Biological Chemistry*, *280*(2), 1257–1263. https://doi.org/10.1074/jbc.M410039200
Williamson, S. M., Robertson, A. P., Brown, L., Williams, T., Woods, D. J., Martin, R. J., Sattelle, D. B., & Wolstenholme, A. J. (2009). The nicotinic acetylcholine receptors of the parasitic nematode *Ascaris suum*: Formation of two distinct drug targets by varying the relative expression levels of two subunits. *PLoS Pathogens*, *5*(7), 1–11. https://doi.org/10.1371/journal.ppat.1000517
Williamson, S. M., Walsh, T. K., & Wolstenholme, A. J. (2007). The cys-loop ligand-gated ion channel gene family of *Brugia malayi* and *Trichinella spiralis*: A comparison with Caenorhabditis elegans. *Invertebrate Neuroscience*, *7*(4), 219–226. https://doi.org/10.1007/s10158-007-0056-0
Wolstenholme, A. J. (2011). Ion channels and receptor as targets for the control of parasitic nematodes. *International Journal for Parasitology: Drugs and Drug Resistance*, *1*(1), 2–13. https://doi.org/10.1016/j.ijpddr.2011.09.003
Wotring, V. E., Miller, T. S., & Weiss, D. S. (2003). Mutations at the GABA receptor selectivity filter: A possible role for effective charges. *Journal of Physiology*, *548*(2), 527–540. https://doi.org/10.1113/jphysiol.2002.032045
Wu, Z. S., Cheng, H., Jiang, Y., Melcher, K., & Xu, H. E. (2015). Ion channels gated by acetylcholine and serotonin: Structures, biology, and drug discovery. *Acta Pharmacologica Sinica*, *36*(8), 895–907. https://doi.org/10.1038/aps.2015.66
Yang, Z. (2007). PAML 4: Phylogenetic analysis by maximum likelihood. *Molecular Biology and Evolution*, *24*(8), 1586–1591. https://doi.org/10.1093/molbev/msm088
Yoav Biala, Liewald, J. F., Ben-Ami, H. C., Gottschalk, A., & Treinin, M. (2009). The Conserved RIC-3 Coiled-Coil Domain Mediates Receptor-specific Interactions with Nicotinic Acetylcholine Receptors. *Molecular Biology of the Cell*, *20*, 2673–2683. https://doi.org/10.1091/mbc.E08
Zerangue, N., Schwappach, B., Yuh, N. J., & Lily, Y. J. (1999). A new ER trafficking signal regulates the subunit stoichiometry of plasma membrane K(ATP) channels. *Neuron*, *22*(3), 537–548. https://doi.org/10.1016/S0896-6273(00)80708-4
Zheng, F., Robertson, A. P., Abongwa, M., Yu, E. W., & Martin, R. J. (2016). The *Ascaris suum* nicotinic receptor, ACR-16, as a drug target: Four novel negative allosteric modulators from virtual screening. *International Journal for Parasitology: Drugs and Drug Resistance*, *6*(1),

60–73. https://doi.org/10.1016/j.ijpddr.2016.02.001
Zhou, Y., Nelson, M. E., Kuryatov, A., Choi, C., Cooper, J., & Lindstrom, J. (2003). Human α4/β2 acetylcholine receptors formed from linked subunits. *Journal of Neuroscience*, *23*(27), 9004–9015. https://doi.org/10.1523/jneurosci.23-27-09004.2003